**Charles University in Prague, Faculty of Science, Department of Analytical Chemistry**, *Hlavova 2030, 12843, Prague2, Czech Republic*

Prague 28. – 29. 1. 2008
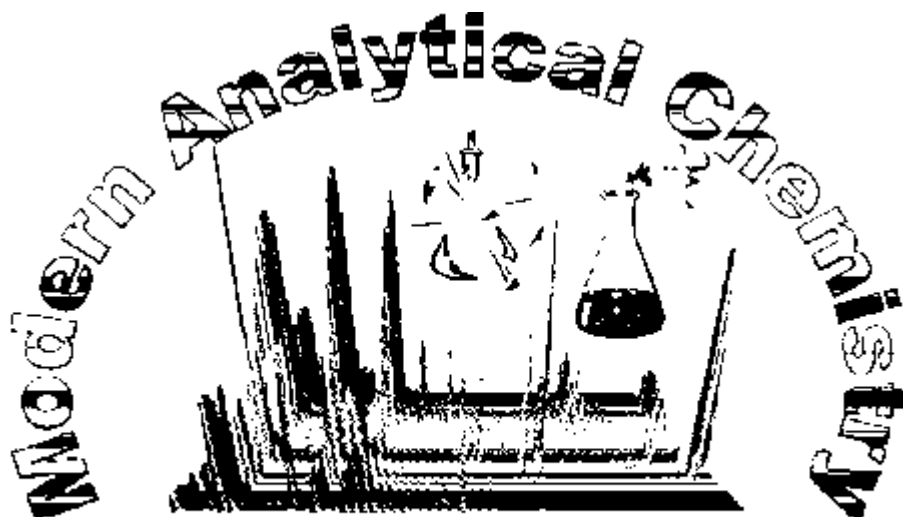
4th International Student Conference

BOOK OF PROCEEDINGS

Prague 2008

We are very grateful to our sponsors for their kind support:

Charles University in Prague, Faculty of Science, Department of Analytical Chemistry, Hlavova 2030, 12843, Prague2, Czech Republic

4th International Student Conference

"Modern Analytical Chemistry"

Prague 28. – 29. 1. 2008

Book of Proceedings

Prague 2008

An Invitation to the 4th International Student Conference

"Modern Analytical Chemistry"

to be held

on January 28 – 29, 2008

at the lecture hall CH2, Faculty of Science,

Department of Chemistry, Albertov 2030, Prague 2

organized by

Charles University in Prague, Faculty of Science, Department of
Analytical Chemistry

and
sponsored by

Zentiva, a.s.

ALS Laboratory Group, ALS Czech Republic, s.r.o.

Quinta Analytica, s.r.o.

PharmaTech, s.r.o.

Shimadzu, GmbH

CZ BIJO, a.s.

Programme

Monday 28th

9.00   11 - 18

GAS CHROMATOGRAPHY IN FOOD ANALYSIS

Antónia Janáčová[a], Ivan Špánik[a] and Tomáš Kowalczuk[b]

[a] *Institute of Analytical Chemistry, Faculty of Food and Chemical Technology Slovak University of Technology, Bratislava, The Slovak Republic; e-mail: antonia.janacova@stuba.sk*
[b] *LECO Corporation, Application laboratory Praque, The Czech Republic*

9.20   19 - 26

DETERMINATION OF GALACTITOL AND GALACTOSE IN URINE FOR GALACTOSAEMIC SUBJECTS BY GAS CHROMATOGRAPHY – MASS SPECTROMETRY

Beáta Meľuchová[a], Eva Pavlíková[a], Žofia Krkošová[a], Róbert Kubinec[a], Helena Jurdáková[a], Jaroslav Blaško[a], Ivan Ostrovský[a], Jozef Višňovský[a], Darina Behúlová[b] and Jozefína Škodová[b]

[a] *Chemical Institute, Faculty of Natural Sciences, Comenius University, Mlynská dolina CH-2, SK-845 45 Bratislava, Slovakia*
[b] *Department of Laboratory Medicine, Comenius University Children`s Hospital, Limbová 1, SK-833 40 Bratislava, Slovakia*

9.40   27 - 35

VARIATIONS IN FATTY ACID COMPOSITION OF PASTURE FODDER PLANTS AND CLA CONTENTS IN EWE MILK FAT ACCORDING TO SEASON

Eva Pavlíková[a], Beáta Meľuchová[a], Jaroslav Blaško[a], Róbert Kubinec[a], Jarmila Dubravská[b], Milan Margetín[c] and Ladislav Soják[a]

[a] *Chemical Institute, Faculty of Natural Sciences, Comenius University, Mlynská dolina, 84215 Bratislava, Slovak republic*
[b] *Grassland and Mountain Agriculture Research Institute, Mládežnícka 36, 97405 Banská Bystrica, Slovak republic*
[c] *Research Institute of Animal Production in Trenčianská Teplá, Hlohovská 2, 94992 Nitra, Slovak republic*

10.00   36 - 42

TWO DIMENSIONAL GAS CHROMATOGRAPHY AS A TOOL FOR BIOSYNTHESIS STUDY OF THE COMPONENTS OF THE MARKING PHEROMONES OF THE MALES SPECIES *Bombus lucorum* AND *Bombus lapidarius*

Petr Žáček[a,b], Anna Luxová[a], Jiří Kindl[a] and Irena Valterová[a]

[a] *Academy of Sciences of the Czech Republic, Institute of Organic Chemistry and Biochemistry, Flemingovo náměstí 2, 166 10 Prague 6, Czech Republic: e-mail: griegzacek@seznam.cz*
[b] *Charles University, Faculty of Science, Albertov 8, 128 40 Prague 2, Czech Republic*

10.20   43 - 48

SEPARATION OF DEFERIPRONE AND ITS IRON CHELATE USING CAPILLARY ELECTROPHORESIS

Eva Svobodová[a], Zuzana Bosáková[a], Pavel Coufal[a] and Jasmina Novakovic[b]

[a] *Charles University in Prague, Faculty of Science, Department of Analytical Chemistry, Albertov 2030, 128 43 Prague 2, Czech Republic; e-mail: svobod15@natur.cuni.cz*
[b] *University of Toronto, Faculty of Pharmacy, 144 College Street Toronto, Ontario Canada M5S 3M2*

10.40   49 - 52

INFLUENCE OF POLYMERIZATION MIXTURE COMPOSITION ON MOLECULARLY IMPRINTED POLYMERS PROPERTIES PREPARED WITH 1--METHYL-2-PIPERIDINOETHYLESTER OF DECYLOXYPHENYLCARBAMIC ACID AS A TEMPLATE

Miroslava Lachová[a], Jozef Lehotay[a], Ivan Skačáni[a] and Jozef Čižmárik[b]

[a] *Institute of Analytical Chemistry, Faculty of Chemical and Food Technology, Slovak University of Technology in Bratislava, Slovak Republic*
[b] *Department of Pharmaceutical Chemistry, Faculty of Pharmacy, Comenius University in Bratislava, Slovak Republic*

11.00   53 - 59

DEVELOPMENT OF A SOLID PHASE EXTRACTION METHOD FOR DETERMINATION OF STYRENE OXIDE ADDUCTS IN HUMAN GLOBIN

Michal Jágr[a], Věra Pacáková[b] and Miroslav Petříček[a]

[a] *Institute of Microbiology, Academy of Sciences of the Czech Republic, Vídeňská 1083, Prague 4, 142 20, Czech Republic, e-mail: jagr@biomed.cas.cz*
[b] *Department of Analytical Chemistry, Faculty o Science, Charles University, Albertov 8, Prague 2, 128 40, Czech Republic*

11.20   60 - 64

ALKYLATION AS A TOOL FOR POSTPOLYMERIZATION SURFACE MODIFICATION OF POLYSTYRENE CAPILLARY MONOLITHIC COLUMNS

Zdeňka Kučerová[a], Michał Szumski[b], Bogusław Buszewski[b] and Pavel Jandera[a]

[a] *University of Pardubice, Faculty of Chemical Technology, nám. Čs. legií 565, CZ-532 10 Pardubice, Czech Republic; e-mail: st8546@student.upce.cz*
[b] *Nicolaus Copernicus University, Faculty of Chemistry, Gagarina 11, PL 87-100 Toruń, Poland*

11.40   65 - 69

USE OF CHIRAL SEPARATIONS FOR THE DETERMINATION OF ENZYME ENANTIOSELECTIVITY

Jiří Břicháč[a,b,c,d], Jiří Zima[b], Michael Kotik[c], Ales Honzatko[a] and Matthew J. Picklo[a]

[a] *Department of Pharmacology, Physiology, and Therapeutics, University of North Dakota, Grand Forks, ND 58203-9024, USA*
[b] *Department of Analytical Chemistry, Charles University in Prague, Albertov 6, 128 43 Prague 2, Czech Republic*
[c] *Laboratory of Enzyme Technology, Institute of Microbiology, Academy of Sciences of the Czech Republic, Vídeňská 1083, 142 20 Prague 4, Czech Republic*
[d] *Department of Membrane Transport Biophysics, Institute of Physiology, Academy of Sciences of the Czech Republic, Vídeňská 1083, 142 20 Prague 4, Czech Republic. E-mail address: brichac@email.cz*

12.00   70 - 76

DETERMINATION OF HERBAL ANTIOXIDANTS

Petr Dobiáš, Martin Adam and Karel Ventura

University of Pardubice, Faculty of Chemical Technology, Department of Analytical Chemistry, Nám. Čs. legií 565, Pardubice, Czech Republic; email: peejay1@seznam.cz

12.20 - 13.30 Lunch

13.30   77 - 82

DETERMINATION OF LINCOMYCIN PRECURSORS IN FERMENTATION BROTH OF *STREPTOMYCES LINCOLNENSIS* USING HIGH PERFORMANCE LC WITH FLUORESCENCE DETECTION

Zdeněk Kameník[a,b], Dana Ulanová[a], Jan Kopecký[a], Karel Nesměrák[b] and Jana Olšovská[a]

[a] *Academy of Sciences of the Czech Republic, Institute of Microbiology, Vídeňská 1083, 142 20 Prague 4, Czech Republic; e-mail: zdenek.kamenik@email.cz*
[b] *Charles University, Faculty of Science, Albertov 8, 128 40 Prague 2, Czech Republic*

13.50   83 - 88

IDENTIFICATION AND QUANTIFICATION OF SELECTED ESTROGENS USING HPLC METHOD

Lucie Loukotková[a], Daniela Zlesáková[a], Květa Kalíková[b], Eva Tesařová[b] and Zuzana Bosáková[a]
[a] *Department of Analytical Chemistry, Faculty of Science, Charles University in Prague, Albertov 2030, 128 43 Prague 2, Czech Republic*
[b] *Department of Physical and Macromolecular Chemistry, Charles University in Prague, Faculty of Science, Albertov 2030, 128 43 Prague 2, Czech Republic*

14.10   166 - 172

HPLC METHOD TO DETERMINE THE RESIDUAL CONCENTRATION OF ESTRONE DURING MOUSE SPERM CAPACITATION *IN VITRO*

Marie Vadinská[a], Zuzana Bosáková[a], Eva Tesařová[b] Jitka Vašínová[c], Michaela Jursová[c] and Kateřina Dvořáková-Hortová[c]
[a] *Department of Analytical Chemistry, Faculty of Science, Charles University in Prague, Albertov 2030, 128 40 Prague 2, Czech Republic, e-mail: vadinskamarie@gmail.com*
[b] *Department of Physical and Macromolecular Chemistry, Faculty of Science, Charles University in Prague, Albertov 2030, 128 40 Prague 2, Czech Republic*
[c] *Department of Developmental Biology, Faculty of Science, Charles University, Viničná 7, 128 44 Prague 2, Czech Republic*

14.30   89 - 94

REDUCTION OF 4-AMINO-3-NITROPHENOL ON BISMUTH-MODIFIED CARBON PASTE ELECTRODE

Hana Dejmková, Jiří Zima and Jiří Barek
Charles University in Prague, Faculty of Science, Department of Analytical Chemistry, UNESCO Laboratory of Environmental Electrochemistry, Albertov 6, 128 43 Praha 2, Czech Republic, e-mail: hdejmkova@seznam.cz

17.00 -   **Social meeting**

Tuesday 29th

9.00   95 - 100

VOLTAMMETRIC CHARACTERIZATION OF VARIOUS BARE AND DNA MODIFIED CARBON PASTE ELECTRODES COVERED WITH MULTIWALLED CARBON NANOTUBES AND CHITOSAN FILMS

Julia Galandová
Institute of Analytical Chemistry, Faculty of Chemical and Food Technology, SlovakUniversity of Technology in Bratislava, Radlinského 9, 812 37 Bratislava, Slovakia, e-mail: julia.galandova@stuba.sk

9.20   173 - 179

VOLTAMMETRIC DETERMINATION OF EPINEPHRINE AT A MODIFIED MINIATURIZED CARBON PASTE ELECTRODE

Zuzana Jemelková, Jiří Zima and Jiří Barek
Charles University in Prague, Faculty of Science, Department of Analytical Chemistry, UNESCO Laboratory of Environmental Electrochemistry, Albertov 6, 128 43 Praha 2, Czech Republic, e-mail: zuzana.jemelkova@seznam.cz

9.40   153 - 157

VOLTAMMETRIC DETERMINATION OF 6-AMINOQUINOLINE AT A CARBON FILM ELECTRODE

Ivan Jiránek and Jiří Barek

Charles University in Prague, Faculty of Science, Department of Analytical Chemistry, UNESCO Laboratory of Environmental Electrochemistry, Albertov 6, 128 43 Praha 2, Czech Republic,e-mail: ijiranek@gmail.com

10.00   101 - 107

TESTING A POSSIBLE ELECTROCHEMICAL RENEWAL OF HANGING MERCURY DROP ELECTRODES

Petra Polášková[a,b] and Ladislav Novotný[a]

[a] *University of Pardubice, Faculty of Chemical technology, nám. Čs. Legií 565, 532 10 Pardubice 19, Czech Republic; e-mail: polaskovap@centrum.cz*
[b] *Charles University, Faculty of Science, Albertov 8, 128 40 Prague 2, Czech Republic*

10.20   108 - 112

POLAROGRAPHIC AND VOLTAMMETRIC DETERMINATION OF SELECTED GENOTOXIC FLUORENE DERIVATIVES USING TRADITIONAL MERCURY ELECTRODES

Vlastimil Vyskočil, Pavol Bologa, Karolina Pecková and Jiří Barek

Charles University in Prague, Faculty of Science, Department of Analytical Chemistry, UNESCO Laboratory of Environmental Electrochemistry, Albertov 6, 128 43, Prague 2, Czech Republic; e-mail: barek@natur.cuni.cz

10.40   180 - 187

VOLTAMMETRIC DETERMINATION OF p-NITROPHENOL USING SILVER AMALGAM PASTE ELECTRODE

Abdul Niaz[a], Jan Fischer[b], Jiří Barek[b], Bogdan Yosypchuk[c], Sirajuddin[a] and Muhammad Iqbal Bhanger[a]

[a] *National Centre of Excellence in Analytical Chemistry, University of Sindh, Jamshoro 76080, Pakistan*
[b] *Charles University in Prague, Faculty of Science, Department of Analytical Chemistry, UNESCO Laboratory of Environmental Electrochemistry, Hlavova 2030, 12843 Prague 2, Czech Republic, e-mail: barek@natur.cuni.cz*
[c] *J. Heyrovsky Institute of Physical Chemistry of ASCR, v. v. i., Dolejšova 3, 182 23 Prague 8, Czech Republic*

11.00   147 - 152

VOLTAMMETRIC DETERMINATION OF 2-NITROPHENOL AT BORON-DOPED DIAMOND FILM ELECTRODE

Jana Musilová[a], Jiří Barek[a], Pavel Drašar[b] and Karolina Pecková[a]

[a] *Charles University in Prague, Faculty of Science, Department of Analytical Chemistry, UNESCO Laboratory of Environmental Electrochemistry, Hlavova 2030, 12843 Prague 2, Czech Republic; e-mail: Jana.Musilova@seznam.cz*
[b] *Institute of Chemical Technology, Faculty of Food and Biochemical Technology, Technická 5, 16628 Prague 6, Czech Republic*

11.20   113 - 117

CHEMICAL VAPOUR GENERATION OF SILVER AS A METHOD FOR SAMPLE INTRODUCTION FOR ATOMIC ABSORPTION SPECTROMETRY

Stanislav Musil[a,b], Jan Kratzer[a,b], Miloslav Vobecký[a], Petr Rychlovský[b] and Tomáš Matoušek[a]

[a] *Institute of Analytical Chemistry of the ASCR v.v.i., Vídeňská 1083, 14220 Prague, Czech Republic; e-mail: stanomusil@biomed.cas.cz*
[b] *Charles University in Prague, Faculty of Science, Department of Analytical Chemistry, Albertov 6, 12843 Prague, Czech Republic*

11.40   118 - 122

NEW ELECTROLYTIC CELLS FOR ELECTROCHEMICAL HYDRIDE GENERATION IN AAS

Jakub Hraníček, Václav Červený and Petr Rychlovský

Charles University, Faculty of Science, Hlavova 8, 128 40 Prague 2, Czech Republic; e-mail: hranicek.jakub@email.cz

12.00   123 - 129

THIOGLYCOLIC ACID AS ON-LINE PRE-REDUCTANT FOR SPECIATION ANALYSIS OF ARSENIC BY SELECTIVE HYDRIDE GENERATION-CRYOTRAPPING-AAS

Stanislav Musil[a,b], Tomáš Matoušek[a] and Petr Rychlovský[b]

[a] Institute of Analytical Chemistry of the ASCR v.v.i., Víděňská 1083, 14220 Prague, Czech Republic; e-mail: stanomusil@biomed.cas.cz
[b] Charles University in Prague, Faculty of Science, Department of Analytical Chemistry, Albertov 6, 12843 Prague, Czech Republic

12.20 - 13.30 Lunch

13.30   130 - 135

BILIRUBIN AND BILIVERDIN: STRUCTURAL STUDIES BY ELECTRONIC AND VIBRATIONAL CIRCULAR DICHROISM

Iryna Goncharova[a] and Marie Urbanová[b]

[a] Institute of Chemical Technology, Prague, Technická 5, Department of Analytical Chemistry, 166 28 Prague 6, Czech Republic; e-mail: gonchari@vscht.cz
[b] Institute of Chemical Technology, Prague, Technická 5, Department of Physics and Measurements, 166 28 Prague 6, Czech Republic

13.50   136 - 141

COMPLEXES OF QUININE DERIVATIVES: VIBRATIONAL AND ELECTRONIC CIRCULAR DICHROISM STUDY

Ondřej Julínek[a] and Marie Urbanová[b]

[a] Institute of Chemical Technology, Prague, Department of Analytical Chemistry, Technická 5, 166 28, Prague, Czech Republic, e-mail: ondrej.julinek@vscht.cz
[b] Institute of Chemical Technology, Prague, Department of Physics and Measurements, Technická 5, 166 28, Prague, Czech Republic

14.10   158 - 165

PREPARATION OF SERS-ACTIVE SUBSTRATES WITH LARGE SURFACE AREA FOR RAMAN SPECTRAL MAPPING AND TESTING OF THEIR SURFACE NANOSTRUCTURE

Vadym Prokopec, Jitka Čejková, Pavel Matějka and Pavel Hasal

Institute of Chemical Technology Prague, Dept. of Analytical Chemistry, Technická 5, Prague 6, 116 28, Czech Republic

14.30   142 - 146

PREPARATION AND CHARACTERIZATION OF NANOPARTICLES

Pavel Řezanka, Kamil Záruba and Vladimír Král

Institute of Chemical Technology Prague, Dept. of Analytical Chemistry, Technická 5, Prague 6, 166 28, Czech Republic; e-mail: pavel.rezanka@vscht.cz

GAS CHROMATOGRAPHY IN FOOD ANALYSIS

Antónia Janáčová[a], Ivan Špánik[a] and Tomáš Kowalczuk[b]

[a] *Institute of Analytical Chemistry, Faculty of Food and Chemical Technology Slovak University of Technology, Bratislava, The Slovak Republic;*
e-mail: antonia.janacova@stuba.sk
[b] *LECO Corporation, Application laboratory Praque, The Czech Republic*

Keywords

GC-MS; GC-O; GCxGC; food analysis; brandy; direct injection; HS; LLE; SPME

Abstract

In this work, the composition of volatile compounds in different wine distillates was studied by GC coupled with MS detector, comprehensive multidimensional gas chromatography and gas chromatography with olfactometry. The effectiveness of direct injection, headspace, SPME and liquid-liquid extraction was compared. The studied samples originate from different geographical region and were produced with different technology.

1. Introduction

Brandy is a general term for distilled product of fermented fruits that usually contains 40–60% ethyl alcohol by volume. The most famous brandies are produced from grape wines by distillation followed by ageing in wooden casks. It is obvious that brandies are a complex mixture of components representing many classes of organic compounds. Many organic compounds are found in brandies while only a few of them are specific for given brand. The formation of overall brandy flavour is influenced by several primary parameters, such as grape cultivars, harvesting time, quality of grape cider, activity of yeasts or fermentation. The most abundant are alcohols, while specific esters are characteristic for overall aroma perception. Both compound groups are formed during fermentation. The distillation process is responsible for relative composition of volatile compounds in final product and consequently for characteristic perceived odour. Other specific aroma active compounds are extracted from wood during brandy maturation. Thus, chemical compounds that give a beverage its characteristic flavour can be used to classify the beverage based on geographical origin or used processing technology.

Various wine distillates are produced in Slovakia, but only 4 are made by classical technology and could be signed as brandy. They are Karpatske brandy special which can be produced only in Little Carpathian wine region, Frucon is produced in town Kosice from grapes harvested in eastern Slovakian wine region and Trencianske brandy special is produced in town Trencin located in middle part of Slovakia. The raw material used for production of this brandy is imported from other EU countries. Vinovica is produced also by classical technology and originated from Little Carpathian wine region the same as Karpatske Brandy Special, but ageing time is not long enough to classify it as brandy. Other studied wine distillates were prepared by other technologies and include two products from Little Carpathian region, Karpatske brandy and Pezignac that are characteristic by addition of honey.

Studied samples were analysed by hyphenated chromatographic that are able to provide powerful analytical methods and instrumentation in order to obtain detailed information about their chemical composition. GC-MS with various sample treatment methods (headspace, direct injection, solid phase microextraction and liquid liquid extraction) have been used to identify volatile organic compounds present in studied wine distillates on both major and trace levels. The aroma profile was investigated by gas

chromatography equipped with olfactometry detector. Finally, brandy samples were analysed by comprehensive two-dimensional gas chromatography with time of light mass spectrometry.

The aim of this work was to characterise brandy composition with various methods. Major goal of this work was to identify organic compounds presented in Slovakian brandies (produced by various technologies and in different geographical regions) that could be used like a potential markers of quality and issue.

2. Experimental
2.1 Samples

In this work, 6 different wine distillates have been studied. The samples can be divided into two major groups. The first group consists of brandies produced by classical technology that is wine distillate aged in wooden barrels for certain period of time. The second group contains wine distillates Pezignac and Karpatske brandy that can be considered as an imitation of classical brandy. These are produced as wine distillates diluted by ethanol from other sources and are characterized by presence of food additives like E150a "Plain caramel", brandy bonificator, honey.

Table 1 The list of studied samples.

Abbreviation	Sample	Producer	Ethanol [%]
KBS	Karpatske brandy special	Vitis Pezinok	40
VIN	Vinovica	Vitis Pezinok	40
PEZ	Pezignac	Vitis Pezinok	38
KB	Karpatske brandy	Vitis Pezinok	40
FRU	Frucon	Frucona Kosice	40
TBS	Trencianske brandy special	Old Herold Trencin	36

2.2 Preseparation techniques

Direct injection (DI): 1 μl of raw sample has been injected directly into GC.

Headspace(HS): 10 ml of sample was inserted into 25 ml head space vial and heated at 70°C for 15 min. A 500 μl of vapour sample was injected into gas chromatograph.

Solid phase microextraction (SPME): SPME fibres coated with polydimethylsiloxane (PDMS) of 100μm, polydimethylsiloxane/di-vinylbenzene (PDMS/DVB) of 65μm and carboxen/polydimethyl-siloxane (CAR/PDMS) of 75μm were used. The fibres were conditioned prior to use by heating in the injection port of the chromatographic system under the conditions recommended by the manufacturer for each fibre coating. All analyses were performed in 15 ml clear glass vials and the solutions were stirred with a PTFE-coated magnetic stir bars. Vials were sealed with hole-caps and PTFE/silicone septa. The temperature was controlled by Heidolph EKT 3001 system. The adsorption of organic compound from 5 ml of sample on SPME fibre took 20 min at 45°C. Desorption was performed in GC injector in splitless mode at 220 °C for 10 min.

Liquid-liquid extraction with Kuderna-Danish preconcen-tration (LLE): 50 ml of sample was extracted with four 12,5ml portions of dichloromethane and NaCl in separated funnel. Collected extracts were preconcentrated Kuderna-Danish distillation with a water bath constantly kept at 85°C.

2.3 GC-MS

Capillary GC was performed using Agilent Technologies 6890 gas chromatograph equipped with split-splitless and headspace injectors and Agilent Technologies 5973 mass

spectrometer. Helium with a flow rate 1 ml/min was used as carrier gas in all analyses. Both, liquid or gaseous samples have been injected into a 30 m DB-FFAP capillary column (30m x 0.25 mm I.D. x 0.25 µm film thickness) via split/splitless injector heated at 250°C. Splitless mode was used in all experiments. The temperature program was tuned for each sample preparation procedure depending on their specific requirements and expected composition of injected sample.

The Mass Spectrometry conditions were: EI ionisation, SCAN mode with a scan frequency 1,2 scan/s and a scan range 29-350 m/z in all experiments. Data handling was performed by means of Agilent Chemstation software. Identification of compounds was performed by comparison of obtained MS spectra with Wiley and NIST MS libraries. The compound was considered as identified, if quality match more than 95 % was reached.

2.4 Enantio-GC-MS

The samples were treated by SPME procedure described in GC-MS. A Perkin Elmer Clarius 500 GC-MS was used for chiral separations with 25 m x 0.25 mm I.D. capillary silica column coated with a 0.25 µm layer of permethylated β-cyclodextrin Chirasil-β-Dex. The GC column was initially programmed at 2°C/min from 40°C (10 min) to 170°C (10 min). Helium was used as the carrier gas at a constant flow of 1 mL/min. The fibre desorption was carried out at 220 °C for 10 min. The injector was operated in splitless mode. MS operated in electron impact ionization with electron energy of 70 eV. The transfer and ion source temperatures were set at 200°C and 230°C, respectively. Scan range was 40-300 mz and acquistion mode 2 scan/s. Data acquisition from the mass spectrometer was accomplished with the TurboMas ver.5.0.0 software. In all instances the volatile compounds in the samples were mainly identified by matching the obtained mass spectra with those provided by the Wiley and NIST libraries. Some peak identities were additionally confirmed by comparison with the mass spectrum and retention time data provided by the standards run under the same experimental conditions.

2.5 GCxGC

An SPME 70 µm carbowax/divinylbenzene StableFlex fibre (CAR/DVB) was used for the extraction of volatiles from the wine distillate. The fibre was conditioned according to manufacturer recommendations prior to use. 1,6 ml sample dilluted with 3,4 ml of water and NaCl were placed in 15 mL vial, and heated for 30 min at 50°C (water bath). Following the preliminary headspace equilibrium procedure, the SPME needle was inserted into the vial, and the fibre exposed to the headspace above the sample for 30 min at 50°C. After sampling, the fibre was thermally desorbed in the GC injection port for 10 min at 220°C.

GC×GC analysis was performed using an Agilent 6890GC coupled to a LECO Pegasus III time-of-flight mass spectrometer. LECO ChromaTOF software was used to evaluate the GC×GC–TOFMS system. Column set consisted of a chiral permethylated β-ChirasilDex (25m x 0,25mm x 0,25µm) first dimension coupled to a polar Supelcowax (2,5m x 0,1mm x 0,1 µm) second dimension placed in second oven with 10°C temperature offset above the main oven. Helium carrier gas at flow 1 ml/min was used for GC × GC–TOFMS analysis. The main GC oven was temperature programmed from 40°C (10 min) to 170°C at 2°C/min hold 10 min. The split/splitless GC injector (220°C) was operated in splitless mode for 10 min. Dual stage jet modulator was used with a modulation period 6s and temperature 30°C above the main oven temperature. The MS transfer line temperature was 220°C and the MS source temperature was 230°C. The TOFMS was operated at a storage rate of 100 Hz EI ionization mode (70eV) and data were collected over a mass range of 35-350 m/z. Total ion chromatograms (TIC) were processed using the automated

data processing software ChromTOF, with a signal-to-noise ratio of 50 and Wiley and NIST spectral libraries were used for peak identification.

2.6 GC-O

Gas chromatograph Hewlett-Packard HP 5890 series II equipped with FID detector and olfactory detector port Gerstel ODP 2 has been used for GC-O measurements. Helium with a flow rate 1,5 ml/min was used as carrier gas in all analyses. 1µl of raw sample has been injected through split/splitless injector heated at 250°C into a 30 m DB-FFAP capillary column with 0,25 mm I.D. and 0,25 µm film thickness. The column temperature was programmed from 35°C (1 min) with a gradient of 3°C/min to 230°C. For GC-O experiments, the effluent of the GC column is eluted to the sniffing port, where odor of individual compounds of aroma extract is detected by human nose. In the sniffing port humidified air (200 ml/min) is added. Olfactive detection was performed by seven panelists who have been chosen from 11 assessors trained in sensory evaluation.

3. Results and Discussion

In the first step, a direct injection of neat sample into the GC-MS was performed. The chromatogram obtained for sample KBS is shown in Fig.1A. It can be seen that from 21 peaks, which are present in the chromatogram at relatively high concentration levels, only 15 have been successfully identified. However, additional 99 peaks were present at trace level. Most from the identified peaks are linear or branched alcohols and carboxylic acids and their ethyl esters.

In headspace injection method, only volatile compounds present in wine distillates are evaporated and injected into the GC. In order to focus volatiles at the column head, a suitable initial low temperature of 35°C was set and held 1 min; then, at 2°C/min temperature increased to 100°C, held 5 min, and at 10°C/min to 220°C. An operating temperature of 70°C and an equilibrium time 20 min were found as optimal headspace conditions. Fig.1B shows the GC-MS chromatogram obtained for sample KBS by a static headspace injection method. It can be seen, that chromatogram is cleaner and poorer on number of presented peaks compare to direct injection. Obviously, only compounds with highest concentration, such as acetaldehyde, ethanol, ethyl acetate, ethyl esters of carboxylic acids, linear and branched alcohols appeared on chromatogram. The average numbers of compounds presented on chromatograms for first group are 18.

SPME represents sorptive technique, which has been used as a sample treatment procedure for isolation of volatile compounds from wine distillates. During optimisation of working conditions, type of SPME fibres, sorption temperature and time have been studied in details. It was found, that the best results are achieved when PDMS or PDMS/DVB fibre is inserted into gaseous phase of sample heated at 40°C for 30 min. The chromatogram obtained for sample KBS using SPME fibre coated with 65 µm layer of PDMS/DVB is shown on Fig.1C. It is obvious that chromatogram contains significantly higher number of compounds compare to previous sample treatment methods. From all 186 peaks only 46 provided satisfactory quality match factor to be considered as identified. These compounds belong to different chemical classes such as organic acids, their various esters, linear and branched alcohols, furan and their derivatives. Also terpenes, like α-amorphene, murrolene, γ-cadinene, cadina-3,9-diene, α-curcumene, (-)-calamenene, 6-methyl α-ionone, β-damascenone and β-damascone were also successfully extracted. These compounds were not present in extracts obtained by other sample treatment procedures. Thus, this method can provide complementary qualitative and quantitative information about terpenes and sesquiterpenes present in wine distillates.

The last studied sample treatment procedure, LLE, allows to determine organic compounds which can be extracted by organic solvents. Various mixtures of organic

solvents for the extraction of volatiles from wine distillates have been described in literature, however, the most frequently used solvent is dichloromethane. Fig.1D shows chromatogram obtained for sample KBS using LLE followed by Kuderna-Danish distillation. More than 240 organic compounds have been found in wine distillates. Slight lower number of compounds (198) was found in sample VIN, which was not aged in wooden barrels. Identified organic compounds belong to different organic classes e.g. ethyl esters of carboxylic acids, linear and branched alcohols, aldehydes, carboxylic acids, furans and their derivatives or phenolic compounds.

Table 2 shows selected compounds obtained by SPME-GC-MS analyses that are unique for particular sample (potential markers of geographical origin). Their presence or absence in chromatogram indicates origin of raw material and place of production. Sample KBS could be described with presence of styrene and absence of rose oxide, 2-methylfuran or 4-terpineol. For VIN, the absence of anisole, hexyl ester of acetic acid or 1,3-dihydroxyacetone dimmer is typical. The presence of 1-phenylethyl acetate or phenylmethyl ester of acetic acid, while absenting components such as diethyl suberate, ethyl orthoformate, ethyl ester 3-methylbutanoic acid is characteristic for TBS. The unique compounds like β-damascenone, tartralin, sorbic acid or glycerol were found in FRU. In this sample missed β-farnesene, geranyl acetate and 2,3-dihydrofarnesol.
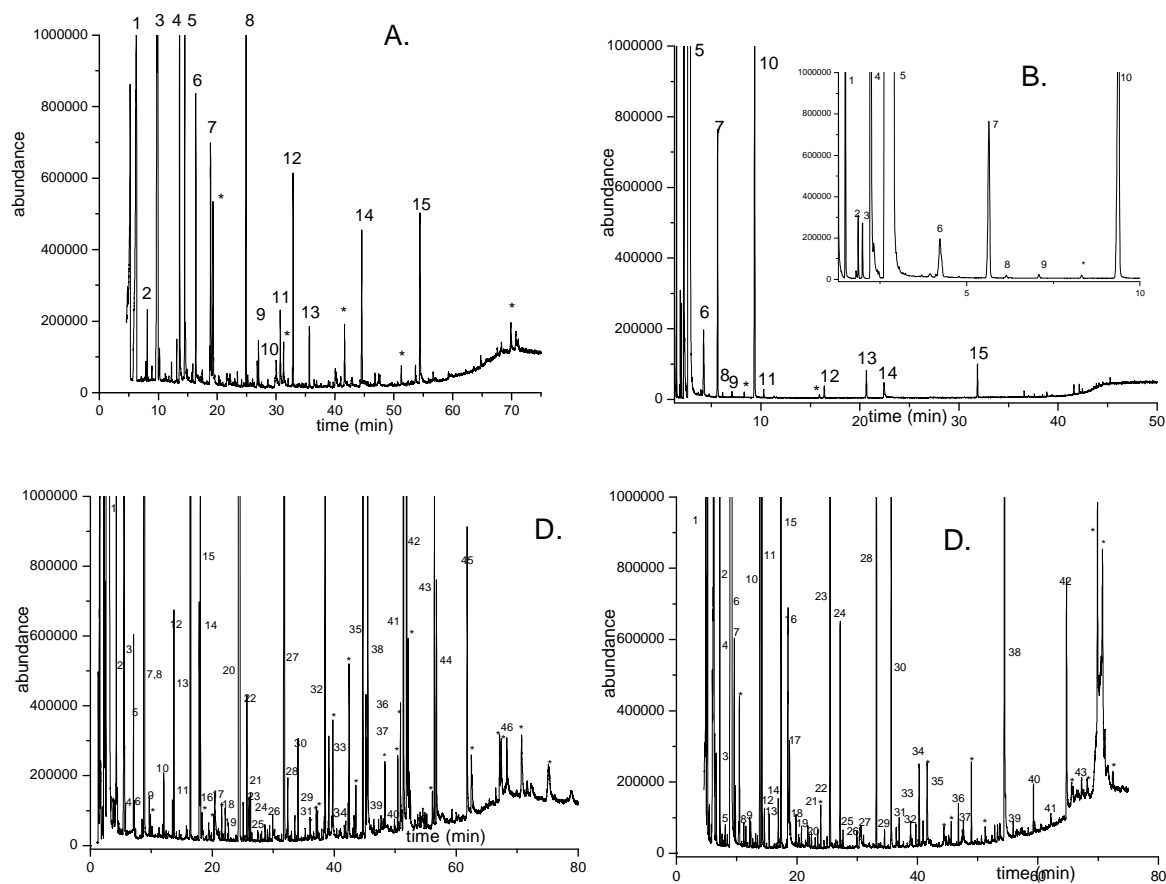
Fig.1 GC-MS chromatograms obtained for sample KBS by (A) direct injection, (B) headspace, (C) SPME and (D) LLE in dichloromethane.

15

Table 2 SPME-GC-MS analyses of wine distillates made by classical technology.

n.	compound	KBS	VIN	TBS	FRU
1	styrene	X			
2	2-methyl-furan		X	X	X
3	2-nonanone		X	X	X
4	4-terpineol		X	X	X
5	benzyl ester cinnamic acid		X	X	X
6	rose oxide		X	X	X
7	1.1-diethoxy-3-methyl-butane	X		X	X
8	1.3-dihydroxyacetone dimer	X		X	X
9	2.6-dihydro-3.5-dihydroxy-6-methyl-4H-pyran	X		X	X
10	5-(ethoxymethyl)-2-furancarboxaldehyde	X		X	X
11	anisole	X		X	X
12	ethyl 9-hexadecenoate	X		X	X
13	furfuryl formate	X		X	X
14	hexyl ester acetic acid	X		X	X
15	propyl ester octanoic acid	X		X	X
16	ethyl ester hydroxy-acetic acid		X		
17	3-methybutyl ester butanoic acid			X	
18	α-methyl-benzenemethanol acetate			X	
19	β-damascenone isomer I			X	
20	1-phenylethanol			X	
21	1-phenylethyl isobutyrate			X	
22	butyl 2-methylbutanoate			X	
23	phenylmethyl ester 3-methyl-butanoic acid			X	
24	phenylmethyl ester acetic acid			X	
25	1.2-cyclopentanedione	X	X		X
26	1.6-dimethyl-4-(1-methylethyl)-naphthalene	X	X		X
27	diethyl suberate	X	X		X
28	ethyl ester 3-ethoxy-propanoic acid	X	X		X
29	ethyl ester 3-methyl-butanoic acid	X	X		X
30	ethyl ester diethoxy-acetic acid	X	X		X
31	ethyl orthoformate	X	X		X
32	β-damascone isomers I, II				X
33	1.1-diethoxy-hexane				X
34	2.3-butanediol				X
35	butyl ester octanoic acid				X
36	ethyl ester 2.4-decadienoic acid				X
37	glycerin				X
38	sorbic acid				X
39	tatralin				X
40	β-damascenone isomer II	X	X	X	
41	2.3-dihydrofarnesol isomers I, II	X	X	X	
42	2-methylpropyl ester 2-hydroxy-benzoic acid	X	X	X	
43	geranyl acetate	X	X	X	
44	phenylmethyl ester 2-methyl-propanoic acid	X	X	X	
45	trans-β-farnesene	X	X	X	

The results obtained by LLE-GC-MS analyses of samples produced in Little Carpathian region are shown in Table 3. They are made from the same grapes, but produced by different procedure. KBS and VIN could be signed like brandy (they do not contain any additives), PEZ and KB are made from the raw wine distillate with ethanol dilution and addition of flavouring mixtures that enhance their sensory and taste properties. Similarly, also in this group an unique compounds that could be considered as markers of processing technology were identified.

Table 3 LLE-GC-MS analyses of samples from Little Carpathian wine region.

n.	compounds	KBS	VIN	KB	PEZ
1	(+/-)-diethyl ester hydroxybutanedioic acid	x	x		
2	1-(2-furanyl)-ethanone	x	x		
3	ethyl citrate	x	x		
4	ethyl ester 2-oxopropanoic acid	x	x		
5	ethyl ester 3-ethoxypropanoic acid	x	x		
6	1-phenylethyl ester 2-methylpropanoic acid			x	x
7	3-methyl-1-butanol acetate			x	x
8	3-phenyl-2-propenyl ester 2-methylpropanoic acid			x	x
9	isoamyl laurate			x	x
10	benzyl benzoate			x	x
11	butyl 2-methylbutanoate			x	x
12	(2,2-diethoxyethyl)-benzene	x		x	
13	(S)-3-ethyl-4-methylpentanol	x		x	
14	2-furancarboxylic acid hydrazide	x		x	
15	limonene	x		x	
16	2,5-furandicarboxaldehyde	x			
17	ethyl 3,3-diethoxypropionate	x			
18	ethyl vanilin		x		
19	2-furanmethanol	x		x	x
20	3-methyl-2-butanoic acid	x		x	x
21	ethyl ester 2-hydroxypropanoic acid	x		x	x
22	hexyl ester acetic acid	x		x	x
23	α-methylbenzenemethanol	x		x	x
24	2-methylpropyl ester 2-hydroxybenzoic acid			x	
25	2-methylpropyl ester 2-methylpropanoic acid			x	
26	butanoic acid	x	x		x
27	3-methylbutyl ester pentadecanoic acid	x	x	x	
28	3-methylbutylester methoxyacetic acid	x	x	x	
29	5-methyl-2-furancarboxaldehyde	x	x	x	
30	ethyl dl-2-hydroxycaproate	x	x	x	
31	ethyl ester butanoic acid	x	x	x	

Based on the previous results, where a lot of chiral compound were identified, next step of the brandy characterisation was chiral analysis. Chiral compounds are distributed in the nature with various enantiomer purities. Determination of enantiomer ratios could provide a very valuable tool for authenticity assesment. Samples were analysed with SPME on chiral column Chirasil-β-Dex. For selected chiral compounds were determinated enantiomer purities. For example limonene, this compound was not detected in FRU and TBS, in VIN and KBS was found with enantiomer excess 4,0% and 4,8%, respectively. The lowest percentage of 2-methylbutyl ester of octanoic acid was found in TBS (12,5%) and the highest value (15,6%) in VIN.

Comprehensive two-dimensional gas chromatography using chiral column in the first and polar column in the second dimension is a powerful tool for complete characterization of complex chiral mixtures such wine distillates. TOFMS detection enables full mass spectral library comparison and provides reliable identification of separated compounds. Thanks to increased separation power by GCxGC the quality of mass spetra is improved compared to one dimensional GC and therefore identification of compounds with similar spectra is easier. Selected chiral compounds were chosen for comparison of samples content. Each wine distillate provides different profile based on amounts of these selected compounds.

The determination of compounds that show real olfactive impact by GC-olfactometry (GC-O) provides beneficial information about compounds that are responsible for characteristic odor of given brandy. Among 200 organic compounds found

in all chromatograms only 71 have showed olfactive properties at given concentration level. The most of aroma active compounds eluted between 25-30 min and 37-45 min. The aroma descriptors found in samples by GC-O showed mostly fruity, alcoholic, caramel and smoked odor properties. The most of aroma active compounds have been found in sample FRU, while VIN showed their minimal content. The identified aroma compounds belong mostly to alcohols, lactones, furan derivatives and aldehydes. The 23 aroma active substances could not be identified, because their concentration was under detection limits of MS or FID detector, while still perceived by the panelists. On the other hand, in some cases the compound was found in chromatogram and identified by GC-MS, however it did not show positive olfactive perception at given concentration level.

4. Conclusion

Wine distillate samples treated by various sample preparation methods were analysed by GC-MS, enantio-GC-MS, enantio-GCxGC and GC-O. Each from these has some advantages and disadvantages and is suitable for another class of compounds. The most powerful GC separation method is without doubt comprehensive two-dimensional gas chromatography. The most suitable sample treatment procedure for GC analysis in terms of the number of extracted compounds is liquid-liquid extraction into CH_2Cl_2. By this method, more than 240 compounds have been extracted from wine distillates produced by classical technology. Furthermore, SPME has shown different selectivity, which allows to determine compounds that could not be extracted by other studied sample preparation methods.

Potential markers of geografical origin or technology procedure were found for each analysed sample. These compounds are very important for the authenticity assesment of an unknown sample.

Acknowledgements

DETERMINATION OF GALACTITOL AND GALACTOSE IN URINE FOR GALACTOSAEMIC SUBJECTS BY GAS CHROMATOGRAPHY – MASS SPECTROMETRY

<u>Beáta Meľuchová</u>[a], Eva Pavlíková[a], Žofia Krkošová[a], Róbert Kubinec[a], Helena Jurdáková[a], Jaroslav Blaško[a], Ivan Ostrovský[a], Jozef Višňovský[a], Darina Behúlová[b] and Jozefína Škodová[b]

[a] *Chemical Institute, Faculty of Natural Sciences, Comenius University, Mlynská dolina CH-2, SK-845 45 Bratislava, Slovakia*
[b] *Department of Laboratory Medicine, Comenius University Children`s Hospital, Limbová 1, SK-833 40 Bratislava, Slovakia*

Abstract

Galactosemia, a metabolic disorder associated with the intolerance to dietary galactose due to an inherited enzymatic deficiency, is indicated by heightened levels of galactose and galactitol in urine. Gas chromatography (GC) with mass spectrometry (MS) detection was evaluated for its ability to screen urinary carbohydrates, particularly galactose and galactitol. The described method uses trimethylsilyl derivates of galactitol and galactose, and needs 100 μl of urine for a single run. Spontaneous urine was obtained from 25 healthy subjects (classified into 5 age groups), from 4 treated patients with classical galactosaemia. The age dependences of galactose and galactitol excretion in urine was found in healthy subjects and treated galactosaemic patients by using reported method.

Recognizing the clinical need for the simultaneous measurement of galactitol and galactose in urine for galactosaemic subjects, we developed the new GC/MS method, permits for the first time, measurement in urine by an accurate and precise single step procedure. This method does not require urine pretreatment before the silylation.

Keywords

Galactose; Galactitol; Carbohydrates; Inherited metabolic disease; Galactosemia

1. Introduction

Metabolism is the sum of all the continuous biochemical reactions of breakdown and renewal of tissues of the body. Enzymes play an indispensable role in facilitating the process by serving as catalysts in the conversion of one chemical (metabolite) to another, often extracting the energy required for the reaction from a suitable high energy source, such as ATP.[1]

„Inborn metabolic disorders (IMDs)" is the term applied to genetic disorders caused by loss of function of an enzyme. Enzyme activity may be low or lacking for variety of reasons. Some IMDs produce relatively unimportant physical features or skeletal abnormalities. Others produce serious disease and even death. Most inborn errors of metabolism are monitored by routine blood or urine tests.[2]

Traditionally the IMDs are categorized as disorders of carbohydrate metabolism, amino acid metabolism, organic acid metabolism, or lysosomal storage diseases.[3]

Galactosemia was first "discovered" in 1908, when Von Ruess reported on a breast-fed infant with failure to thrive, enlargement of the liver and spleen, and "galactosuria" in publication entitled "Sugar Excretion in Infancy". This infant ceased to excrete galactose through the urine when milk products were removed from the diet. The toxic syndrome,

galactosemia, is associated with an intolerance to dietary galactose as a result of certain enzymatic deficiencies.[4]

Malfuctions in the following three enzymes, which participate in the normal metabolism of galactose (Fig.1), are known to be causes of galactosemia: galactose-1-phosphate uridyltransferase (GALT), galactokinase and uridine diphosphate-galactose-4-epimerase.[5,6] Inborn errors of metabolic result in defects in these enzymes that are categorized as Type I (classical, deficiency galactose-1-phosphate uridyltransferase), Type II (deficiency galactokinase) and Type III (deficiency uridine diphosphate-galactose-4-epimerase) galactose-mias, respectively.

Increased galactitol concentration is a common feature in GALT deficiency and has been implicated in galactosaemic cataract formation (Holton et al 2001). As conversion of galactose to galactitol by aldose reducatase representants a dead – end metabolic pathway (Weinstein and Segal 1968), galactitol removal is a confined to renal excretion. The recently observed age – dependent decrease of endogenous galactose formation in galactosaemic patients (Wendel *et al.* 2002).

Classical galactosemia (GALT deficiency), an autosomal recessive disorder occurs in the population with an incidence of approximately 1:40–60 000. Galactose-1-phosphate, a metabolite derived from ingestion of galactose, is considered to be toxic in several tissues particularly in the liver, brain and renal tubules.[7]

Galactose is a monosaccharide present in many polysaccharides, where the most clinically important source is the disaccharide lactose. Lactose is the predominant carbohydrate in human and most other animal milk, including cow's milk, therefore many commercially available infant formulas contain lactose.

Monosaccharide analysis by GC (with FID or MS detection) requires derivatization to increase their volatility and decrease interaction with the analytical system. The simplest and most rapid for routine analysis is silylation to procedure trimethylsilyl (TMS) derivates.[8] GC faced problems of multiple peaks due to the anomers of cyclic forms[9] and long reactions times and multiple steps sample preparation[10-12]. The multiple peak problems were as in the early studies of Sweeley *et al.*[13] prior to the derivatizationstep. Reduction to alditols have the advantage that each sugar generate only one peak, while trimethylsilyl (TMS) oximes give 2 peaks, but hydroxylamine reactions are more selective. Alditols preparation also include cation-exchange steps and boric acid removal[10], in the TMS-oxime preparation, all reactions are carried out in the same vial and consecutively.
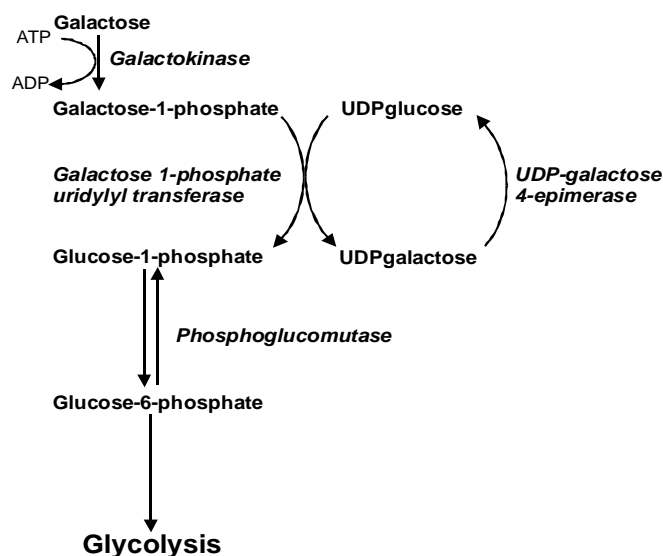
Fig.1 Major steps in the intermediary metabolism of galactose.

2. Experimental
2.1 Patients
Spontaneous urine was obtained from 25 healthy subjects (classified into 5 age groups), from 4 treated patients with classical galactosaemia.

2.2 Chemicals
All chemicals were of analytical reagent grade. Carbohydrate standards (D-glucose, D-fructose, D-mannitol) were purchased from Merck (Bratislava, Slovakia) and carbohydrate standards (D-galactose, D-galactitol) were purchased from CMS Chemicals (Bratislava, Slovakia). Derivatizations of carbohydrates were performed using hexamethyldisilane (HMDS) with trimethyl-chlorsilane (TMCS) and pyridine as catalyst, all supplied from Sigma Aldrich (St. Louis, MO, USA).

Urine samples were obtained from Department of Laboratory Medicine of Comenius University Children´s Hospital, Bratislava, Slovakia.

2.3 Sample preparation
Urine samples from patients were frozen immediately after collection and kept at – 20 °C until analyzed. 100 µl aliquots of each urine sample were taken and trimethylsilylated with 3 ml silylating reagent HMDS: TMCS: Pyridine in the volume ratio of 1: 1: 1 at 70 °C for 70 min. 1 µl portion of derivatized sample (model and sample solution) was injected to the chromatograph.

2.4 GC – MS analysis
The analysis was performed on 6890 N/5973 N GC–MS Agilent Technologies (USA) by electron ionization at 70 eV using an DB–Dioxin column 60 m x 250 µm x 0.25 µm (J&W Scientific, Folson, CA, USA). The injector was held at 300 °C and was operated in splitless mode. The purge flow of 9.5 ml min^{-1} was started 2 min after the sample injection. The initially column temperature was 90 °C, then the temperature was increased to 250 °C at rate of 10 °C.min^{-1}, and kept at the final temperature of 250 °C for 5 min. High purity helium was used as carrier gas with inlet pressure of 200 kPa. MS data were obtained in SIM-mode (m/z–73, 204, 205, 217, 319, 422, 435, 437). Transfer line temperature was 280 °C. Quadrupole conditions were follows: electron energy 70 eV and ion source temperature 230 °C.

Compound identification was performed by comparison with the chromatographic retention characteristics and mass spectra of authentic standards, reported mass spectra and mass spectral library of GC-MS data system. Compounds were quantified SIM peak area, and converted to compound mass using calibration curves of galactitol and galactose.

3. Results and discussion
Fig.2 shows typical GC-MS chromatogram of fructose, glucose, galactose, mannitol and galactitol TMS derivates obtained using silylation reagent (HMDS:TMCS:Pyridine 1:1:1). Chromatographic analysis can be accomplished in less than 16 min, without loss of resolution between critical pairs.
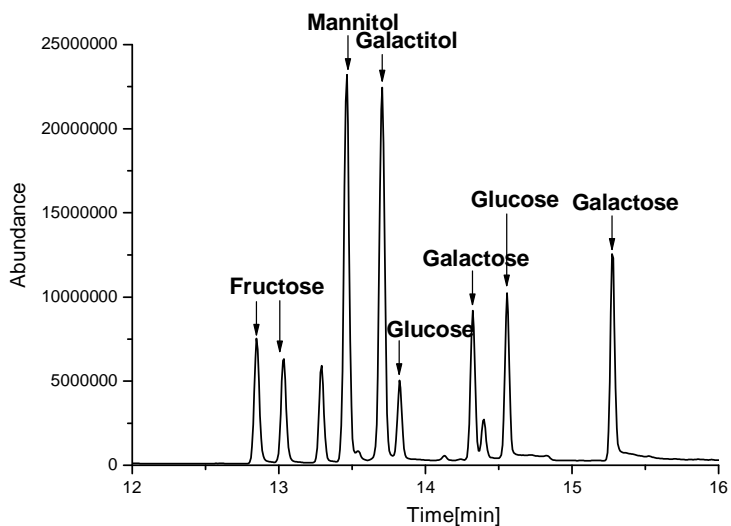
Fig.2 Total ion GC-MS chromatogram of TMS carbohydrate derivatives.
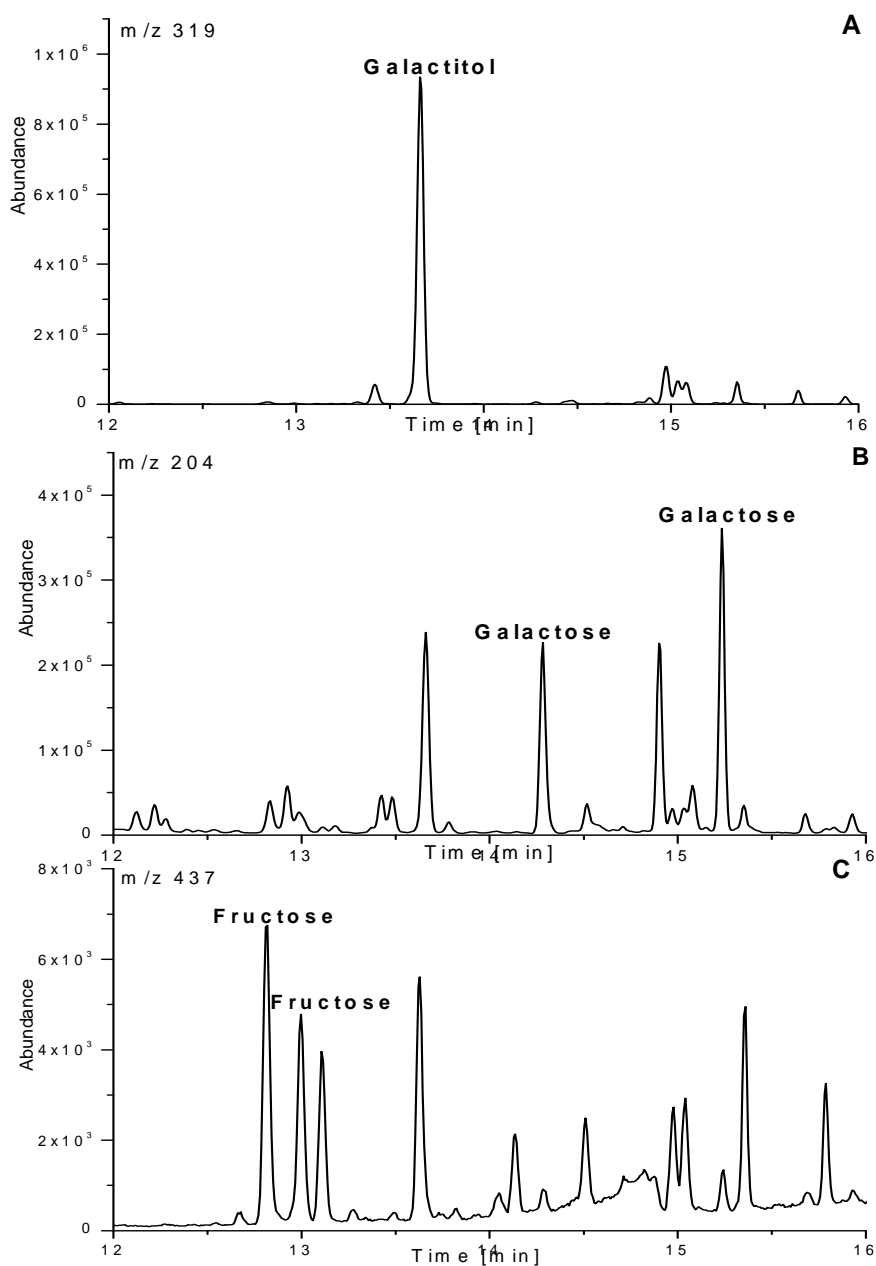
Fig.3 SIM GC-MS chromatograms of galactitol (A), galactose (B) and fructose (C) TMS-derivates of untreated patient.

Due to the α and β configurations of the OH group on pyrano-ring galactose and glucose yields two major GC peaks, whereas fructose produced three GC major peaks due to the α and β configurations of the OH group on pyrano- and furano-ring. These isomers are also present in urine samples and are commonly summed to report one value. The mass spectra of saccharide with the pyrano-ring (5C) are characterized by the fragment ion of *m/z* 204 (galactopyranose as trimehtylsilyl, Fig.3) and therewith the furano-ring (4C) are characterized by the *m/z* 437 fragment ion, whereas the fragmentation of alcohol saccharides (galactitol and mannitol) are yield the *m/z* 319 (galactitol as TMS, Fig.3).

These three fragments are used as key ions for identification of these two sugars as TMS derivatives.

3.1 Calibration

Calibration of galactitol and galactose as done in the range 1-1000 mg.l⁻¹, which encompass concentrations, known to exist in urine of healthy individuals. The calibrators were treated by the same procedure as described above.

Typical calibration curves of galactitol and galactose are shown in the Fig. 4.
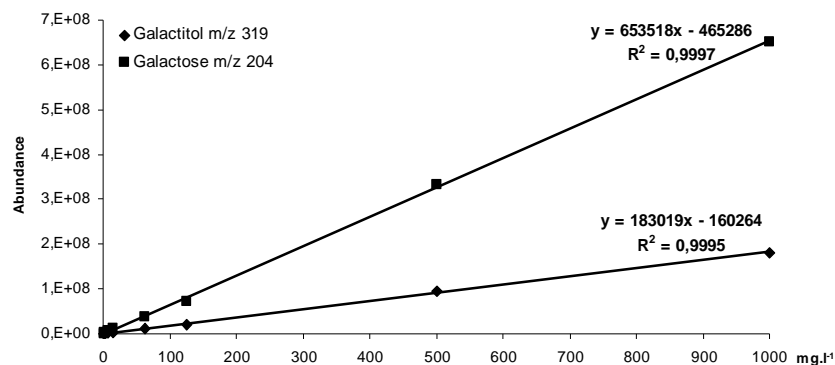
Fig.4 Calibration curves of galactitol and galactose.

Quantitation of galactose and galactitol in urine samples from 41 subjects was determined by application of the calibration curve.

The creatinine level of each sample was determined using the enzymatic method.

3.2 Repeatability

Repeatability of the proposed analytical procedure was assign by the relative standard deviation (RSD) of replicate measurements. The RSD values ranged from 3.61 to 9.74 %, and demonstrated reasonable repeatability of the method.

Table 1 The repeatability of the analytical procedure.

			1	2	3	4	5	Average	RSD [%]
28	**Galactitol**		240.5	227.9	213.9	206.9	228.6	223.6	5.9
	Galactose		29.8	30.4	25.9	24.9	27.6	27.7	8.5
29	**Galactitol**	**[mg.l⁻¹]**	31.1	37.5	29.9	31.4	35.3	33.0	9.7
	Galactose		69.6	72.4	66.5	70.3	65.4	68.8	4.2
30	**Galactitol**		142.0	159.6	163.9	149.1	157.9	154.5	5.7
	Galactose		3.2	3.2	3.5	3.2	3.2	3.3	3.6

3.3 Age dependence

Age dependence of urine concentration of galactitol corrected to creatinine content in healthy subjects is shown in Fig.5. The age dependences of urinary galactitol and galactose are very similar. Urinary galactose and galactitol excretion in controls is age dependent with highest concentrations at a younger age.

Age dependent experimental data were best fitted to a simple growth-related model assuming an exponential decrease with age until adulthood. Among number of growth-related model tested, the best fit was obtained using model

$$y = a.e^{\left(-x/b\right)} + c \, ,$$

where y is creatinine corrected concentration of galactitol or/and galactose, x is age in months, and a, b, c are model fit parameters.
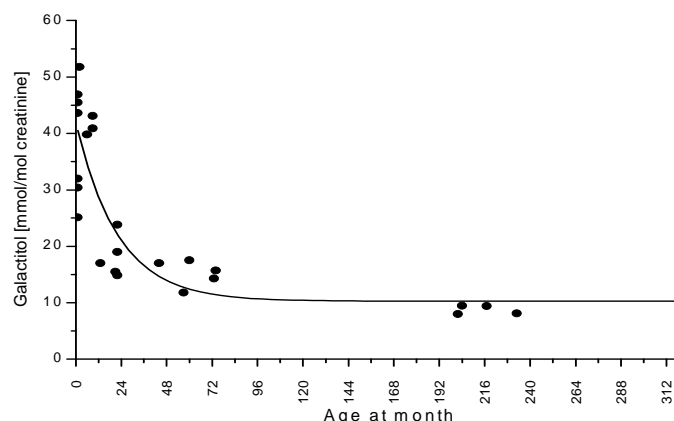
Fig.5 Age dependence of urinary excretion of galactitol in healthy subjects. Metabolite concentrations were calculated as concentrations corrected to creatinine content.

Fig.6 shows a chromatogram of urine from galactosaemic patient demonstrating the presence of the two metabolites. The peaks were identified by their fragmentation pattern and corresponding position of standards added to the urine.

Although the compounds are present in urine of healthy persons, the peak abundances in the chromatograms are much in samples of galactosaemia, which fact can serve as a new way of affected patients diagnosing and monitoring.
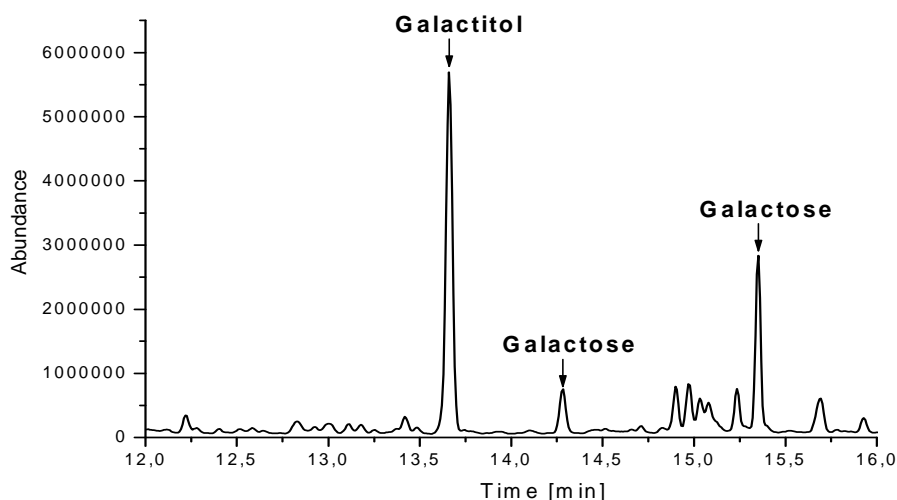
Fig.6 TIC GC – MS chromatogram of untreated galactosaemic patient.

The table 2 shows the galactose and galactitol concentrations for the samples of healthy subjects and treated galactosemic patients.

Table 2 The galactose and galactitol concentrations for the samples.

Sample	Galactitol	Galactose	Creatinine	Galactitol	Galactose	Age group
	[mg.l^{-1}]			[mmol.mol^{-1} creatinine]		[month]
1	8.6	136.2	1.1	43.6	688.0	
2	17.7	190.4	1.7	57.8	622.4	
3	14.1	26.2	1.2	65.5	121.4	0 - 1
4	8.2	12.9	1.0	45.5	71.6	
5	5.8	12.4	1.0	32.0	68.7	
6	19.4	35.6	2.3	46.9	85.9	
7	11.2	1.0	1.2	51.8	4.5	
8	10.3	16.4	1.4	40.9	65.0	1 - 12
9	33.0	28.7	4.6	39.8	34.7	
10	11.6	10.2	1.5	43.1	37.8	
11	19.8	28.5	7.1	15.5	22.3	
12	5.8	2.6	1.9	17.0	7.6	
13	32.2	36.3	7.5	23.8	26.9	12 - 24
14	14.2	27.2	5.3	14.9	28.5	
15	11.0	3.3	3.2	19.0	5.7	
28*	116.1	15.6	2.2	293.1	39.3	
16	7.2	17.1	2.3	17.5	41.3	
17	25.3	61.3	11.9	11.8	28.6	
18	19.5	31.6	7.6	14.3	23.1	
19	11.0	18.1	3.9	15.7	25.8	24 - 180
20	21.8	31.7	7.1	17.0	24.8	
29*	183.2	25.9	7.7	132.2	18.7	
30*1*	142.0	3.2	2.8	282	6	
21	12.9	25.5	7.4	9.6	19.1	
22	9.2	18.7	6.3	8.1	16.5	
23	26.6	41.4	18.4	8.0	12.5	180 and more
24	36.9	45.5	21.6	9.5	11.7	
25	35.7	59.7	21.0	9.4	15.8	
28*1*	240.5	29.8	10.2	131	16	

* - galactosaemic treated patients

4. Conclusion

Analysis of galactitol and galactose in spontaneous urine samples using a GC-MS analytical method was demonstrated here. The result of this study shows that GC-MS has potential to serve as a rapid, high throughput technique with low sample requirement for screening and monitoring of the metabolic disease galactosemia. The speed of analysis and the potential throughput are particularly appealing advantages of GC over the current techniques. Proposed GC-MS method requires a minimal volume for a reliable diagnosis (100 μl of urine for a single run). The study has proven that the analysis time can be dramatically shortened by direct one step silylation of the aqueous carbohydrate samples with mixture of HMDS, TCMS and pyridine.

These results indicate that GC-MS could serve as a more rapid and less costly alternative for carbohydrate screening and monitoring of urine for galactosuyemia diagnosis.

References

[1] Clarke J.T.R.: *Clinical Guide to Inherited Metabolic Diseases, Port Chester, Cambridge University Press, 2002*.

[2] Kavitha S.; Sarbadhikari S.N.; Ananth N.R.: *J. of Health and Allied Sciences **5** (3) (2006)*.

[3] http://en.wikipedia.org/wiki/Inborn-error-of-metabolism

[4] Schadewaldt J.; Killius S.; Kamalanathan L.; Hammen H.W.; Straβburger K.; Wendel U.: *J. Inherit. Metab. Dis. **26** (2003), 459–479*.

[5] Burtis C.A.; Ashwood E.R.: *Tietz Textbook of Clinical Chemistry, W. B. Saunders, Philadelphia, PA, 1999*.

[6] Eastly C. J. et al.: *J. Chromatogr. A **1004** (2003), 29-37*.

[7] Holton J.B.; Walter J.H.; Tyfield L.A. in: *The Metabolic and Molecular Bases of Inherited Diseases. Scriver C.R. et al. (Eds.), McGraw-Hill, New York, 2001, p. 1553*.

[8] Rojas-Escudero E. et al.: *J. Chromatogr. A **1027** (2004), 117 – 120*.

[9] Martinez-Castro; Paez M.I.; Sanz J.; Garcia-Raso J.; Sauracalixto F.; Garcia-Raso A.: *J. Chromatogr. **389** (1987), 9–20*.

[10] Bradbury A.G.W.; Halliday D.J.; Medcalf D.G.: *J. Chromatogr. **213** (1981), 146–150*.

[11] Molnár-Perl I.; Morvai M.: *J. Chromatogr. **520** (1990), 201–207*.

[12] Molnár-Perl I.; Morvai M.; Knausz D.: *J. Chromatogr. **552** (1991), 337–344*.

[13] Sweeley C.C.; Bentley R.; Makita M.; Wells W.W.: *J. Am. Chem. Society **85** (1963), 2497–2508*.

VARIATIONS IN FATTY ACID COMPOSITION OF PASTURE FODDER PLANTS AND CLA CONTENTS IN EWE MILK FAT ACCORDING TO SEASON

Eva Pavlíková[a], Beáta Meľuchová[a], Jaroslav Blaško[a], Róbert Kubinec[a], Jarmila Dubravská[b], Milan Margetín[c] and Ladislav Soják[a]

[a] *Chemical Institute, Faculty of Natural Sciences, Comenius University, Mlynská dolina, 84215 Bratislava, Slovak republic*
[b] *Grassland and Mountain Agriculture Research Institute, Mládežnícka 36, 97405 Banská Bystrica, Slovak republic*
[c] *Research Institute of Animal Production in Trenčianská Teplá, Hlohovská 2, 94992 Nitra, Slovak republic*

Abstract

The relations between fatty acids (FA) composition of pasture fodder plants and the content of conjugated linoleic acid (CLA) cis-9,trans-11 C18:2 in ewes´ milk fat during natural pasture season (April - September) were investigated. The extracts of ewes milk fat samples as well as the pasture samples were analysed for fatty acid composition by capillary gas chromatography- mass spectrometry (GC-MS). The content of α-linolenic, linoleic, and palmitic acids in pasture plants predominated and varied significantly during pasture season. The most abundant fatty acid compound in pasture plants was α-linolenic acid, its content decreased from 62 % to 39 % (of total FA) from May to August, and subsequently increased to the slightly lower value (56 %) from August to September, than that at the beginning of pasture season. Similarly the content of CLA in ewes´ milk decreased from 2.4 % in May to 1.3 % in August and subsequently increased to 2.6 % in September. The ratio of linoleic to α-linolenic acids in the pasture sample increased from 0.23 in May to 0.51 in August and subsequently decreased to 0.32 in September, thus to the ratio similar than that at the beginning of pasture season. The seasonal variations in this ratio in the pasture reversely correlated with the corresponding content of CLA in milk fat. The results confirm that the seasonal variations of CLA content in ewe milk fat are determined by seasonal variations in α-linolenic acid content in grass lipids.

Keywords

Botanical composition; Pasture fatty acid; Conjugated linoleic acid; Ewe milk

1. Introduction

An increasing interest in enhancing the conjugated linoleic acids (CLA) content in food products is connected with its potential anti-carcinogenic, anti-atherogenic, anti-diabetic, anti-obesity and immu-nomodulatory functions found in animal models. There are 14 possible CLA positional isomers counting from carbons 2,4- to carbons 15,17-C18:2. Each positional isomer has four geometric isomers cis,trans; trans,cis; cis,cis; and trans,trans for a total of 56 possible isomers. The double bond positions of CLA isomers actually identified in rumen milk fat range from 6,8- to 12,14-C18:2 in most of the possible geometrical configuration for a total of 20 isomers.[1] Recent reports suggest that each conjugated fatty acid isomer has different physiological functions.[2]

Conjugated linoleic acid occurs naturally in many foods, however, ruminant milk fat is the richest natural common source of CLA in foodstuffs. Cow milk fat contains approx. 0.6 % CLA of total fatty acids (FA), and concentrations of CLA in ewe milk was found to be around 1 % of total fatty acids.[3] The major cis-9,trans-11 C18:2 isomer, which is responsible for CLA anti-carcinogenic properties, growth promoting and antiatherogenic

properties, comprises about 75-90 % of total CLA in ruminant milk fat. Most studies of dairy products simply quantify the most prominent peak assigned to CLA as fatty acid methylesters (FAME) by gas chromatography (GC). This main peak includes also minor CLA isomers trans-7,cis-9 and trans-8,cis-10 C18:2. More detailed analysis of CLA isomers in milk fat allows high-resolution mass spectroscopy (MS) of 4,4-dimethyloxazoline (DMOX) derivatives and quanti-fication by Ag+-HPLC.[1]

The presence of CLA in milk fat from ruminants relates to the isomerization and biohydrogenation of unsaturated fatty acids by rumen bacteria as well as the Δ9-desaturase activity in the mammary gland. α-Linolenic (cis-9,cis-12,cis-15 C18:3) and linoleic (cis-9, cis-12 C18:2) acids are the predominant unsaturated fatty acids in forages. The cis-9,trans-11 CLA in milk fat is derived from linoleic acid and α-linolenic acid as a lipid substrate of fodder. Linoleic acid is first isomerized to the cis-9,trans-11 C18:2 by cis-12,trans-11 isomerase and then hydrogenated by Butyrivibrio fibrisolvens to trans-11 C18:1 (VA) in the rumen. These initial steps occur rapidly. The biohydrogenation of trans-11 C18:1 to stearic acid appears to involve a different group of organisms and occurs at a slow rate. For this reason, VA typically accumulates in the rumen. This main trans FA is responsible for the formation of the CLA isomer cis-9,trans-11, which occurs by desaturation (Δ9-desaturase) of the ruminally derived VA in the mammary gland. The pathway for the formation of the CLA cis-9,trans-11 from α-linolenic acid in the rumen involves an initial isomerization to a conjugated triene (cis-9,trans-11,cis-15 C18:3), followed by reduction of double bond at carbons 9, 15 and 11 to yield the trans-11,cis-15 C18:2, trans-11 C18:1 and C18:0 FAs, respectively, but not cis-9,trans-11 CLA, as intermediates.[4]

Variation in CLA content in milk of ruminants has been associated with several factors such as stage of lactation, parity and breed. However, diet is the most important factor influencing milk CLA concentration. The CLA concentration is higher in milk from animal fed pasture than those fed dry diets, and decreases with increasing growth stage of forage or maturity.[5] It was shown that abrupt change from indoor feeding (grass silage, hay and beets) to grazing cows on pasture increased cow milk fat CLA content up to 2.54 %, what is 550 % of the original level until, d 29.[6] This may be the time required for adaptation of the rumen microbes to the changing diet as well as the physiology of milk fat synthesis on the basis of type and quantity of FAs supplied through the diet. It was also shown that only 4d were needed to bring the milk fat CLA and VA contents back to their original level once the cows were withdrawn from pasture and put back on a similar total mixed rations (TMR) diet.

The seasonal changes in CLA and VA in milk fat are related to variations in pasture quality. Only few studies have investigated the relation of pasture plant species consumed by the ewes on their fatty acid composition of milk fat. Nudda *et al.* (2005) estimated that CLA concentration in ewe milk fat decreased as lactation progressed and noted that it is probably due to variation in pasture availability and fatty acid composition of grass lipids. The cis-9,trans-11 CLA content declined from 2.2 % to 1.14 % from March to June.

Highest contents of CLA (and VA) in milk were observed when ewes grazed fresh pastures. A possible explanation for CLA content can be found in the variation of animal diet during the survey period, particularly in the progressive variation of FAs profile as grass matured. The main fatty acid in grass lipids is α-linolenic acid that decreases, both in absolute and relative values, as grass matures. Such a decrease of α-linolenic acid could have resulted in a decrease of VA produced in the rumen by biohydrogenation and, consequently, in a reduction of CLA that is mostly synthesized in the mammary gland from VA by Δ9-desaturase. It is also possible that something in green grass enhances the growth of particular bacteria in the rumen that are responsible for producing CLA or blocks the final reduction of VA to C18:0.

Estimated daily intake of CLA in humans range in different countries from 0.015 to 1 g (Ref. *4,8*). These amounts are lower than those indicated to provide anticarcinogenic effect in laboratory animals. The greatest potential for increasing the CLA intake of humans is to consume high-CLA containing dairy products (milk and cheese). The procedures aimed to increase the main conjugated octadecadienoic acid cis-9,trans-11 isomer as well as content of α-linolenic acid in ewes´ milk fat under field conditions by dietary means are interesting. The composition of the fodder is very important, as already stated in previous investigations on grass, forage preservation, grass versus hay, silage versus hay and botanical composition of dry forage or pasture grass.[9,10] Milk and dairy products from pasture-fed animals are naturally enriched and have the higher content of CLA than those fed by TMR. The CLA-enriching effect of pasture has been attributed to the effects on biohydrogenation and the provision of α-linolenic acid as a lipid substrate for the formation of VA in the rumen and its subsequent desaturation to cis-9,trans-11 CLA in the mammary gland. The dietary substrates high in α-linolenic acid appear to facilitate establishment of rumen microflora that associated with the deposition of CLA in milk.

The aim of this work is to determine the CLA content of ewes´ milk as well as the corresponding content of α-linolenic and linoleic acids in pasture during the pasture season. The CLA content in milk is correlated with botanical families and individual plant pasture species to determine whether the CLA content of milk fat during season is affected by the variation of botanical composition of pasture, respectively which plants could be responsible for the occurrence of CLA in milk fat.

2. Materials and Instruments

The botanical composition of the pasture consumed by dairy sheep from April till September in the experimental farm of the Research Institute of Animal Production in Trenčianská Teplá (Midwest Slovakia) was determined. Botanical composition of a grassland sample from the farm of Liptovská Anna (North Slovakia) obtained in September was also analysed for comparison. The botanical families and main plant species of pasture samples were determined in the Grassland and Mountain Agriculture Research Institute in Banská Bystrica (Slovakia) by the method of projective dominants once a month.[11] Prepared four herbage samples: mean herbage sample, samples of dominant grasses, dominant legumes, and dominant herbs were analysed by GC-MS on the content of individual FAs.

A flock of 350 dairy ewes in the farm of Trenčianská Teplá was kept indoors and fed with TMR till middle of April. Subsequently, till middle of September the ewes grazing natural pastures. The average ewes´ milk samples, similarly as the pasture samples, were analyzed for fatty acid composition by GC-MS procedures.[1] The milk samples from the farm of Liptovská Anna obtained in September were also analysed for comparison.

Lipids from milk samples were extracted using chloroform- methanol mixture (2:1), obtained extracts were filtered through anhydrous sodium sulfate, then dried and stored under nitrogen at -18 °C. Lipids from dried plant samples were extracted using similar procedures.

GC-MS measurement of plant and milk extracts were performed on an Agilent Technologies 6890 N gas chromatograph with a 5973 Network mass- selective detector. Fatty acid methyl esters were separated using capillary column 60m x 0.25mm I.D. coated with a film thickness of 0.25 µm of DB-23 stationary phase (J&W Scientific) by programmed column temperature of 70-240 °C.

Identification of separated compounds was obtained on the basis of standard reference materials. Heptadecanoic acid was used as the internal standard for quantification. The quantified fatty acids in plant samples were: C10:0, C12:0, C14:0, C15:0, C16:0, C16:1, C18:0, C18:1, C18:2, C18:3, C20:0, C22:0, and C24:0. Similarly, in milk fat were analysed C4-C24 fatty acid methyl esters. The measured content of CLA in ewes´ milk fat is a total content of three CLA isomers cis-9,trans-11 + trans-7,cis-9 + trans-8,cis-10 C18:2, which are gas chromatographically unseparated.

3. Results and Discussion
3.1. Fatty acid composition of pasture plants

Significant differences were found in the composition of botanical families as well as of individual plant species during pasture season from April through September. The investigated pasture is composed of three botanical families: *Poaceae* (P), *Fabaceae* (F) and *Herbaceae* (H). The *Poaceae* was dominant botanical family in the pasture through pasture season. The variations of botanical families during pasture season for the average pasture samples as a percentage of total number of plant species are presented in Fig.1. From April to August, the content of *Poaceae* in average pasture sample increased from 52 % to 81 %, and in September it decreased to 60 %. The content of *Fabaceae* decreased from 20 % in April to 7 % in August, and increased to 30 % in September. The content of *Herbaceae* decreased from 28 % in April to 10 % in September.
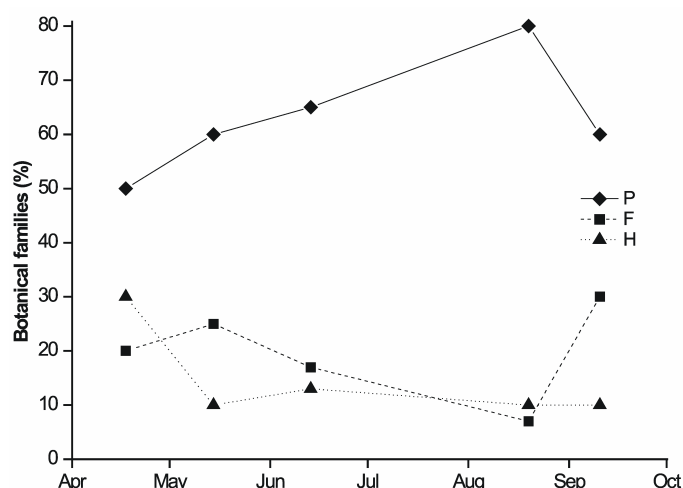
Fig.1 Variations in the content of botanical families as a percentage of total number of species during pasture season in average pasture samples. *P- Poaceae, F- Fabaceate, H- Herbaceae.*

Twenty seven plant species was identified in pasture, 12 species in April, 16 species in May, 15 species in June, 17 species in August and 12 species in September. There are the pasture seasonal variations in individual plants. In May, the most abundant plant species are *Bromus inermis* (P) 42 %, *Trifolium repens* (F) 26 % and *Festuca rubra* (P) 11 %. In August the most abundant species are *Festuca rubra* (P) 46 %, *Poa pratensis* (P) 16 % and *Bromus inermis* (P) 12 %. In September the most abundant plant species are *Dactylis glomerata* (P) 30 %, *Trifolium repens* (F) 18 % and *Trifolium pratense* (P) 12 %. This composition of pasture fodder plants is partially different from that published by Collomb *et al.* (2002) for the alpine lowlands (altitude 600-650 m a.s.l.), from major plants only *Trifolium repens*, *Dactylis glomerata* and *Trifolium pratense* were present in both pastures.

Fatty acid composition of plant species from pasture fodder were established by GC-MS. A total of 14 C10-C24 fatty acids were analysed in plant samples. α-Linolenic, linoleic and palmitic acids predominated in the lipids accounting from 75 % to 93 % of total fatty acids. α-Linolenic acid was the most abundant fatty acid in all analysed botanical species. Fig.2 presents the seasonal variations of α-linolenic acid as well as linoleic acid and palmitic acid in average pasture fodder plant samples. The content of α-linolenic acid significantly decreased from 62 % to 39 % from May to August, and subsequently significantly increased to 56 % from August to September. The content of α-linolenic acid in pasture at the end of pasture season is similar or slightly lower than that at the beginning of pasture season.
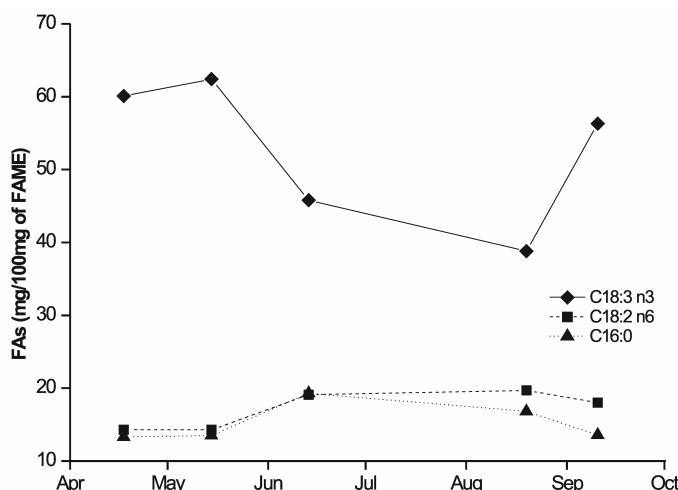
Fig.2 Variations in the content of α-linolenoic, linoleic and palmitic acids during pasture season in average pasture samples. *C18:3 n3- α-linolenoic acid, C18:2 n6- linoleic acid, C16:0- palmitic acid.*

The established contents of α-linolenic acid in pasture at the beginning and the end of pasture season are higher than published contents representing 48 % to 56 % of total fatty acids.[8] The content of linoleic acid in pasture increased from 14 % to 20 % from April to August, and subsequently moderate decreased to 18 % in September. There is inverse patter of these dependences for α-linolenic and linoleic acid at the beginning and the end of pasture season. The dominant saturated fatty acid in all of the investigated plant species was palmitic acid, and its content in average pasture sample increased from May (13 %) to June (19 %) and subsequently decreased from August to September (up to 14 %).

Seasonal variations in the content of α-linolenic acid in individual plant species are presented in Fig.3. The characteristic variations for individual plant species are quite similar, from May to August the content of α-linolenic acid decreased and subsequently to September increased. The except is *Festuca rubra* with increasing content of α-linolenic acid from 36 % in June to 42 % in August. This plant was only in small content (6 %) present in September pasture sample and for the content of α-linolenic was not analysed.
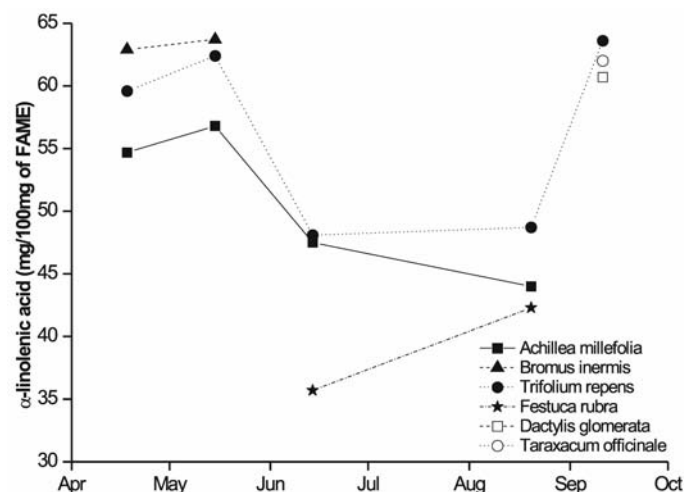
Fig.3 Variations in the content of α-linolenoic acid during pasture season in individual pasture plant species.

Seasonal variations in the content of linoleic acid of individual plant species are presented in Fig.4. Generally, the content of linoleic acid increased from May to June and subsequently to September decreased, except from *Festuca rubra*, which increased from 21 % in June to 25 % in August.
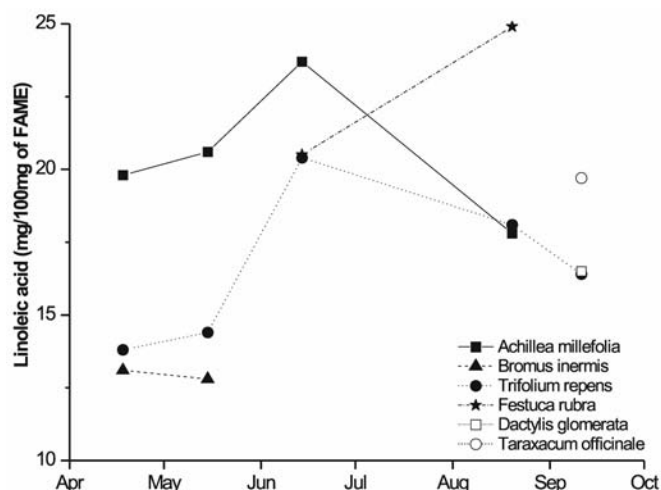
Fig.4 Variations in the content of linoleic acid during pasture season in individual pasture plant species.

With regard to the composition of fatty acid groups in average pasture fodder sample, the content of polyunsaturated FA during pasture season decreased from 74 % in April to 59 % in August, and subsequently increased to 74 % in September. Monounsaturated fatty acids during pasture season increased from 4 % in April, to 11 % in August, and subsequently decreased to 5 % in September. Saturated even fatty acids increased during pasture season from 18 % in April to 26 % in August, and subsequently decreased to 18 % in September. Saturated odd fatty acid increased during pasture season from 0.3 % in May to 2.6 % in August and subsequently decreased to 0.4 % in September.

The fat content in analyzed average samples of pasture plants increased from 3.4 % in April up to 3.8 % in June, decreased to 3.2 % in August, and subsequently increased to 4.2 % in September. This trend in plants fat content for the beginning and end of pasture season is similar to published in work of Dhiman *et al.* (2005).

3.2. Content of CLA in milk fat during pasture season

The CLA content in milk fat can be modified by feeding that influence the pattern of fat precursors that the mammary gland removes from blood for fat synthesis. The measured CLA values of ewes´ milk fat during pasture season from April to September are presented in Fig.5.

From May to the end of July the CLA content decreased from 2.4 % to 1.3 % (as a percent of total fatty acids) and subsequently increased to 2.6 % in the middle of September. For comparison, Nudda *et al.* (2005) published a monotony decreasing content of CLA during ewes´ pasture season from 2.2 % in March to 1.1 % in June. The decrease of CLA content through May- July may be due to decrease in forage quantity and quality as pasture plants mature from the vegetative to the reproductive stage. The increase of CLA content in milk fat from 1.3 % in the end of July to 2.6 % in mid-September is connected with a pasture regrowth including high content of *Dactylis glomerata* (30 %), which is characteristic by high content of α-linolenic acid (61 %). High content of α-linolenic acid in *Dactylis glomerata* was determined also by Clapham *et al.* (2005) before.
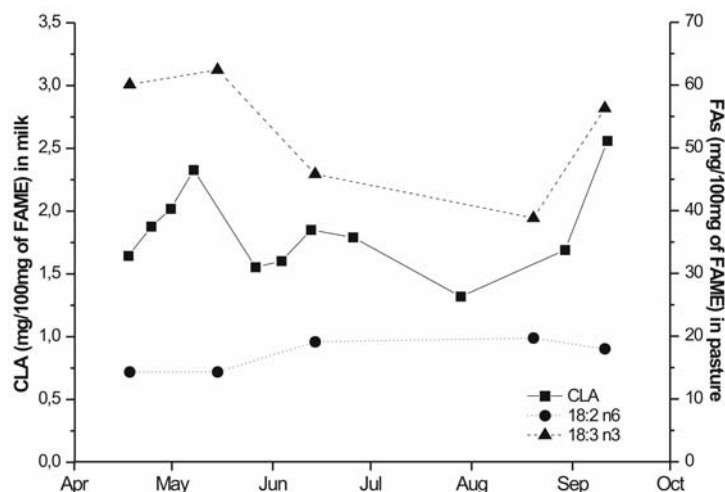
Fig.5 Variations in the content of CLA in ewe milk fat, and content of α-linolenoic and linoleic acids during pasture season in average pasture samples. *C18:3 n3- α-linolenoic acid, C18:2 n6- linoleic acid, C16:0- palmitic acid.*

Obtained data on variation of fatty acid composition in pasture during pasture season were compared with the corresponding content of CLA in milk fat of ewes, which were fed on the studied pasture. The determined contents of CLA in milk fat from April to September given in Fig.5 are compared with determined contents of α-linolenic and linoleic acids in pasture during pasture season. The content of CLA correlates positively with the content of α-linolenic acid in pasture, whereas the content of linoleic acid in pasture correlated inversely with the content of CLA in milk fat at the beginning and at the end of pasture season. Increased CLA fat content may be related to the ratio of linoleic to α-linolenic acids content in the pasture. The ratio of linoleic to α-linolenic acids in the average pasture sample increased from 0.23 in May to 0.51 in August and subsequently decreased to 0.32 in September, thus to the ratio similar than that at the beginning of pasture season. The seasonal variations of the ratio of linoleic to α-linolenic acids in the pasture reversely correlated with the corresponding content of CLA in milk fat. Follows, that the variation of CLA content during pasture season is substantially determined by the content of α-linolenic acid in pasture. It is in agreement with observation of Dhiman *et al.* (2000) that supplemental α-linolenic acid increased CLA concentration in cow milk when

the ratio of linoleic to α-linolenic acids in diet was 1:1 or less. Moreover, the high concentration of soluble fiber and fermentable sugars in fresh grass may create an environment in the rumen without lowering the ruminal pH that is favorable for the growth of the microbes responsible for CLA and VA production.[8]

Some deviations in CLA content from monotony of given dependence during season pasture in Fig.5, e.g. as the decrease of CLA values at the end of May, are connected with hydro-metheorological effects (dryness). They are more pronounced in the case of a shortage of fodder pasture, which was characteristic for studied pasture in summer-time. The highest content of CLA about 2.5 % in milk fat obtained at the beginning of May and in the middle of September is in agreement with corresponding highest content of α-linolenic acid in pasture in these months. This CLA content is comparable with published highest CLA content of ewes´ milk obtained by pasture feeding.

Very similar results on the FA composition of pasture fodder (60 % of α-linolenic acid) for corresponding CLA content in milk fat (2.6 %) were observed for another pasture site in North Slovakia (Liptovská Anna) measured in September. Altitude of pasture site at Trenčianská Teplá (280 m a.s.l) is quite different from that of in Liptovská Anna (950 m a.s.l.), nevertheless, the content of α-linolenic acid in both pastures as well as the content of CLA in milk fat in September is very similar. Thus, the CLA concentration of ewe milk fat does not depend on altitude in this altitude range of both pasture sites but on pasture feed characteristics. This is in agreement whith results obtained by Leiber *et al.* (2007).

4. Conclusions

The study demonstrated that during pasture season the content of α-linolenic, linoleic, and palmitic acids in pasture plants vary significantly. The measured data showed that the CLA content in ewes´ milk fat was primarily dependent on the α-linolenic acid content of pasture fodder plants. The CLA content in milk fat during pasture season from April to August decreased, and subsequently increased in September to the value similar to that at the beginning of pasture season. Analogical results were obtained for seasonal variation in α-linolenic acid content in pasture fodder plants. The seasonal variations of the ratio of linoleic to α-linolenic acids content in pasture reversely correlated with the content of CLA in milk fat. The results confirm that the seasonal variations of CLA content in ewe milk fat are determined by seasonal variations in α-linolenic acid content in pasture fodder plants.

Acknowledgements

References

[1] Kramer J.K.G.; Cruz-Hernandez C.; Deng Z.; Zhou J.; Jahreis G.; Dugan M.E.R.: *Am. J. Clin. Nutr.* **79** *(2004), 11375-11455.*
[2] Nagao K.; Yanagita T.: *J. Biosci. Bioeng.* **100** *(2005), 152-157.*
[3] Luna P.; Fontecha J.; Juárez M.; de la Fuente M.A.: *J. Dairy Res.* **72** *(2005), 415-424.*
[4] Collomb M.; Schmid A.; Sieber R.; Wechsler D.; Ryhänen E.L.: *Int. Dairy J.* **16** *(2006), 1347-1361.*

[5] Leiber F.; Bartl K.; Hochstrasser R.; Wettstein H.R.; Kreuzer M.: *Journal of Mountain Agriculture on the Balkans (2007), 162-167.*

[6] Khanal R.C.; Olson K.C.: *J. Nutr. 3 (2004), 82-98.*

[7] Nudda A.; McGuire M.A.; Battacone G.; Pulina G.: *J. Dairy Sci. 88 (2005), 1311-1319.*

[8] Dhiman T.R.; Nam S.H.; Ure A.L.:. *Crit. Rev. Food Sci. Nutr. 45 (2005), 463-482.*

[9] Morand-Fehr P.; Fedele V.; Decandia M.; Le Frileux Y.: *Small Rumin. Res. 68 (2007), 20-34.*

[10] Sanz Sampelayo M.R.; Chilliard Y.; Schmidely P.; Boza J.: *Small Rumin. Res. 68 (2007), 42-63.*

[11] Regal V.; Krajčovič V.: *Forage (in Czech), SZN, Praha, (1963), 466 pp.*

[12] Collomb M.; Bütikofer U.; Sieber R.; Jeangros B.; Bosset J.O.: *Int. Dairy J. 12 (2002), 661-666.*

[13] Clapham W.M.; Foster J.G.; Neel J.P.S.; Fedders J.M.: *J. Agric. Food Chem. 53 (2005), 10068-10073.*

[14] Dhiman T.R.; Satter L.D.; Pariza M.W.; Galli M.P.; Albright K.; Tolosa M.X.: *J. Dairy Sci. 83 (2000), 1016-1027.*

[15] Pulina G.; Nudda A.; Battacone G.; Cannas A.: *Anim. Feed Sci. Technol. 131 (2006), 255-291.*

TWO DIMENSIONAL GAS CHROMATOGRAPHY AS A TOOL FOR BIOSYNTHESIS STUDY OF THE COMPONENTS OF THE MARKING PHEROMONES OF THE MALES SPECIES *Bombus lucorum* AND *Bombus lapidarius*

Petr Žáček[a,b], Anna Luxová[a], Jiří Kindl[a] and Irena Valterová[a]

[a] *Academy of Sciences of the Czech Republic, Institute of Organic Chemistry and Biochemistry, Flemingovo náměstí 2, 166 10 Prague 6, Czech Republic: e-mail: griegzacek@seznam.cz*
[b] *Charles University, Faculty of Science, Albertov 8, 128 40 Prague 2, Czech Republic*

Abstract

Biosynthesis of the bumblebees males' marking pheromone of species *Bombus lucorum* and *Bombus lapidarius* was studied. Deuterated fatty acids were applied to the abdomen of the bumblebee's body. After a few days of incubation extracts of labial glands and fat bodies were analyzed. Two dimensional gas chromatography separation with MS detection technique has been optimised and used for analysis of the tissue. Decarboxylation, reduction, and esterification of applied labelled fatty acids have been found. Prolongation of deuterated precursor's carbon chain has been observed, too but no shortening.

Keywords
Comprehensive two dimensional gas chromatography; labial gland; fat body; Bombus lucorum, Bombus lapidarius; marking pheromone

1. Introduction

Bumblebees belong to the social species of insect similar to bees, ants, or termites. Communication by means of chemical compounds coordinates all aspect of their life in colony.

This study is focused on biosynthesis of the components of the male marking pheromones of species *Bombus lucorum* and *Bombus lapidarius*. Premating behavior of bumblebee males has been studied for long time mainly by Swedish authors[1,2]. Majority of bumblebee species exhibit a patrolling behaviour. They fly around the nest or maximally few hundred meters away from it and mark prominent objects in their territories (stones, leafs) with a pheromone secretion from the labial gland[3,4]. The marked places attract conspecific females for mating[5]. The composition of the secretion is species-specific[1]. The gland secretion of species *Bombus lucorum* contains mainly ethyl esters of fatty acids, chiefly 53% ethyl (Z)-tetradec-9-enoate (Ref. *6*) while main components of the labial gland secretion of *Bombus lapidarius* are hexadecan-1-ol (31%) and (Z)-tetradec-9-en-1-ol (52%). Biosynthesis of these components has been discussed[7]. It was suggested, that these compounds are produced from saturated fatty acids by means of specific enzymes. There are available some experimental data[8] from a recent time which show us first look on the biosynthetic pathways of the pheromone formation. Authors applied labelled $[^2H_{31}]$-hexadecanoic acid into the head capsule and abdomen of the bumblebee's body. After a certain time of incubation in living animals hexane extracts of dissected labial glands and fat bodies were analysed. GC/MS was used for analysis. In labial glands of species *B. lucorum* 2 metabolites of the applied compounds have been found: ethyl $[^2H_{31}]$-hexadecanoate and ethyl $[^2H_{29}]$-hexadec-9-enoate. Analysis of fat body showed that labelled compounds incorporated into the triacylglycerols (TAG) as acids. In case of species *B. lapidarius* there have also been found 2 metabolites in labial gland: $[^2H_{31}]$-hexadecan-1-ol and $[^2H_{29}]$-hexadec-9-en-1-ol. Similary to *B. lucorum* precursors

incorporated into TAG. No prolongation or shortening of deuterated carbon chain was found. This study follows the previous work, but it uses a new analytical tool for separation and identification of labelled compounds. Two dimensional gas chromatography with MS (TOF) detector (GC/GC-TOF) is a new method which is used for biosynthetic studies for the first time.

2. Experimental
2.1 Animals
The males of bumblebee species *B. lucorum* and *B. lapidarius* were obtained from laboratory colonies from cooperating laboratory in Faculty of Science of Masaryk University in Brno.

2.2 Chemicals
Compounds labelled by deuterium have been used: $[^2H_{27}]$-tetradecanoic acid (Aldrich), $[^2H_{31}]$-hexadecanoic acid (Aldrich), $[^2H_{35}]$-octadecanoic acid (Aldrich). For extractions of the tissue redistillated hexane purchased from Merck was used. The same hexane was used as a blank. <u>Application mixture</u>: 4 µg of labelled compound were dissolved in 100 µl of mixture of solvents: dimethylsulfoxide:ethanol:water 7:2:1. No mixtures of labelled precursors were done in this study.

2.3 Application/Dissection
All animals were approximately 2 days old when labelled compounds were applied. Application dose was 2 µl of the application mixture per animal and the solution was injected into the abdomen. Labial glands and the peripheral fat bodies (fat body) were dissected after 2 or 4 days of incubation. The dissected labial glands were extracted with hexane: 100µl per gland. All samples were stored in freezer (-30^oC) until their analyses. The dissected fat body was used for further treatment (Preparation of derivatives).

2.4 Preparation of Derivatives
The dissected fat body was dissolved with 100 µl of mixture (methanol:chloroform 1:1 + BHT (butylatedhydroxytoluene) as an antioxidant) then homogenized and next 100 µl of chloroform was added. Mixture was fractionated on precleaned glass thin layer chromatography plates (TLC) (75 x 59 mm, coated with Adsorbosil-Plus (Applied Science Labs), layer thickness 0.2 mm, added gypsum (12%)) using mixture hexane:diethylether:formic acid 80:20:1 as a mobile phase. Spots were visualized by spraying Rhodamine 6G solution (0.05% in ethanol). Three fractions were obtained: 1.: hydrocarbons ($R_f = 0.91$), 2.: triacylglycerols (TAG) ($R_f = 0.59$), 3.: mixture of mono and diacylglycerols ($R_f = 0.24$). Each of the fractions was extracted with approximately 0.5 ml of ether and cleaned on silica gel column. The cleaned extract was put over to the ampoule of known weight. Then the extract was dried by argon flow until there was no solvent. After that the ampoule was dried under vacuum until constant weight. Fractions of TAG and MAG + DAG were transesterified[9] and analysed as fatty acids methyl esters by GC/GC-TOF.

2.5 Chromatographic Analyses
All analyses were done using GC/GC-TOF-MS Pegasus 4D from LECO, Co. (USA). This system consists of gas chromatograph Agilent 6890N with split/splitless injector. Inside the GC oven a dual-stage jet modulator and the secondary oven were mounted. Resistively heated air was used as a medium for hot jets, while cold jets were supplied by gaseous nitrogen, secondary cooled by liquid nitrogen. Second part of this system was mass spectrometer with mass analyser Time Of Fly (TOF) LECO Pegasus III.

Separation parameters: Split (1/20); constant He column flow 1ml/min column, inlet temperature 250°C, injection volume 2 µl (1 µl sample + 1 µl hexane), modulation time: 3 s (hot pulse 0.6 s); modulation temperature offset: 30°C.

First dimension column: Length 30 m, ID 250 µm, film thickness 0.25 µm, phase DB-5 (J & W Scientific, USA). Temperature gradient was applied: 40°C (2 min), then 5°C/min to 320°C (5 min).

Second dimension column: length 1.79 m, ID 100 µm, film thickness 0.1 µm, phase BPX-50 (SGE, Australia). Temperature gradient was applied: 45°C (2 min), then 5°C/min to 325°C (5 min).

MS parameters: Electron ionisation mode (-70 eV), acquisition rate 150 Hz, mass range 29-500 amu, ion source temperature 220°C, transfer line temperature 250°C, detector voltage −1750 V. ChromaTOF software (LECO, Co.) was used for the processing of collected data.

2.6 Comprehensive Two Dimensional Gas Chromatography

Separation in this system is provided by two different separation mechanisms. After injection a sample comes to the first column, which is usually an ordinary nonpolar column of the same parameters as for one dimensional GC. Then the sample, already separated in first column, continues to the modulator. Zones of compounds are focused by means of timed cold and hot pulses there and injected to the second column (usually polar). This column is only a few meters long, more than two times thinner and situated in a second oven, which can be heated independently. This column is connected with MS detector with TOF mass analyser (Fig.1). The software reconstructs first dimension of separation by means of chromatographic data resulted from separation from secondary column and visualises the whole chromatogram as a contour plot or 3D visualisation (Fig.2). Main advantages of this system: 1) separation according two different mechanisms, 2) focusation of the chromatographic zones in cryogenic modulator – increasing sensitivity, 3) obtaining true baseline – more accurate quantification.

Biological aspect of this study the will not be discussed in this paper.
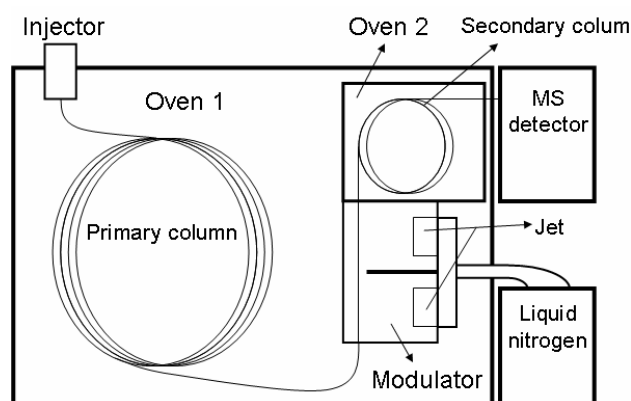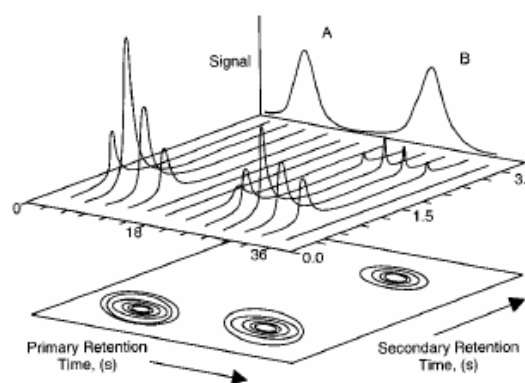
Fig.1 Schema GC/GC/MS.   **Fig.2** Data visualization.

3. Results and Discussion
3.1 Identification of the labelled compounds

Previous study[8] found in LG and fat body (TAG) metabolites which had the same length of carbon chain coming from the labelled acid only. Analysis by means GC/GC-TOF-MS found much more compounds isotopically labelled (Tables 1 and 2). However, only some of them could have been sprightly identified according their MS spectra. Full

identification of metabolites which have partly deuterated carbon chain will not be probably possible because it is very difficult to synthesise them in laboratory. In this case identification by way of two retention indexes and mass spectra must have been sufficient. Deuterated compounds are eluted from the first dimensional column (non-polar) slightly sooner then their non-deuterated (native) analogs. The same behaviour is observed in the second dimension (used polar column) (Fig.3).

Hydrocarbons: In both species deuterated hydrocarbons were observed: CD_3-$(CD_2)_n$-$(CH_2)_m$-CH_3 where n = 12 (precursor was $[^2H_{27}]$-tetradecanoic acid), n = 14 (precursor was $[^2H_{31}]$-hexadecanoic acid) or n = 16 (precursor was $[^2H_{35}]$-octadecanoic acid) and m = 1,3,5,7,9,11,..-this number depends on incorporation of deuterium to the bumblebee organism and concentration of the extract. The most abundant are C23 and C25 hydrocarbons in both species. But their relative response in comparison to response of all compounds in the sample was approximately 0.01 %. Molecular ion could have been observed very rarely. Typical fragments for deuterated compounds in MS spectrum are m/z = 46 and 50 ($[C_3D_5]^+$, $[C_3D_7]^+$, respectively. These fragments are analogs of m/z = 41 and 43 in native hydrocarbons. Pattern of the spectrum is similar but in deuterated hydrocarbons abundance of fragment 46 is higher or comparable to 50. The same situation is in case of unsaturated hydrocarbons. Branched carbon chains do not appear in the tissue. Spectrum became quite difficult if the hydrocarbons were partly deuterated and partly non-deuterated. Then the final spectrum is a mixture of both. Then the identification by means in comparison of retention behaviour of native and partly deuterated compounds is sufficient. All compounds appeared in the analysed material consisted of long carbon chain (10-30C) with a functional group in position 1. It means that in the mass spectrum fragments similar to hydrocarbons, especially fragments 46 and 50 arise. If they both appeared in the spectrum there was no doubt that the compound originated from applied deuterated compounds.

Alcohols: Acid group in labelled acid is reduced to alcohol group, which means that methyl groups next to the hydroxyl contain hydrogens: CD_3-$(CD_2)_m$-$(CH_2)_n$-OH, (m = 12 and n = 1) if $[^2H_{27}]$-tetradecanoic acid is applied and (m = 14 and n = 2) if $[^2H_{31}]$-hexadecanoic acid is applied. Molecular ion was not observed because alcohols loose DOH by deuterium rearrangement, so mass $[M-19]^+$ was observed. Typical fragment of native primary alcohols is m/z = 31 $[CH_2=O^+H]$, if deuterated m/z = 34. Secondary and tertiary alcohols do not appear in analyzed material. This fragment appeared in spectrum but it was not as intensive as in the native analog. Next typical fragment in deuterated alcohols (saturated and unsaturated) m/z = 62 $[CD_3$-CD=CD-$C^+D_2]$, which comes from m/z = 55. Fragments 46 and 50 are also very abundant.

Esters: Esters found in the analysed samples had general formula as follows: CD_3-$(CD_2)_l$-$(CH_2)_m$-COO-$(CH_2)_n$-CH_3 (Tables 1 and 2). In cases of (MAG + DAG) and TAG the methyl group arises from transesterification of the proper glycerides. In LG extracts the ethyl group was connected by enzymatic system of the animal.

Identification of esters is very easy. There are 2 very important fragments. One comes from McLafferty rearrangement of γ hydrogen: $[CX_2=C(O^+H)$-OR], X = D if the ester came from labelled acid which was prolonged by 2 or more carbons. R can be methyl or ethyl group. Second fragment arises from γ bond splitting. The exact mechanism is still unknown. The fragment is formally represented by formula $[CX_2$-$CX_2=C(O)$-OR$]^+$. If the ester was saturated intensities of these two fragments were far the most intensive in the

spectrum. In unsaturated ester their intensities were comparable with abundances of fragments 46 and 50. Molecular ion was usually observed.

For deuterated metabolites found in the tissue see Tables 1 and 2.

Table 1 Deuterated compounds found in *B. lucorum* species.

B. lucorum	**Deuterated metabolites**		
	Labial gland	Fat body	
Applied acid		MAG + DAG	TAG
[$^2H_{27}$]-tetradecanoic acid CD_3-$(CD_2)_{12}$-COOH 8 animals	E.[d] tetradecanoate, E.[d] tetradecenoate[a,e] CD_3-$(CD_2)_{12}$-COO-CH_3 Hexadecanol CD_3-$(CD_2)_{12}$-$(CH_2)_3$-OH Hydrocarbons[a,b] CD_3-$(CD_2)_{16}$-(CH_2)n-CH_3	M.[c] tetradecanoate CD_3-$(CD_2)_{12}$-COO-CH_3 M.[c] hexadecanoate CD_3-$(CD_2)_{12}$-$(CH_2)_2$-COO-CH_3 M.[c] octadecanoate CD_3-$(CD_2)_{12}$-$(CH_2)_4$-COO-CH_3	M.[c] tetradecanoate CD_3-$(CD_2)_{12}$-COO-CH_3 M.[c] hexadecanoate CD_3-$(CD_2)_{12}$-$(CH_2)_2$-COO-CH_3 M.[c] octadecanoate CD_3-$(CD_2)_{12}$-$(CH_2)_4$-COO-CH_3

Table 2 Deuterated compounds found in *B. lapidarius* species.

B. lapidarius	**Deuterated metabolites**		
	Labial gland	Fat body	
Applied acid		MAG + DAG	TAG
[$^2H_{27}$]-tetradecanoic acid CD_3-$(CD_2)_{12}$-COOH 12 animals	Hexadecanol, Hexadecenol[a] CD_3-$(CD_2)_{14}$-$(CH_2)_3$-OH Hydrocarbons[a,b] CD_3-$(CD_2)_{14}$-(CH_2)n-CH_3	M.[c] tetradecanoate CD_3-$(CD_2)_{12}$-COO-CH_3 M.[c] hexadecanoate CD_3-$(CD_2)_{12}$-$(CH_2)_2$-COO-CH_3	M.[c] tetradecanoate CD_3-$(CD_2)_{12}$-COO-CH_3 M.[c] hexadecanoate, M.[c] hexadecenoate[a] CD_3-$(CD_2)_{12}$-$(CH_2)_2$-COO-CH_3
[$^2H_{31}$]-hexadecanoic acid CD_3-$(CD_2)_{14}$-COOH 11 animals	Hexadecanol, Hexadecenol[a] CD_3-$(CD_2)_{16}$-CH_2-OH Hydrocarbons[a,b] CD_3-$(CD_2)_{16}$-(CH_2)n-CH_3	M.[c] hexadecanoate CD_3-$(CD_2)_{12}$-$(CH_2)_2$-COO-CH_3	M.[c] hexadecanoate, M.[c] hexadecenoate[a] CD_3-$(CD_2)_{14}$-COO-CH_3
[$^2H_{35}$]-octadecanoic acid CD_3-$(CD_2)_{16}$-COOH 26 animals	Hydrocarbons[a,b] CD_3-$(CD_2)_{16}$-(CH_2)n-CH_3	M.[c] octadecanoate, CD_3-$(CD_2)_{16}$-COO-CH_3	M.[c] octadecanoate, M.[c] octadecenoate[a] CD_3-$(CD_2)_{16}$-COO-CH_3

[a] *Position of the double bond was not determined*, [b] *Odd carbon number only (C23 and C25 were most abundant)*, [c] *Methyl*, [d] *Ethyl*, [e] *Two isomers with different position of double bond were observed.*
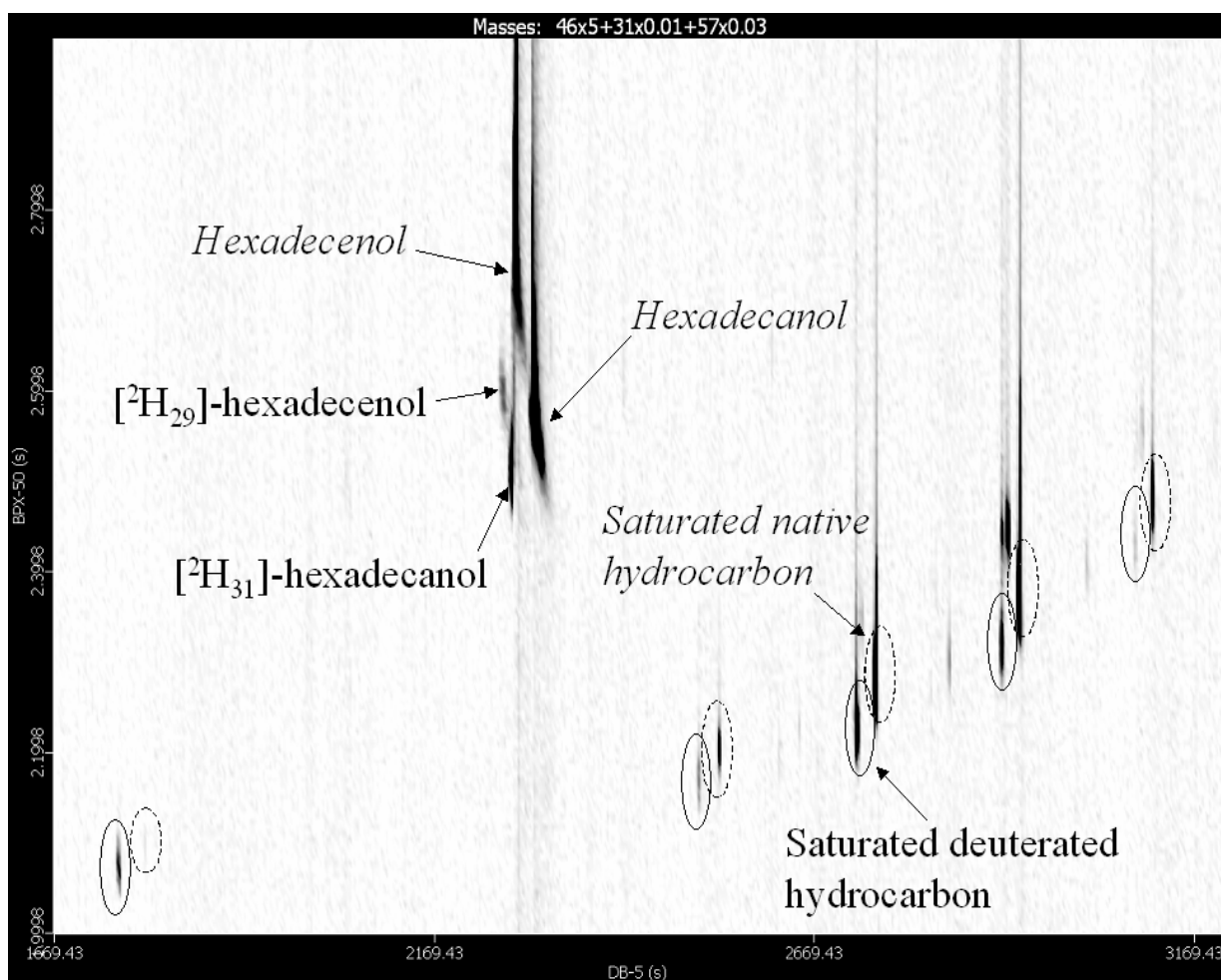
Fig.3 Chromatogram of the hexan extract of the labial gland species *B. lapidarius* ([^{2}H$_{31}$]-hexadecanoic acid was applicated).

4. Conclusions

Deuterated compounds were found in the all types of tissue except of hydrocarbon fraction from fat body (Tables 1 and 2). Quantification has not been done yet, but correlation between abundance of native compounds and their deuterated analogs was observed. Prolongation of deuterated precursor's carbon chain has been observed. No deuterated metabolites with shorter carbon chain than the applied precursor have been observed.

References

[1] Bergström G.; Svensson B.G.; Appelgren M.; Groth I.: *Academic Press, London and New York **Vol. 19** (1981), p. 175.*

[2] Kullenberg B.; Bergström G.; Ställberg-Stenhagen S.: *Acta Chem. Scand. **24** (1970), 1481.*

[3] Morse D.H.: *Social Insect (H.R. Hermann, Ed.), Academic Press, New York. **Vol. III** (1982), p. 245.*

[4] Bergström G.; Kullenberg B.; Bringer B.; Carlberg B.; Cederberg B.: *Zoon Suppl. **1** (1973), 25.*

[5] Kullenberg B.: *Zoon Suppl. **1** (1973), 31.*

[6] Urbanová K.; Valterová I.; Hovorka O.; Kindl J.: *Eur J Entomol **98** (2001), 111-115.*

[7] Lanne B.S.; Bergström G.; Wassgren A.B.;Törnbäck B.: *Comp Biochem Physiol **88B** (1987), 631-636.*

[8] Luxová A.; Valterová I.; Stránský K.; Hovorka O.; Svatoš A.: *Chemecol **13** (2003), 81-87.*

[9] Stránský K.; Jursík T.: *Fett/Lipid **98** (1996), 65-67.*

SEPARATION OF DEFERIPRONE AND ITS IRON CHELATE USING CAPILLARY ELECTROPHORESIS

Eva Svobodová[a], Zuzana Bosáková[a], Pavel Coufal[a], Jasmina Novakovic[b]

[a] Charles University in Prague, Faculty of Science, Department of Analytical Chemistry, Albertov 2030, 128 43 Prague 2, Czech Republic; e-mail: svobod15@natur.cuni.cz
[b] University of Toronto, Faculty of Pharmacy, 144 College Street Toronto, Ontario, Canada M5S 3M2

Abstract

A CE method has been developed for separation and quantification of deferiprone and its iron chelate. Experimental conditions were selected to optimize the separation of studied analytes and minimize dissociation of the chelate. Electrophoretic measurements were carried out using two types of background electrolytes (borate buffer and tris(hydroxymethyl)aminomethane hydrochloride (TRIS-HCl)) of different pH values (7 – 10). The effect of the applied voltage (5 – 25 kV) and the addition of anionic surfactant (SDS) or chiral selectors (native and derivatized cyclodextrins) into the running electrolyte on the separation of deferiprone and its chelate was investigated. The best separation was achieved using 10 mM TRIS-HCl, pH 7.5 with 10 mM 2-hydroxypropyl-β-cyclodextrin within 13 min, at the wavelenght of 280 nm and the applied voltage of 10 kV. The optimized separation conditions were utilized for calibration of the free deferiprone and its iron-chelate.

Keywords

CZE; MEKC; separation; deferiprone; iron-chelate; cyclodextrin derivatives

1. Introduction

Capillary zone electrophoresis (CZE) and micellar electrokinetic chromatography (MEKC) are efficient separation techniques well established for the analysis of biologically active compounds[1-3]. Both methods can be used for analytical purposes as well as for pharmacological studies. The separation mechanism, orthogonal to high performance liquid chromatography (HPLC), is a promising tool to solve difficult analytical tasks.

Iron is a transitional metal, involved in redox processes and essential for life, but potentially toxic in excess. Iron, excessively absorbed from food or released from proteins, can participate in generation of toxic oxyradicals and in subsequent oxidative damage of biological molecules[4]. Excess iron can be removed by chelatation.

The deferiprone (1,2-dimethyl-3-hydroxypyrid-4(1H)-one), known as L1 or CP20 belongs to the group of effective iron chelators and is clinically used for iron removal in thalassemic patients. The iron-chelate (iron-deferiprone) complex contains one to three chelate rings (it depends on the pH value of environment) and iron is coordinated by two vicinal oxygen atoms. The chelator/chelate equilibrium is affected by a number of factors and can easily be disturbed during the separation processes[5-7].

The objective of this work is to find experimental conditions for separation of the free deferiprone and its iron complex (see Fig.1), simultaneously minimizing dissociation of the created chelate. The test complex $Fe(L1)_3$ is tightly bounded above pH = 7 (ref. *5*).
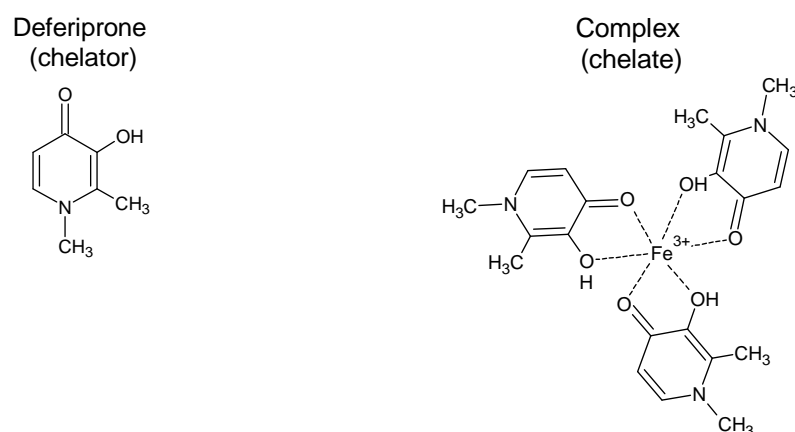
Fig.1 Structures of the studied analytes.

2. Experimental
2.1 Instrumentations

The CE measurements were carried out using a CE^{3D} electrophoretic instrument (Agilent Technologies, Waldbronn, Germany) with a diode array detector operated at 214 and 280 nm. An untreated fused-silica capillary (CACO s.r.o., Bratislava, Slovakia) of $L_D = 55.8$ cm, $L_C = 69.4$ cm, i.d. $= 75$ μm and o.d. $= 380$ μm was used. The separation voltage of 5 to 25 kV and the hydrodynamic sample injection at 2 kPa for 5 s were applied.

Between individual analyses, the capillary was washed with 1 M HCl for 5 min, deionized water for 2 min, 1 M NaOH for 5 min, deionized water for 2 min and finally with the background electrolyte for 5 min, all steps at 100 kPa.

2.2 Chemicals

The deferiprone (L1) was provided by ApoPharma Inc., Toronto, Canada. Iron(III) ($Fe(NO_3)_3$ p.a.) and $Na_2B_4O_7 \cdot 10\ H_2O$, p.a. were purchased from Lachema (Brno, Czech Republic); NaOH (p.a.) and HCl (35%, p.a.) from Lach-Ner (Neratovice, Czech Republic). Tris(hydroxymethyl)aminomethane hydrochloride (TRIS-HCl) and sodium dodecylsulfate (SDS) were obtained from Merck (Darmstadt, Germany). Cyclodextrins (hydroxypropyl-β-cyclodextrin, sulfated β-cyclodextrin, γ-cyclodextrin and hydroxypropyl-γ-cyclodextrin,) were delivered by Fluka (Buchs, Switzerland). Deionized water was used in all experiments.

2.3 Preparations

Two types of the background buffers – 40 mM borate buffer, pH 6.9-10.0 and 10 mM TRIS-HCl, pH 7.5 – 9.0 – were used as constituents of background electrolyte (BGE). The buffer pH was adjusted with 1.0 M NaOH to the required value. The running buffer composed of 10 mM TRIS-HCl, pH 7.5 was combined with cyclodextrins in the BGE. The MEKC running electrolyte was prepared by mixing the 10 mM TRIS-HCl, pH 7.5 with 50 mM sodium dodecylsulfate (SDS).

For preparation of the iron-deferiprone complex, an 8 mM solution of deferiprone in 10 mM TRIS-HCl, pH 7.5 and a 2 mM solution of iron(III) in the same buffer were mixed together at a 1:1 volume ratio. After 30 min needed for completion of the reaction, the mixture contained the complex and the free ligand, both at the 1 mM concentration.

3. Results and Discussion
3.1 Optimization of the separation conditions

The type of buffer, its concentration and pH value used in background electrolytes as well as the presence of an organic modifier or other the BGE additives are the major

factors controlling the separation properties of BGE in CZE and MEKC. To find an appropriate separation system for the mixture of deferiprone and its iron chelate, two types of buffers of different pH values without or with the presence of BGE additives were studied. All the tested separation media are summarized in Table 1.

Table 1 Buffer components used for preparation of the CZE and MEKC background electrolytes of various pH values and voltages (V) applied.

Background electrolyte	pH	V (kV)
10 mM $Na_2B_4O_7 \cdot 10\,H_2O$	6.9	25
	7.6	25
	8.0	25
	8.5	25
	9.9	25
	9.9	20
	10.0	25
10 mM TRIS-HCl	7.5	10
	7.5	25
	8.2	25
	9.0	25
50 mM SDS in 10 mM TRIS-HCl	7.5	10
	7.5	15
	7.5	20
	7.5	25
10 mM hydroxypropyl-β-cyclodextrin in 10 mM TRIS-HCl	7.5	10
5 mM sulfated β-cyclodextrin in 10 mM TRIS-HCl	7.5	5
	7.5	10
10 mM γ-cyclodextrin in 10 mM TRIS-HCl	7.5	10
	7.5	5
10 mM 2-hydroxypropyl-γ-cyclodextrin in 10 mM TRIS-HCl	7.5	10

As the first choice, the 40 mM borate buffer was selected as the CZE running electrolyte. The effect of the buffer pH (6.9 – 10.0) on separation of the complex and the free ligand was studied. This composition of the BGE provided comigrations of both analytes and no separation was observed. Partial splits of peaks corresponding to the individual solutes appeared with increasing pH value of the borate buffer. This peak deformation could be caused by presence of different charged forms of deferiprone and iron-deferiprone complex. Therefore, the borate buffer was replaced by the 10 mM TRIS–HCl buffer that is more compatible with biological media and permits application of a higher voltage.

The effect of the buffer pH (7.5 – 9.0) and the separation voltage (10 – 25 kV) on migration of analytes in the TRIS – HCl buffer was studied. Under all tested conditions, mixture of the complex and the ligand (Fe(L1)$_3$/L1 (in a ratio of 0.5 mM/4.5 mM) migrated with the electroosmotic flow in one peak and was not separated (see Fig.2).
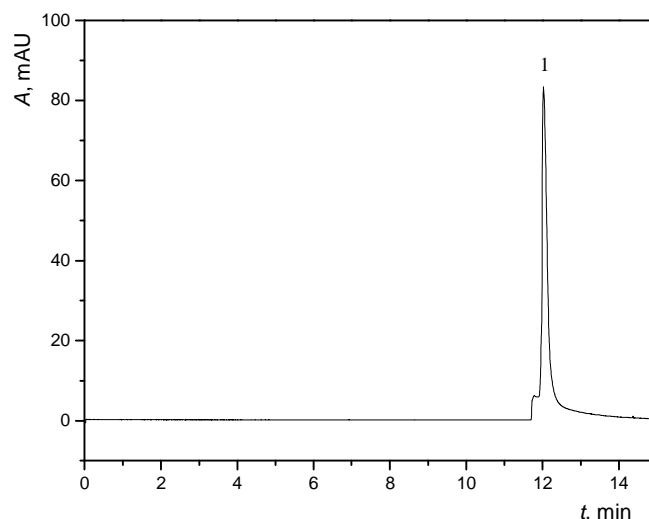
Fig.2 Electropherogram of the mixture Fe(L1)$_3$/L1 in ratio 0.5 mM/4.5 mM; *10 mM TRIS-HCl, pH 7.5, UV detection at 280 nm, injection 20 kPa for 5 s, voltage 10 kV, electrical current 5.5 μA.*

MEKC provides possibilities to separate charged analytes as well as neutral ones. The separation of neutral species requires addition of surfactants to the running buffer. SDS is the most common anionic surfactant which migrates toward the anode, that is obviously in opposite direction to the EOF. To improve the separation, the running buffer containing 10 mM TRIS-HCl, pH 7.5 with addition of 50 mM SDS (at various voltages applied) was tested for the separation of deferiprone and its iron complex. MEKC was shown to provide a poor separation of the studied analytes. A decrease in the applied voltage resulted in a negligible improvement of separation of the test compounds (see Fig.3).
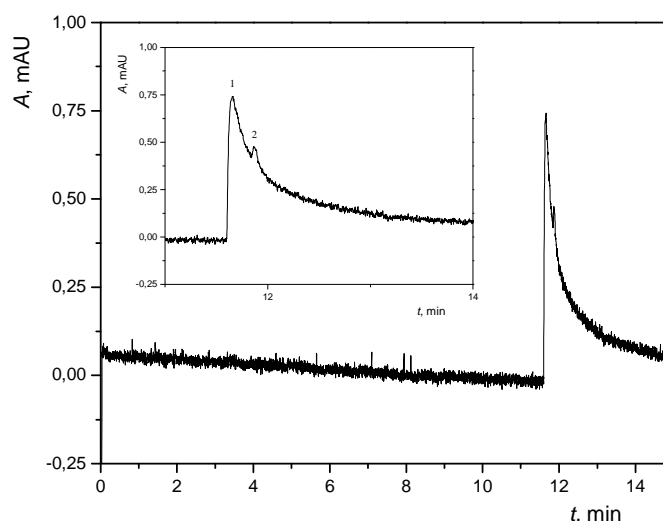
Fig.3 Electropherogram of the mixture Fe(L1)$_3$/L1 in ratio 0.5 mM/4.5 mM, (**1**) complex, (**2**) chelator; *50 mM SDS in 10 mM TRIS-HCl, pH 7.5, UV detection at 280 nm, injection 20 kPa for 5 s, voltage 10 kV, electrical current 12 μA.*

Cyclodextrins (CDs) are mostly used as chiral selectors in chiral separations. In some cases, (when steric arrangement plays an important role in separation mechanism) they were successfully used for non-chiral separations. Their selectivity results from inclusion of hydrophobic portion of the solute in the cavity and also from the hydrogen

bonding to the hydroxyl moieties. CD derivatives can provide alter selectivity and improve detection properties or solubilization. The additions of 5 mM sulfated β-cyclodextrin, 10 mM hydroxypropyl-β-cyclodextrin, 10 mM γ-cyclodextrin or 10 mM hydroxypropyl-γ-cyclodextrin into 10 mM TRIS-HCl, pH 7.5 was tested. In contrast to MEKC separation system, the use of CD derivatives as BGE constituents brought a noticeable improvement in the separation. Among all the tested separation systems, the best separation of the mixture chelate/chelator was achieved in the BGE containing 10 mM TRIS-HCl, pH 7.5 with 10 mM hydroxypropyl-γ-cyclodextrin (Fig.4).
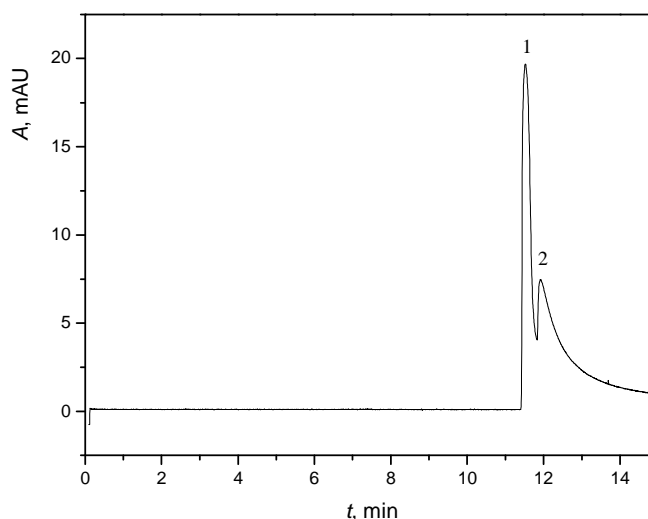
Fig.4 Electropherogram of the mixture Fe(L1)$_3$/L1 in ratio 0.5 mM/4.5 mM, (1) complex, (2) chelator;
10 mM 2-hydroxypropyl-γ-cyclodextrin in 10 mM TRIS-HCl, pH 7.5, UV detection at 280 nm, injection 20 kPa for 5 s, voltage 10 kV, electrical current 5.9 μA.

3.2 Calibration

The optimized separation conditions (10 mM 2-hydroxypropyl-γ-cyclodextrin in 10 mM TRIS-HCl, pH 7.5, 10 kV, injection 20 kPa for 5 s) were used for quantification of deferiprone and the iron-deferiprone complex. Calibration dependencies of the complex and the free ligand were determined within concentration intervals $5 \cdot 10^{-6}$ – $5 \cdot 10^{-4}$ mol·L^{-1} and $4 \cdot 10^{-4}$ – $4 \cdot 10^{-3}$ mol·L^{-1}, respectively. Measurements at all concentration levels were repeated four times ($n = 4$) and mean values of the peak area were subjected to linear regression. The regression coefficients of calibration equations are shown in Table 2:

Table 2 Regression coefficients of the calibration dependencies.

Analyte	Slope, k mAU·s·mol^{-1}·L	Intercept, q mAU·s	Correlation coefficient, r
Fe(L1)$_3$	68.98	48.87	0.9957
L1	137.96	-10.45	0.9763

4. Conclusion

The obtained results demonstrate that a partial separation of deferiprone and its iron-chelate and a sufficient sensitivity of the UV detection has been achieved only in the separation media containing derivatized cyclodextrins. The addition of 10 mM hydroxypropyl-γ-cyclodextrin into 10 mM TRIS-HCl, pH 7.5 has provided the best separation condition for Fe(L1)$_3$ and L1. The separation mechanism is probably based on a distinct interaction of L1 and sterically bulk Fe(L1)$_3$ with the cyclodextrin cavity. The

optimized separation conditions were utilized for calibration of the free deferiprone and its iron–chelate.

Influence of the temperature and the capillary deactivation on separation of the free deferiprone and its iron–chelate is still under investigation.

References

[1] Di Marco, V.B.; Dean, A.; Ferlin, M.G.; Yokel, R.A.; Li, H.; Venzo, A.; Bombi, G.G.: *Eur. J. Inorg. Chem. (2006), 1284-1293*.

[2] Merkofer, M.; Domazou, A.; Nauser, T.; Koppenol, W.H.: *Eur. J. Inorg. Chem. (2006), 671-675*.

[3] Novakovic, J.; Tesoro, A.; Thiessen, J.J.; Spino, M.: *Eur. J. Drug. Metab. Ph. 29 (4) (2004), 221-224*.

[4] Altomare, C.; Cellamare, S.; Summo, L.; Fossa, P.; Mosti, L.; Carotti, A.: *Bioorg. Med. Chem. 8 (2000), 909-916*.

[5] Pacáková, V.; Coufal, P.; Štulík, K.: *J. Chromatogr. A 834 (1999), 257-275*.

[6] Liu, D.Y.; Gosriwatana, I.; Liu, S.L.; Liu, Z.D.; Hider, R.C.: *J. Pharm. Pharmacol. 50 (1998), 126*.

[7] Blatný, P.; Kvasnička, F.; Kenndler, E.: *J. Chromatogr. A 757 (1997), 297-302*.

INFLUENCE OF POLYMERIZATION MIXTURE COMPOSITION ON MOLECULARLY IMPRINTED POLYMERS PROPERTIES PREPARED WITH 1--METHYL-2-PIPERIDINOETHYLESTER OF DECYLO-XYPHENYLCARBAMIC ACID AS A TEMPLATE

Miroslava Lachová[a], Jozef Lehotay[a], Ivan Skačáni[a] and Jozef Čižmárik[b]

[a] *Institute of Analytical Chemistry, Faculty of Chemical and Food Technology, Slovak University of Technology in Bratislava, Slovak Republic*
[b] *Department of Pharmaceutical Chemistry, Faculty of Pharmacy, Comenius University in Bratislava, Slovak Republic*

Abstract

Molecularly imprinted polymers (MIP) were synthesized and tested. 1-methyl-2-piperidinoethylester of 4-decyloxyphenylcarbamic acid was used as template for molecular imprinting. Monomers acrylamide, methacrylic acid and 4-vinylpiridine were used for MIP preparation. Methanol, acetonitrile and toluene were used as porogens. Non-imprinted blank polymers (NIP) were prepared for each MIP. These were used to study of nonspecific interaction between polymer and analyte. Prepared polymers were used as sorbents for solid-phase extraction (SPE). In this work the influence of polymerization mixture composition on polymer capacity and selectivity was studied.

Keywords

Molecularly imprinted polymers; Solid-phase extraction; HPLC; Phenylcarbamic acids

1. Introduction

Molecular imprinting (MI) is a technique used for the preparation of polymers with synthetic recognition sites having a predetermined selectivity for a specified analyte. The imprint is obtained by the polymerization of functional and crosslinking monomers in the presence of a template (target) molecule. The resultant imprints possess a steric (size and shape) and chemical (spatial arrangement of complementary functional groups) memory for the template molecule. Removal of the template from the polymer matrix creates vacant recognition sites that enable the polymer to selectively rebind the imprint molecule from a mixture of closely related compounds[1].

A technology, using selective solid phases based on MIPs in molecularly imprinted solid-phase extraction (MISPE), is an active area of research. Analytes can adsorb to MIPs via selective and non-selective adsorption. If the analyte associate with the MIP by ionic or hydrophobic interactions, then aqueous solutions of the analyte can be loaded directly. Subsequently, the non-selectively bound components can be removed by washing with organic solvent, and the analyte of interest, retained on the MIP, will switch from non-selective to selective binding[2]. MIP adsorbants have been used in pharmaceutical[3], environmental[4] and food analysis[5].

2. Experimental
2.1 Materials

1-methyl-2-piperidinoethylesters of alkoxyphenylcarbamic acids were synthesized on Pharmaceutical Faculty. Acetonitrile, methanol, toluene, methacrylic acid and diethylamine were purchased from Merck, 4-vinylpyridine was obtained from Aldrich,

acrylamide and azobisizobutylonithrile were obtained from Fluka, and acetic acid was purchased from Lachema.

2.2 HPLC analysis

An HP 1100 system (Hewlett-Packard, Germany), consisting of a pump with a degasser, a diode-array detector (DAD) a 20 μl injector and a HP ChemStation were used. Analyses were carried out on the analytical column Separon SGX C18 (125 x 4 mm, 7 μm) (Watrex, USA) at laboratory temperature. Mobile phase consisted of methanol, acetonitrile, acetic acid and diethylamine (80:20:0.1:0.2) at a flow rate of 0.5 ml/min. Izokratic elution was used. Diode-array detector worked in the range of 190 – 400 nm and the chromatograms were acquired at wavelength of 240 nm.

2.3 Polymer preparation

The molecularly imprinted polymer was prepared according to Zhang *et al´s* method. For synthesis of MIPs template (1-methyl-2-piperidinoethylester of decoxyphenylcarbamic acid) was used as hydrochloride and base, respectively. The base was used mainly for polymers prepared in acetonitrile and toluene because of better solubility of base template in these solvents. The composition of polymerization mixtures is shown in Table 1.

Table 1 Composition of polymers.

Polymer	Template	Porogene	Monomer
MIP1	Base	Methanol	Acrylamide
MIP2	Hydrochloride	Methanol	Acrylamide
NIP1,2	-	Methanol	Acrylamide
MIP3	Base	Acetonitrile	Acrylamide
NIP3	-	Acetonitrile	Acrylamide
MIP4	Base	Toluene	Acrylamide
NIP4	-	Toluene	Acrylamide
MIP5	Hydrochloride	Methanol	4-vinylpyridine
NIP5	-	Methanol	4-vinylpyridine
MIP6	Base	Acetonitrile	4-vinylpyridine
NIP6	-	Acetonitrile	4-vinylpyridine
MIP7	Base	Toluene	4-vinylpyridine
NIP7	-	Toluene	4-vinylpyridine
MIP8	Hydrochloride	Methanol	Methacrylic acid
MIP9	Base	Methanol	Methacrylic acid
NIP8,9	-	Methanol	Methacrylic acid
MIP10	Base	Acetonitrile	Methacrylic acid
NIP10	-	Acetonitrile	Methacrylic acid
MIP11	Base	Toluene	Methacrylic acid
NIP11	-	Toluene	Methacrylic acid

2.4 Evaluation of MIP

100 mg of each cartridge were packed in 3 ml polypropylene cartridges. The cartridges capacity was tested in methanol, acetonitrile, water and toluene. Prior to applying the solution of p-decoxy-phenylcarbamic acid, the polymer was pre-equilibrated with 5 ml of methanol and then with 5 ml of solvent in which the capacity was studied. Aliquots (1 ml) of analyte solution (0.5 μg/ml) were applied gradually onto the cartridge until release was detected. In the case of toluene, solution of analyte dissolved in toluene

was applied, the cartridge was dried, the adsorbed analyte was eluted by methanol - acetic acid mixture (95:5). Eluent was dried, resolved in methanol and measured by HPLC.

Selelectivity of MIP3, MIP 9, MIP10 and MIP11 for ester of p-methoxyphenylcarbamic acid and of o-decoxyphenylcarbamic was tested. Selectivity of MIP3 and MIP 11 in acetonitrile and of MIP9 and MIP10 in methanol was determined. The procedure was the same as described for ester of p-decoxyphenylcarbamic acid. The concentration of ester of p-methoxyphenylcarbamic acid and o-decoxyphenylcarbamic acid was 0.5 µg/ml.

3. Results and discussion

1-methyl-2-piperidinoethylesters of phenylcarbamic acids are potential anaestethics[7]. Basic chromatographic parameters are described in Renčová´s article[8].
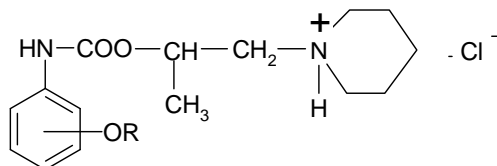
Fig.1 Structure of compounds used in research. R= -CH$_3$ and C$_{10}$H$_{21}$ in orto and para position.

3.1 Capacity of polymers

The resultant values of polymer capacities are shown in Table 2.

Table 2 Binding capacities of prepared polymers. *RSD = 4.5 – 13.5 %, n = 3.*

Polymer	Capacity (µg of analyte/100 mg of polymer)		
	Acetonitrile	Methanol	Toluene
MIP1	0.1	0	-
MIP2	0	0	-
NIP1,2	0.1	0.1	-
MIP3	2.5	0.5	-
NIP3	0.4	0.4	-
MIP4	0.7	0.1	1.2
NIP4	0.5	0	0.9
MIP5	0.2	0.1	-
NIP5	0.3	0	-
MIP6	0.5	0.2	-
NIP6	0.6	0	-
MIP7	0.7	0.1	0.4
NIP7	0.8	0.1	0.4
MIP8	3.8	2.0	-
MIP9	28.0	8.0	-
NIP8,9	4.0	1.9	-
MIP10	20.4	20.2	-
NIP10	10.7	5.9	-
MIP11	76.0	32.0	61.1
NIP11	9.7	6.2	6.6

The highest values of binding capacities were obtained using water for sample loading for MIPs and also for NIPs.The whole amount of loaded analyte was sorbed on the sorbents It means that nonselective sorption takes place. This allows to use water samples for extraction.

The capacity in methanol is low for polymers prepared with acrylamid and vinylpiridine, respectively. It can be caused by stronger interaction between methanol and analyte than between polymer and analyte. Methanol is polar solvent which cancel the hydrogen bonding between analyte and monomer. This speculation doesn´t fit for polymers

prepared with methacrylic acid as functional monomer. Polarity and functional groups of monomer propably play important role during polymerization.

Noticeable specific binding capacity can be observed for MIP3 in acetonitrile, (prepared from acrylamide in acetonitrile). High values of binding capacity were obtained on MIP9, MIP10 and MIP11 prepared with methacrylic acid as the functional monomer. It can be observed, that the less polar solvent the higher binding capacity.

3.2 Selectivity of MIPs

Selectivity of MIP3, MIP9, MIP10 and MIP11, respectively was tested. Influence of length of alkoxy- chain was tested using by ester of p-methoxyphenylcarbamic acid. The influence of position of alkoxy- chain was investigated by measuring of MIPs´ capacity for ester of o-decoxyphenylcarbamic acid. The polymer capacities of MIPs and relevant NIPs are shown in Table 3.

Table 3 Binding capacities of prepared polymers. *RSD = 4.5 – 9.1 %, n = 3.*

	Capacity (µg of analyte/100 mg of polymer)		
	Ester of p-decoxyphenylcarb. acid (template)	Ester of p-methoxyphenylcarb. acid	Ester of o-decoxyphenylcarb. acid
MIP3	2.5	1.3	1.9
NIP3	0.4	0.3	0.4
MIP9	8.0	9.2	4.8
NIP9	1.9	1.9	1.8
MIP10	20.2	18.1	10.2
NIP10	5.9	3.2	6.2
MIP11	76.0	75.1	76.2
NIP11	9.7	10.2	8,0

As it is obvious from Table 3, capacity of MIP3 is lower for analyte with shorter alkoxy- chain than for template. Therefore the length of alkoxy- chain impacts the capacity of analyte and MIP3 can recognize template molecule from structurally related compounds. In the case of MIPs prepared from methacrylic acid the influence of alkoxy chain length wasn´t established.

The influence of alkoxy chain position was also tested. The difference between capacity values of the template and the analyte with alkoxy chain in orto- position is not very leap. But in the case of MIP9 and MIP10, the capacity of MIPs is two times higher for template than for the analyte with alkoxy chain in orto- position.

References
[1] Poole C.F.: *TrAC 22 (6) (2003), 362-373.*
[2] Ensing K.; Majors R.E.: *LC-GC Europe (2002), 16-22.*
[3] Caro E., Marcé R.M.; Cormack P.A.G.; Sherrington D.C.; Borrull F.: *Anal. Chim. Acta 562 (2006), 145-151.*
[4] Moullec S.; Bégos A.; Pichon V.; Bellier B.: *J. Chromatogr. A 1108 (2006), 7-13.*
[5] Karasová G.; Lehotay J.; Sádecká J.; Skačáni I.; Lachová M.: *J. Sep. Sci. 28 (18) (2005), 2468-2476.*
[6] Zhang T.; Liu F.; Chen W.; Wang J.; Li K.: *Anal. Chim. Acta 450 (2001), 53-61.*
[7] Pokorná M.; Čižmárik J.; Sedlárová E.; Račanská E.: *Čes. a Slov. Farm. 45 (1999), 80-86.*
[8] Renčová M.; Čižmárik J.; Lehotay J.; Hroboňová K.: *Čes. a Slov. Farm. 51 (2002), 150-153.*

DEVELOPMENT OF A SOLID PHASE EXTRACTION METHOD FOR DETERMINATION OF STYRENE OXIDE ADDUCTS IN HUMAN GLOBIN

Michal Jágr[a], Věra Pacáková[b] and Miroslav Petříček[a]

[a] *Institute of Microbiology, Academy of Sciences of the Czech Republic, Vídeňská 1083, Prague 4, 142 20, Czech Republic, e-mail: jagr@biomed.cas.cz*
[b] *Department of Analytical Chemistry, Faculty o Science, Charles University, Albertov 8, Prague 2, 128 40, Czech Republic*

Abstract

The styrene-7,8-oxide (SO) adducts with amino acids in human globin are studied as potential biomarkers of the exposure to styrene. There is a strong effort to develop a suitable analytical method for determination of the SO adducts with cysteine (SO-Cys), histidine (SO-His), and lysine (SO-Lys). In this paper a simple method for solid phase extraction (SPE) of the SO adducts from human globin hydrolysates is described.

Various SPE sorbents were tested and the extraction procedure was then optimized. Average recoveries for SO-Cys (~50 %), SO-His (~80 %), and SO-Lys (~90 %) adducts were obtained on cartridges Strata-X. Levels of the SO adducts in globin samples were determined by coupling of SPE with gas chromatography. Content of the most abundant SO adducts regioisomers was in the range 0.4-135 μmol/g globin.

Keywords

Styrene oxide; adducts; solid phase extraction; cysteine; histidine; lysine

1. Introduction

Styrene-7,8-oxide is the main intermediate involved in the metabolism of styrene, which is used as a globally important industrial monomer in the production of plastics, synthetic rubbers and resin[1,2].

In humans, SO is formed *in vivo* by oxidation of styrene. This conversion is catalyzed in livers by cytochromes P450. The main part of formed SO is further metabolized to mandelic acid and phenylglyoxylic acid, which are excreted in urine. Minor part of SO alkylates various nucleophilic sites at blood proteins or DNA to form stable covalent compounds, so called adducts. Determination of the SO adducts affords informations about internal dose of the SO or styrene obtained by people or laboratory animals. Dosimetry of the SO adducts with globin presents several advantages over determination of urinary metabolites, especially the long lifespan and easy availability of the protein adducts.[3,4]

Reaction of SO with a nucleophilic group (an amino acid residue) in proteins may occur via both electrophilic epoxidic carbons (Cα or Cβ), giving rise to two regioisomeric products: 2-hydroxy-1-phenylethyl (21HPE), and 2-hydroxy-2-phenylethyl (22HPE) adducts, respectively. The occurrence of the SO adducts with individual amino acids in the form of two or more regioisomers was reported.[5,6]

Various procedures have been developed to determine the particular types of the SO adducts with globin. The modified Edman degradation procedure has been used to determine SO adducts with N-terminal valine (SO-Val).[7,8] Levels of the SO-Val adducts in humans profesionally exposed to styrene *in vivo* proved to be very low and hard to detect. Vodička et al. were able to determine SO-Val adducts at a level of low pmol/g globin.[9]

SO-Cys adducts have been determined using the Raney-Nickel cleavage, releasing the SO moiety in the form of phenylethanols, that were determined by gas chromatography[10]. Unexpected high background levels of phenylethanols were observed in unexposed subjects (level ca. nmol/g globin), while occupational exposures to styrene did not result in significant increase of the SO-Cys adduct levels.

Several recent studies combined tryptic hydrolysis of the SO-modified globin with mass spectrometry analysis of the resulting digest. Histidine imidazole residues were identified as the dominant binding sites for SO in human globin[11]. Similarly, in other studies, histidine was confirmed to be the main target of SO alkylation, followed by cysteine and N-terminal valine.[12,13]

The above mentioned methods are of limited applicability for routine use, mainly due to very low content of the SO adducts in globin. The main aim of this work was to find a suitable system for enrichment of the SO adducts in samples of human globin hydrolysate. SPE was used for this purpose.

In the last decade, Black et al. used SPE for extraction of the Nτ-(2-hydroxyethylthioethyl)histidine adducts from globin hydrolysate[14]. Authors were able to determine these adducts in the samples obtained from human casualties of sulphur mustard poisoning. Histidine adducts with benzo[*a*]pyrenediolepoxide were extracted by SPE and determined by μHPLC/MS/MS with the sensitivity of the method at a level of fmol/g (ref. *15*). Acrylamide adducts with valine were extracted on SPE columns Strata-X and then assessed in another study.[16]

Various SPE resins were tested in this study for extraction of the SO adducts from human globin hydrolysate. The procedure was then optimized and applied to samples of human globin treated with SO *in vitro*. The levels of the SO adducts in these samples were then determined by gas chromatography with flame-ionization detector.

2. Experimental
2.1 Chemicals

Methanol p.a. was purchased from Lachema (Czech Republic), trifluoroacetic acid (TFA) was from Riedel de Haën. N,N-Dimethylformamide (DMF), N-*tert*-butyldimethylsilyl-N-methyl-trifluoroacetamide (MTBSTFA), norleucine, and acetonitrile p.a. were purchased from Fluka (Switzerland). Standards of twenty proteinogenic amino acids were obtained from Calbiochem (USA). Standards of the SO-Cys, SO-His, and SO-Lys adducts (their structure is shown in Fig.1) have been synthesized as described in previous study[17], as well as the preparation of the SO-modified globin samples (SO-Gb) and their enzymatic hydrolysis with pronase.

2.2 Instrumentation

GC analyses were performed on Agilent 6890N gas chromatograph equipped with an autosampler Agilent 7693 and a flame-ionization detector. Analyses were carried out on a DB-5ms fused silica capillary column (length 30 m, i.d. 0.25 mm, film thickness 0.25 μm) purchased from J&W Scientific. The carrier gas (N_2) linear velocity was maintained at 30 cm/sec. Temperatures: injector 270 °C, detector 250 °C, column temperature program started at 70 °C for 2 min, then a gradient 12 °C/min. to 300 °C was used and finally the temperature was kept at 300 °C for 10 min.

Solid phase extraction was performed at a 12-port SPE vacuum manifold (Supelco).
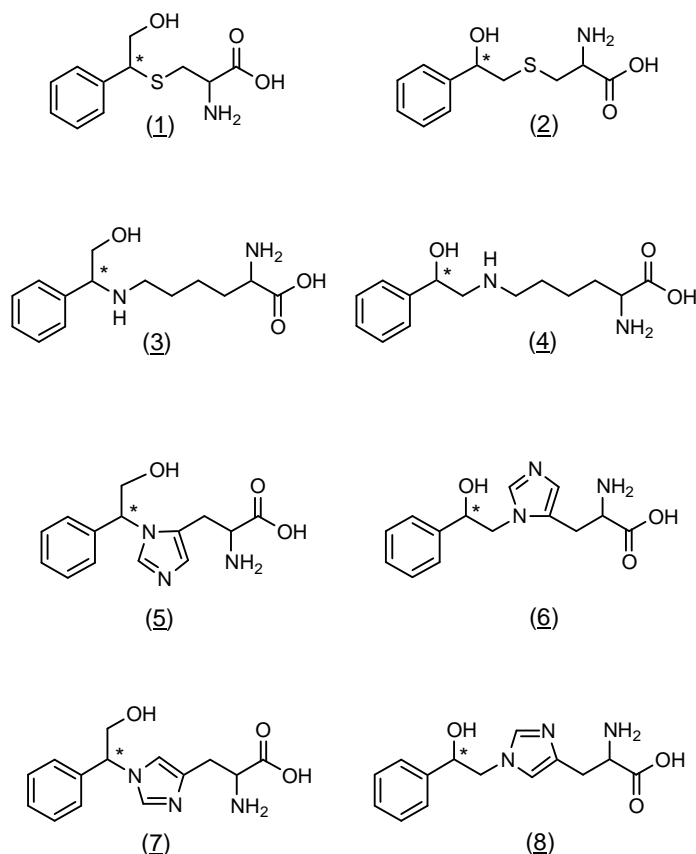
Fig.1 <u>1</u>: S-(21HPE)cysteine; <u>2</u>: S-(22HPE)cysteine; <u>3</u>: Nω-(21HPE)lysine; <u>4</u>: Nω-(22HPE)lysine; <u>5</u>: Nπ-(21HPE)histidine; <u>6</u>: Nπ-(22HPE)histidine; <u>7</u>: Nτ-(21HPE)histidine; <u>8</u>: Nτ-(22HPE)histidine.

2.3. SPE procedures
2.3.1 Sorbent comparison

Amino acids (Ala, Val, Glu, Asp, Lys, Ser, His, Thr, Phe, Tyr and Trp; c = 0.1 mg/ml) and the SO adducts (SO-Cys, SO-His and SO-Lys; c = 0.01 mg/ml) were mixed and dissolved in phosphate buffer (pH = 8.0) to prepare a standard solution. The 3 ml-polypropylene SPE cartridges (60 mg or 100 mg) were obtained from the following manufacturers: Strata (Phenomenex), Oasis (Waters) and Discovery (Supelco).

Prior to extraction, the cartridges were prewashed with 2 ml of methanol and then with 2 ml of distilled water. After application of the sample (1 ml), the cartridges were washed with 3 ml of water and dried by air flow. Elution was performed with 3 ml of organic solvent mixture (acetonitril/methanol/0.1 % TFA, 45/45/10, v/v/v). The eluates were evaporated in a Gyrovap vacuum concentrator and stored at dry place before derivatization.

2.3.2 Recovery assays

Samples of human control globin hydrolysate (c = 5 mg/ml) were spiked with SO adducts. The amount of the SO adducts added was: 1, 5, 10, 50, 100 or 500 nmol/g globin. 1 ml of the sample was applied onto preconditioned Strata-X SPE cartridge (60 mg/3 ml) and the cartridges were washed with three different volumes of water (3, 5 or 7 ml). Retained SO adducts were eluted with 3 ml of „organic solvent mixture", eluate was then dried and derivatized.

The same samples of globin hydrolysates spiked with SO adducts (in the range of 0-500 nmol/g globin), that were not treated with SPE, were set as 100 % for recovery studies. These samples were also used for construction of calibration curves. All samples were analyzed in triplicates.

2.3.3 Determination of the SO adducts

16 ml of human globin hydrolysate at c = 5 mg/ml (that was obtained by hydrolysis of 80 mg of SO-Gb sample) was applied onto preconditioned SPE cartridges Strata-X Giga Tubes (1 g/12 ml). The cartridges were then washed with 48 ml of water and the SO adducts were eluted with 24 ml of organic solvent mixture. Eluates were then concentrated, dried and derivatized before GC analysis.

2.4 Derivatization and gas chromatography analysis

30 μl of internal standard (norleucine, c = 0.2 mg/ml) was added to each sample before drying and derivatization. Dry samples were subjected to derivatization with a MTBSTFA reagent according to a procedure described by Mawhinney *et al.*[18]. The solution (50 μl) was then extracted by 50 μl of dry heptane (50 μl), shaken and 1 μl of heptane phase was injected splitless into GC.

3. Results and discussion

Analytical method described in previous study[17] is suitable for determination of the SO adducts in biological material at a relatively high level (ca. μmol/g globin). On the other hand, the level of the SO adducts in samples obtained from laboratory animals or people exposed to styrene and SO *in vivo* is very low (ca. nmol-pmol/g globin). Determination of such low levels reaches the limit of detection of commonly used analytical methods.

So, there is a need to improve sensitivity of the used methods by introducing an additional analytical step to the protocol. In this study, the SO adducts are extracted from the globin samples by using SPE and thus they are concentrated. The SPE procedure is based on relatively higher hydrophobicity of the SO adducts in comparison to the most of proteinogenic amino acids. It enables good retention of the SO adducts on unpolar SPE sorbents, while other more polar amino acids are washed out. The desired SO adducts are then eluted by organic solvent, concentrated and determined.

3.1 Sorbent comparison

Various types of unpolar sorbents were chosen to cover a wide range of their chemical properties. Results of these preliminary experiments are summarized in Table 1.

Good recoveries of the SO adducts (almost > 50 %) were obtained on three of the tested sorbents (Strata-X, Strata-SDB L and Oasis-HLB). These cartridges were developed in last decade and are composed mainly of polystyrene-divinylbenzene copolymer. Good recoveries of the SO adducts on these polymeric sorbents could be obtained due to polar groups in the polymeric matrix, which increases the efficiency of the extraction process.

Surprisingly poor recoveries (< 5 %) of the SO adducts were obtained on the other tested unpolar sorbents (e.g. C_{18}, C_8, phenyl). Recoveries of the amino acids on all tested sorbents were almost low (< 1 %) except for phenylalanine and tryptophan. Cartridges Strata-X were chosen for further optimization of the SPE method.

Table 1 Recoveries (in %) of the studied SO adducts and amino acids on tested SPE resins.

SPE cartridge	SO-Cys: 1	SO-His: 8	SO-Lys: 3	Ala	Tyr	Phe	Trp
Strata C-18	3,5	4,2	4,5	< 0,1	< 0,1	1,3	2,5
Strata C-8	0,3	0,4	0,4	< 0,1	< 0,1	< 0,2	< 0,2
Strata Ph	0,5	1,6	1,7	0,2	0,3	0,5	0,9
Strata NH2	0,3	0,9	1,2	< 0,1	< 0,1	< 0,1	< 0,1
Strata CN	0,2	< 0,1	0,2	< 0,1	< 0,1	< 0,1	< 0,1
Strata-X	53,4	67,2	83,6	0,5	1,1	5,8	23,5
Strata SDB-L	45,0	64,9	76,3	0,3	1,0	4,6	19,6
Oasis-HLB	51,2	66,9	78,3	0,4	1,2	5,2	24,1
Discovery DSC C-18	1,2	1,5	1,6	< 0,1	< 0,1	0,4	0,9
Discovery DSC C-8	< 0,2	< 0,2	< 0,2	< 0,1	< 0,1	< 0,2	< 0,2
Discovery DSC Ph	0,3	0,5	0,5	< 0,2	< 0,2	< 0,2	< 0,2
Discovery DSC NH2	< 0,1	< 0,1	< 0,1	< 0,1	< 0,1	< 0,1	< 0,1
Discovery DSC CN	< 0,1	< 0,1	< 0,1	< 0,1	< 0,1	< 0,1	< 0,1

3.2 Recovery assays

The next step was optimization of the wash volume and recovery assays of the SO adducts. Control human globin was subjected to enzymatic hydrolysis by pronase. Hydrolysate was then divided into 1 ml aliquots (c = 5 mg/ml). Each aliquot was spiked with internal standard (norleucine) and with the SO adducts. Analysis of the globin samples afforded linear seven-point calibration curve for the SO adducts, with $R^2 \geq 0.9997$. Relative standard deviation of the compound area was < 1 % for samples spiked with 100-500 nmol of the adducts and < 10 % for other samples.

Other aliquots of globin hydrolysate, that were spiked with SO adducts were applied onto preconditioned SPE Strata-X cartridges. Then they were washed with three different water volumes (3, 5 and 7 ml) to study the influence of washing volume on recovery of the SO adducts. Results are shown in Table 2. Nε-(21HPE)lysine was almost quantitatively recovered on all investigated washing volumes (86-104 %). Similarly, a bit lower recoveries were gained for Nτ-(22HPE)histidine (65-86 %). Recoveries of S-(21HPE)cysteine range from 23 % to 58 %. Dependence of S-(21HPE)cysteine recovery on washing volumes was observed. Higher recoveries (53-58 %) of this regioisomer were obtained when 3 ml wash volume was used. The lowest recoveries were obtained (23-30 %) when cartridges were washed with 7 ml of water.

It follows from the results obtained that especially SO-Cys adducts can be partly removed from the sorbent Strata-X even with water. Using washing volumes < 3 ml is not sufficient to remove the most of other amino acids (data not shown), but on the other hand, washing volumes > 3 ml cause severe loss of the S-(21HPE)cysteine adducts.

Table 2 Recoveries of the studied SO adducts from spiked human globin obtained on Strata-X SPE cartridges.

Amount of SO adducts in sample (nmol/g)	Wash volume (ml H_2O)	Recovery (%)		
		S-(21HPE)cysteine	Nε-(21HPE)lysine	Nτ-(22HPE)histidine
500	3	55	99	71
500	5	33	95	75
500	7	26	98	69
100	3	57	98	75
100	5	31	87	66
100	7	24	104	67
50	3	55	89	72
50	5	36	99	67
50	7	23	98	67
10	3	53	86	75
10	5	38	92	69
10	7	30	98	76
5	3	53	86	71
5	5	38	92	65
5	7	30	102	86
1	3	58	89	66
1	5	39	94	78
1	7	27	97	65

3.3 Determination of the SO adducts

80 mg of samples of the SO-modified human globin was digested by Pronase giving rise to 16 ml pf hydrolysate. The hydrolysate was then extracted on Strata-X Giga Tubes. The determined levels of the SO adducts were corrected in accordance with average recoveries of the SO adducts mentioned in previous section. Determined levels of the SO adducts in SO-Gb samples are presented in Table 3. The levels are in the range 0.4-135 μmol/g globin.

Table 3 Recoveries of the studied SO adducts from samples of human globin modified with SO (SO-Gb) at a molar ratio SO vs. globin: 100:1; 10:1 and 0.625:1.

Globin sample	SO adduct level (μ mol/g globin)		
	S-(21HPE)cysteine	Nε-(21HPE)lysine	Nτ-(22HPE)histidine
SO-Gb 100:1	10,5	34,7	135
SO-Gb 10:1	5,80	11,0	39,3
SO-Gb (*R*)-SO 0,625:1	0,59	0,85	1,98
SO-Gb (*S*)-SO 0,625:1	0,42	0,83	1,30

Sensitivity of the used method of detection was also tested. It was ca 0.1 nmol of SO adduct per sample. On presumption that 0.1 nmol of the adducts can be isolated by SPE

from 100 mg of the globin sample, it would be possible to detect the SO adducts in globin samples at the level of ca. 1 nmol/g globin.

4. Conclusion

The analytical method for solid phase extraction of the SO adducts from human globin hydrolysate was developed. The method is able to selectively extract the SO adducts from more than 99 % of proteinogenic amino acids. SPE was used in coupling with gas chromatography and flame ionization detector and the SO adducts in SO-modified human globin were determined. The method will be applied for determination of the SO adducts in real samples of globins from laboratory animals or people exposed to styrene and SO *in vivo*.

Acknowledgment

References

[1] Sumner S.C.J.; Fennell T.R.: *Crit. Rev. Toxicol. 25 (1994), S11-S33.*

[2] Vodička P.; Koskinen M.; Naccarati A.; Oesch-Bartlomowicz B.; Vodičková L.; Hemminki K.; Oesch F.: *Drug Metab. Rev. 38 (2006), 805-853.*

[3] Phillips D. H.; Farmer P. B.: *Crit. Rev. Toxicol. 24 (1994), S35-S46.*

[4] Farmer P. B.: *Mutat. Res. 428 (1999), 69-81.*

[5] Hemminki K.: *Arch. Toxicol. Suppl. 9 (1986), 286-290.*

[6] Jágr M.; Mráz J.; Ctibor K.; Stránský V.; Pospíšil M.: *Biomed. Papers 149 (2005), 82-86.*

[7] Osterman-Golkar S.; Christakopoulos A.; Zorzec V.; Svensson K.: *Chem.-Biol. Interact. 95 (1995), 79-87.*

[8] Pauwels W.; Veulemans H.: *Mutat. Res. 418 (1998), 21-33.*

[9] Vodička P.; Tvrdik T.; Osterman-Golkar S.; Vodičková L.; Peterková K.; Souček P.; Šarmanová J.; Farmer P. B.; Granath F.; Lambert B.; Hemminki K.: *Mutat. Res. 445 (1999), 205-224.*

[10] Yeowell-O´Connell K.; Jing Z.; Rappaport S. M.: *Cancer Epidemiol. Biomarkers Prev. 5 (1996), 205-215.*

[11] Kaur S.; Hollander D.; Haas R.; Burlingame A. L.: *J. Biol. Chem. 264 (1989), 16981-16984.*

[12] Badghisi H.; Liebler D. C.: *Chem. Res. Toxicol. 15 (2002), 799-805.*

[13] Basile A.; Ferranti P.; Mamone G.; Manco I.; Pocsfalvi G.; Malorni A.; Acampora A.; Sannolo N.: *Rapid Commun. Mass Spectrom. 16 (2002), 871-878.*

[14] Black R. M.; Clarke R. J.; Harrison J. M.; Read R. W.: *Xenobiotica 27 (1997), 499-512.*

[15] Helleberg H.; Törnqvist M.: *Rapid Commun. Mass Spectrom. 14 (2000), 1644-1653.*

[16] Ospina M.; Vesper H. W.; Licea-Perez H.; Meyers T.; Mi L.; Myers G.: *Advances in Exp. Medicine and Biology 561 (2005), 97-107.*

[17] Jágr M.; Mráz J.; Linhart I.; Stránský V.; Pospíšil M.: *Chem. Res. Toxicol. 20 (2007), 1442-1452.*

[18] Mawhinney T. P.; Robinett R. S. R.; Atalay A.; Madson M. A.: *J. Chromatogr. 358 (1986), 231-242.*

ALKYLATION AS A TOOL FOR POST-POLYMERIZATION SURFACE MODIFICATION OF POLYSTYRENE CAPILLARY MONOLITHIC COLUMNS

Zdeňka Kučerová[a], Michał Szumski[b], Bogusław Buszewski[b] and Pavel Jandera[a]

[a] *University of Pardubice, Faculty of Chemical Technology, nám. Čs. legií 565, CZ-532 10 Pardubice, Czech Republic; e-mail:* st8546@student.upce.cz
[b] *Nicolaus Copernicus University, Faculty of Chemistry, Gagarina 11, PL 87-100 Toruń, Poland*

Abstract

Polystyrene capillary columns were synthesized in fused silica capillaries. The polymerization mixture comprised styrene and divinylbenzene as the monomers, propan-1-ol and formamide as the porogen system and azobisisobutyronitrile as the initiator of the polymerization. The monoliths were subsequently alkylated with linear C18 groups to improve the retention and the chromatographic resolution of phenolic acids and flavones. Two different approaches were used for the alkylation procedure, namely the Friedel-Crafts reaction and the grafting. A new thermally initiated grafting procedure was developed and optimized in order to speed up and simplify the alkylation process. All the columns were characterized with respect to the hydrodynamic properties, porosity and chromatographic properties.

Keywords

Alkylatio; Monolithic columns; Polystyrene columns; Liquid chromatography; Electrochromatography

1. Introduction

Polystyrene monolithic columns can be directly used for reversed-phase chromatography due to the hydrophobicity of monomers. Chemical modification of the monolithic bed is necessary for other chromatographic modes or capillary electrochromatography (CEC). It can be done in two main ways[1].

A change in the monomer mixture composition is the first approach. Incorporation of methacrylic acid increases the electroosmotic flow; therefore it is used for CEC. The proportion 1:1 to styrene is usually used[1,2]. 4-vinylbenzyl chloride can be used to introduce reactive groups into the (co)-polymer monolithic matrix, which are suitable for further chemical reactions to prepare ion exchangers[3,4] or monoliths with highly hydrophilic surface grafted to the hydrophobic polymeric skeleton[5]. The use of 4-octylstyrene instead of styrene was investigated to improve the separation of peptides without the need of any additional surface reaction or modification[6].

The second approach is the modification after the polymerization. Friedel-Crafts reaction is used for introduction of alkyls, usually C18 chains. Polystyrene monoliths[7] or beads[8] have been alkylated using this method. 1-chlorooctadecane in the presence of different catalysts and solvents was used as the reactant. The use of alkylated stationary phases improved the separation of proteins and oligonucleotides in the μ-HPLC mode because alkylation provides encapsulation. Another possibility of the post-polymerization change of the surface chemistry is grafting monomers by covalent bonds onto the polymer surface. The grafted products can be uncrosslinked (sol) and crosslinked (gel). Viklund *et al.*[9] grafted polystyrene monolith with 3-sulfopropyl methacrylate in dimethyl sulfoxide and obtained a monolithic column suitable for cation-exchange separation of a protein mixture.

The goal of this study was to compare the selectivity and the resolution of μ-HPLC and CEC separation of a phenolic acid mixture and flavones on non-modified and alkylated polystyrene monolithic columns. The alkylation was carried out in two different ways. The first one was Friedel-Crafts alkylation using the procedure described in literature[7]. The second approach was a newly developed grafting procedure using stearyl methacrylate as a grafting reactant. The procedure was optimized in the terms of the temperature, time, the concentration of the grafting reactant and the solvent.

2. Experimental
2.1 Capillary pretreatment

The capillary wall modification procedure was carried out based on the results of Courtois *et al.*[10]. The fused silica capillary was rinsed and filled with 1 M NaOH. Both ends were sealed and the capillary was left in the oven for 2 h at 120°C. Subsequently, NaOH was washed out with redistilled water and acetone. The capillary was then dried in the stream of nitrogen for 1 h and then in the oven with 120°C for another 1 h. The silanization solution contained 10% (v/v) 3-(trimethoxysilyl)-propylmethacrylate in toluene. The silanization solution was degassed in the stream of nitrogen for 10 min and filled into the capillary, where the silanization took 2 h at room temperature. Both ends were sealed. The solution was then washed out with toluene and the capillary was dried in the stream of nitrogen for 1 h. The inner surface hydrophobicity was evaluated by the measurement of the wetting angle and only capillaries showing wetting angle greater than 70° were used for further experiments.

2.2 Column preparation

100 μm I.D. fused silica capillaries were used for all experiments. Friedel-Crafts alkylation and preparation of the polystyrene monoliths was carried out following the procedure presented by Huang *et al.*[7]. The only difference was the use of a water bath instead of an oven for polymerization and alkylation.

The grafting procedure employed reaction mixture prepared by mixing 25% (w/v) of stearyl methacrylate and azobisisobutyronitrile (1% of the stearyl methacrylate amount) in dimethyl formamide (DMF)[11]. The mixture was homogenized and degassed in the stream of nitrogen for 10 min. The column was then filled with the mixture pressurizing the vial by a nitrogen source of 0.8 MPa. The ends were sealed and the column was put into the 65°C hot water bath for 9 h.

The detection window was prepared inserting part of the column into a hot tungsten wire loop, while flushing the column with methanol. The columns were then cut into the desired total length 33.5 cm, having 25.0 cm to the detection window.

3. Results and discussion
3.1 Hydrodynamic properties

The column hydrodynamic permeability was measured as the dependence of methanol flow rate on the back pressure. The measured plots were linear within the range of 5 – 25 MPa, indicating good mechanical stability of the monoliths. The data obtained for non-modified column (NM) and the column alkylated using Friedel-Crafts alkylation (FC) show very similar slopes within the range of the reproducibility of the polystyrene monoliths production (8%). On the other hand, the hydrodynamic permeability of the grafted column (GR) decreased of 38% comparing to the NM column. The lower hydrodynamic permeability is probably a consequence of the decrease of the flow-through pores diameter in the monolith structure, indicating formation of a thin polymer layer in the pores during the grafting procedure, which decreased the flow-through pores volume.

3.2 Column porosity

Column porosity controls the hydrodynamic permeability. The inverse size-exclusion chromatography (ISEC) was used for the determination of the total column porosity, ε_T. The ISEC experiments were carried out with toluene and narrow distribution polystyrene standards with molecular masses within the range of 660 – 2,000,000 and tetrahydrofuran as the mobile phase.

Total column porosities, ε_T, and the interstitial porosities, ε_0, of NM and FC columns were very similar (Table 1). The difference was within the measurement errors. It could indicate that the alkyl chains were linked to benzene rings or remaining vinyl groups without any significant change in the monolith structure. The results obtained for the GR column were quite different. The total column porosity and the interstitial porosity significantly decreased in comparison to NM column.

Table 1 Column properties. *ε_T is the total column porosity, ε_0 is the flow-through porosity and ε_i is the mesopore porosity.*

Column	NM	FC	GR
ε_T	0.706	0.702	0.655
ε_0	0.661	0.653	0.598
ε_i	0.045	0.049	0.057

3.3 Column efficiency in μ-HPLC and CEC

The column efficiency was obtained by measuring the band spreading of thiourea with 5 mM phosphate buffer pH 7.5 as the mobile phase, which is considered to be a non-retained compound under the conditions of the experiment. The van Deemter plots indicated greater band spreading due to the bed non-uniformities and mass transfer resistance with parabolic flow profile than with plug-like profile flow (Fig.1A). The column efficiency in CEC did not depend on the linear velocity of the mobile phase. This behavior enables rapid separations without the loss in the resolution. Typically, plate height increases with increasing linear velocity in μ-HPLC. The practical consequence of this behavior was poorer resolution of phenolic acids at higher separation velocities. The comparison of the columns showed the best μ-HPLC efficiency for GR column. Voltage-driven flow provided comparable efficiency for all the monoliths (Fig.1B).
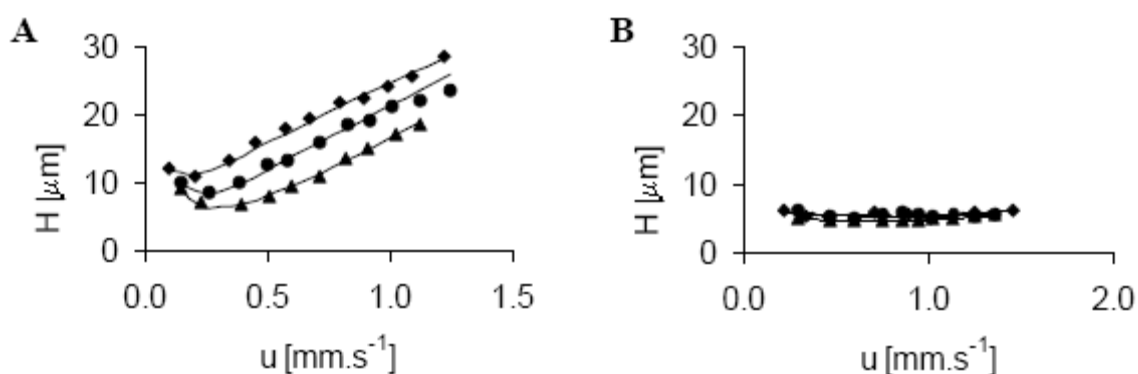
Fig.1 Van Deemter plots for (**A**) pressure-driven (*μ*-HPLC) and (**B**) voltage-driven (CEC) conditions. ◆*NM column,* ● *FC column,* ▲ *GR column.*

3.4 Grafting procedure – separation of antioxidants

No separation of phenolic acid mixture was achieved using NM column in neither μ-HPLC nor CEC with purely aqueous mobile phases, due to the insufficient retention on

the stationary phase. Friedel-Crafts alkylation increased the retention and improved the resolution by decreasing the polarity of the monolithic polymer (Fig.2A). The effect of the alkylation was reproducible; however the used procedure was time consuming. Thermally initiated grafting was used as an alternative. The concentration of the C18 reactant, the type of the solvent, the reaction temperature and time are the factors influencing most significantly the retention properties of the monolithic column. Chromatographic resolution of the two least retained phenolic acids was selected at the criterion of the procedure performance.

The type of the solvent influences the result in the most significant way. DMF as the solvent of stearyl methacrylate provided much better separation in comparison with propan-2-ol and toluene. DMF is a poor solvent for polystyrene and could enhance the stearyl methacrylate affinity to the monolith. As anticipated, the increase in reaction time increased the resolution. The increase of the reaction time from 6 to 9 hours improved the resolution from 0.3 to 0.6. The column permeability of the grafted column decreased to approx. 60% of the original value after 9 hours long grafting. The optimized content of stearyl methacrylate was 25% w/v and the optimal grafting temperature was 65°C. The capillaries prepared in this way provided the resolution for the phenolic acids better than 1.0, which was comparable with FC column (Fig.2B).
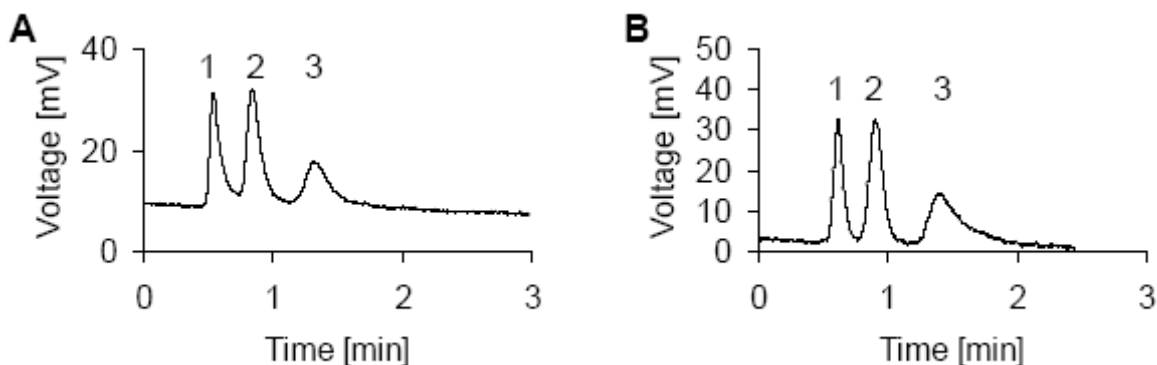
Fig.2 μ-HPLC separation of phenolic acids on FC (**A**) and GR (**B**) column. *Conditions: mobile phase, 10 mM ammonium acetate buffer, pH 3.0; detection, UV (214 nm). Sample: (1) gallic acid, (2) syringic acid, (3) ferulic acid.*
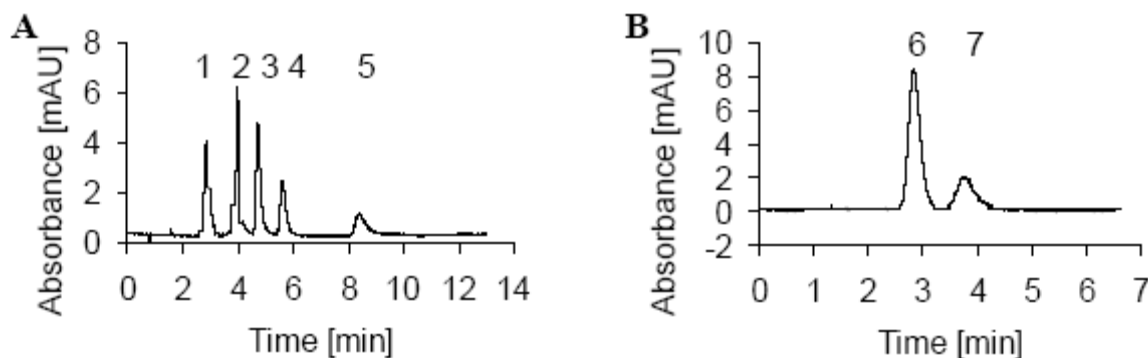
Fig.3 CEC separation of antioxidant mixtures on FC (**A**) and GR (**B**) column. *Conditions (A): mobile phase, 5 mM phosphate buffer, pH 2.5; voltage, -20 kV; L_{ef} = 25.0 cm; injection, 3 s, -5 kV; detection, UV (210 nm). Sample: (1) thiourea, (2) gallic acid, (3) vanillic acid, (4) syringic acid, (5) ferulic acid. Conditions (B): mobile phase, 20% methanol in 5 mM phosphate buffer pH 2.5; applied voltage, -20 kV; L_{ef} = 8.5 cm; injection, 3 s, -10 kV; detection, UV (210 nm). Sample: (6) rutin, (7) hesperidin.*

Both alkylated columns were also tested under CEC conditions. Fig.3A shows the separation of phenolic acids on FC column and Fig.3B presents the separation of two flavones on GR column.

4. Conclusions

The alkylation is an effective tool for post-polymerization surface modification to control the retention properties of the polystyrene monolithic columns. Linear C18 chains were linked to polystyrene monoliths using two different approaches – Friedel-Crafts reaction and a newly optimized thermally initiated grafting method. Both alkylation procedures improved the retentivity and the resolution of the stationary phase. The newly introduced grafting method provided comparable resolution of the tested phenolic acid mixture as the Friedel-Crafts method; however both alkylated monoliths had different structure. Friedel-Crafts alkylation did not affect the hydrodynamic and porous properties; however it decreased the polarity of the stationary phase. The grafting decreased the hydrodynamic permeability of the column, the total column porosity and the interstitial porosity. As a consequence, the grafted monolith provided slower analysis.

References
[1] Xiong B.; Zhang L.; Zhang Y.; Zou H.; Wang J.: *J. High Resol. Chromatogr. 23 (2000), 67-72.*
[2] Jin W.; Fu H.; Huang X.; Xiao H.; Zou H.: *Electrophoresis 24 (2003), 3172-3180.*
[3] Legido-Quigley C.; Marlin N.; Smith N.W.: *J. Chromatogr. A 1030 (2004), 195-200.*
[4] Gusev I.; Huang X.; Horváth C.: *J. Chromatogr. A 855 (1999), 273-290.*
[5] Wang Q.C.; Svec F.; Frechet J.M.J.: *Anal. Chem. 65 (1993), 2243-2248.*
[6] Ro K.W.; Liu J.; Busman M.; Knapp D.R.: *J. Chromatogr. 1047 (2004), 49-57.*
[7] Huang X.; Zhang S.; Schultz G.A.; Henion J.: *Anal. Chem. 74 (2002), 2336-2344.*
[8] Huber C.G.; Oefner P.J.; Bonn G.K.: *Anal. Biochem. 212 (1993), 351-358.*
[9] Viklund C.; Nordström A.; Irgum K.; Svec F.; Fréchet J.M.J.: *Macromolecules 34 (2001), 4361-4369.*
[10] Courtois J.; Szumski M.; Byström E.; Iwasiewicz A.; Shchukarev A.; Irgum K.: *J. Sep. Sci. 29 (2006), 14-24.*
[11] Kučerová Z.; Szumski M.; Buszewski B.; Jandera P.: *J. Sep. Sci. 30 (2007), 3018-3026.*

USE OF CHIRAL SEPARATIONS FOR THE DETERMINATION OF ENZYME ENANTIOSELEC-TIVITY

<u>Jiří Břicháč</u>[a,b,c,d], Jiří Zima[b], Michael Kotik[c], Ales Honzatko[a] and Matthew J. Picklo[a]

[a] *Department of Pharmacology, Physiology, and Therapeutics, University of North Dakota, Grand Forks, ND 58203-9024, USA*
[b] *Department of Analytical Chemistry, Charles University in Prague, Albertov 6, 128 43 Prague 2, Czech Republic*
[c] *Laboratory of Enzyme Technology, Institute of Microbiology, Academy of Sciences of the Czech Republic, Vídeňská 1083, 142 20 Prague 4, Czech Republic*
[d] *Department of Membrane Transport Biophysics, Institute of Physiology, Academy of Sciences of the Czech Republic, Vídeňská 1083, 142 20 Prague 4, Czech Republic. E-mail address: brichac@email.cz*

Abstract

   Enantioselective enzyme prefers one enantiomer as a substrate or preferentially forms one enantiomer over the other in a chemical reaction. To study implication of enantioselectivity in biomedicine and biotechnology, we developed chiral separation methods. Determination of various epoxides and diols formed by their hydrolysis were performed using chiral cyclodextrine-based gas chromatography. Developed methods were successfully applied for the determination of enantioselectivity of microbial epoxide hydrolases.

   **Furthermore, we elucidated the basis of enantioselective oxidation of lipid peroxidation product *trans*-4-hydroxy-2-nonenal (HNE). Enzyme kinetics measurement of oxidation of HNE enantiomers by aldehyde dehydrogenases to *trans*-4-hydroxy-2-nonenoic acid (HNEA) were performed using UV spectrometry, HPLC and LC-MS/MS. Moreover, direct and indirect RP-HPLC methods for enantioseparation of HNEA were developed and validated.**

Keywords

   Chiral separatio; HPLC; GC; enantioselectivity; lipid peroxidation; aldehyde dehydrogenase; epoxide hydrolase

1. Introduction

   Enantioselectivity is the ability of chiral environment to distinguish between two enantiomers. Enantioselective enzyme, receptor, catalyst or chiral selector preferentially interact with or preferentially form in a chemical reaction one enantiomer over the other. Enantioselective enzymes are very useful biocatalyzators allowing cheap preparation of optically pure chemicals. Moreover, enantioselective enzymes play important role in metabolic pathways of chiral compounds. Chiral separations play crucial role in studying of implication of enantioselectivity in biomedicine and biotechnology.

   The first part of this work is devoted to the determination of enantioselectivity of microbial epoxide hydrolases using chiral gas chromatography (GC). Chiral epoxides prepared by an enzyme kinetic resolution of racemates can serve as valuable building blocks in an organic synthesis[1]. We tested hypothesis, that microorganisms isolated from a harsh industrial environment might be the promising source of novel enantioselective epoxide hydrolases. In order to measure the enantioselectivity, we developed methods for analyses of chiral epoxides and their corresponding diols using a chiral GC on cyclodextrine-based stationary phases.

   In the second part of this study we elucidated the basis of enantioselective oxidation of *trans*-4-hydroxy-2-nonenal (HNE) by brain mitochondria. HNE is a cytotoxic α,β-unsaturated aldehyde implicated in the pathology of multiple diseases involving

oxidative damage[2]. Detoxification of HNE to *trans*-4-hydroxy-2-nonenoic acid (HNEA), mediated by aldehyde dehydrogenases (ALDHs), is a major route of metabolism in many systems. We showed previously that HNE is detoxified (*R*)-enantioselectively to HNEA by respiring rat brain mitochondria[3,4]. Here we describe enzyme kinetics measurement of oxidation of HNE enantiomers by ALDHs to HNEA using UV spectrometry, HPLC and LC-MS/MS[5].

Further study of the role of enantioselectivity in HNE metabolism is restricted by the fact that no method is available for the enantioseparation of HNEA. Therefore, we developed reversed-phase high-performance liquid chromatography (RP-HPLC) methods for HNEA enantioseparation. In general, chiral carboxylic acids can be determined indirectly by RP-HPLC as diastereomeric amides using derivatization with chiral amines. For direct enantioseparation of carboxylic acids, a polysaccharide based chiral stationary phase (CSP) Chiralpak AD-RH can be used. We employed both direct and indirect approach to separate HNEA enantiomers using RP-HPLC[6].

2. Experimental
2.1 Chemicals and Reagents
All reagents were of analytical reagent grade or higher purity. HNE dimethylacetal and HNE and HNEA enantiomers were synthesized as described previously[3].

2.2 Determination of Enantioselectivity of Microbial Epoxide Hydrolases Using Gas Chromatography
Epoxides and diols were quantified and their enantiomeric excesses (*ee*) determined by GC with chiral columns on a Hewlett-Packard 5890A gas chromatograph equipped with a flame ionization detector (FID) using H_2 as carrier gas. *tert*-Butyl glycidyl ether (TBE) and its corresponding diol were separated using CP-Chirasil-DEX CBcolumn (Chrompack, 25 m, 0.25 mm i.d., 0.25 μm film thickness) with a start temperature of 50 °C for 5 min, followed by a gradient of 5 °C/min. A β-DEX 225 column (Supelco, 30 m, 0.25 mm i.d., 0.25 μm film thickness) at an isothermal temperature of 107 °C was used for analysis of benzyl glycidyl ether and 3-benzyloxy-1,2-propanediol after derivatization into its acetonide. The same column at an isothermal temperature of 71 °C was used for analysis of allyl glycidyl ether (AGE) and the derivatized corresponding diol (AGD). Other experimental details can be found elsewhere[1].

2.3 Enantioselectivity of HNE Detoxification
Preparation of recombinant rat ALDH5A and ALDH2 enzymes and measurement of enzyme activity of ALDH5A is described elsewhere[5].

Because of the low K_M of ALDH2 for HNE, we measured the ALDH2 enzyme activity via monitoring the formation of HNEA by liquid chromatography – tandem mass spectrometry (LC-MS/MS) when determining K_M and V_{max} parameters as described previously with some modifications[3]. LC-MS/MS system consisted of an Agilent 1100 series HPLC system (Agilent Technologies, Santa Clara, CA) coupled to an API 3000 electrospray (ESI) triple quadrupole mass spectrometer (MDS Sciex, Concord, Canada). A 10 μL portion of the sample was injected onto a chromatographic column Luna C8(2) 150 × 2.1 mm i.d., 3 μm, (Phenomenex, Torrance, CA). HNEA eluted at 4.4 min in isocratic mode in the mobile phase ACN-30 μM ammonium acetate, pH 3.8 (45:55, v/v), at a flow rate of 150 μL/min.

2.4 Direct and Indirect HPLC Enantioseparation of HNEA
Derivatization of HNEA enantiomers using (1*S*,2*S*)-(+)-2-amino-1-(4-nitrophenyl)-1,3-propanediol (ANPAD, "dextrobase") in the presence of the coupling agent *N*-(3-

dimethylaminopropyl)-*N'*-ethylcarbodiimide hydrochloride (EDC) and the additive 1-hydroxybenzotriazole (HBT) is described elsewhere[6]. Indirect separation of HNEA-ANPAD diastereomers was performed using an RP Spherisorb ODS2 250 mm×4.6 mm I.D., 5 μm (Waters). HNEA-ANPAD diastereomers were separated isocratically in a mobile phase consisting of MeOH–5mM ammonium acetate, pH 7.0 (39:61, v/v), followed by a washing gradient program. The mobile phase flow rate was 1.5 mL/min and absorbance was monitored at 211 nm. The injection volume was 80 μL.

Direct separation of HNEA enantiomers was performed using a CSP Chiralpak AD-RH 150 mm×2.1 mm I.D., 5 μm (Chiral Technologies, West Chester, PA, USA). The mobile phase consisted of MeOH–ACN–5mM ammonium acetate, pH 3.5 (52:5:43, v/v/v) and the flow rate was 0.1 mL/min. Absorbance was monitored at 210 nm. The injection volume was 20 μL.

3. Results and Discussion
3.1 Determination of Enantioselectivity of Microbial Epoxide Hydrolases Using Gas Chromatography

Chiral GC-FID methods were developed and optimized for determination of various epoxides and diols (Fig.1). Highly polar diols were derivatized to corresponding acetonides. Conditions for analysis were optimized, including selection of CSP, optimization of column temperature program and optimization of derivatization conditions (for final conditions see experimental section). Developed methods were successfully applied for the determination of enantioselectivity of microbial epoxide hydrolases.
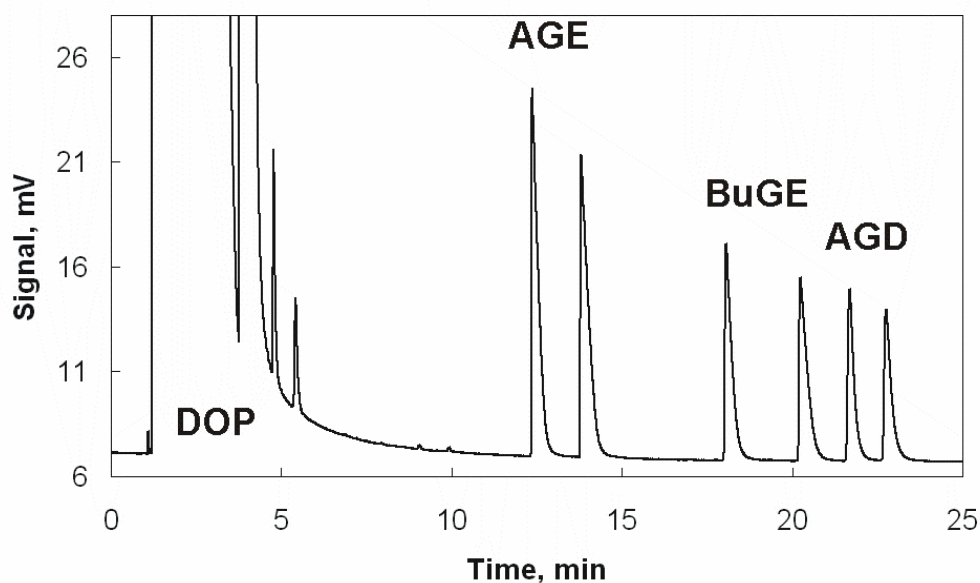
Fig.1 GC-FID separation of AGE and AGD derivatized to its acetonide (both $c_{enantiomer}$ = 8 mM). Butyl glycidyl ether (BuGE) was used as an internal standard ($c_{enantiomer}$ = 3.5 mM). Elution order of the enantiomers was not determined, because optically pure AGE, AGD and BuGE were not available. 2,2-dimethoxypropane (DOP) is derivatization and extraction agent. *Chromatographic conditions are described under experimental section.*

3.2 Enantioselectivity of HNE Detoxification

Recombinant rat ALDH5A and ALDH2 containing *N*-terminal polyhistidine tags were prepared as described elsewhere[5]. During the affinity chromatography, six histidine tagged proteins interact with nickel immobilized on nitrilotriacetic acid agarose (Ni-NTA Agarose) stationary phase. Proteins of just over 50 kDa were obtained as judged by SDS-PAGE analysis. Enzyme kinetics measurement of oxidation of HNE enantiomers by ALDHs and by rat brain mitochondria lysate were performed using UV spectrometry,

HPLC and LC-MS/MS. Based on kinetic parameters of purified recombinant enzymes, it was concluded, that rat ALDH5A enantioselectively oxidized (R)-HNE, whereas rat ALDH2 was not enantioselective.

3.3 Direct and Indirect HPLC Enantioseparation of HNEA

Direct and indirect RP-HPLC methods for enantioseparation of HNEA were developed and validated.

The indirect separation method was based on the derivatization of HNEA enantiomers with the chiral derivatization agent ANPAD in a phosphate buffer–methanol (MeOH) mixture in the presence of the coupling agent EDC and the additive HBT. Various RPs were screened for efficiency to separate HNEA-ANPAD diastereomers. Optimal separation conditions were achieved using a stationary phase Spherisorb ODS2 and mobile phase MeOH–5mM ammonium acetate, pH 7.0 (39:61, v/v). (R)- and (S)-HNEA-ANPAD eluted at 40 and 43 min, respectively, with resolution $R_s = 2.26$.

The direct enantioseparation of HNEA was performed using saccharide-based CSP Chiralpak AD-RH and ternary mobile phase MeOH–ACN–5mM ammonium acetate, pH 3.5 (58:4:38, v/v/v). Resolution R_s of (R)- and (S)-HNEA was 1.78. Validation parameters of both direct and indirect separation methods were determined, including linear range, LOQ, precision and stability[6]. The accuracy of enantiomeric ratio of the mixture (ER) was estimated by analyzing enantiomerically enriched samples containing various ER of HNEA. Difference in ER obtained by direct and indirect separation method was less than 0.7%, showing excellent accuracy. The indirect separation method was applied for determination of ER of HNEA formed in rat brain mitochondria by enzymatic oxidation of HNE. Oxidation of 160 μM rac-HNE by aldehyde dehydrogenases present in rat brain mitochondria led to (R)-enantioselective formation of HNEA.

Finally, conditions for direct enantioseparation of HNEA using LC-ESI-MS/MS were optimized (Fig.2). Determination of HNEA was linear in the range of 0.4 – 25 pmol with $r^2 = 0.9988$ for both enantiomers. As an internal standard, isotopically labeled d_{11}-HNEA was used.
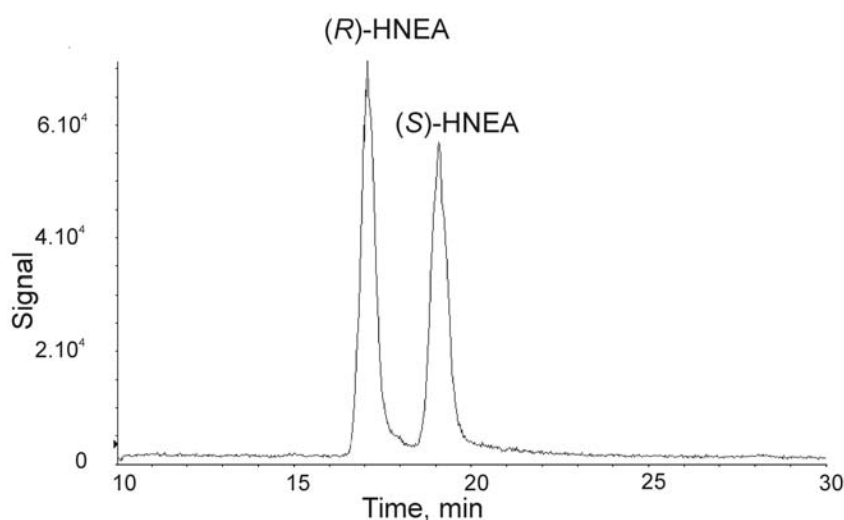
Fig.2 LC-ESI-MS/MS separation of (R)- and (S)-HNEA (both 500 nM) spiked into rat brain homogenate and purified by solid phase extraction (SPE). *20 μL of sample was injected onto CSP Chiralpak AD-RH 150 mm×2.1 mm I.D., 5 μm. Mobile phase ACN-0.1% acetic acid (24:76, v/v) was used with flow rate 0.1 mL/min. HNEA enantiomers were detected by tandem mass spectrometry in multiple reaction mode (MRM) using 171.2/99.2 parent/daughter ions.*

4. Conclusion

Chiral separation methods were developed and used as a tool for answering emerging questions in biomedicine and biotechnology. Screening of enantioselectivity of epoxide hydrolases produced by various microorganisms was performed and enantioselective enzymes were found using chiral GC on cyclodextrine-based stationary phases. Enantioselective metabolism of lipid peroxidation product HNE was studied using enzyme kinetic measurement and chiral liquid chromatography. Difference in ability to detoxify individual HNE enantiomers by ALDHs was found.

Acknowledgment

References

[1] Kotik M.; Brichac J.; Kyslik P.: *J. Biotechnol. 120 (2005), 364-375*.
[2] Kubatova A.; Honzatko A.; Brichac J.; Long E.; Picklo M.J.: *Redox. Rep. 12 (2007), 16-19*.
[3] Honzatko A.; Brichac J.; Murphy T.C.; Reberg A.; Kubatova A.; Smoliakova I.P.; Picklo M.J., Sr.: *Free Radical Biol. Med. 39 (2005), 913-924*.
[4] Honzatko A.; Brichac J.; Picklo M.J.: *J. Chromatogr. B Analyt. Technol. Biomed. Life. Sci. 857 (2007), 115-122*.
[5] Brichac J.; Ho K.K.; Honzatko A.; Wang R.; Lu X.; Weiner H.; Picklo M.J., Sr.: *Chem. Res. Toxicol. 20 (2007), 887-895*.
[6] Brichac J.; Honzatko A.; Picklo M.J.: *J. Chromatogr. A 1149 (2007), 305-311*.

DETERMINATION OF HERBAL ANTIOXIDANTS

Petr Dobiáš, Martin Adam and Karel Ventura

University of Pardubice, Faculty of Chemical Technology, Department of Analytical Chemistry, Nám. Čs. legií 565, Pardubice, Czech Republic; email: peejay1@seznam.cz

Abstract

The method for HPLC-UV analysis of antioxidant mixture (esculetin, 7-hydroxycoumarine, scopoletin, rutin, xanthotoxin, 5-methoxypsoralen and quercetin) was developed. Ultrasonic extraction methods were used for isolation of these antioxidants from these plants - *Mentha longifolia L.*, *Mentha spicata*, *Ruta graveolens*, *Plantago lanceolata L.* and *Coriandrum sativum*. Both of these methods, ultrasonic probe and ultrasonic bath method, were optimised and compared.

Keywords

Antioxidant; High-Performance Liquid Chromatography; Ultrasonic Extraction

1. Introduction

The terms antioxidants, antioxidative activity and free radicals are popular for nutritionists and other health professionals[1]. The last few years it has been published a lot of information about the role of oxidative stress causing[2], and the potential therapeutic role of antioxidants preventing, a number of serious diseases such certain cancers[3] or cardiovascular diseases[4].

Free radicals are very reactive compounds[5], which are formed in human organism owing to external environment (smoking, exhaust gases, UV radiation and stress) and also internal environment (purine metabolism, adrenaline synthesis). Activity of these matters is tied by antioxidants. These decrease probability of free radicals creation or divert them to less reactive or non-reactive states[6].

Antioxidants can be divided to 2 groups, synthetic and natural. In almost all plants there can be discovered natural antioxidants[7]. The most important groups of natural antioxidants are vitamin E (tocopherols), flavonoids and coumarines[8]. Synthetic antioxidants are usually prepared in laboratories and mostly out of other chemical components. In the food industry adding natural antioxidants have appeared as an alternative to synthetic antioxidants and these are now generally preferred by consumers.

Ultrasonic extractions in liquid and gas environment are prejudiced by cavitation factor and by microfluctuation or surface instability[9] which is formed on liquid-liquid or gas-liquid interface of phases. The grinded sample is mixed with the suitable solvent and is placed into the ultrasonic bath where the working temperature and extraction time are set[10]. Also ultrasonic probe can be used. Moreover, it allows prejudicing the extraction by amplitude selection[11].

2. Experimental part

Analysed plant samples were provided by Botanicus s.r.o. (Ostrá, Czech Republic). Those were *Mentha longifolia L.*, *Mentha spicata*, *Ruta graveolens*, *Plantago lanceolata L.* and *Coriandrum sativum*. Each plant was divided to leaves, flowers and stems, which were dried in laboratory temperature. These were stored in dark vessels in room temperature. Samples of leaves, which were used for extractions, were powdered in grinding mortar because of better extraction.

Plant sample amount (cca 0.75 g) was inserted into glass flask and 40 ml of solvent (30 % ACN) was added. Then the flask was placed into ultrasonic bath. Extraction was

carried out in the temperature 25 °C for 10 minutes. The frequency was 35 kHz. Ultrasonic bath SONOREX RK 31 from Bandelin electronic GmbH & Co. KG (Berlin, Germany) was used. Obtained extract was filtrated through Target, PTFE 0.45 μm filter (Fisher Scientific, Pardubice, Czech Republic). This extract was analysed by HPLC-UV.

By ultrasonic probe extraction method the plant sample amount (cca 0.75 g) was placed into glass homogenization vessel, which has three shoulders. Then 50 ml of solvent (30 % ACN) was added. After this the ultrasonic probe was inserted. Extraction was 25 minutes long, the amplitude was set at 60 % (equal to 90 W), without pulse changing and without controlled temperature. Obtained extract was filtrated again trough filter paper and Target, PTFE 0.45 μm filter. Ultrasonic probe SONOPULS HD 3200 for 2-1000 ml from Bandelin electronic GmbH & Co. KG (Berlin, Germany) was used. It allows set homogenization time, amplitude and pulsation. The instrument is equipped with titan probe (SH 70 G, 65 % maximum amplitude – 98 W) and homogenization vessel (thermostatic KG 3 and circulation RZ 3).

Plant extracts were analysed by HPLC-UV method. Liquid chromatograph GBC LC 1445 with LC 1150 pump, ERC-3415 degasser, LC 1650 detector and LC 1210 UV detector (everything from GBC, Australia) were used. It was also used LiChrospher® 100 CN (5 μm) column with LiChrospher® 100 CN (5 μm) guard column in LiChroCart® 250-4 HPLC-Cartridge implementation from Merck (Darmstadt, Germany). The results were evaluated by WinChrom 1.35 software (GBC, Australia). Gradient was formed from 2 mobile phases, A (ACN) a B (H₂O): 0 – 20 minutes 95 % to 90 % mobile phase A, 20 – 50 minutes 90 % to 0 % mobile phase A. 1 ml/minute flow rate was used. Antioxidants were detected by UV-detector in 335 nm (esculetin, 7-hydroxycoumarine and scopoletin) and 235 nm (rutin, xanthotoxin, 5-methoxypsoralen, quercetin) wavelengths. Quantification was performed by standard addition method. Injected volume was 20 μl. Antioxidant standard mixture chromatogram is on figure 1.

HELIOS Gamma UV–Vis spectrometer (Thermo Fisher Scientific, Inc., Waltham, USA) was used for wavelength detection of each antioxidant.
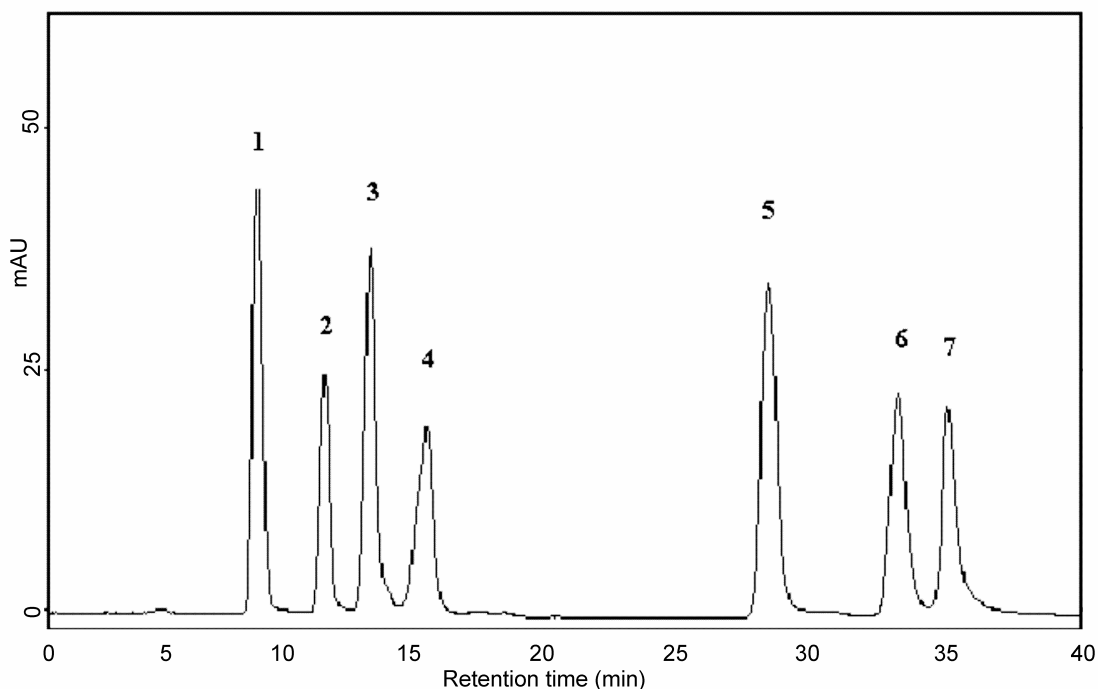
Fig.1 Chromatogram of antioxidant standards. *1) esculetin, 2) 7-hydroxycoumarine, 3) scopoletin, 4) rutin, 5) xanthotoxin,6) 5-methoxypsoralen, 7) quercetin*

3. Results and discussion

Then antioxidant standard UV spectra were measured because of choosing wavelengths for its detection during HPLC analysis. UV spectra were measured between 200 - 400 nm and are shown on figures 2 and 3.

Optimisation of individual extraction parameters for each extraction method was made. First of all suitable solvent was chosen. Because of our previous experiences[12] the 30 % acetonitrile has been selected. By this solvent the highest amount of extracted antioxidants was obtained.
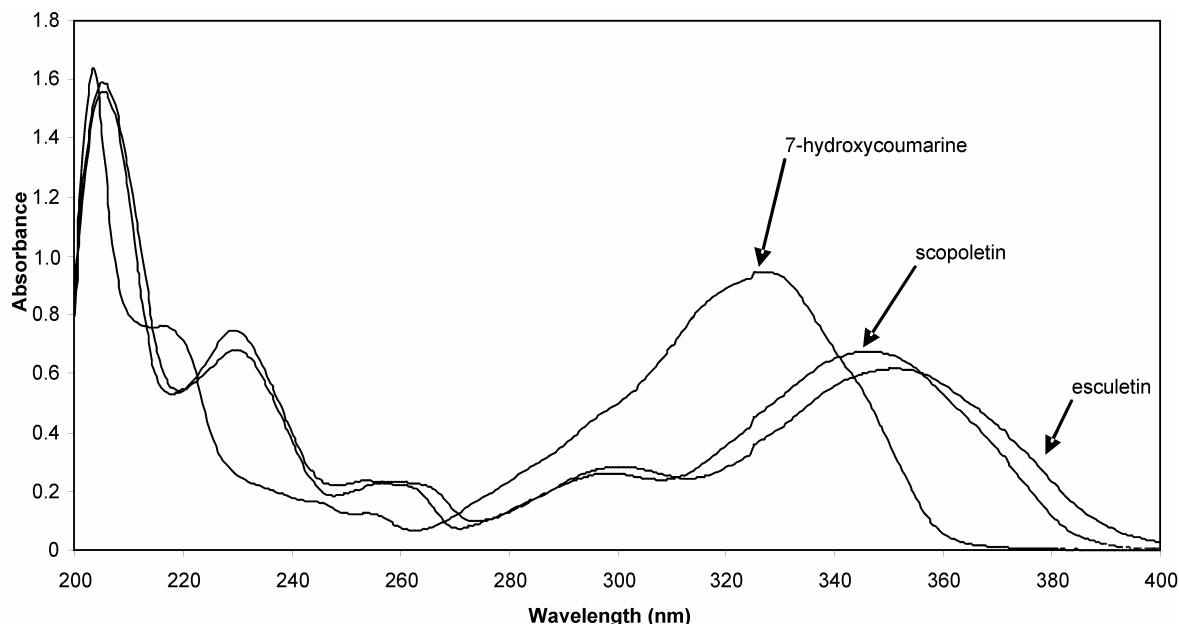
Fig.2 UV spectra of esculetin, 7-hydroxycoumarine and scopoletin

For UV detection of antioxidant mixture 2 wavelenghts – 335 nm for esculetin, 7-hydroxycoumarine and scopoletin and 235 nm for rutin, xanthotoxin, 5-methoxypsoralen and quercetin were chosen. These were selected in relation to sufficient sensitivity of the method.
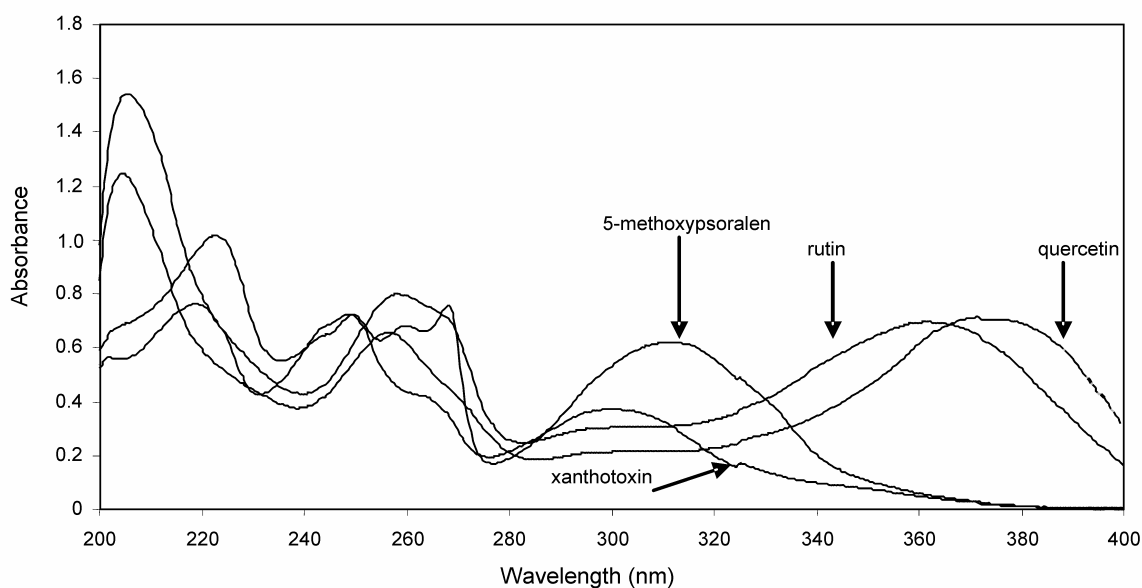
Fig.3 UV spectra of rutin, xanthotoxin, 5-methoxypsoralen and quercetin.

For the method with ultrasonic bath there were performed only the extraction time and temperature optimisations. Extraction temperature optimisation was made at first. These experiments were performed at 40 minutes using 30 % acetonitrile as the extraction solvent. For temperature optimisation the values of 25 (laboratory temperature), 35, 40, 45 and 55 °C were tested. For this optimisation 0.75 g of *Achyllea millefolium* dried flowers and 40 mL of the solvent were used. In this sample the rutin and quercetin antioxidants were contained. By the evaluation of these compounds the 25 °C was chosen and used for further experiments. As shown in the figure 4 the extraction of antioxidants in the ultrasonic bath was only slightly influenced by the selected temperature and maximum contents were gained at room temperature.
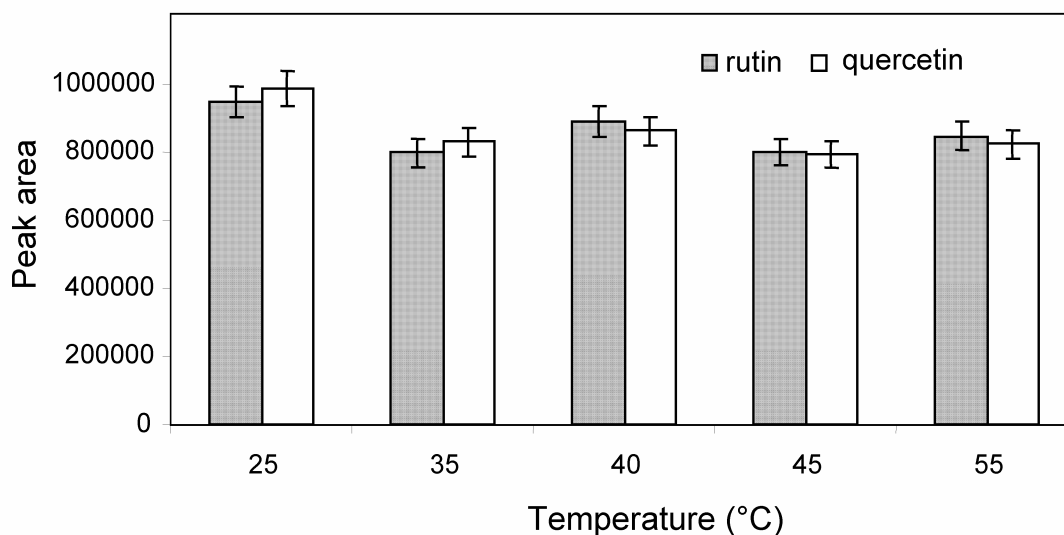
Fig.4 Quercetin and rutin quantity dependency on extraction temperature in the ultrasonic bath method.

The extraction time optimisation was performed at the optimised temperature using 30 % acetonitrile as the extraction solvent. Tested time periods were 5, 10, 15, 20, 25, 30, 40 and 60 min, respectively. The aliquot 0.75 g of *Achyllea millefolium* dried leaves was used for this optimisation, when quercetin and esculetin are included in. The appropriate peak areas were increasing until the extraction time of 25 min, which is depicted in the figure 5. Based on these results the extraction time 25 min was chosen for the future experiments. After this time period no improvements at the peak areas of target compounds were observed.
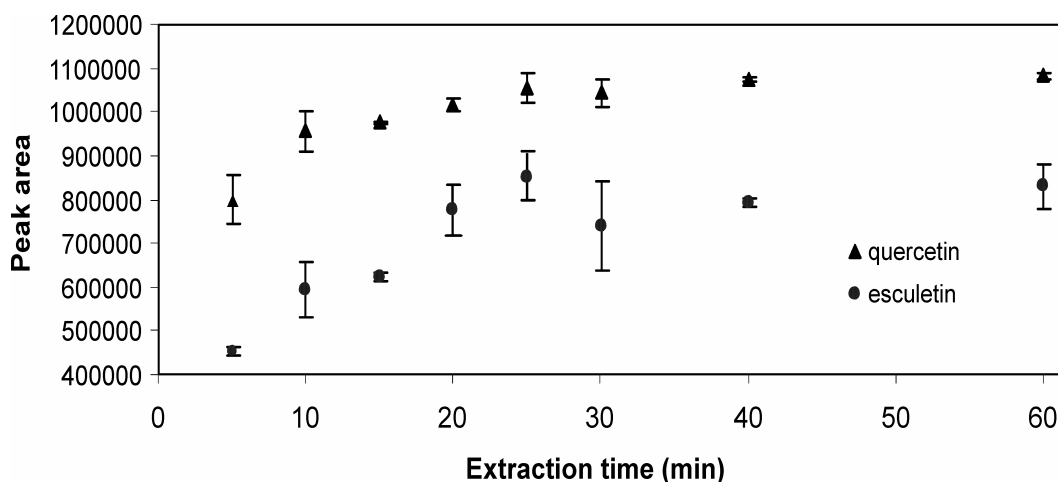
Fig.5 Quercetin and esculetin quantity dependency on extraction time in the ultrasonic bath method.

Also by the ultrasonic probe extraction method optimisations of each factor, which were extraction time, extraction temperature, generator's output (amplitude) and ultrasonic energy pulsation possibility, was made. Homogenization vessel, which has 3 shoulders, was used, because of better sample circulation and extraction recovery. It was necessary to change solvent volume to 50 ml, but the sample weight was used the same as by ultrasonic bath method. As optimised extraction time was chosen 25 minutes again, as optimised temperature was chosen room temperature also. Extractions were made without pulsation using 60 % amplitude, which equals to 90 W generator output.

Sample amount was chosen 0.75 g because of expected antioxidant quantity. Ultrasonic bath method values are shown in table 1. Ultrasonic probe values are shown in table 2.

Table 1 Antioxidant contents in herbs extracted by ultrasonic bath.

	Antioxidant content [mg/100 g of dried leaves]				
	R. graveolens	*C. sativum*	*P. lanceolata*	*M. spicata*	*M. longifolia*
esculetin	< LoQ*	< LoQ	441.3 ± 8.2	< LoQ	< LoQ
7-hydroxy-coumarine	< LoQ	< LoQ	< LoQ	< LoQ	< LoQ
scopoletin	< LoQ	< LoQ	< LoQ	165.7 ± 8.5	45.26 ± 5.2
rutin	1180 ± 45	245.54 ± 3.5	< LoQ	156.7 ± 7.8	246.6 ± 2.3
xanthotoxin	91.1 ± 3.6	< LoQ	< LoQ	< LoQ	< LoQ
5-methoxy-psoralen	133.2 ± 5.3	< LoQ	< LoQ	< LoQ	< LoQ
quercetin	321.8 ± 5.1	55.67 ± 2.6	< LoQ	< LoQ	< LoQ

* *< LoQ ... under limit of quantification*

Table 2 Antioxidant contents in herbs extracted by ultrasonic probe.

	Antioxidant content [mg/100 g of dried leaves]				
	R. graveolens	*C. sativum*	*P. lanceolata*	*M. spicata*	*M. longifolia*
esculetin	< LoQ*	< LoQ	352.7 ± 8.7	< LoQ	< LoQ
7-hydroxy-coumarine	< LoQ	< LoQ	< LoQ	< LoQ	< LoQ
scopoletin	< LoQ	< LoQ	< LoQ	101.7 ± 8.2	39.36 ± 5.1
rutin	890 ± 23	210.56 ± 8.7	< LoQ	102.3 ± 6.2	210.4 ± 5.9
xanthotoxin	81.8 ± 4.7	< LoQ	< LoQ	< LoQ	< LoQ
5-methoxy-psoralen	77.1 ± 2.4	< LoQ	< LoQ	< LoQ	< LoQ
quercetin	231.1 ± 6.3	42.97 ± 2.5	< LoQ	< LoQ	< LoQ

* *< LoQ ... under limit of quantification*

Chromatogram of *Ruta graveolens* obtained by the ultrasonic bath method is presented on figure 6.

4th International Student Conference: "Modern Analytical Chemistry"
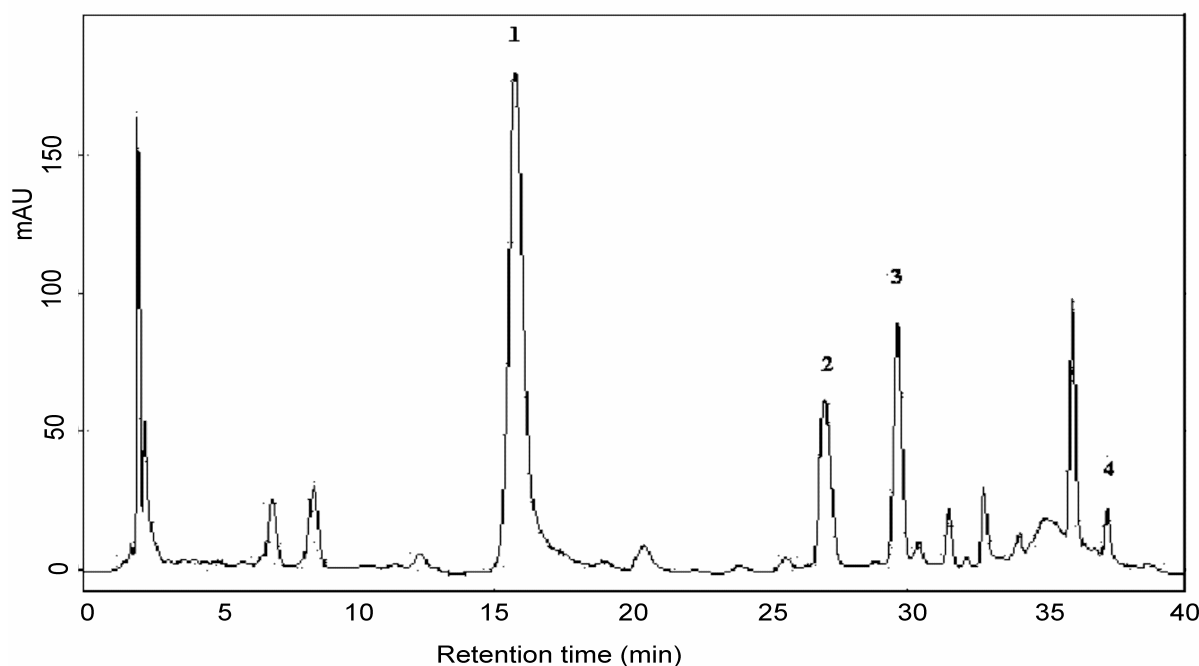
Fig.6 *Ruta graveolens* chromatogram gained by the ultrasonic bath method. *1) rutin, 2) xanthotoxin, 3) 5-methoxypsoralen, 4) quercetin*

Also detection limits (LoD) for each antioxidant were measured and then limits of quantification (LoQ) were counted. These formulas were used:

$$LoD = 3 \cdot \sigma$$

$$LoQ = 10 \cdot \sigma$$

σ is retention time signal noise for each antioxidant. Results are shown in table 3.

Table 3 Limits of detection and quantification for each antioxidant.

antioxidant	LoD (ng/ml)	LoQ (ng/ml)
esculetin	73,8	245,1
7-hydroxycoumarine	55,6	185,2
scopoletin	85,8	285,8
rutin	65,3	217,4
xanthotoxin	26,4	87,9
5-methoxypsoralen	45,5	151,6
quercetin	37,2	123,9

4. Conclusion

Antioxidant identification and quantification was peformed in leaves of these plants - *Mentha longifolia*, *Mentha spicata*, *Ruta graveolens*, *Plantago lanceolata* and *Coriandrum sativum*. There were ultrasonic bath extraction and ultrasonic probe extraction methods used. Both methods were optimised. Gained extracts were analysed by the HPLC-UV method. Both extraction methods are simple and could be used for antioxidant extractions from plants. Higher values were reached by ultrasonic bath extraction method.

75

Acknowledgment

References

[1] Pelli K.; Lyly L.: *Antioxidants in the diet, Institut National de la Recherche Agronomique, France, 2003.*

[2] Kishk Y.F.M.; Al-Sayed H.M.A.: *LWT 40 (2007), 270.*

[3] Ningappa M.B.; Dinesha R.; Srinivas R.: *Food Chem. 106 (2008), 720.*

[4] Valko M.; Liefritz D.; Moncol J.; Cronin M.T.D.; Mazur M.; Telser J.: *Int. J. Biochem. Cell Biol. 39 (2007), 44.*

[5] Wu S.J.; Ng L.T.: *LWT accepted 2007.*

[6] Rodrígueza J.; Olea-Azara C.; Cavieresb C.; Norambuenab E.; Delgado-Castroc T.; Soto-Delgadoc J.; Araya-Maturanac R.: *Bioorgan. Med. Chem. 15 (2007), 7058.*

[7] Dall´Acqua S.; Cervellati R.; Loi M.C.; Innocenti G.: *Food Chem. 106 (2008), 745.*

[8] Cherng J.M.; Chiang W.; Chiang L.C.: *Food Chem. 106 (2008), 944.*

[9] Christian G.D.: *Analytical chemistry, John Wiley & Sons, New York, 1986.*

[10] Hromádková Z.; Ebringerová A.: *Ultrason. Sonochem. 10 (2003), 127.*

[11] Rial-Otero R.; Carreira R.J.; Cordeiro F.M.; Moro A.J.; Santos H.M.; Vale G.; Moura I.; Capelo J.L.: *J. Chromatogr. A 1166 (2007), 101.*

[12] Bajer T.; Adam M.; Galla L.; Ventura K.: *J.Sep. Sci. 30 (2007), 122.*

DETERMINATION OF LINCOMYCIN PRECURSORS IN FERMENTATION BROTH OF *STREPTOMYCES LINCOLNENSIS* USING HIGH PERFORMANCE LC WITH FLUORESCENCE DETECTION

<u>Zdeněk Kameník</u>[a,b], Dana Ulanová[a], Jan Kopecký[a], Karel Nesměrák[b] and Jana Olšovská[a]

[a] *Academy of Sciences of the Czech Republic, Institute of Microbiology, Vídeňská 1083, 142 20 Prague 4, Czech Republic; e-mail: <u>zdenek.kamenik@email.cz</u>*
[b] *Charles University, Faculty of Science, Albertov 8, 128 40 Prague 2, Czech Republic*

Abstract

   Two routine reversed-phase high performance liquid chromatography (HPLC) methods with fluorescence detection for determination of lincomycin precursors in fermentation broth of *Streptomyces lincolnensis* and genetically modified *Streptomyces lincolnensis* were developed. The first one enables simultaneous detection and quantitation of methylthiolincosamide (MTL) and N-demethyllincomycin (NDL), whereas the second one is suitable for 4-propylproline (PPL) analysis. Both methods are based on the pre-column derivatization of MTL and NDL with 4-chloro-7-nitrobenzofurazan (NBF) and PPL with *o*-phthaldialdehyde-2-mercaptoethanol (OPA). The methods are relatively simple due to the lack of fermentation broth purification step. Both methods were successfully validated with LLOQ values of 2.50, 3.75 and 3.75 for MTL, NDL and PPL, respectively.

Keywords

   Methylthiolincosamide; N-demethyllincomycin; propylproline; o-phthaldialdehyde; 4-chloro-7-nitrobenzofurazan; derivatization; fluorescence detection; Streptomyces lincolnensis

1. Introduction

   Lincomycin produced by *Streptomyces lincolnensis* and its semi--synthetic derivative clindamycin are widely used in the clinical practice. The aglycone PPL and the sugar moiety MTL are two basic precursors in lincomycin biosynthesis. These two parts are condensed to NDL in a reaction catalyzed by NDL-synthetase. Finally, NDL is converted to lincomycin A by S-adenosyl methionine dependent NDL-methyltransferase. The complete lincomycin biosynthetic pathway has not been described yet. At the present time lincomycin biosynthetic genes are studied using REDIRECT inactivation kit[1]. Determination of PPL, MTL and NDL in mutant strains helps to elucidate single steps in the pathway.

   The complex matrix of fermentation broth including organic and inorganic compounds makes the main problem in developing the method for MTL, NDL and PPL analysis. Within the selectivity, the other requirement of developed method is high sensitivity, because the expected concentration level of precursors is about 10 μg ml^{-1}. Further, other criteria such as run time, price, equipment and simplicity are included.

   It has not been reported an analysis of neither PPL nor NDL, to date. Nevertheless, it is possible to adopt methods for determination of structurally related compounds including proline and lincomycin for PPL and NDL, respectively.

   Methods for analysis of proline based on the pre-column derivatization with subsequent fluorescence detection seem to be most suitable for PPL analysis considering selectivity (complex matrix) and sensitivity requirements. As far as NDL assay is

concerned, an analysis of another lincomycin precursor[2] - MTL - can be applied thanks to the presence of secondary amino group in its molecule. A different approach to NDL analysis, determination of lincomycin using UV detection and SPE purification[3], worths considering as well.

2. Experimental
2.1 Chemicals, standard solutions

Solvents used in HPLC were of HPLC gradient grade. Acetonitrile (ACN) was purchased from J.T. Baker (Holland), methanol from Merck (Germany). All other chemical including derivatization agents were obtained from Sigma (Germany). All chemicals were stored according to the producer instructions.

PPL, MTL and NDL standards were prepared at Institute of Microbiology, Academy of Sciences of the Czech Republic, their structure and purity were proved by nuclear magnetic resonance and mass spectrometry. The standard stock solutions were prepared in double distilled water at a concentration level of 1 mg ml^{-1}. The solutions were stable at 4 °C for 5 days.

2.2 Derivatization procedure
PPL

The following procedure was used to obtain optimal conditions for OPA derivatization of PPL. 100 µl of 10 mM solution of chloramin-T in 400 mM Na$_3$BO$_3$ (pH 9.5) and DMSO, 4:1 (v/v) was pre-heated in a water bath (70 °C) for 1 min. 100 µl of PPL standard or real sample was added, the mixture was mixed and heated at 70 °C for another minute. After that 100 µl of 300 mM NaBH$_4$ in 600 mM LiOH was added, the mixture was mixed, heated at 70 °C for 10 min and centrifuged at 13 400 ppm. 45 µl of the mixture was added to 10 µl of derivatization agent (5 mg of OPA diluted in 50 µl of ACN, 50 µl of 200 mM Na$_3$BO$_3$ - pH 9.5 and 4 µl of mercaptoethanol).

MTL, NDL

For MTL and NDL derivatization, 250 µl of 30 mg ml^{-1} NBF solution was mixed with 50 µl of 1 M NaHCO$_3$ and 200 µl of standard or real sample. The mixture was vortexed for 20 s, put in a water bath (70 °C) for 4 h and freezed at –20°C for 20 min.

2.3 Chromatographic conditions

HPLC analyses were performed with a Waters system equipped with flow controller 600 and autosampler 717, and Millenium 32 software was used for data processing. 25µl of sample mixture was loaded onto analytical C$_{18}$ (250 × 4.6 mm i.d.; particle size, 5 µm; Phenomenex) column kept at room temperature, connected to a security guard C$_{18}$ cartridge (30 × 20 mm i.d.; particle size, 5 µm; Phenomenex).

The mobile phase consisted of solvents A: 20 mM ammonium formiate, pH adjusted with NH$_4$OH (25 %) on the value of pH 4.7; acetonitril 10:1 (v/v) and B: acetonitril.

PPL

The linear gradient elution at a flow rate of 1.25 ml min^{-1} is described in tab. 1, the column effluent detected a scanning fluorescence detector 474 (λ_{ex} = 240 nm; λ_{em} = 417 nm) with a gain switch from 10 to 100 at 6 min of analysis.

MTL, NDL

The linear gradient elution at a flow rate of 1 ml min^{-1} is described in Table 1. The column effluent detected a scanning fluorescence detector 474 (λ_{ex} = 420 nm; λ_{em} =

525 nm) with gain set on the value of 100 for the whole analysis.

Table 1 Gradient elution.

PPL		MTL, NDL	
Time (min)	B (%)	Time (min)	B (%)
0	30	0	15
1	30	5	33
13	65	15	44
15	100	16	100
19	100	20	100
20	30	21	15

2.4 Method validation

Selectivity. Sample matrix without a content of PPL and sample matrix containing neither MTL nor NDL was used to evaluate the method selectivity.

Calibration curve. Calibration curves over linear ranges from 3.75 to 100 µg ml^{-1} for PPL, from 2.50 to 40.0 µg ml^{-1} for MTL and from 3.75 to 40.0 for NDL were determined. Stock solution of PPL (1 mg ml^{-1}) or MTL and NDL (a mixture; 0.5 mg ml^{-1} of both) was spiked into a matrix without a content of the spiked compound to required concentrations. The applied range is sufficient with regards to expected levels of analytes in real samples.

Lower limit of quantification. LLOQ was determined as the lowest concentrations of PPL, MTL and NDL quantified with precision (RSD) and accuracy lower than 20 %. Six replicates of samples spiked with PPL (3.75 µg ml^{-1}), MTL (2.50 µg ml^{-1}) and NDL (3,75 µg ml^{-1}), respectively, concentrations at which the signal-to-noise ratio was found to be larger than 10, were measured.

Accuracy and precision. To evaluate the precision and accuracy of the assay, quality control samples were prepared at concentrations of 3.75, 40.0, 100; 2.50, 15.0, 40.0 and 3.75, 15.0, 40.0 µg ml^{-1} for PPL, MTL and NDL, respectively. For precision and accuracy six replicates of quality control samples at each concentration were assayed on the same day (intra-day assay).

3. Results and discussion
3.1 Method development
PPL

Several derivative agents including DNS-Cl, FMOC, AQC and OPA were evaluated. Following its characteristics and pre-experiments, OPA was chosen for PPL derivatization, even though it reacts with primary amino groups only and therefore PPL has to be oxidized using chloramin-T before the derivatization[4].

In order to achieve as low LLOQ as possible, several steps in the derivatization procedure were modified, concentration of chloramin-T, NaBH$_4$ and OPA, temperature and time of oxidative reaction, pH of Na$_3$BO$_3$ solution and the amount of added sample into the reaction. The parameters that showed a necessity of modification are presented further.

Concentration of OPA. Solution of OPA agent on three concentration levels, 5.0, 25, 50 µg ml^{-1}, was tested. The volume of added mercaptoethanol remained unaltered in order not to change the rate of the amount of substance between OPA and MCE. The usage of ten times more concentrated OPA solution yielded 2.3 times higher response. Therefore 50 mg ml^{-1} OPA solution was used for further derivative reactions.

Temperature of oxidative reaction. The influence of derivatization reaction temperature on oxidative reaction in the interspace from 50 °C to 80 °C with 5 °C steps

was tested. The efficiency of oxidation increased from 50 °C to 70 °C, after that it stagnated or even slightly decreased. Reaction temperature of 70 °C was determined as the most suitable.

pH of Na_3BO_3 solution. pH condition of oxidative and derivative reactions was tested simultaneously in the range from pH 7.0 to 10 with resulting pH 9.5 as optimal.

Sample volume added to the reaction. The excess of oxidative and derivative agents was tested simultaneously. To simplify the experiment, it was proceeded as a dependence of derivatized product concentration on the amount of added sample into the reaction. Sample volumes of 25, 50, 100, 125 and 150 μl were examined resulting in the optimal volume of 100 μl.

In order to develop a suitable and relatively simple mobile phase supporting efficient separation of PPL derivate from matrix interferents, several buffers were examined, potassium phosphate, natrium borate and ammonium formiate. The usage of ammonium formiate yields the best separation efficiency expressed by the resolution. In addition, ammonium formiate is compatible for possible MS experiments. It was ascertained that the separation is independent on pH of mobile phase (buffer). Therefore, ammonium formiate of pH 4.7 was selected. The value is reliable not only for PPL derivate separation, but also for column long lifetime.The sample was eluted by gradient elution, which was modified in order to separate the analyte from the matrix.

Detection. There were compared three published wavelengths[4,5,6] and as optimal λ_{ex} = 336 nm and λ_{em} = 425 nm was chosen. The gain of the detector was set on the value of 10 with a switch to 100 at 6 min of the analysis to avoid response overloading caused by the matrix and to obtain maximum sensitivity for PPL.

MTL, NDL

The method for lincomycin determination[3] is not applicable to NDL analysis due to matrix interference. However, NDL can be derived with a fluorescent agent as well as MTL in the already existing method[2]. Moreover, application of this method for NDL analysis enables simultaneous determination of both lincomycin precursors.

Three parameters of derivatization reaction (reaction temperature, time and sample volume added to the reaction) were optimized to obtain the most sufficient conditions for MTL as well as NDL derivatization.

Reaction temperature. The temperature was tested in the range from 55 °C to 75 °C in 5 °C steps. It was found out that the derivatization of NDL is independent on temperature, whereas derivatization of MTL yields better results with increasing temperature. Therefore, the temperature of 75 °C was chosen for MTL and NDL simultaneous derivatization.

Reaction time and sample volume added to the reaction. The reaction was tested for 1-5 h duration in 1 h steps; the volume of added sample was tested from 200 to 400 μl in 50 μl steps. It was shown that both parameters sufficient for MTL derivatization, reaction time of 4 h and 200 μl of added sample[2] are reliable for NDL as well.

Aside from potassium phosphate buffer[2], ammonium formiate and sodium borate were examined resulting a good efficiency of separation if ammonium formiate, which is also compatible with MS, was used. It was shown that the separation of MTL as well as NDL derivatives is pH independent so the value of pH 4.7 was chosen on the basis of the buffer stability and column maintenance.

Furthermore, the elution gradient was modified to separate analytes from the matrix.

3.2 Method validation

Selectivity. The selectivity was performed to determine the optimal conditions for

quantification of PPL, MTL and NDL in fermentation broth of *Streptomyces lincolnensis*. Under chromatographic conditions described in this study all three analytes were well separated. No significant interferring components of sample matrix were detected by fluorescence detection under chromatographic parameters used. See Fig.1 and 2.
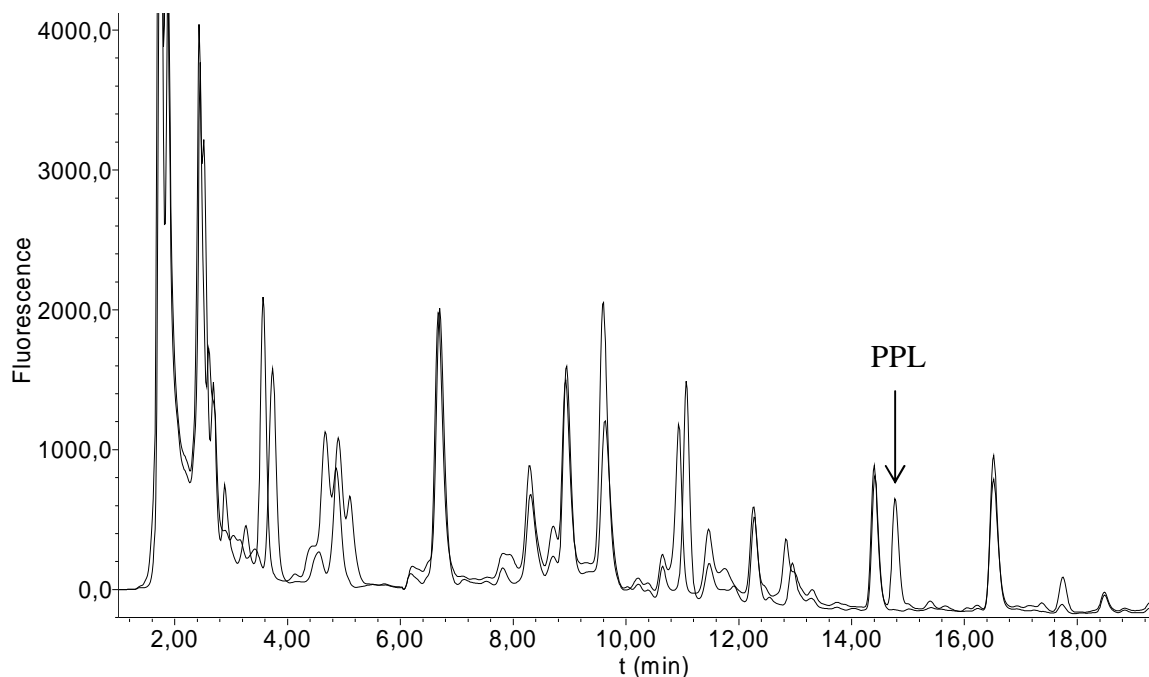
Fig.1 Overlay of PPL (30 μg ml⁻¹) spiked in matrix (fermentation broth of *S. lincolnensis*) and matrix itself.
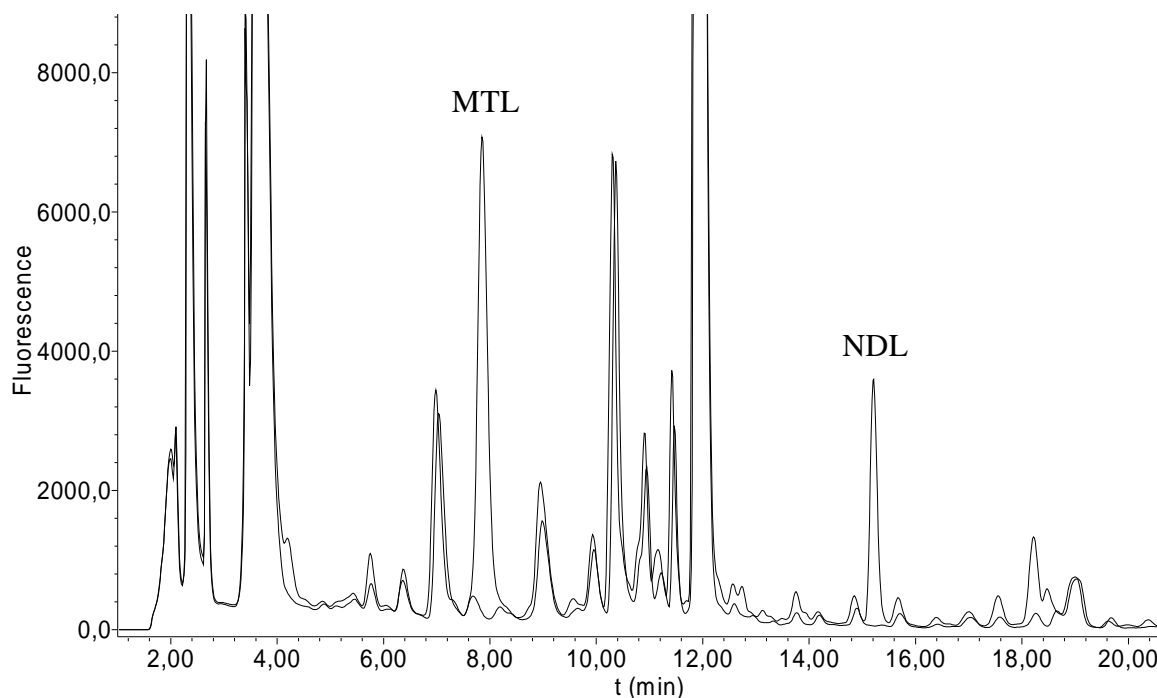
Fig.2 Overlay of MTL and NDL (30 μg ml⁻¹) spiked in matrix (fermentation broth of S. lincolnensis) and matrix itself.

Calibration curve and LLOQ. The calibration curves were prepared at six concentration levels, 3.75, 7.50, 15.0, 30.0, 50.0, 100; 2.50, 5.00, 7.50, 15.0, 20.00, 40.0 and 3.75, 5.00, 7.50, 15.0, 20.0, 40.0 μg ml⁻¹ for PPL, MTL and NDL, respectively. All characteristics of the calibration curves including LLOQ values are shown in table 2.

Table 2 Parameters of calibration curves and LLOQ values for PPL, MTL and NDL.

Analyte	Retention time (min)	Regression equation	Correlation coefficient	LLOQ ($\mu g\ ml^{-1}$)
PPL	14.7	$2.19 \cdot 10^5 - 4.38 \cdot 10^4$	0.9995	3.75
MTL	7.4	$2.38 \cdot 10^6 - 1.55 \cdot 10^6$	0.9999	2.50
NDL	14.9	$9.14 \cdot 10^5 - 2.64 \cdot 10^6$	0.9998	3.75

Accuracy and precision. The accuracy and precision of the assays are summarized in table 3. The accuracy for PPL ranged from 98.4 to 112 % with the precision (RSD) from 2.6 to 6.5 %, for MTL from 98.0 to 109 % with the precision (RSD) from 2.4 to 8.8 % and for NDL ranged from 99.0 to 111 % with the precision (RSD) from 1.9 to 4.9 %.
These results indicate that the presented method has satisfactory accuracy, precision and reproducibility.

Table 3 Precision and accuracy of PPL, MTL and NDL in fermentation broth of *Streptomyces lincolnesis* (n=6).

	Spiked ($\mu g\ ml^{-1}$)	Measured ($\mu g\ ml^{-1}$)	RSD (%)	Accuracy (%)
PPL	3.75	3.69	6.53	98.4
	40.0	44.3	2.56	111
	100	112	3.68	112
MTL	2.50	2.57	8.82	103
	15.0	16.4	2.40	109
	40.0	39.2	4.69	98.0
NDL	3.75	3.93	4.32	105
	15.0	14.8	1.94	99.0
	40.0	44.3	4.87	111

4. Conclusion

Two assays for three lincomycin precursors, MTL, NDL and PPL, are described. The methods are selective, sensitive and reproducible. Last but not least advantages of the newly developed assays are the simplicity and high-throughput.

Acknowledgment

References

[1] Gust B.; Challis G.L.; Fowler K.; Kieser T.; Chater K.F.: *Proceedings of the National Academy of Sciences of the United States of America* **100** *(2003), 1541-1546.*
[2] Yurek D.A.; Kuo M.S.; Li G.P.: *J. Chromatogr. A* **502** *(1990), 184-188.*
[3] Olsovska J.; Jelinkova M.; Man P.; Koberska M.; Janata J.; Flieger M.: *J. Chromatogr. A* **1139** *(2007), 214-220.*
[4] Cooper J.D.H.; Lewis M.T.; Turnell D.C.: *J. Chromatogr. A* **285** *(1984), 484-489.*
[5] Cunico R.L.; Schlabach T.: *J. Chromatogr. A* **266** *(1983), 461-470.*
[6] Wu G.: *J. Chromatogr. A* **641** *(1993), 168-175.*

IDENTIFICATION AND QUANTIFICATION OF SELECTED ESTROGENS USING HPLC METHOD

Lucie Loukotková[a], Daniela Zlesáková[a], Květa Kalíková[b], Eva Tesařová[b] and Zuzana Bosáková[a]

[a] *Department of Analytical Chemistry, Faculty of Science, Charles University in Prague, Albertov 2030, 128 43 Prague 2, Czech Republic*
[b] *Department of Physical and Macromolecular Chemistry, Charles University in Prague, Faculty of Science, Albertov 2030, 128 43 Prague 2, Czech Republic*

Abstract

A growing interest is focused on environmental contaminants, which may disrupt endocrine system of organisms. Estrogens are considered to belong to chemicals that negatively affect the endocrine system, even when present in very low concentrations. They are discharged into environment as a result of an increasing application of drugs, excretion of human metabolites etc. Although estrogens are present in very low amounts, their impact on certain fish and other wildlife and humans is significant.

Various methods have been developed for determination of estrogens. Due to the fact that low detection limits are required, these methods mostly involve MS or fluorescence detection hyphenated to a separation technique (GC, LC).

This work has been focused just on the separation. We have optimized and compared isocratic and gradient elution systems for separation of five estradiols, namely estrone (E1), estriol (E3), ethinylestradiol (EE), mestranol (M) and 17α-estradiol (αE2) in HPLC. The chromatographic systems have consisted of a C18 stationary phase and various mobile phases. The optimized mobile phase composition has been acetonitrile/water 40/60 (*v/v*) in the isocratic mode. However the analysis time of the last eluting analyte – mestranol – has been to long under isocratic conditions. Therefore, separation has been improved using gradient elution: starting from the same basic mobile phase and employing a linear gradient between 15th and 16th minute to 100% acetonitrile.

Keywords

Endocrine disruptors; estrogen hormones; HPLC analysis; isocratic elution; gradient elution

1. Introduction

A wide variety of artificial chemicals are currently being released into the environment subsequently contaminating precious global resources with potentially deleterious effects.[1] Some of these chemicals, such as endocrine disruptors (EDCs)[2], are connected with adverse effects on reproductive systems in wildlife and human, even when present at very low concentrations[3].

Endocrine disruptor is an exogenous substance or mixture that alters function(s) of the endocrine system and consequently, may cause adverse health effects in an intact organism, its progeny or its (sub)populations.[4] EDCs may have different mechanisms of action. They can mimic or antagonize functions of steroid hormones, disrupt biosynthesis or metabolism of steroids or alter hormone receptor populations. Modification of sexual development and reproductive function in reptiles, birds, amphibians, crustaceans and fish by environmental exposure to EDCs has been reported.[4] In mammals, the evidence of endocrine disruption is less unambiguous; however EDCs are believed to exert similar

83

effects on human reproductive health and also can be involved in the initiation of some hormone-dependent cancers[4].

The group of endocrine disruptors includes 4-nonylphenol (NP), which is the biodegradation metabolite of non-ionic surfactants that has been shown to be present in the environment (river water, sewage sludge and fish tissues). Another representative of the group of endocrine disruptors is bisphenol A (BPA) that is mainly used in the manufacture of polycarbonate plastics and epoxy resins. It is of great concern that these materials are used as food and beverage containers and as the lining of metal cans, from which BPA leaches into food.[3] Natural and synthetic hormones, such as 17β-estradiol (βE2), 17α-estradiol (αE2), estriol (E3), estrone (E1) and ethinylestradiol (EE), which is a synthetic contraceptive chemical, also belong to endocrine disruptors. The study of the metabolism of estrogens suggests that these compounds absorbed by intestine are glucuronidated and sulfated in liver and kidney and excreted as glucuronide and sulfate by urine[3].

Many techniques have been developed for determination of estrogens in water, sediment, tissue, plasma or human urine. Based on their principle, these techniques can be divided into three groups. The first one is biomonitoring (mostly using GloFish); the second group contains immunochemical methods such as enzyme-linked immuno-sorbent assay (ELISA)[5,8,9], radioimmunoassay (RIA) and flow injection analysis (FIA). The last techniques are represented by analytical separation methods such as gas chromatography or high-performance liquid chromatography, mostly with MS detection[1,7,11], MS/MS[10,12], UV or fluorescence detections[6,4]. Sample preconcen-tration or derivatization is usually required, as very low concentrations of the estrogens should be monitored in environmental samples.

Herein, we report a development of a simple HPLC method with UV detection for analysis of estradiol analogues that will be used for determination of these pollutants in natural- and wastewater samples.

2. Experimental
2.1 Reagents

Acetonitrile and methanol, both p.a., were purchased from Sigma-Aldrich (Steinheim, Germany). Deionised water was used throughout the experiments (Milli-Q water purification system Millipore, Milford, MA, USA).

Estrone, ethinylestradiol, 17α-estradiol, estriol and mestranol (M), for structures see Fig.1, all VETRANAL®, analytical standards, have been purchased from Sigma-Aldrich (Steinheim, Germany).

2.2 Instrumentation

The HPLC equipment - the Waters Alliance system (Waters Chromatography, Milford, MA, USA) comprised a Waters 2695 Separation Module, a Waters 2996 Photodiode Array Detector, a Waters 717plus Autosampler and a Waters Alliance Series column heater. Signal was processed and data were handled with the PC Empower software from Waters Chromatography (Milford, MA, USA). Commercially available steel column Supelcosil TM LC- 18-DB (250 x 4.6 mm I.D., octadecyl bonded to silica gel, particle size 5 μm) was purchased from Supelco (Bellefonte, Pennsylvania, USA).

2.3 Separation conditions

The mobile phases consisted of water and acetonitrile (ACN). The amount of the organic modifier present in the mobile phase was varied during the method optimalization experiments.

All the standards of estrogens (E1, αE2, EE, E3 and M, Fig.1) were diluted in water for optimalization process and in methanol for the LOD and LOQ determinations. (Higher

concentration than 50 μg/mL led to the sample precipitation in water.) The concentration of all the stock solutions of the standards was 1 mg/mL. The solutions were stored at 5 °C.

The mobile phase flow rate was 1.3 mL/min. Detection was performed at the wavelength of 200 nm. The measurements were carried out at the laboratory temperature of 20 °C.

Estrone (E1)

17α-estradiol (αE2)

Mestranol (M)

Estriol (E3)

17α-ethinylestradiol (EE)
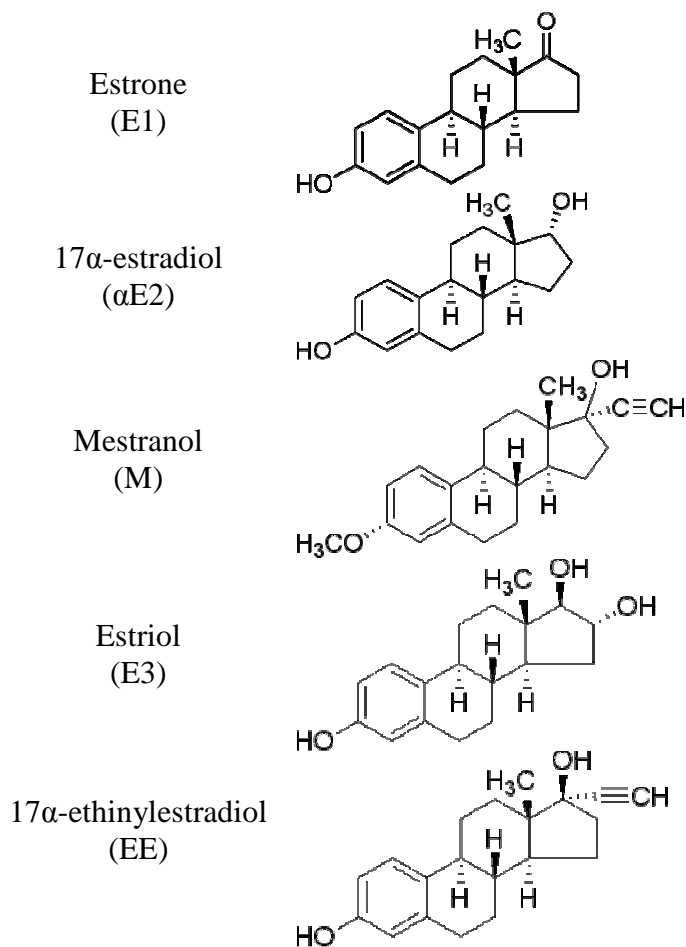
Fig.1 Structures of studied estrogen analogues.

3. Results and Discussion
3.1 Optimalization of separation conditions

Important endocrine disruptors - estrogens occur in wastewaters in very low concentrations. Therefore, a method for their analysis should involve a preconcentration step, mostly solid-phase extraction (SPE), and a suitable separation technique combined with sensitive MS or fluorescence detections.

This work deals just with the development and optimization of a simple HPLC method for determination of the estrogen derivatives. A Supelcosil TM LC-18-DB column was used as the separation stationary phase. The mobile phase contained acetonitrile and water and the content of the organic modifier was varied. Both isocratic and gradient elution modes were tested and compared. The flow rate was optimized as well.

When isocratic elution was performed, the optimized mobile phase composition found was ACN/water 40/60 (*v/v*). At the flow rate 1mL/min all the estrogens (E1, αE2, E3, EE) eluted within 20 minutes except of mestranol that had very long retention - 110 minutes. The retention time of mestranol decreased to 89 minutes when the flow rate was increased to 1.3 mL/min (Fig.2).
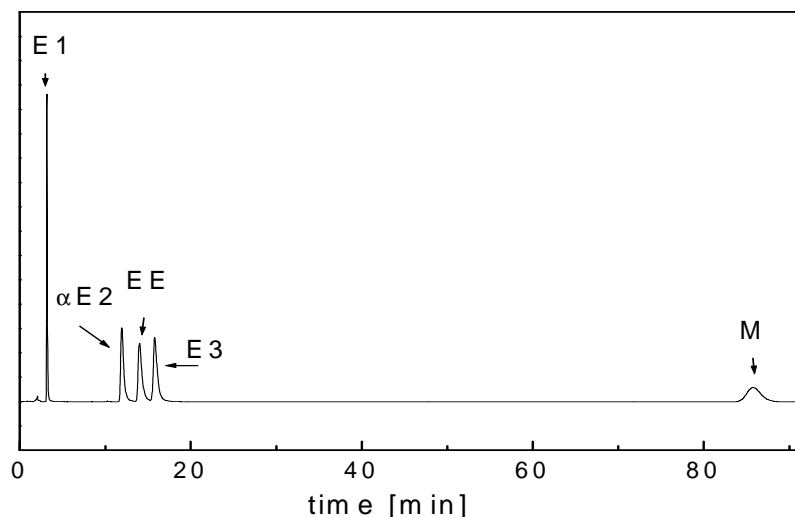
Fig.2 Chromatogram of separation of selected estrogens - estrone (E1), ethinylestradiol (EE), 17α-estradiol (αE2), estriol (E3) and mestranol (M). *Supelcosil TM LC-18-DB column (250 x 4.6 mm I.D.); mobile phase, ACN/water 40/60 (v/v); flow rate, 1.3 mL/min; UV detection, 200 nm; column temperature, 20 °C.*

Several types of gradient elutions can be used that result in improved separation of analytes. First of all the gradient of mobile phase composition, i.e. organic modifier contents, ionic strength or pH of the aqueous portion can be employed, but also temperature or even flow rate gradients can be performed. Linear, concave and convex concentration gradients were tested in this work (see Fig.3). The basic mobile phase composition was ACN/water 40/60 (*v/v*) in all cases and applying the gradient the amount of ACN was increased up to 100 % (for the gradients tested see Table 1). The linear gradient of ACN/water (*v/v*) mobile phase composition was chosen from the gradient profiles available as the next step in method optimization. ACN/water 40/60 (*v/v*) with the linear gradient to 100 vol. % of acetonitrile applied from 15 to 16 minute provided separation of all the analytes within 20 minutes. The mobile phase flow rate was kept at a constant value of 1.3 mL/min. Chromatogram of the separation under gradient elution is shown in Fig.4. Shorter retention and better peak shape and efficiency were obtained when gradient elution was employed.
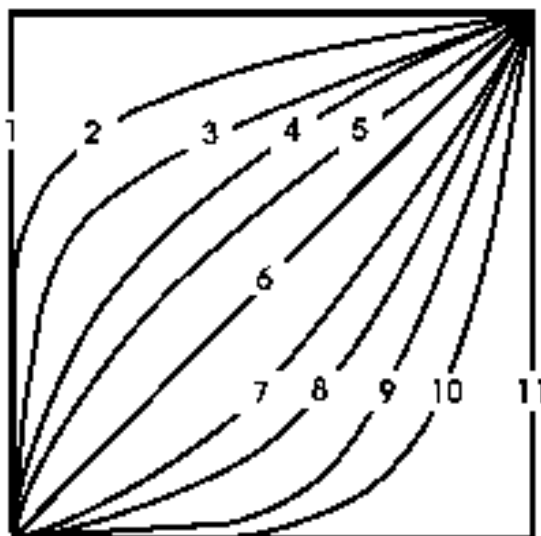
Fig.3 Gradient curves available on the instrument used.
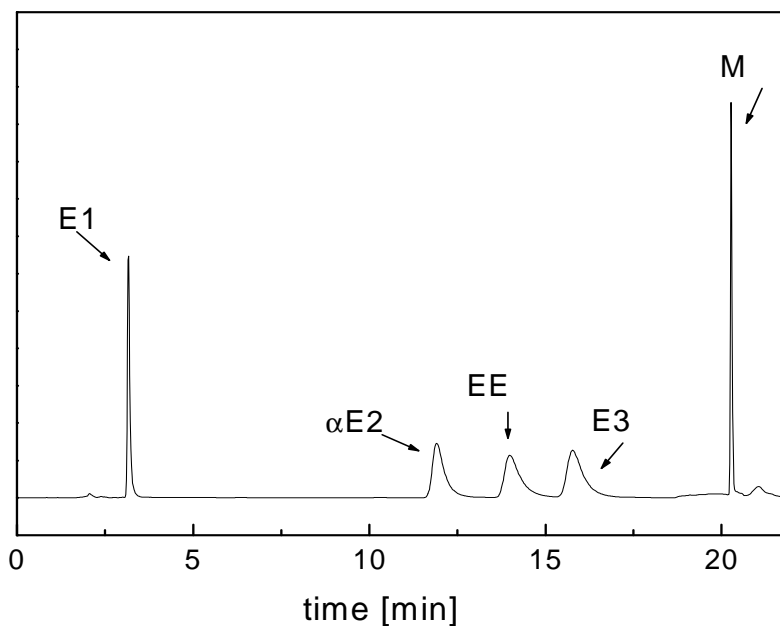
Fig.4 Chromatogram of the separation of selected estrogens - estrone (E1), ethinylestradiol (EE), 17α-estradiol (αE2), estriol (E3) and mestranol (M). *Supelcosil TM LC-18-DB column (250 x 4.6 mm I.D.); mobile phase, ACN/water 40/60 (v/v), 0. – 15. min, with a linear gradient to 100 vol. % of acetonitrile applied from 15. to 16. min; flow rate, 1.3 mL/min; UV detection, 200 nm; column temperature, 20 °C.*

Table 1 Gradient elution conditions tested in this work.
The basic mobile phase composition: ACN/water 40/60 (v/v), 0. – 15. min, with a linear gradient to 100 vol. % of acetonitrile; stationary phase, Supelcosil TM LC-18-DB column (250 x 4.6 mm I.D.); flow rate, 1.3 mL/min; UV detection, 200 nm; column temperature, 20 °C.

Gradient curve corresponding to Fig.3	Gradient type	Running time of the gradient
Nr. 6	Linear	16. - 17. minute
Nr. 6	Linear	15. - 16. minute
Nr. 6	Linear	13. - 16. minute
Nr. 2	Convex	16. - 17. minute
Nr. 10	Concave	16. - 17. minute

3.2 Calibration

Limits of detection (LOD) and limits of quantification (LOQ) for the individual estrogens were determined under the optimized linear concentration gradient conditions. The measurements were carried out within the concentration range from 5.0 μg/mL to 200 μg/mL. The dependence of the peak height on the analyte concentration was linear over the whole studied range. The limits of detection and quantification were obtained from the regression analysis as the background noise multiplied by three and ten, respectively. The results measured for the individual estrogens are summarized in Table 2. As follows from the Table 2, the lowest LOD and LOQ values have been obtained for mestranol and estrone, i.e. for the first and last eluting peaks in the gradient mode. LOD and LOQ of αE2, EE and E3 have been almost eight times higher than the values of M and E1.

Table 2 LOD and LOQ obtained for the individual estrogen hormones. *Conditions: Supelcosil TM LC-18-DB column (250 x 4.6 mm I.D.); mobile phase, ACN/water 40/60 (v/v) with linear gradient to 100 vol. % of ACN applied from 15 to 16 minute; flow rate, 1.3 mL/min, UV detection, 200 nm.*

	LOD		LOQ	
	µg/mL	10^{-5} mol/L	µg/mL	10^{-5} mol/L
E1	0.160	0.043	0.533	0.144
αE2	0.687	0.186	2.290	0.621
EE	0.875	0.259	2.920	0.864
E3	0.803	0.231	2.680	0.770
M	0.101	0.031	0.337	0.105

4. Conclusion

The optimized separation conditions (HPLC with UV detection) for the analysis of five estrogen analogues (estradiols) were found. The optimized mobile phase composition was ACN/water 40/60 (*v/v*) with a linear gradient to 100 vol. % of acetonitrile applied from 15. to 16. min. The limits of detection and limits of quantification determined under these optimized conditions for the individual estrogens ranged between 0.26 – 0.03 mol/L and 0.86 – 0.11 mol/L, respectively.

We plan a further improvement of the proposed analytical method in the near future: (i) a better quality C18 column will be used, which could provide more symmetrical peaks; (ii) more sensitive fluorescence detection will be employed under the optimized separation conditions (using gradient elution again); (iii) various possibilities of preconcentration – solid phase extraction columns - will be tested. As the final step estrogens in real water samples will be determined.

Acknowledgment

References

[1] Watabe Y.; Kubo T.; Nishikawa T.; Fujita T.; Kaya K.; Hosoya K.: *J. Chromatogr. A* **1120** *(2006), 252-259.*
[2] Lintelmann J.; Katayama A.; Kurihara N.; Shore L.; Wenzel A.: *Pure Appl. Chem.* **75** *(2003), 631-681.*
[3] Mao L.; Sun Ch.; Zhang H.; Li Y.; Wu D.: *Anal. Chim. Acta* **522** *(2004), 241-246.*
[4] Reine J.; Vriese E.; Glatt H.; Vermeulen N.P.E.: *Anal. Biochem.* **357** *(2006), 85-92.*
[5] Li Z.; Wang S.; Lee N.A.; Allan R.D.; Kennedy I.R.: *Anal. Chim. Acta* **503** *(2004), 171-177.*
[6] Yoon Y.; Westerhoff P.; Snyder S.A.; Esparza M.: *Water Res.* **37** *(2003), 3530-3537.*
[7] Nakamura S.; Sian T.H.; Daishima S.: *J. Chromatogr. A* **919** *(2001), 275-282.*
[8] Farré M.; Brix R.; Kuster M.; Rubio F.; Goda Y.; Lopez de Alda M.J.; Barceló D.: *Anal. Bioanal. Chem.* **385** *(2006), 1001-1011.*
[9] Suzuki Y.; Maruyama T.: *Water Res.* **40** *(2006), 1061-1069.*
[10] Mitani K.; Fujioka M.; Kataoka H.: *J. Chromatogr. A* **1081** *(2005), 218-224.*
[11] Hu J.; Zhang H.; Chang H.: *J. Chromatogr. A* **1070** *(2005), 221-224.*
[12] Huang Ch.H.; Sedlak D.L.: *Environ. Toxicol. Chem.* **20** *(2001), 133-139.*
[13] Ferguson P.L.; Iden Ch.R.; McElroy A.E.; Brownawell B.J.: *Anal. Chem.* **73** *(2001), 3890-3895.*

REDUCTION OF 4-AMINO-3-NITROPHENOL ON BISMUTH-MODIFIED ELECTRODES

Hana Dejmková, Jiří Zima and Jiří Barek

Charles University in Prague, Faculty of Science, Department of Analytical Chemistry, UNESCO Laboratory of Environmental Electrochemistry, Albertov 6, 128 43 Praha 2, Czech Republic, e-mail: hdejmkova@seznam.cz

Abstract

Electrochemical behaviour of glassy carbon paste electrode (GCPE) and bismuth-modified glassy carbon paste electrode (Bi-GCPE) was compared for cathodic reduction of 4-amino-3-nitrophenol using differential pulse voltammetry and HPLC with electrochemical detection. Generally, the performance of both electrodes is similar. BiGCPE showed in DPV some favourable properties, eg. less negative reduction potential of the analyte and lower sensitivity to oxygen. However, its application is limited to acidic media due to the narrow potential window. The presence of oxygen complicated the HPLC electrochemical detection and related baseline fluctuation caused high detection limit.

Keywords

Carbon paste electrode, bismuth, differential pulse voltammetry, HPLC, aminonitrophenol

1. Introduction

Nowadays, mercury electrodes are less employed in electroanalysis because of adverse effect of liquid mercury on the environment. Bismuth electrodes, introduced several years ago, offer interesting properties to stand in their place: bismuth toxicity is low compared to mercury, but its electrochemical properties are very similar, including high hydrogen overpotential, low background current and high reversibility of electrochemical reaction.[1]

There are several varieties of bismuth-modified electrodes. Bismuth bulk electrodes are rather rare because of difficult surface treatment. Most common are electrodes composed of bismuth film electrochemically deposited on glassy carbon or carbon paste electrode. For oganic compound analysis, ex situ film plating is necessary, which is experimentally more demanding.[1] Recently introduced carbon paste electrode with admixed bismuth powder combines modification by bismuth with properties of carbon paste electrodes, eg. easily renewable surface.[2,3]

Bismuth-based electrodes were successfuly used for anodic stripping voltammetry of metals.[4] Studies dealing with direct reduction of organic substances are less common [5-7] and they are dealing with bismuth film electrodes only.

Aim of this study is to compare the electrochemical behaviour of bare carbon paste electrode and carbon paste electrode with admixed bismuth powder on the instance of cathodic reduction of 4-amino-3-nitrophenol (4A3NP) using differential pulse voltammetry and HPLC with electrochemical detection.

2. Experimental
2.1 Apparatus

Differential pulse voltammetry (DPV) measurements were carried out using Eco-Tribo-Polarograph, controlled by software Polar Pro 5.1 (both PolaroSensors, Prague, Czech Republic). HPLC system consisted of degasser, high-pressure pump Beta 10,

injector valve with 20 μL loop, Gemini 3μm C18 110A, 150 × 4.6 mm column (Phenomenex, USA) with chemically bonded C18 phase, UV/VIS detector Saphire 800 (all Ecom, Czech Republic) and amperometric detector ADLC 2 (Laboratorní přístroje, Czech Republic) connected in series. The HPLC system was controlled via Clarity 2.3 software (DataApex, Czech Republic) working under Windows XP (Microsoft).

Three-electrode arrangement was used both for DPV and electrochemical detection with platinum auxiliary electrode and Ag/AgCl (1 M KCl) reference electrode RAE 113 (Monokrystaly Turnov, Czech Republic), which all the potential values are referred to. Working electrodes are described below.

2.2 Working electrodes

Glassy carbon paste electrode (GCPE) was prepared by mixing 250 mg of glassy carbon microparticles (Alfa Aesar, Germany) with 100 μL of mineral oil (Fluka).

Bismuth-modified carbon paste electrode (Bi-GCPE) were prepared by mixing 150 mg of glassy carbon microparticles and 90 mg of bismuth powder (100 mesh, Aldrich) with 100 μL of mineral oil.[3]

The paste mixtures were packed in piston-driven holders with inner diameter of 3 mm. Electrode surface was renewed befor each DPV measurement and once a day in flow detection measurements. To remove oxygen, the potential of – 1.0 V was applied for 60 s in a stirred solution prior to each measurement.

2.3 Chemicals

The stock solution (c = $1 \cdot 10^{-3}$ mol·L^{-1}) of 4-amino-3-nitrophenol (4A3NP, CAS Number 610-81-1, Aldrich) was prepared by dissolving the exact amount of the substance in methanol (for HPLC, LachNer, Neratovice, Czech Republic) and was kept at laboratory temperature.

Britton-Robinson (B-R) buffers served as supporting electrolyte for DPV, 0.01 mol·L^{-1} phosphate buffer was used for preparation of mobile phases in HPLC. All chemicals used for buffer preparation were of analytical grade purity and obtained by Lachema Brno, Czech Republic. Deionized water (Millipore) was used throughout.

2.4 Procedures

Differential pulse voltammograms were carried out at following scan parameters: scan rate 20 mV·s^{-1}, pulse amplitude 50 mV and pulse duration 80 ms. Solutions were prepared by exact dilution of methanolic stock solution by B-R buffers. Oxygen of the solution was removed by purging by nitrogen.

Samples for injection into HPLC system were prepared by exact dilution of the stock solutions to contain the required amount of the analyte in 50% methanol (v/v in water). The mobile phase contained 50 % of methanol and 50 % of phosphate buffer pH 4 (v/v) and its flow rate was 0.5 mL·min^{-1}. Detection wavelength of 216 nm was selected from UV spectra of the analyte.[8]

Calibration dependences were evaluated by least squares linear regression method.

3. Results and discussion
3.1 Differential pulse voltammetry

At first, the influence of pH on voltammetric behaviour of 4A3NP was investigated. As can be seen in Fig.1, the main drawback of Bi-GCPE is narrow potential window compared to GCPE. Potential window is limited towards less negative potentials by the value of approximately –250 mV (due to the oxidation of bismuth) and towards more negative potentials by value of approx. –1000 mV, while GCPE extends to values

higher than –1400 mV. Therefore, pH range for the measurement using Bi-GCPE is limited to values lower than pH 7, as the peak is not observable in more alkaline solutions.

On the other hand, addition of bismuth decreases the sensitivity of the electrode to the oxygen. Oxygen signal, caused mainly by oxygen dissolved in the carbon paste, was hardly notable in measurements carried out using Bi-GCPE. GCPE, however, shows stable oxygen peak in spite of reduction pretreatment.

Notable is also the potential shift of the peak of 4A3NP for about 30 mV towards less negative potentials.
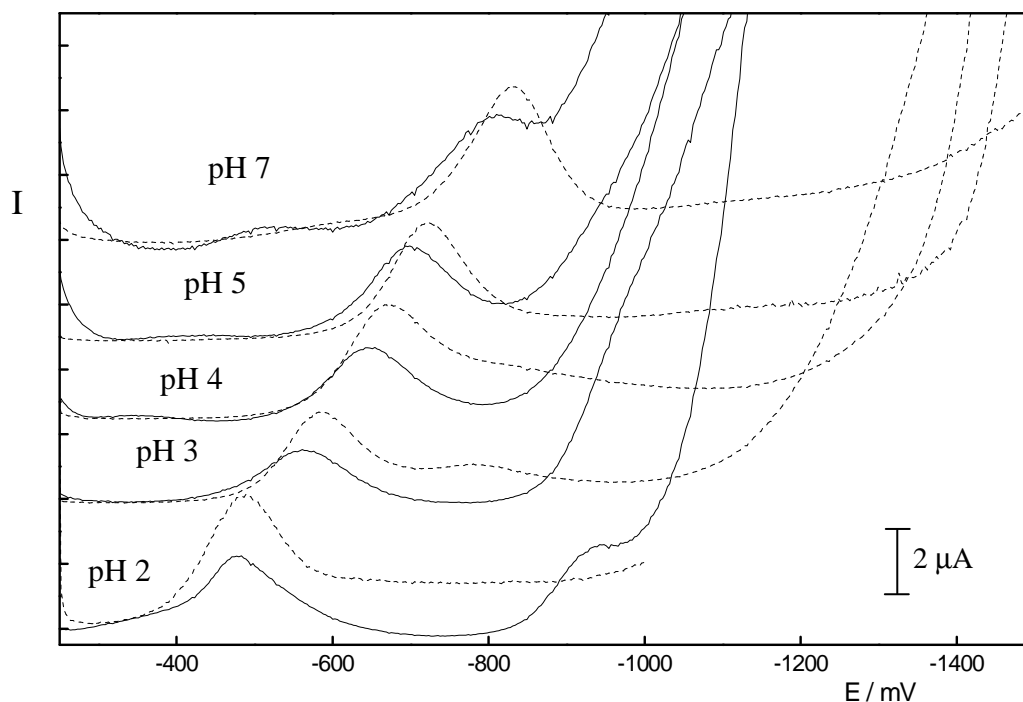
Fig.1 Voltammograms of 4A3NP obtained using GCPE (dashed line) and Bi-GCPE (solid line). *DPV, supporting electrolyte B-R buffer (10 % of methanol), scan rate 20 mV·s⁻¹, pulse amplitude 50 mV and pulse duration 80 ms.*

For further measurements, pH 4 was chosen as optimal and calibration dependences were measured in the range from $1 \cdot 10^{-4}$ mol·L⁻¹ to $2 \cdot 10^{-6}$ mol·L⁻¹. The obtained calibration dependences are linear in the studied concentration range. (Fig.2) Calculated parameters of the dependences are summarized in Table I. Quite a high intercept is caused by the nonideal baseline shape and consequent difficult evaluation.

The limits of determination were calculated as the concentration of the analyte, which gave the signal equal to ten times the standard deviation estimated from the lowest measurable concentration. The value reaches $1.5 \cdot 10^{-6}$ mol·L⁻¹ using Bi-GCPE and $2.4 \cdot 10^{-6}$ mol·L⁻¹ using GCPE.
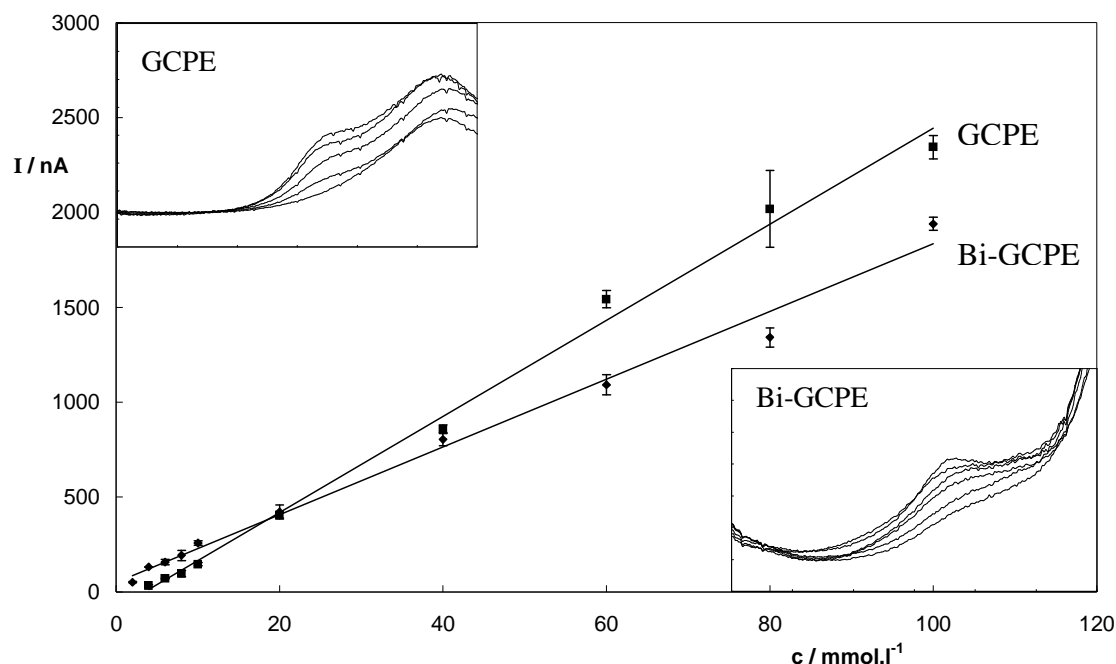
Fig.2 Calibration dependences of 4A3NP obtained using Bi-GCPE and GCPE supplemented by voltammograms of the lower part of concentration range. *DPV, supporting electrolyte B-R buffer pH 4 (10 % of methanol), scan rate 20 mV·s^{-1}, pulse amplitude 50 mV and pulse duration 80 ms.*

Table 1 Characteristics of the calibration dependences of 4A3NP obtained using Bi-GCPE and GCPE.

Electrode	Concentration range (mol·L^{-1})	Slope (mA·L·mol^{-1})	Intercept (nA)	Correlation coefficient	Limit of determination (mol·L^{-1})
Bi-GCPE	$2 \cdot 10^{-6} - 1 \cdot 10^{-4}$	17.8	50.4	0.9953	$1.5 \cdot 10^{-6}$
GCPE	$4 \cdot 10^{-6} - 1 \cdot 10^{-4}$	25.3	87.1	0.9974	$2.4 \cdot 10^{-6}$

3.2 HPLC with electrochemical detection

In the next step, the possibility of employing Bi-GCPE as the working electrode in electrochemical detector was tested. Hydrodynamic voltammograms were measured (Fig.3). The potential of the wave obtained using Bi-GCPE is less negative than potential obtained using GCPE in the same way as in DPV measurements. Optimal potential – 0.9 V (Bi-GCPE) and –1.1 V (GCPE) was chosen for calibration dependences measurement.

The obtained calibration dependences are linear in the studied concentration range, as can be seen in Fig.4. The parameters of the calibration dependences are summarized in Table II. The presence of oxygen caused baseline fluctuation, which disabled the detection for lower concentrations. Unlike in DPV, Bi-GCPE exhibits the same sensitivity to the oxygen influence as GCPE. Resulting limit of determination, which was calculated as concentration of the analyte, which gave the signal equal to ten times the baseline noise, is therefore very high, reaching the value $1.1 \cdot 10^{-5}$ mol·L^{-1} using Bi-GCPE and $0.9 \cdot 10^{-5}$ mol·L^{-1} using GCPE. In contrast, limit of determination obtained by spectrophotometric measurements is $2.1 \cdot 10^{-8}$ mol·L^{-1}.
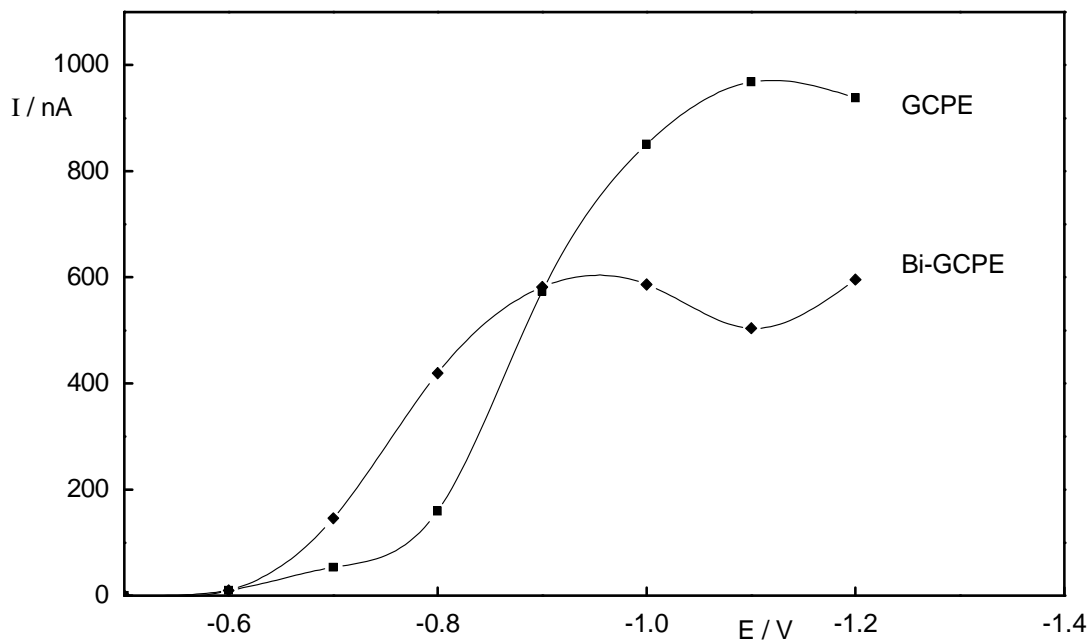
Fig.3 Hydrodynamic voltammograms of 4A3NP. *Gemini 3μm C18 110A, 150 × 4.6 mm column, mobile phase 0,01 mol·L⁻¹ phosphate buffer pH 4 : methanol (1:1, v/v), c = 1·10⁻⁴ mol·L⁻¹ .*
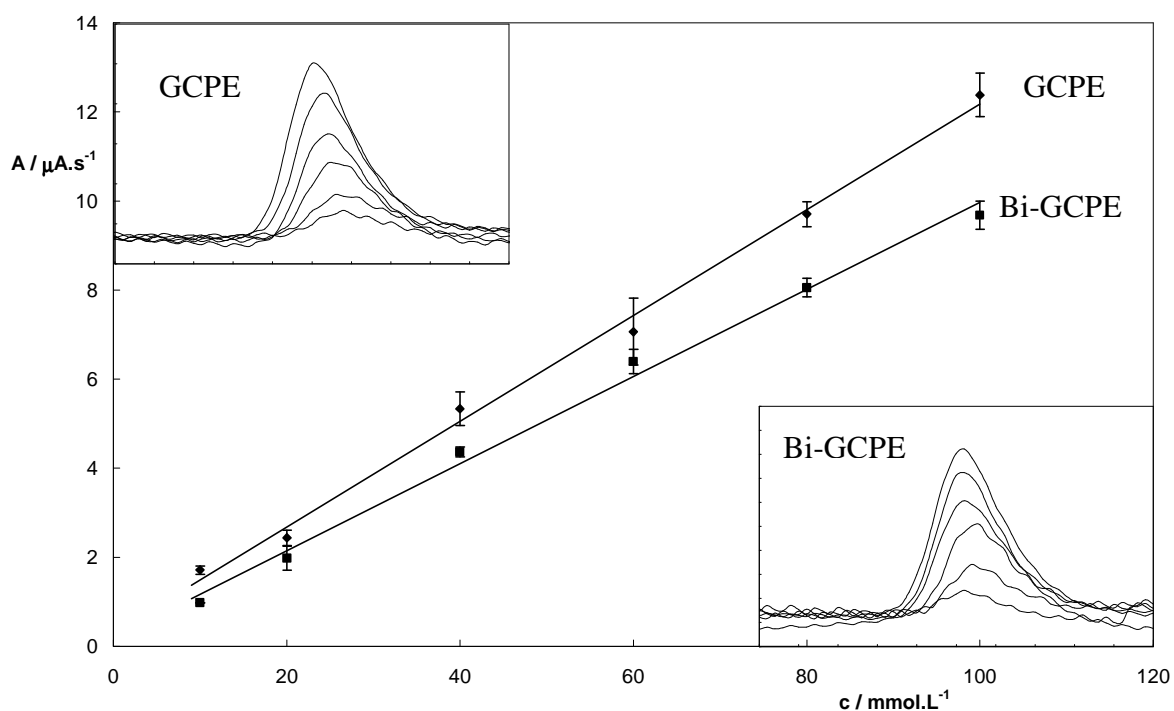
Fig.4 Calibration dependences of peak area of 4A3NP obtained using Bi-GCPE and GCPE, supplemented by corresponding chromatograms. *Gemini 3μm C18 110A, 150 × 4.6 mm column, mobile phase 0,01 mol·L⁻¹ phosphate buffer pH 4 : methanol (1:1, v/v), Bi-GCPE: E_{DET} = –0.9 V, GCPE: E_{DET} = –1.1 V.*

Table 2 Characteristics of the calibration dependences of 4A3NP obtained using Bi-GCPE and GCPE as electrochemical detector in HPLC, calculated of the peak area.

Detection	Concentration range (mol·L^{-1})	Slope [a] (mA.s^{-1}·L·mol^{-1})/ (10^{-3}AU.s^{-1}.L. mol^{-1})	Intercept [a] (μA.s^{-1})/ (mAU.s^{-1})	Correlation coefficient	Limit of determination (mol·L^{-1})
Electrochemical Bi-GCPE	1·10^{-5} – 1·10^{-4}	97.8	0.19	0.9972	1.1·10^{-5}
Electrochemical GCPE	1·10^{-5}– 1·10^{-4}	118.6	0.31	0.9978	9.0·10^{-6}
Spectrophoto-metric	1·10^{-6}– 1·10^{-4}	12.1	25.3	0.9986	2.1·10^{-8}

[a] first unit reffers to electrochemical measurements, second to spectrophotometric measurements

4. Conclusion

The applicability of the bismuth-modified electrodes for cathodic reduction of 4A3NP is limited. Bismuth film modified carbon paste electrodes show favourable characteristics, eg. less negative reduction potential and lower sensitivity to oxygen. However, their application is limited to acidic media due to the narrow potential window. Limit of determination obtainable using developed method is 1.5·10^{-6} mol·L^{-1} using Bi-GCPE and 2.4·10^{-6} mol·L^{-1} using GCPE. The presence of oxygen complicated the HPLC electrochemical detection and related baseline fluctuation caused high detection limit, 1.1·10^{-5} mol·L^{-1} using Bi-GCPE and 9.0·10^{-6} mol·L^{-1} using GCPE.

References
[1] Švancara I.; Vytřas K.: *Chem. Listy* **100** (2006), 90-113.
[2] Hočevar S.B.; Švancara I.; Vytřas K.; Ogorevc B.: *Electrochim. Acta* **51** (2005) 706-709.
[3] Švancara I.; Baldrianová L.; Tesařová E.; Hočevar S.B.; Elsuccary S.A.A.; Economou A.; Sotiropoulos S.; Ogorevc B.; Vytřas K.: *Electroanalysis* **18** (2006), 177-185.
[4] Wang J.: *Electroanalysis* **17** (2005), 1341-1346.
[5] Hutton E.A.; Ogorevc B.; Hočevar S.B.; Weldon F.; Smyth M.R.; Wang J.: *Electrochem. Comm.* **3** (2001), 707.
[6] Hutton E.A.; Ogorevc B.; Smyth M.R: *Electroanalysis* **16** (2004), 1616-1621.
[7] Arribas A.S.; Bermejo E.; Chicharro M.; Zapardiel A.: *Electroanalysis* **18** (2006), 2331 – 2336.
[8] Dejmková H.; Zima J.; Barek J.: *Proceedings of 3rd International Student Conference of Modern Analytical Chemistry (2007), 40-48.*

VOLTAMMETRIC CHARACTERIZATION OF VARIOUS BARE AND DNA MODIFIED CARBON PASTE ELECTRODES COVERED WITH MULTIWALLED CARBON NANOTUBES AND CHITOSAN FILMS

Julia Galandová

Institute of Analytical Chemistry, Faculty of Chemical and Food Technology, SlovakUniversity of Technology in Bratislava, Radlinského 9, 812 37 Bratislava, Slovakia, Corresponding author: julia.galandova@stuba.sk

Abstract

Modified carbon paste electrodes are a very active area of electrochemical research. We report the comparison of various types of carbon pastes used as voltammetric electrode materials. The carbon powder (C), the glassy carbon micro spheres (GCS) and multi walled carbon nanotubes (MWNT) together with Nujol as the pasting liquid were used to prepare the pastes. These pastes were modified by chitosan (CHIT) and DNA. Individual electrode substrates were characterized by cyclic voltammetry with $K_3[Fe(CN)_6]$ as a well known redox probe. Finally, the CV responses of such electrodes were compared with that of the screen printed carbon paste electrode (SPCE).

Keywords

Carbon paste electrodes, glassy carbon microspheres, multiwalled carbon nanotubes, chitosan, DNA-based biosensor, screen printed carbon paste electrode

1. Introduction

DNA-based electrochemical biosensors are today of great interest as effective devices for the DNA research as well as testing of drugs and other chemicals interacting with immobilized DNA. An improvement of the biosensor signal, both its sensitivity and specificity, belongs to tasks of numerous investigations. New construction elements and detection schemes are permanently proposed. As signal transducers, simple and inexpensive electrode substrates are favorably used. Carbon paste electrodes typically possess wide working potential window, low backround current, simple renewal and are widely used as bare or chemicaly modified electrodes for electroanalysis of inorganic ions, organic compounds, polutants, pharmaceutics and drugs.[1] Both, glassy and vitreous carbons (GC) as the substrates and films offer to electroanalytical chemistry excellent properties like good electrical conductivity, hardness and resistance to corrosion.[2] GC spheres (GCS) are obtained by atomizing polymer of furfuryl alcohol containing pore forming agents in the form of either dissolved high bowling organics or disperse carbon black.[3] Thus, their porosity, pore size and surface area should be controlled. With the increased temperature, the size and the volume of the micropores increases and the size distribution is more narrow which enhances the homogenity of electroanalytical results. The heterogenous rate constant for ferricyanide is higher at the paste prepared with GCS than that with CP.[4]

Carbon nanotubes (CNT) including multiwalled carbon nanotubes (MWNT) represent known nanomaterials that display attractive structural, mechanical and electronic properties leading to improved electrochemical activity of many analytes.[5] Polymeric materials have also been widely used at sensors, actuators, high sensitive membranes, energy storage and others. Among them, chitosan (CHIT) as a polysaccharide containing free amino groups and hydroxyl groups, having good film-forming ability, high water

permeability, good adhesion, is perspective for biosensing.[6] It is biocompatible, biodegradable and non-toxic cationic polymer that forms polyelectrolyte complexes with negatively charged molecules including DNA.[7]

The anion $[Fe(CN)_6]^{3-/4-}$ is a redox probe frequently used in cyclic voltammetry (CV) for testing of new types of electrode materials because of its electrochemical reversibility at many electrode substrates. Its monolayer adsorption was also reported.[8] At the DNA-based biosensors, it can be used as a simple redox probe in the solution phase where its voltammetric signal decreases comparing to bare electrode due to electrostatic repulsion by the immobilized negatively charged DNA backbone.[9] At carbon paste electrodes, however, problems with the CV behavior of $[Fe(CN)_6]^{3-/4-}$ can occur due to insulating properties of pasting liquids.[10] This can be eliminated by lowering the content of the binder in the paste.

The aim of this work is to improve the double stranded DNA detection by the $[Fe(CN)_6]^{3-/4-}$ redox probe using an effective combination of carbon paste as the electrode material and MWNT and CHIT as the electrode modifiers. The carbon substrates such as glassy carbon microspheres (GCS), multiwalled carbon nanotubes (MWNT) and simple carbon powder (CP) in mineral oil were investigated for this purpose.

2. Experimental
2.1 Chemicals

Calf thymus double-stranded DNA was purchased from Merck, Germany. Its stock solution (0.1 mg.ml^{-1}) was prepared in 0.01 mol.dm^{-3} Tris-HCl + 1 mM EDTA, pH 8.0 and stored at $-4°C$. Polysaccharide CHIT of high relative molecular mass (M= 600 000), degree of deacetylation 85% was from Fluka, Germany. Its 0.5% solution (pH 5.0) in 1% acetic acid was filtered through a simple filter paper strip. The CHIT solution of pH 3.3 was prepared by adjusting the pH value of CHIT pH 5 with 1% acetic acid.

Glassy carbon spheres (GCS) of 0.4-12 μm, type 2 (Alfa Aesar, Germany), carbon powder, crystallic graphite 2 μm, (Maziva Týn, Czech Republic) were used. Multiwalled carbon nanotubes (MWNT) (OD 40-60 nm, ID 5-10 nm, length 0.5-500 μm) were obtained from Aldrich, Germany. For their dispergation, 1 mg.ml^{-1} pure dimethylformamide (DMF) from Lachema Brno, Czech Republic, was used. Nujol was purchased from Fluka, BioChimika, Germany (absorption $\lambda = 260$-280 nm, $A_{max} = 0.6$-0.9). The redox probe the $1 \cdot 10^{-3}$ mol.dm^{-3} K$_3$[Fe(CN)$_6$] was prepared in 0.1 mol.dm^{-3} phosphate buffer solution pH 7.0. Deionized and double distilled water was used throughout.

2.2 Apparatus

Mini- and microelectrode system UMμE, three electrode set (working electrode, silver/silver chloride/sat. KCl, reference electrode and Pt wire - auxiliary electrode) were putted into glassy electrochemical cell. Software Polar 5.1 (Eko-Tribo-Polarograf, version 3.0, Polaro-Sensors, Prague, Czech Republic) was used. The working electrode was teflon enclosure with slewing piston with renewable filling.

2.3 Electrodes preparation and Procedure

The carbon material (500 mg of GCS, 250 mg of CP or MWNT) and 200 μl of mineral oil (Nujol) were mixed to the form of homogenous paste. Finally, the cavity (d = 2 mm) of the Teflon electrode holder was filled with corresponding paste. The modified electrodes were prepared via renewal of carbon paste surface by cutting and subsequent covering by dropp of 2 μl of the CHIT and DNA aqueous solutions or the dispersion of MWNT in DMF and allowing to dry.

Prior to measurement the electrode was immersed into $1 \cdot 10^{-3}$ mol.dm^{-3} K$_3$[Fe(CN)$_6$] in 0.1 mol.dm^{-3} PBS pH 7.0 for 120 s under stirring. The cyclic voltammograms were

recorded within the potential range from 600 to –400 mV at scan rate 50 mV.s^{-1} and potential step 5 mV.s^{-1}.

3. Results and Discussion
3.1 CV signals at carbon paste electrodes without DNA

Cyclic voltammograms of the $1 \cdot 10^{-3}$ mol.dm^{-3} K$_3$[Fe(CN)$_6$] redox probe at various bare carbon paste electrodes were poorly developed (Fig.1) what is typical for many carbon materials. Covering the CPE and GCSPE with a layer of MWNT dispersed in DMF has clearly improved the CV picture, particularly at MWNT/GCSPE where ΔE_p of only 174 mV was observed in comparison to 572 mV at bare GCSPE together with an increase in the CV peaks currents (Fig.2). This is due to the electroconductivity of MWNT. Therefore, the GCSPE was chosen for further investigation.

Certain electroconductivity of chitosan is known,[11] therefore, its effect on the redox probe CV picture was also tested. The CHIT solutions of pH 5.0 and 3.3 were applied to modify the GCSPE surface. The presence of CHIT causes an increase in the [Fe(CN)$_6$]$^{3-}$ current response, particularly for CHIT pH 5.0. The CV records at CHIT/GCSPE prepared by using CHIT pH 5.0 exhibits ΔE_p which varied from 69 mV for the first cycle to 76 mV for the eighth cycle. At CHIT pH 3.3, the ΔE_p values have varied from 153 mV for the first cycle to 167 mV for the eighth cycle.
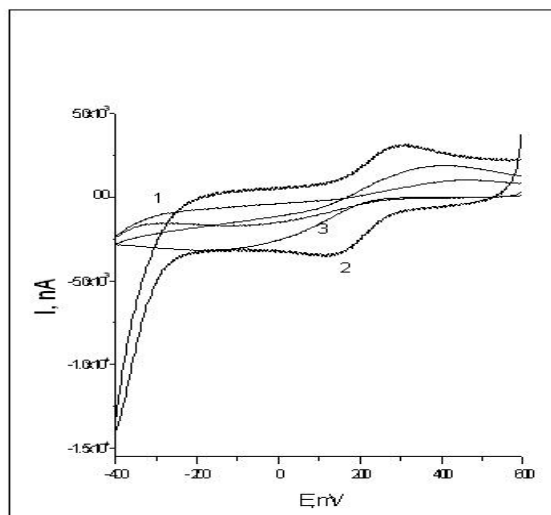
Fig.1 Cyclic voltammograms of $1 \cdot 10^{-3}$ mol.dm^{-3} K$_3$[Fe(CN)$_6$] in 0.1 mol.dm^{-3} PBS pH 7.0 at GCSPE (1) CPE (2) and MWNTPE (3).
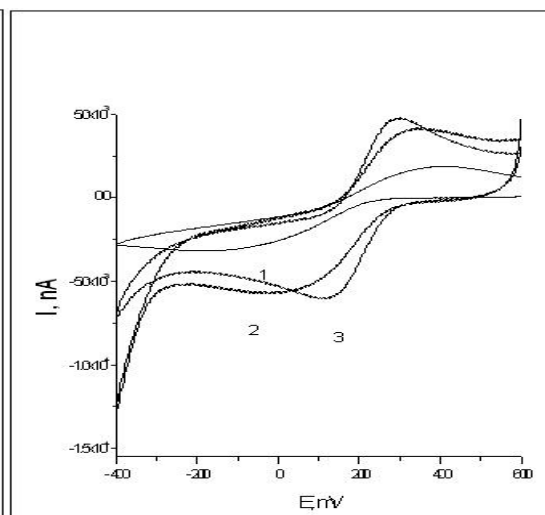
Fig.2 Cyclic voltammograms of $1 \cdot 10^{-3}$ mol.dm^{-3} K$_3$[Fe(CN)$_6$] in 0.1 mol.dm^{-3} PBS pH 7.0 at MWNTPE (1), MWNT/CPE (2) and MWNT/GCSPE (3).

The increased current response and small peak potential separation ΔE_p at both CHIT layers could be ascribed to retaining of [Fe(CN)$_6$]$^{3-}$ ions by the protonated NH$_2$ groups of CHIT similarly to [12] where a residual redox activity from the ferricyanide ions trapped within the chitosan film at the gold electrode was observed. An accumulation of [Fe(CN)$_6$]$^{3-}$ into the CHIT layer has been confirmed in a separate experiment using 5 min electrode incubation in $1 \cdot 10^{-3}$ M K$_3$[Fe(CN)$_6$] prior to the CV measurement. The Fig.3 presents consecutive CVs of the redox probe at CHIT(pH 5.0)-MWNT/GCSPE. The mixture of MWNT in CHIT was sonificated for 5 min before use of this composite. It can be seen that this modification gives very high current response with rather small ΔE_p (102 mV).

97
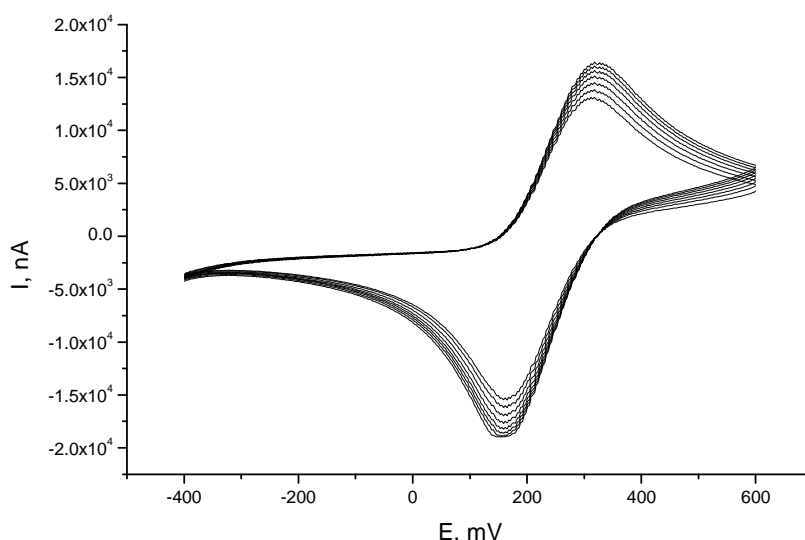
Fig.3 Eight consecutive cyclic voltammograms of $1 \cdot 10^{-3}$ mol.dm^{-3} [Fe(CN)$_6$]$^{3-}$ in 0.1 M PBS pH 7.0 as a redox probe at CHIT(pH 5.0)–MWNT/GCSPE without previous activation of the surface.

In our previous study[9], a good dispergation of MWNT within the chitosan matrix deposited on a screen-printed carbon electrode has been shown. Moreover, a formation of a polyelectrolyte complex between the negatively charged dsDNA backbone and positively charged protonated aminogroups of chitosan is of interest for the DNA fixation. Therefore, the effect of such a complex was tested. Summarization of the results obtained by cyclic voltammetry on GCSPE is in Table 1.

In addition the mixed coverage, used at CHIT-DNA/GCSPE did not cause any significant change in the current response in comparison to the layer-by-layer technique. Also the double concentration of the redox probe did not affect the signal at DNA/MWNT/GCSPE markedly.

Table 1 CV parameters of $1 \cdot 10^{-3}$ mol.dm^{-3} K$_3$[Fe(CN)$_6$] in 0.1 M PBS pH 7.0 at various GCSPE. *Conditions: the potential range from 600 to -400 mV, scan rate 50 mV/s. CHIT solution used was of pH 5.0.*

Electrode	E_{pc}, mV	E_{pa}, mV	I_{pc}, μA	I_{pa}, μA	ΔE_p, mV	(I_{pa}/I_{pc})
GCSPE	-90	482	-	-	572	-
MWNT/GCSPE	124	300	-4.46	4.33	174	0.97
CHIT /GCSPE (1st cycle)	206	275	-1.69	2.90	69	1.72
CHIT /GCSPE (8st cycle)	200	276	-7.56	6.23	76	0.82
CHIT/GCSPE (8st cycle) after accumulation of the redox probe	196	276	7.67	7.37	80	0.96
CHIT-MWNT/GCSPE	189	290	-20.16	15.58	102	0.77
DNA/GCSPE	-95	446	-0.75	0.45	541	0.60
DNA/MWNT/GCSPE	116	308	-4.02	3.66	192	0.91
DNA/CHIT/GCSPE	190	315	-6.29	8.61	125	1.37
DNA/CHIT-MWNT/GCSPE	192	300	-20.15	16.26	108	0.81

An influence of the electrode surface activation for CHIT-MWNT/GCSPE was tested according to Ref. [13] It was seen, that the electrochemical activation by CV sweeps between 0.45 and 1.00 V at 100 mV.s^{-1} causes the decrease in current response and that there is practically no influence on the peak potential separation (84 *vs* 87 mV).

A replacement of mineral oil with CHIT was also tested in order to simplify the electrode preparation. The CHIT-GCSPE was prepared as described in Experimental, the mineral oil was replaced by 250 µl of chitosan solution pH 5.0. However, chitosan has not been found as a suitable "pasting liquid" for GCS because the CV peaks were ill developed.

3.2 Comparison of CV signals at various DNA modified carbon paste materials

The voltammograms of $1 \cdot 10^{-3}$ mol.dm^{-3} K$_3$[Fe(CN)$_6$] in 0.1 mol.dm^{-3} PBS pH 7.0 obtained at DNA modified paste electrodes with and without CHIT are depicted in Fig.4 and 5. Higher current response at the electrodes with CHIT pH 5.0 interface should indicate the defective immobilization of DNA on this polymer matrix.
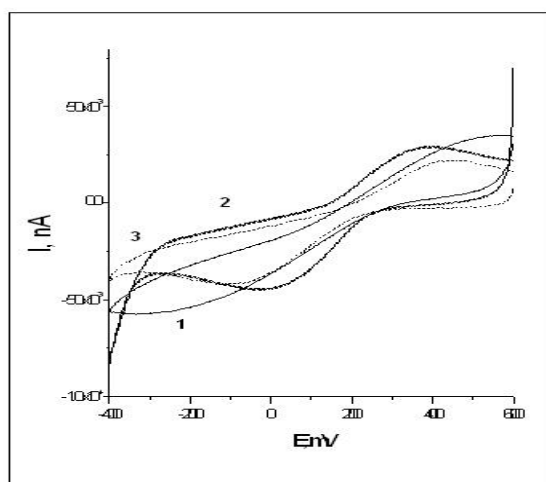
Fig.4 Cyclic voltammograms of $1 \cdot 10^{-3}$ mol.dm^{-3} [Fe(CN)$_6$]$^{3-}$ in 0.1 mol.dm^{-3} PBS pH 7.0 at DNA/MWNTPE (1), DNA/CPE (2), DNA/GCSPE (3).
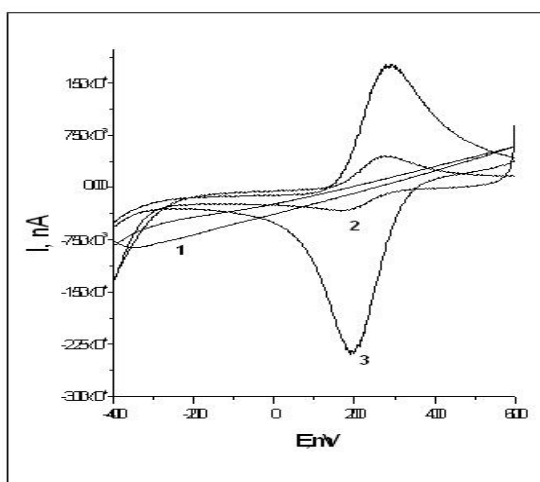
Fig.5 Cyclic voltammograms of $1 \cdot 10^{-3}$ mol.dm^{-3} [Fe(CN)$_6$]$^{3-}$ in 0.1 mol.dm^{-3} PBS pH 7.0 at DNA/CHIT/MWNTPE (1), DNA/CHIT/CPE (2), DNA/CHIT/GCSPE

Cyclic voltammetry of the redox probe at CPEs (paste formed of carbon powder in mineral oil) was performed. From the results the effect of the modifiers can be seen, Table 2.

Table 2 The CV parameters of 1×10^{-3} mol.dm^{-3} [Fe(CN)$_6$]$^{3-}$ in 0.1 mol.dm^{-3} PBS pH 7.0 at carbon powder paste electrodes.

Modifier (2 µl)	E_{pc}, mV	E_{pa}, mV	I_{pc}, µA	I_{pa}, µA	ΔE_p, mV	(I_{pa}/I_{pc})
CPE	150	292	-1.16	0.93	142	0.80
DNA /CPE	-23	397	-0.72	0.75	420	1.04
MWNT/CPE	76	345	-1.96	1.95	269	0.99
DNA/CHIT pH 5/CPE (1st cycle)	182	275	-2.31	1.18	93	0.51

The cyclic voltammetry on MWNTPE (paste formed of multiwalled carbon nanotubes in mineral oil) was also performed. After immobilization with CHIT and DNA layers the peaks were poorly defined. Thus the comparison with bare MWNTPE is impossible.

4. Conclusions

According to the results obtained for the MWNTPE, CPE and GCSPE electrodes it can be concluded that the last one should be very suitable platform for the DNA immobilization and detection. The reduction current response of the redox probe at CHIT(pH 5.0)-MWNT/GCSPE is approximately the same as that at the SPCE screen printed electrode. However, the peak potential values differ and are shifted to more positive values. The use of chitosan does not represent a convenient platform for the modification of CHIT-MWNT/GCSPE by DNA compared to the screen printed carbon electrode.

Acknowledgement

References

[1] Kalcher K.; Kauffmann J.M.; Wang J.; Švancara I.; Vytřas K.; Neuhold C.; Yang Z.: *Electroanal. 7 (1995), 5.*
[2] Yosypchuk B.; Barek J.; Fojta M.: *Electroanal. 18 (2006), 1126.*
[3] Levendis Y.A.; Fagan R.C.: *Carbon 27 (1989), 265.*
[4] Wang J.; Kirkoz U.A.; Mo J.W.; Lu J.; Nasser Kawde A.; Muck A.: *Electrochem. Commun. 3 (2001), 203.*
[5] Tan X.; Li M.; Cai P.; Luo L.; You X.: *Anal. Biochem. 337 (2005), 111.*
[6] Zhang M.; Smith A.; Gorski W.: *Anal. Chem. 76 (2004), 5045.*
[7] Kara P.; Kerman K.; Ozkan D.; Meric B.; Erdem A.; Nielsen P.E.; Oszos M.: *Electroanal. 24 (2002), 1685.*
[8] Chen P.; McCreery R.L.: *Anal. Chem. 68 (1996), 3958.*
[9] Galandova J.; Zyiatdinova G.; Labuda J.: *Anal. Sci., submited.*
[10] Svancara I.; Schachl K.: *Chem. Listy 93 (1998), 490.*
[11] Finkenstadt V.L.: *Appl. Microbiol. Biotech. 67 (2005), 735.*
[12] Zangmeister R.A.; Park J.J.; Rubloff G.W.; Tarlov M.J.: *Electrochim. Acta 51 (25) (2006), 5324.*
[13] Jiang L.; Wang R.; Li X.; Jiang Li.; Lu G.: *Electrochem. Commun. 7 (2005), 597.*

TESTING A POSSIBLE ELECTROCHEMICAL RENEWAL OF HANGING MERCURY DROP ELECTRODES

Petra Polášková[a,b] and Ladislav Novotný[a]

[a] *University of Pardubice, Faculty of Chemical technology, nám. Čs. Legií 565, 532 10 Pardubice 19, Czech Republic; e-mail: polaskovap@centrum.cz*
[b] *Charles University, Faculty of Science, Albertov 8, 128 40 Prague 2, Czech Republic*

Abstract

The aim of the work was to compare voltammetric results obtained using a mechanically renewed hanging mercury drop electrode (HMDE) and an electrochemically renewed HMDE in presence of one selected surface active organic depolarizer and one surface inactive inorganic depolarizer. The measurements were performed in solutions containing 2-aminoantraquinone (2-AA) and $Cd(NO_3)_2$. They confirmed a reasonable applicability of a purely electrochemical renewal of the electrode surface of HMDE for voltammetric purposes.

Keywords

Voltammetry; hanging mercury drop electrode; 2-amino-anthraquinone

1. Introduction

Renewed hanging or stationary mercury electrodes (HMDE) represent a very useful tool for voltammetric trace analysis[1-3] as well as electrochemical study of bioactive species[4-6]. Recent development in the field of the stationary mercury-based electrodes has brought suggestion of numerous new types of useful designs and applications concerning, e.g., the miniaturized electromechanically renewed electrodes[7] HMDE/SMDE and the mercury modified solid amalgam[8-10] (incl. composite amalgam[8] and plastic-tip or glas-tip[8,11]) electrodes. In the HMDEs the mercury flow is stopped by different closure mechanisms operating, e.g., a needle valve. In distinction to the ideally renewable dropping mercury electrode DME the HMDE carries with itself its own "history" from the beginning of its polarization. A mechanical renewal of the HMDE produces a very good quality of its surface close to that of DME, nevertheless a reproducibility (or repeatability) of the drop-size can be limited. To a certain measure the reproducibility and the stability of HMDE depends on the type of capillary used and on the quality of the closures.

On the other hand an electrochemical renewal of the HMDE-surface could eliminate the above-mentioned irreproducibility of the drop-size. Therefore, a combination of the mechanical with purely electrochemical renewal[8] of the electrode surface of HMDE seems to be useful for many electroanalytical applications. The aim of the present communication is to give a brief report on testing the electrochemical renewal of HMDE.

2. Experimental
2.1 Chemicals

Stock solution of $1 \cdot 10^{-5}$ mol.L^{-1} 2-aminoanthraquinone [2-AA, (Sigma – Aldrich, CZ)] in methanol (Lachema, CZ) and aqeous 0.01 mol.L^{-1} $Cd(NO_3)_2$ were prepared from analytical reagent grade chemicals with the redistilled water. They were stored at the laboratory temperature. Working standard solutions were prepared daily by dilution of the stock solutions.

Britton – Robinson buffer (BrRo-buffer) was prepared by mixing 0.04 M phosphoric acid, 0.04 M acetic acid and 0.04 M boric acid (Lachema, CZ).

2.2 Voltammetric measurements

Direct current (DCV) or differential pulse (DPV) voltammetric measurements were performed with the PC-controlled Eco-Tribo Polarograph (ECO-TREND PLUS and ROTKEV, Prague), using a three electrode configuration. The working electrode was the pen-type hanging mercury drop electrode (HMDE) with a drop area of cca 0.4 mm^2. The reference electrode was an Ag/AgCl/KCl (3 mol.L^{-1}), a Pt wire was used as auxiliary electrode. The measured solutions were deaerated by nitrogen. The pH values were measured using pH and conductivity meter (Jenway 4330, UK). Parameters of DPV-scans: scan rate 20 mV.s^{-1}, sampling time 50 ms, pulse amplitude –50 mV, pulse frequency 5 Hz.

3. Results and discussion
3.1 Measurements in solutions containing a surface active depolarizer

Using the mechanically renewed HMDE 2-AA gave sharp cathodic diferential pulse (DP) voltammetric peaks at about –0.5 V and –0.6.V (vs. Ag/AgCl) in Britton-Robinson buffer:methanol (1:1), pH = 6,7 (Fig.1) under the following parameters: t_{bubl} = 300 s; electrochemical pretreatment at E_{in} = 0 V; E_{fin} = –1 V; number of scans N = 3; $t_{stirr.}$ = 5 s; E_{rest} = –0.1 V; t_{rest} = 600 s; initial potential E_{in} = 0 V, final potential E_{fin} = –1.400 V, scan rate v = 0.02 V.s^{-1}; the applied voltammetric conditions agree well with previous voltammetric studies of 2-AA[4]. The curves were registered starting 0 V (vs. Ag/AgCl). The growth of the DP voltammetric (DPV) peak I (at –0.5 V) with increasing concentration c followed a hyperbolic dependence in the given concentration range 0 to 2·10^{-6} mol.L^{-1} (Fig.2). It indicated presence of the adsorption mechanism mixed with the faradaic process.
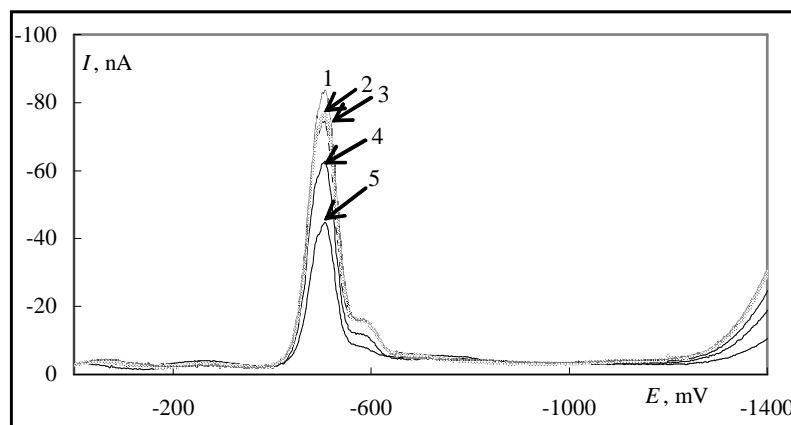
Fig.1 DP voltammograms of 2-AA, mechanical renewal, *in BrRo buffer:MeOH 1:1; pH = 6.7; scan rate 20 mV.s^{-1}, concentration 1.8·10^{-6} mol.L^{-1}(1); 1.5·10^{-6} mol.L^{-1}(2); 1.1·10^{-6} mol.L^{-1}(3); 7.0·10^{-7}mol.L^{-1} (4); 2.5·10^{-7} mol.L^{-1}(5).*
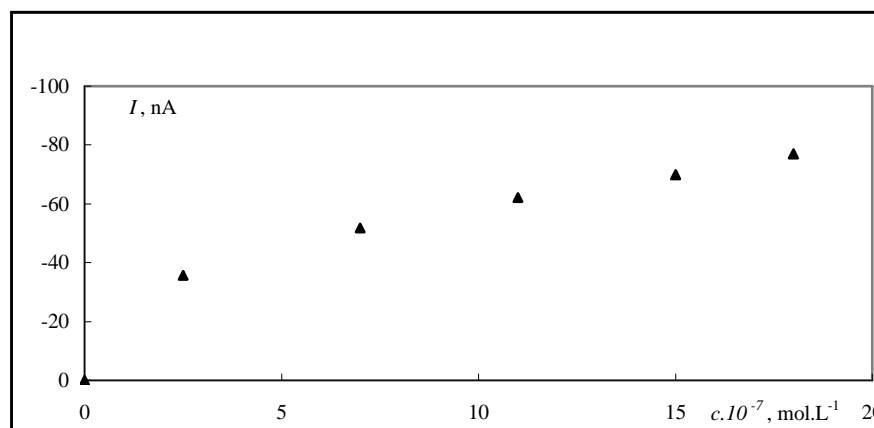
Fig.2 ΔI vs. c dependence of 2-AA, mechanical renewal, *BrRo buffer:MeOH 1:1; pH = 6.7; scan rate 20 mV.s^{-1}.*

It is in accordance with DC-voltammetry registered at various scan rates v (Fig.3). As shown in Fig.4 a DCV-signal ΔI_{DC} depends non-linearly on $v^{0.5}$, which corresponds with electrosorption activity of 2-AA.
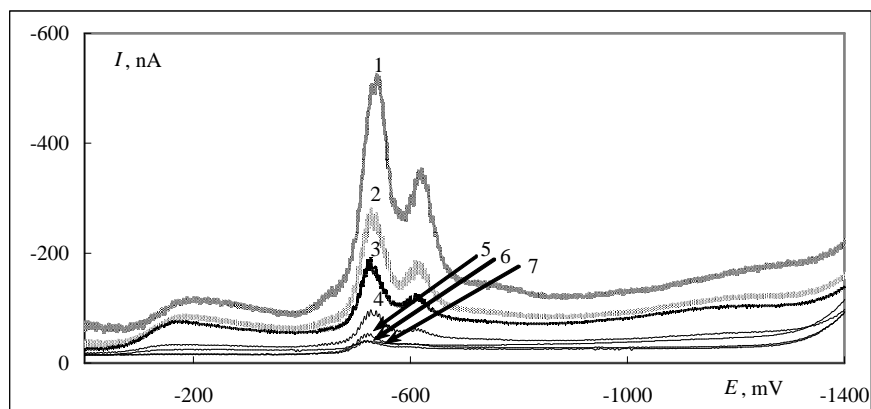
Fig.3 DC voltammogram of 2-AA (c = $4 \cdot 10^{-6}$ mol.L^{-1}), mechanical renewal, *in BrRo buffer:MeOH 1:1*; *pH = 6.7; scan rate 500 mV.s^{-1}(1), 200 mV.s^{-1}(2), 100 mV.s^{-1}(3), 50 mV.s^{-1}(4), 20 mV.s^{-1}(5), 10 mV.s^{-1}(6), 5 mV.s^{-1}(7).*
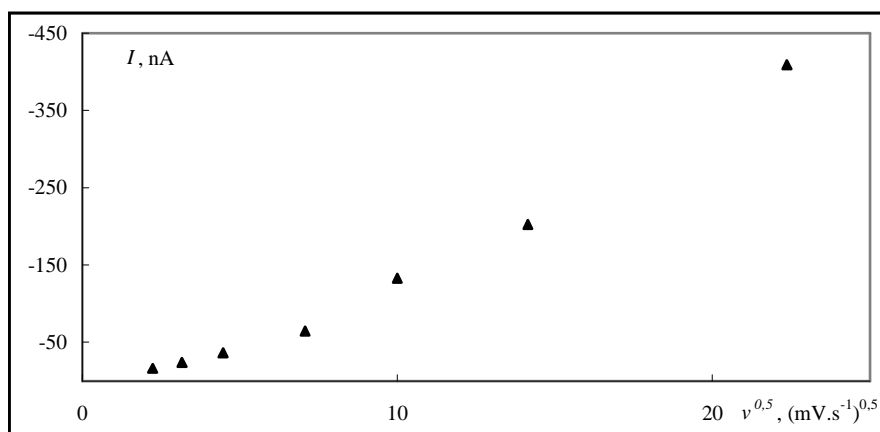
Fig.4 ΔI vs. $v^{1/2}$ dependence of 2-AA (c= $4 \cdot 10^{-6}$ mol.L^{-1}), mechanical renewal, *in BrRo buffer:MeOH 1:1*; *pH = 6.7; scan rate 5; 10; 20; 50; 100; 200; 500 mV.s^{-1}.*

Application of purely electrochemically pretreated HMDE produced analogous sharp cathodic DPV-peaks at the same depolarization potentials as mentioned above (Fig.5). ΔI-c dependence (Fig.6) was of a parabolic shape exhibiting a more flat course approaching the linear dependence. It is so probably due to a time-dependent competition between adsorption of 2-AA and other multi-partical electrosorption interactions in the electrode boundary. Nevertheless, a reasonable sensitivity and good reproducibility (Fig.7, 8) outlined a good analytical applicability of this procedure.

103
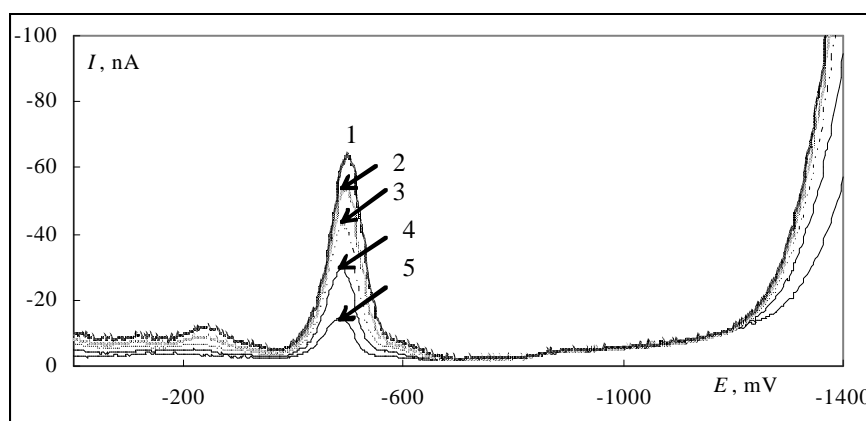
Fig.5 DP voltammograms of 2-AA, electromechanical renewal, *in BrRo buffer: MeOH 1:1*; *pH = 4.6; scan rate 20 mV.s⁻¹, concentration 1.8·10⁻⁶ mol.L⁻¹(1); 1.5·10⁻⁶ mol.L⁻¹ (2); 1.1·10⁻⁶ mol.L⁻¹(3); 7.0·10⁻⁷mol.L⁻¹ (4); 2.5·10⁻⁷ mol.L⁻¹(5).*
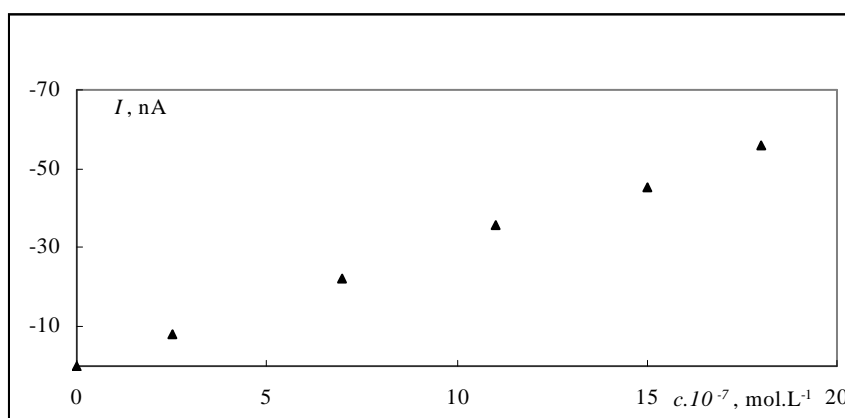
Fig.6 ΔI vs. *c*[2-AA] dependence, electromechanical renewal, *in BrRo buffer:MeOH 1:1.*
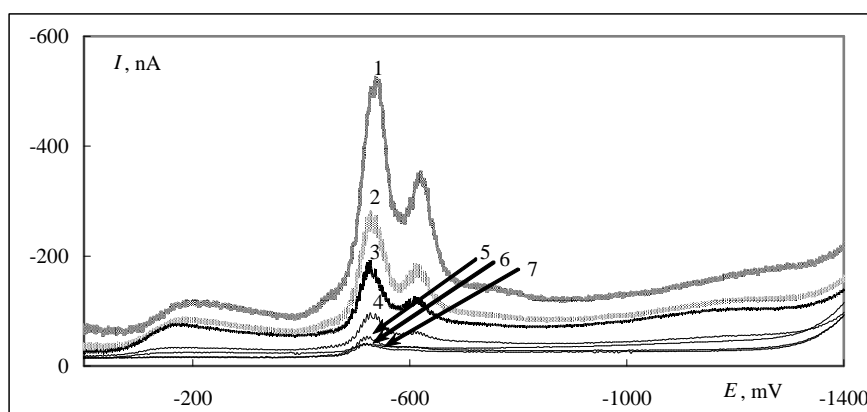
Fig.7 DC voltammograms of 2-AA (*c*= 4·10⁻⁶ mol.L⁻¹), mechanical renewal, *in BrRo buffer:MeOH 1:1; pH = 6.7; scan rate 500 mV.s⁻¹(1), 200 mV.s⁻¹(2), 100 mV.s⁻¹(3), 50 mV.s⁻¹(4), 20 mV.s⁻¹(5), 10 mV.s⁻¹(6), 5 mV.s⁻¹(7).*
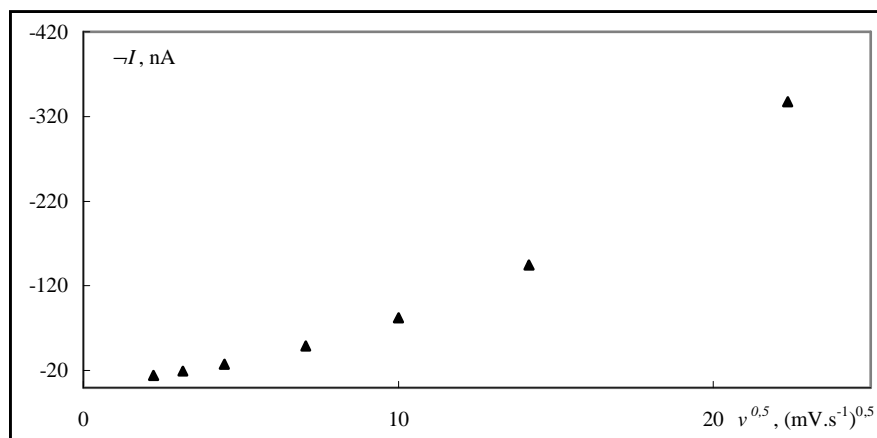
Fig.8 ΔI vs. $v^{1/2}$ dependence of 2-AA ($c = 4 \cdot 10^{-6}$ mol.L^{-1}), electromechanical renewal, *in BrRo buffer:MeOH 1:1*; *pH = 6.7.*

3.2 Measurements in solutions under a diffusion controlled process

Analogous DPV-calibration recordings of $Cd(NO_3)_2$ (Fig.9) using the mechanical renewal of HMDE were carried out. As expected, the evaluated peak heights ΔI_{DPV} proportionally increased with concentration c (Fig.10). In addition, electrochemical signals of present traces of air oxygen were observed not significantly interfering with Cd-peaks.
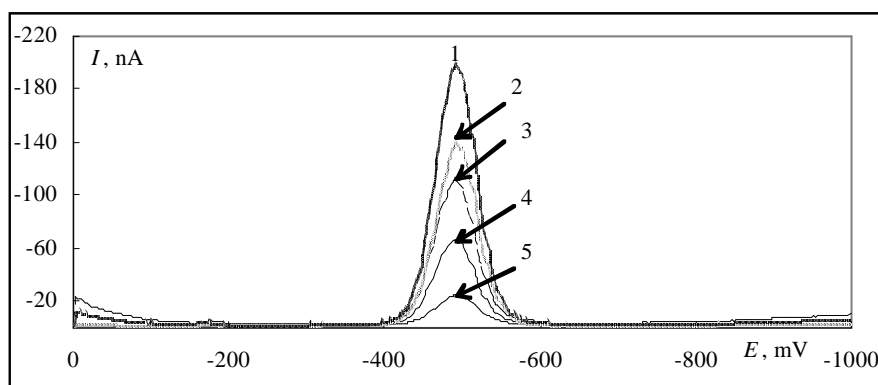
Fig.9 DP voltammograms of $Cd(NO_3)_2$, mechanical renewal, *in BrRo buffer: MeOH 1:1*; *scan rate 20 mV.s^{-1}, concentration 1.7·10^{-2} mol.L^{-1}(1); 1.5·10^{-2} mol.L^{-1}(2); 1.1·10^{-2} mol.L^{-1}(3); 7.0·10^{-3}mol.L^{-1} (4); 2.5·10^{-3} mol.L^{-1}(5).*
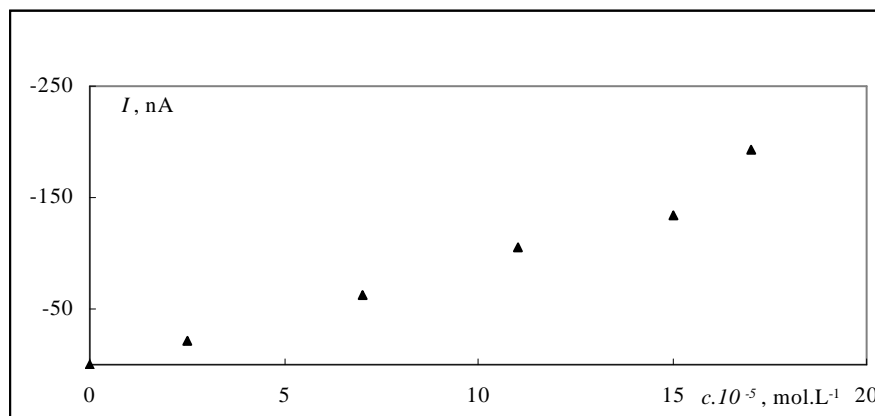
Fig.10 ΔI vs. $c[Cd(NO_3)_2]$ dependence, mechanical renewal, *in BrRo buffer: MeOH 1:1*; *pH = 4.7.*

In case of DC-voltammetry at constant c an increasing scan rate caused linear rise of the registered DC-signal of Cd^{2+} (Fig.11), in agreement with theory of diffusion controlled processes.
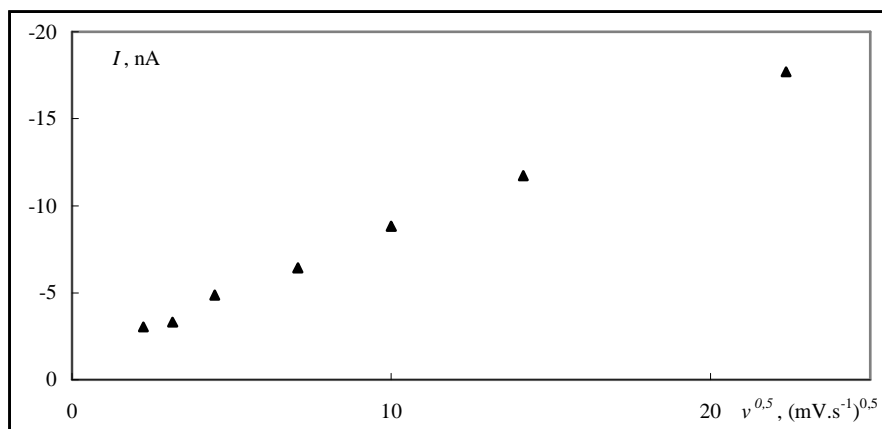
Fig.11 ΔI vs. $v^{1/2}$ dependence of Cd^{2+} (c = $4 \cdot 10^{-6}$ mol.L^{-1}), mechanical renewal, *in BrRo buffer:MeOH 1:1*; *pH = 4.6.*

DP-measurements using the electrochemically pretreated HMDE provided a good voltammetric signal (Fig.12), increasing proportionally with rising concentration of Cd^{2+} (Fig.13). ΔI_{DC} vs. $v^{1/2}$ dependence exhibited a slightly hyperbolic course (Fig.14), that is probably connected with "history" of polarization of the given HMDE.
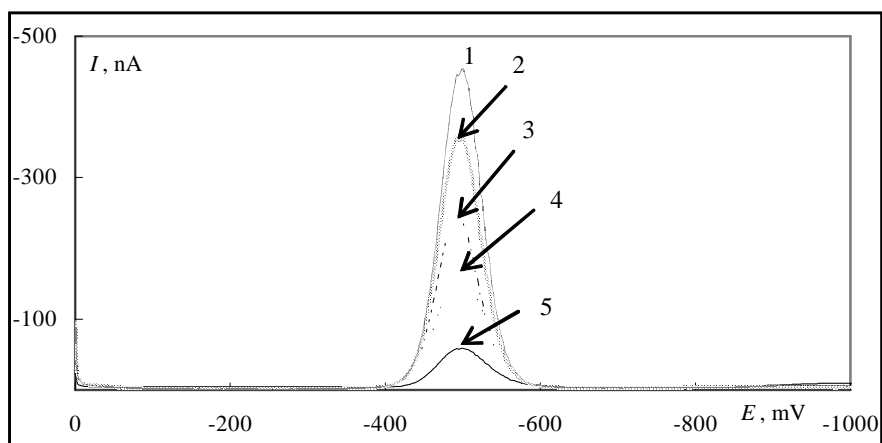
Fig.12 DP voltammograms of $Cd(NO_3)_2$, electromechanical renewal, *in BrRo buffer: MeOH 1:1*; *pH = 4.6; scan rate 20 mV.s^{-1}, concentration $1.7 \cdot 10^{-2}$ mol.L^{-1}(1); $1.5 \cdot 10^{-2}$ mol.L^{-1}(2); $1.1 \cdot 10^{-2}$ mol.L^{-1}(3); $7.0 \cdot 10^{-3}$ mol.L^{-1} (4); $2.5 \cdot 10^{-3}$ mol.L^{-1}(5).*
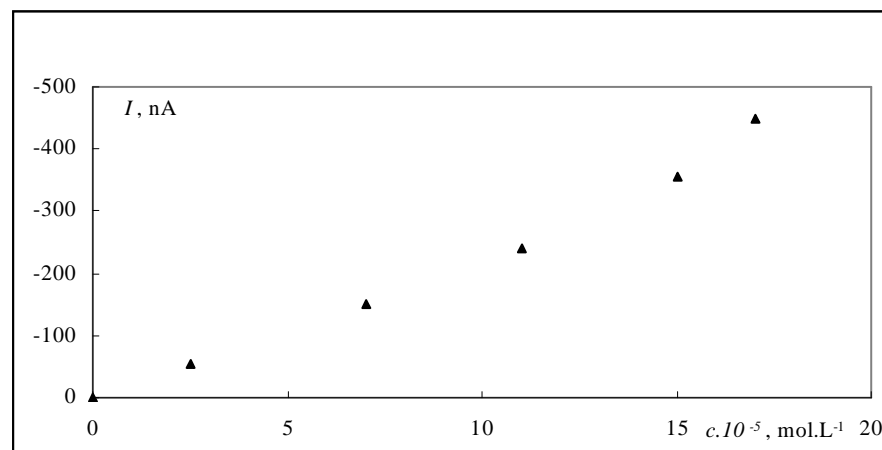
Fig.13 ΔI vs. $c[Cd(NO_3)_2]$ dependence, mechanical renewal, *in BrRo buffer: MeOH 1:1*; *pH = 4.7.*
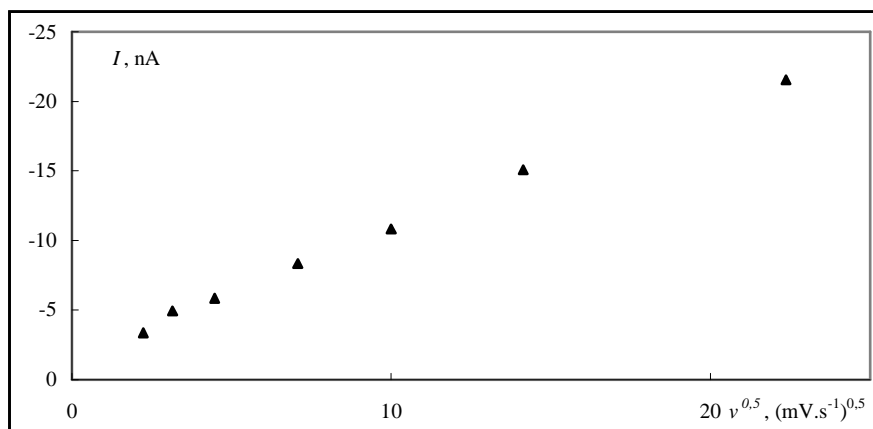
Fig.14 ΔI vs. $v^{1/2}$ dependence of Cd^{2+} ($c = 4 \cdot 10^{-6}$ mol.L^{-1}), electromechanical renewal, *in BrRo buffer: MeOH 1:1; pH = 4.6.*

4. Conclusion

The obtained results confirmed a reasonable applicability of a purely electrochemical renewal of the electrode surface of HMDE for voltammetric purposes. However, in distinction to the mechanically renewed HMDE it brings adequate consequences connected with the "history" of polarization of the electrode interface.

References

[1] Barek J. a kol.: *Možnosti inovací v elektroanalytické chemii. in PACI (Eds: ESF; VŠCHT), Praha 2006.*

[2] Wang J.: *Analytical Electrochemistry. VCH Publ., New York 1994.*

[3] Štulík K.; Kalvoda R. (Eds): *Electrochemisrty for Environmental Protection. UNESCO ROSTE, Venice 1996.*

[4] Ayyildiz H.F.; Topkafa M.; Kara H.; Barek J.; Pecková K.: *Chem. Anal. - Warsaw., submitted.*

[5] Paleček E.; Fojta M.: *Anal. Chem. **73** (2001), 74A.*

[6] Jelen F.; Yosypchuk B.; Kouřilová A.; Novotný L.; Paleček E.: *Anal. Chem. **74** (2002), 4788.*

[7] Novotný L.: *Chem. Listy **95** (2001), 147.*

[8] Novotný L.: *Čs. patenty, PUV 7103-1997; PV 1-2001; PUV 19501-2007, Praha.*

[9] Novotný L.;Yosypchuk B.: *Chem. Listy **94** (2000), 1118.*

[10] Yosypchuk B.; Novotný L.: *Crit. Rew. Anal. Chem. **32**(2) (2002), 141.*

[11] Novotný L.: *Electroanalysis **12** (2000), 1240.*

POLAROGRAPHIC AND VOLTAMMETRIC DETER-MINATION OF SELECTED GENOTOXIC FLUORENE DERIVATIVES USING TRADITIONAL MERCURY ELECTRODES

Vlastimil Vyskočil, Pavol Bologa, Karolina Pecková and Jiří Barek

Charles University in Prague, Faculty of Science, Department of Analytical Chemistry, UNESCO Laboratory of Environmental Electrochemistry, Albertov 6, 128 43, Prague 2, Czech Republic; e-mail: barek@natur.cuni.cz

Abstract

The use of direct current tast polarography, differential pulse polarography, differential pulse voltammetry and adsorptive stripping voltammetry for the determination of trace amounts of selected genotoxic fluorene derivatives was studied at mercury working electrodes (2-nitrofluorene, 2,7-dinitrofluorene, 9-fluorenone, 2-nitro-9-fluorenone and 2,7-dinitro-9-fluorenone were chosen as model substances). The negative influence of these compounds on environment and living organisms was discussed. Possible practical applicability of developed methods in environmental analyses was outlined.

Keywords

Genotoxicity; Fluorene nitro derivatives; Mercury electrodes; Polarography; Voltammetry; Solid Phase Extraction

1. Introduction

The emissions of gasoline and diesel engines contribute significantly to the environmental pollution. Certain part of exhaust particulates consists of nitrated polycyclic aromatic hydrocarbons (NPAHs). NPAHs belong among the substances whose occurrence in the environment can be causally connected with an increased cancer rate[1]. During eighties and nineties of the last century, the research team around Lennart Möller has investigated genotoxic effects of NPAHs on living organisms and their DNA.[2] Carcinogenic 2-nitrofluorene has been chosen as a model compound[3] and lately, studies of 2,7-dinitrofluorene influence were realized, too.[4] Main problem in NPAHs effect on organisms is the fact that the pernicious tumor grow can be provoked by small amount of carcinogen and the disease can manifest itself after many years since the initiatory exposition. That is why the need for extremely sensitive and selective methods of NPAHs determination is still growing. Nitro compounds belong between relatively easy reducible compounds, chemically as well as electrochemically. Therofore, nitro group containing chemical carcinogens are suitable candidates for the application of modern polarographic and voltammetric methods on mercury electrodes. Despite the enormous and ever-increasing importance of solid electrodes, carbon paste electrodes, screen printed electrodes, and chemically modified electrodes, mercury electrodes are still the best electrochemical sensors available for these purposes.[5-7]

We have focused in our work on important group of NPAHs – fluorene nitro derivatives. Many nitrated fluorene derivatives have been found and studied in exhaust gas.[8,9] Concentrations of some of the fluorene and fluorenone nitro derivatives determined in exhaust particulates extracts were 1.8 μg g^{-1} for 2-nitrofluorene (Ref. *8*), 4.2 μg g^{-1} for 2,7-dinitrofluorene, and 8.6 μg g^{-1} for 2,7-dinitro-9-fluorenone (Ref. *9*), respectively. The main danger of these compounds should be seen in raising hazard of ground-water contamination. Therefore, we developed sensitive polarographic and voltammetric

methods for determination of these compounds in aqueous and/or methanolic-aqueous medium.

Studied compound were chosen to cover a wide scale of fluorene nitro derivatives: 2-nitrofluorene (2-NF), 2,7-dinitrofluorene (2,7-DNF), 9-fluorenone (9-FN), 2-nitro-9-fluorenone (2-NFN) and 2,7-dinitro-9-fluorenone (2,7-DNFN). All these compounds are at present known as chemical mutagens and their genotoxicity was proven.[10]

2. Experimental Part
2.1 Reagents

The stock solutions of tested substances [2-NF ($1 \cdot 10^{-3}$ mol L^{-1}), 2,7-DNF ($1 \cdot 10^{-4}$ mol L^{-1}), 9-FN ($5 \cdot 10^{-4}$ mol L^{-1}), 2-NFN ($5 \cdot 10^{-4}$ mol L^{-1}) and 2,7-DNFN ($2 \cdot 10^{-4}$ mol L^{-1}); all Sigma-Aldrich, Prague, Czech Republic] in methanol (Lachema, Brno, Czech Republic) were prepared by dissolving an accurately weighed amount of pure substance in 100 ml of the solvent. The different concentrations of stock solutions were used due to their different solubility in methanol. Solutions with lower concentrations were prepared daily by diluting the stock solution with methanol. Other chemicals (boric acid, glacial acetic acid, phosphoric acid, sodium hydroxide, potassium chloride, all p.a. purity) were supplied by Lachema, Brno, Czech Republic. Deionized water from Millipore, USA, was used. All the solutions were stored in the dark.

2.2 Apparatus

All polarographic and voltammetric measurements were carried out using Eco-Tribo electrochemical analyzer driven by PolarPro 5.1 software (all Polaro-Sensors, Prague, Czech Republic). The software worked under the operational system Microsoft Windows XP Professional (Microsoft Corporation, USA). Measurements were carried out in a three-electrode system – platinum electrode PPE (Monokrystaly, Turnov, Czech Republic) as auxiliary electrode, silver/silver chloride reference electrode RAE 113 (1 mol L^{-1} KCl) (Monokrystaly, Turnov, Czech Republic) and dropping mercury electrode (DME) or hanging mercury drop minielectrode (HMDE) as working electrode. For DCTP and DPP techniques, work with the DME was carried out at a polarization rate of 4 mV s^{-1}, the controlled drop time was 1 s, and the modulation amplitude in DPP was -50 mV. DPV and AdSV measurements using HMDE (type UMµE, Polaro-Sensors, Prague, Czech Republic) were carried out at a polarization rate of 10 mV s^{-1}, the valve opening time was 300 ms, pulse amplitude -50 mV and pulse width 80 ms.

2.3 Procedures

Unless stated otherwise, appropriate amount of given stock solution was measured into a polarographic vessel, methanol was added to total requested volume and the solution was filled up to 10.0 ml with Britton-Robinson (BR) buffer of appropriate pH. All curves were measured 3 times. Oxygen was removed from the measured solutions by bubbling with nitrogen for five minutes.

3. Results and Discussion

At first the influence of pH and the composition of the supporting electrolyte on the polarographic and voltammetric behaviour of the test substances were investigated. Because of the low solubility of the tested fluorene derivatives in water, a mixture of BR buffer with methanol was used as the supporting electrolyte. The influence of pH at voltammetric behaviour of 9-NF and 2,7-DNFN is shown in Fig.1 and Fig.2 for the sake of illustration. The nitro group is reduced to the hydroxylamino group or even to the amino group in dependence of medium pH. The carbonyl group is reduced to the –OH group.

109

Detailed mechanisms of electrochemical reduction of studied fluorene derivatives were satisfactorily explained.[11,12]
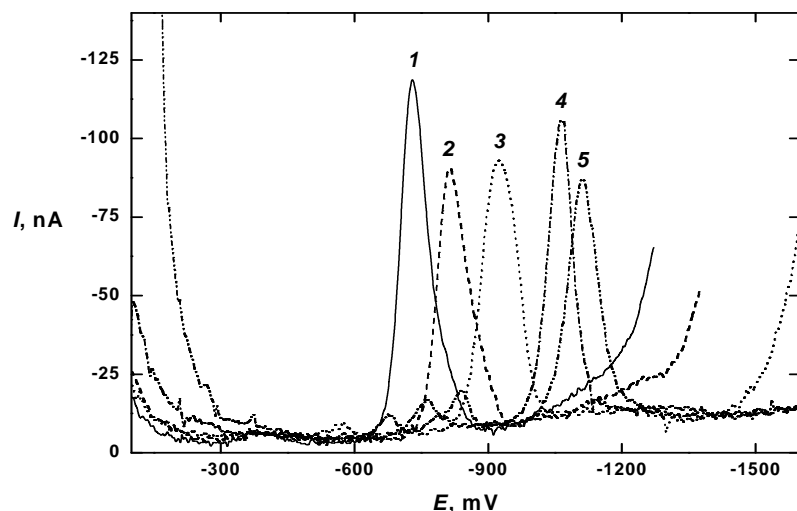

Fig.1 Selected DP voltammograms of 9-FN (c = $1 \cdot 10^{-5}$ mol L^{-1}) at HMDE *in methanol – BR buffer (1:1); resulting pH 3.3 (1), 4.9 (2), 7.6 (3), 10.6 (4), 12.6 (5).*
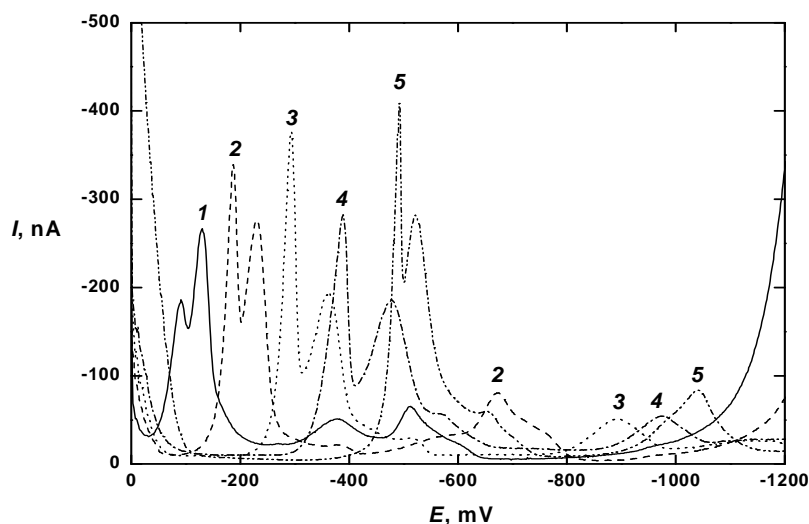

Fig.2 Selected DP voltammograms of 2,7-DNFN (c = $1 \cdot 10^{-5}$ mol L^{-1}) at HMDE in methanol – BR buffer (1:1); resulting pH 2.7 (1), 4.9 (2), 7.0 (3), 9.3 (4), 11.2 (5).

Optimum conditions for the determination of the tested substances under which the best developed and most easily measured curves were obtained are summarized in Table 1, including reached limits of quantification (L_Q). Optimum conditions for AdSV were found on the basis of investigation of the influence of potential of accumulation (E_{acc}) and time of accumulation (t_{acc}) on the height and shape of the AdSV peaks.

The practical applicability of the voltammetric methods was demonstrated by the determination of traces of 2-NFN and 2,7-DNFN added to drinking and river water and by monitoring the chemical destruction of the test substances and the recovery factor of solid phase extraction used for preconcentration. It has been found that the recovery of the extraction-voltammetric determination at concen-trations around $5 \cdot 10^{-8}$ mol L^{-1} of 2-NFN is cca 90% in spiked drinking water[13]. In the case of 2,7-DNFN, the recovery at concentrations around $5 \cdot 10^{-8}$ mol L^{-1} of 2,7-DNFN was cca 95% in spiked drinking water and cca 80% in spiked river water[14]. It is evident that we could reach the similar results with the other investigated fluorene derivatives.

110

Table 1 Polarographic and voltammetric determination of selected fluorene derivatives at mercury electrodes.

Substance	Formula	Technique	Medium	L_Q [mol L^{-1}]	Reference
2-nitrofluorene		DCTP at DME	methanol – BR buffer pH 12 (1:1)	$4 \cdot 10^{-6}$	[15]
		DPP at DME	methanol – BR buffer pH 12 (1:1)	$4 \cdot 10^{-7}$	[15,16]
		DPV at HMDE	methanol – BR buffer pH 12 (1:9)	$4 \cdot 10^{-8}$	[15,16]
		AdSV at HMDE[a]	methanol – BR buffer pH 12 (1:9)	$3 \cdot 10^{-9}$	[15,16]
2,7-dinitrofluorene		DCTP at DME	methanol – BR buffer pH 2 (1:1)	$2 \cdot 10^{-6}$	[15]
		DPP at DME	methanol – BR buffer pH 2 (1:1)	$2 \cdot 10^{-7}$	[15,16]
		DPV at HMDE	methanol – BR buffer pH 12 (1:1)	$1 \cdot 10^{-8}$	[15,16]
		AdSV at HMDE[b]	methanol – BR buffer pH 3 (1:9)	$4 \cdot 10^{-9}$	[15,16]
9-fluorenone		DCTP at DME	methanol – BR buffer pH 10 (1:1)	$3 \cdot 10^{-6}$	–
		DPP at DME	methanol – BR buffer pH 7 (1:1)	$5 \cdot 10^{-7}$	–
		DPV at HMDE	methanol – BR buffer pH 3 (1:1)	$2 \cdot 10^{-8}$	–
2-nitro-9-fluorenone		DCTP at DME	methanol – BR buffer pH 4 (1:1)	$4 \cdot 10^{-6}$	[13]
		DPP at DME	methanol – BR buffer pH 4 (1:1)	$3 \cdot 10^{-7}$	[13]
		DPV at HMDE	methanol – BR buffer pH 11 (1:1)	$4 \cdot 10^{-8}$	[13]
		AdSV at HMDE[c]	methanol – BR buffer pH 11 (1:1)	$3 \cdot 10^{-9}$	[13]
2,7-dinitro-9-fluorenone		DCTP at DME	methanol – BR buffer pH 11 (1:1)	$1 \cdot 10^{-6}$	[14]
		DPP at DME	methanol – BR buffer pH 11 (1:1)	$2 \cdot 10^{-7}$	[14]
		DPV at HMDE	methanol – BR buffer pH 11 (1:1)	$2 \cdot 10^{-8}$	[14]
		AdSV at HMDE[d]	methanol – BR buffer pH 11 (1:9)	$4 \cdot 10^{-9}$	[14]
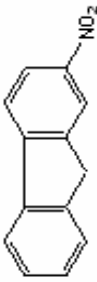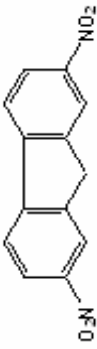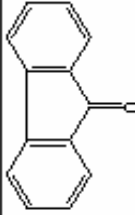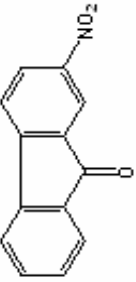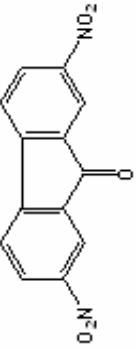
[a] – $t_{acc} = 600\,s$, $E_{acc} = -300\,mV$; [b] – $t_{acc} = 300\,s$, $E_{acc} = 0\,mV$; [c] – $t_{acc} = 180\,s$, $E_{acc} = -200\,mV$; [d] – $t_{acc} = 60\,s$, $E_{acc} = -300\,m$

Acknowledgement

References

[1] Jacob J.; Karcher W.; Belliardo J.J.; Dumler R.; Boenke A.: *Fresenius. J. Anal. Chem.* **340** *(1991), 755-767.*

[2] Moller L.: *Environ. Health Perspect.* **102** *(1994), 139-146.*

[3] Moller L.; Rafter J.; Gustafsson J.A.: *Carcinogenesis 8 (1987), 637-645.*

[4] Moller L.; Cui X.S.; Torndal U.B.; Eriksson L.C.: *Carcinogenesis* **14** *(1993), 2627-2632.*

[5] Barek J.; Mejstrik V.; Muck A.; Zima J.: *Crit. Rev. Anal. Chem.* **30** *(2000), 37-57.*

[6] Barek J.; Cvacka J.; Muck A.; Quaiserova V.; Zima J.: *Fresenius. J. Anal. Chem.* **369** *(2001), 556-562.*

[7] Barek J.; Fogg A.G.; Muck A.; Zima J.: *Crit. Rev. Anal. Chem.* **31** *(2001), 291-309.*

[8] Schuetzle D.: *Environ. Health Perspect.* **47** *(1983), 65-80.*

[9] Campbell R.M.; Lee M.L.: *Anal. Chem.* **56** *(1984), 1026-1030.*

[10] Sax N.I.; Lewis R.J.: *Dangerous Properties of Industrial Materials. John Wiley & Sons, New York, USA 2000.*

[11] Gary J.T.; Day R.A.: *J. Electrochem. Soc.* **107** *(1960), 616-618.*

[12] Vyskocil V.; Barek J.; Cizek K.; Zawada Z.: *Modern Analytical Chemistry 2007. Proceeding from 3rd International Student Conference, pp. 132-141. Czech Chemical Society, Prague 2007.*

[13] Bologa P.; Barek J.: *XXV. Moderní elektrochemické metody. Proceeding from International Seminar, pp. 17-21. Czech Chemical Society, Prague 2005.*

[14] Vyskocil V.; Jiranek I.; Barek J.; Peckova K.; Zima J. in *Sensing in Electroanalysis,* **Vol. 2** *(Eds: Vytras K. and Kalcher K.), University of Pardubice, Pardubice 2007, pp. 105-119.*

[15] Pumera M.: *Diploma Thesis. Charles University in Prague, Prague 1997.*

[16] Barek J.; Pumera M.; Muck A.; Kaderabkova M.; Zima J.: *Anal. Chim. Acta* **393** *(1999), 141-146.*

CHEMICAL VAPOUR GENERATION OF SILVER AS A METHOD FOR SAMPLE INTRODUCTION FOR ATOMIC ABSORPTION SPECTROMETRY

Stanislav Musil[a,b], Jan Kratzer[a,b], Miloslav Vobecký[a], Petr Rychlovský[b] and Tomáš Matoušek[a]

[a] *Institute of Analytical Chemistry of the ASCR v.v.i., Víděňská 1083, 14220 Prague, Czech Republic; e-mail: stanomusil@biomed.cas.cz*
[b] *Charles University in Prague, Faculty of Science, Department of Analytical Chemistry, Albertov 6, 12843 Prague, Czech Republic*

Abstract

A method of silver chemical vapour generation as a sample introduction technique for analytical atomic spectrometry is presented. In principle, the analyte is converted to volatile compounds by means of reaction with tetrahydroborate in acidic environment analogously to classical hydride generation. The atomization of silver in externally heated multiatomizer was employed. Optimization of reaction and atomization parameters was carried out to achieve maximum sensitivity and method robustness. The efficiency of the chemical vapour generation and distribution of residual analyte were studied by means of radiotracer experiments.

Keywords

Chemical vapour generation; silver; analytical spectrometry

1. Introduction

Chemical vapour generation (CVG) of transition and noble metals[1] as a sample introduction method for analytical atomic spectrometry emerged in recent years as an extension of the classical method of hydride generation. The same chemical scheme, i.e. reduction of analyte by tetrahydroborate in acidic environment is employed[2,3]. However, very little is known about the actual reaction mechanism and identity of the volatile metal compounds.

The practical potential of the CVG of metals lies in separation of analyte from the matrix and high analyte introduction efficiency which increases sensitivity and decreases limits of detection. The futher advantage is the possibility of analyte collection and preconcentration prior to detection by methods already established for volatile hydrides. Nevertheless, this promising technique is still in its infancy. The generation efficiency[4] is still relatively low ranging from single to tens of per-cent compared to efficiencies approaching 100 % typical for classical hydride generation. For ilustration, by using neutron activation analysis Ag generation efficiency was 7 %(Ref. 5) and in recent studies even over 20 % of Ag was found in the gaseous phase[6]. The relatively low efficiency is probably also a source of low stability and reproducibility of the signals. Huge inconveniences are also caused by memory effects. Therefore, the improvement in the CVG efficiency is an essential task before this technique enters a stage of routine analysis. It was found recently that surfactants in the reaction mixture enhance the Ag efficiency of the CVG process by 1-2 orders of magnitude, possibly by stabilization of the volatile species, modification of surface of a gas-liquid separator or enhancing release of volatile species from solution[6]. Futhermore, the enhancement can be performed by permanent reaction modifier which can be an efficient catalyzer for decomposition of tetrahydroborate. The rate of the CVG reaction and its efficiency is thus enhanced 2-3

times. The modification by palladium for the CVG of silver has suficient stability and achieves permanent stabilization of sensitivity[7].

The general aims of this study were to optimize conditions of the CVG procedure of silver with the quartz multiatomizer- atomic absorption spectrometry detection, and to assess the efficiency of generation by means of radiotracer experiments.

2. Experimental
2.1 Instrumentation

The detection was performed by an atomic absorption spectrometer Perkin-Elmer 503 with silver HCl lamp (Perkin-Elmer) operated at 12 mA. A multiple microflame quartz tube atomizer (multiatomizer)[8] heated eletrically was employed for atomization with 20 ml·min^{-1} of air as outer gas.

2.2 Standards and reagents

Deionized water (Ultrapur 40, Watrex, USA) was used for preparation of all solutions. Ag standard solutions were prepared by dilution of 1000 µg·ml^{-1} stock solution (BDH, UK) in 0.6 M HNO$_3$ (Lach-Ner, s.r.o., Czech Republic). A reducing solution containing 2.4% (m/v) NaBH$_4$ (FLUKA, Germany) and 13 µg·ml^{-1}Antifoam B emulsion (Sigma, USA) in 0.1% (m/v) KOH (Lach-Ner, s.r.o., Czech Republic) was prepared fresh daily. 20 µg·ml^{-1} Triton X-100 (Aldrich Chemical Co., USA) in 0.1M HNO$_3$ was used as a reaction modifier. As a waste stabilizer 0.5M NaOH solution (Lach-Ner, s.r.o., Czech Republic) was employed.

2.3 System for CVG

A scheme of the system in flow injection (FI) mode is shown in Fig.1. All reagents were pumped by means of peristaltic pump 1 at the rates of 0.5 ml min^{-1}. The manifold was built from PTFE T-junctions and PTFE tubing. A sample is injected into a flow of 0.6 M HNO$_3$ by a six-port injection valve with 228 µl sample loop volume. After mixing with reaction modifier the mixture comes to special arrangement (Fig.2). The reduction proceeds at a tip of three concentric capillaries: the two inner ones (i.d. 0.25 mm and 0.53 mm) are made of deactivated fused silica tubing and used for a introduction of sample/standard and reductant solutions, respectively; the outermost one (i.d. 1 mm) is made of PTFE and served to introduce purge gas (Ar at the rate of 50 ml·min^{-1}). The three concentric capillaries enter a glass gas-liquid separator (GLS). A miniature spray chamber is attached to the GLS to prevent large aerosol droplets entering the multiatomizer. The permanent modification of the generator was carried out by means of 4 ml of 10 µg·ml^{-1} Pd solution (BDH, UK) in 0.1M HNO$_3$ and 20 µg·ml^{-1} Triton X-100 which formed Pd deposits in the system after reduction by NaBH4.

The waste stabilizer was employed for neutralization of the reaction mixture. It prevents production of hydrogen gas in the waste tubing, which aids to maintain stable liquid level within the GLS. Waste from the GLS was pumped out by peristaltic pump 2 at variable speed to assure stable liquid level.
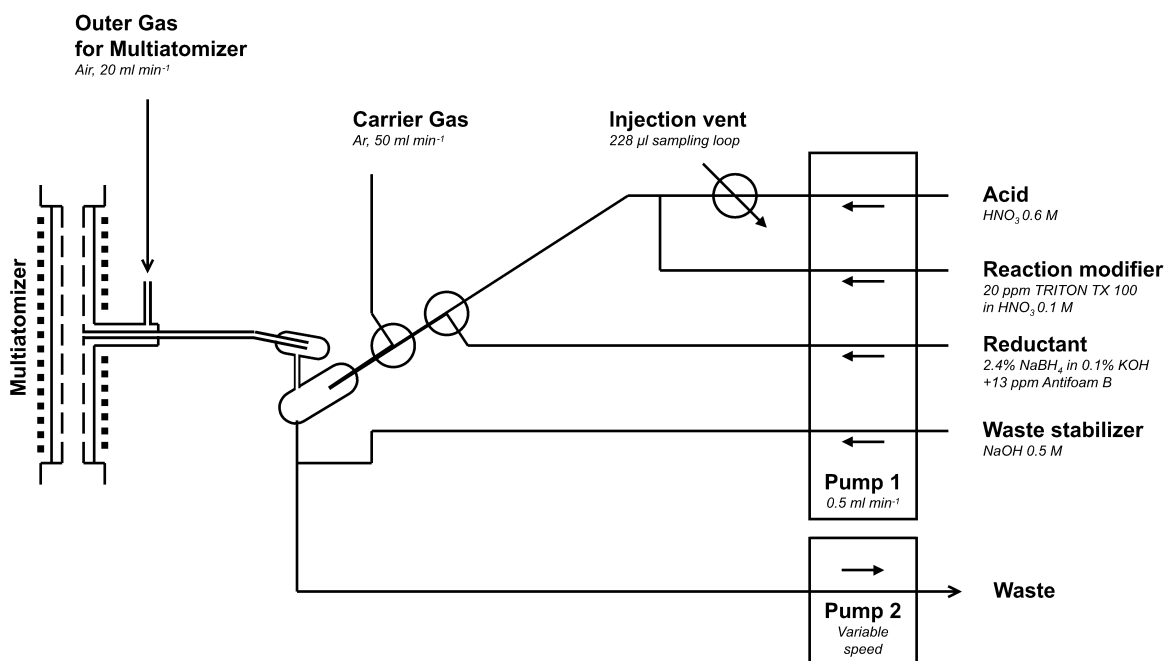
Fig.1 FI mode of CVG
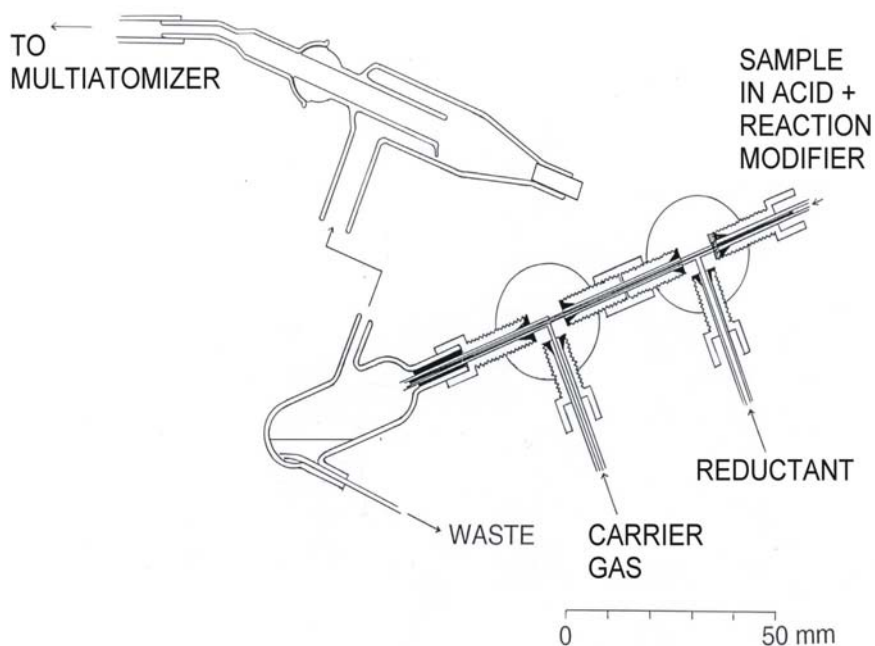
Fig.2 The detailed scheme of the CVG setup

2.4 Preparation of radiotracer

A radioactive indicator [111]Ag (half-life 7.45 days) of high specific activity was prepared by irradiation of palladium by thermal neutrons in research nuclear reactor LVR-15 (Nuclear Research Institute Řež plc) by [110]Pd(n,γ)[111]Pd(β−)[111]Ag process followed by chemical separation and isolatotion of radionuclide [111]Ag on anion exchanger (as chlorocomplex).

2.5 111Ag radiotracer experiments

The determination of the CVG efficiency was carried out by means of two tandem syringe filter units (30 mm diameter, 0.2 μm pore size) which captured the analyte from the gaseous phase before the entry to multiatomizer. The scintillation γ-counter Minaxi 5000 series (Packard) was used for measurements of gamma activity in leachates of these filters and other parts of the apparatus. For spatial distribution of activity, the image plate autoradiography (Fuji Film Imager Plate, BAS 5000 Scanner) was employed.

3. Results and discussion

The signal of FI measurements are shown in Fig.3, which presents a comparison of signals at the different reagent flow rates. The highest peak area response was gained at the rates of acid, reaction modifier and reductant 0.2 ml·min^{-1}, however, the peak was too broad. Therefore the flow rate 0.5 ml·min^{-1} of reagents was employed for futher analysis. It is also very important to ensure the decrease of the signal to the baseline at the end of measurement time. In general, the reproducibility of peak area response was about 4 % at 100 ng·ml^{-1} level.
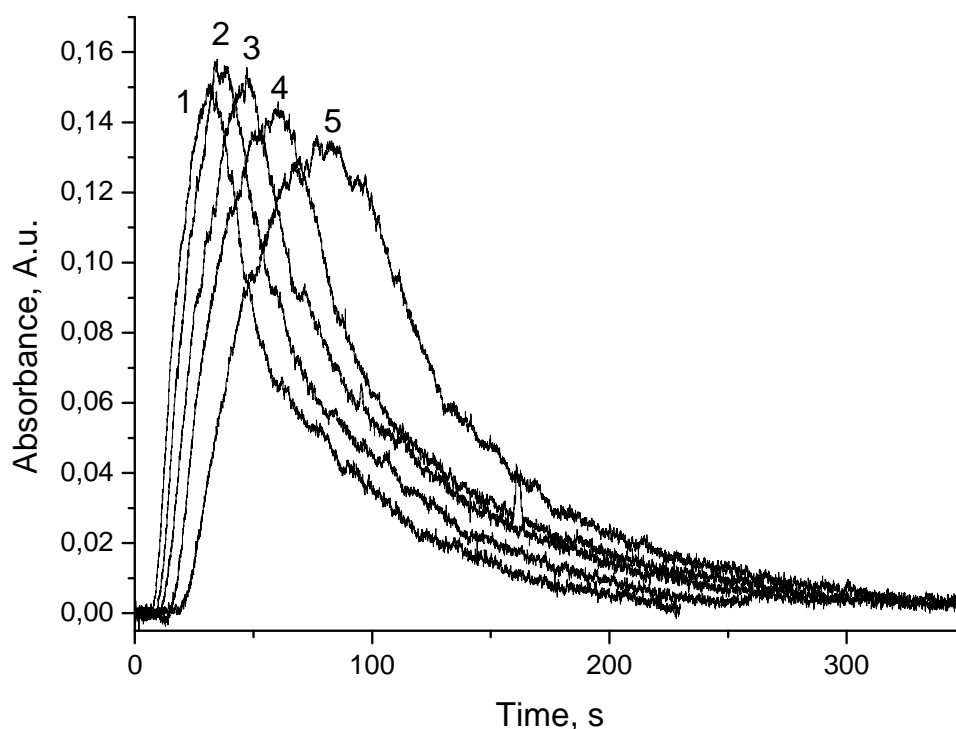
Fig.3 The optimalization of reagents flow rate; *1 – 0.6 ml·min^{-1}, 2 – 0.5 ml·min^{-1}, 3 – 0.4 ml·min^{-1}, 4 – 0.3 ml·min^{-1}, 5 – 0.2 ml·min^{-1} (100 ng·ml^{-1} Ag).*

As shown in Fig.4, higher atomization temperature increases sensitivity. On the other hand, severe corrosion of quartz was observed, probably due to high aerosol carryover to the atomizer at high temperature. 900°C was chosen as a compromise. The atomization temperature dependence along with other results, such as little influence of outer gas introduction, imply the mechanism of thermal decomposition of analyte in the multiatomizer. This contrasts with the hydrogen radical mechanism proven in atomization of "classical" hydrides.

Relative and absolute limits of detection (3σ, 228μl sample loop) measured at optimized conditions were determined as 3.5 ng·ml^{-1} and 0.8 ng, respectively.
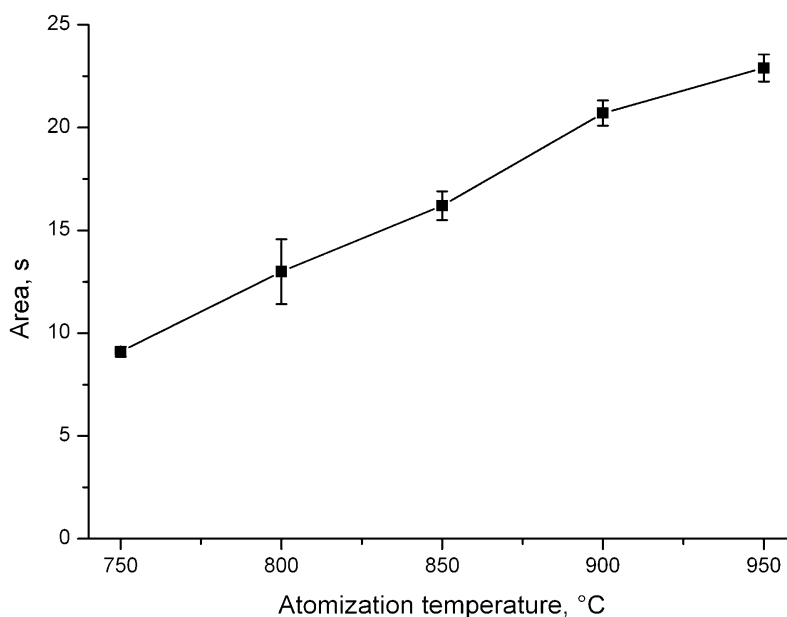
Fig.4 The atomization temperature; *100 ng·ml⁻¹ Ag.*

The [111]Ag radiotracer experiments were employed for determination of the CVG efficiency and the spatial distribution of residual [111]Ag in the apparatus. It was found that 23 % of analyte was converted to the gaseous phase. However, only 8 % was found in filters placed at the entrance to the atomizer. The rest was lost on the way to the filters, especially in the spray chamber. About 40 % of analyte remained in the waste liquid, the rest was deposited on the wall of apparatus: 15 % in the waste conduit, 12 % on the wall of the GLS and about 4 % on the tip of the cappilary, where sample is mixed with the reductant.

4. Conclusion

The CVG procedure for silver was optiomized in order to achieve maximum sensitivity and method robustness. The optima-tization of atomization temperature indicates the thermal decomposition of analyte in the multiatomizer. The radiotracer experiments proved that 23% of analyte is converted to the gaseous phase, but 8 % of analyte actually enters the atomizer which can be considered as the intoduction efficiency.

Acknowledgement

References

[1] Pohl P.; Prusisz B.: *Anal. Bioanal. Chem.* **388** *(2007), 753-762.*
[2] Dědina J.; Tsalev D.L.: *Hydride generation atomic absorption spectrometry. Chichester, Wiley (1995).*
[3] Pohl P.: *Trends Anal. Chem.* **23** *(2004), 21-27.*
[4] Matoušek T.: *Anal. Bioanal. Chem.* **388** *(2007), 763-767.*
[5] Matoušek T.; Dědina J.; Vobecký M.: *J. Anal. Atom. Spectrom.* **17** *(2002), 52-56.*
[6] Matoušek T.; Sturgeon R.E.: *J. Anal. Atom. Spectrom.* **18** *(2003), 487-494.*
[7] Matoušek T.; Sturgeon R.E.: *J. Anal. Atom. Spectrom.* **19** *(2004), 1014-1016.*
[8] Matousek T.; Dedina J.; Selecka A.: *Spectrochim. Acta B* **57** *(2002), 451-462.*

NEW ELECTROLYTIC CELLS FOR ELECTRO-CHEMICAL HYDRIDE GENERATION IN AAS

Jakub Hraníček, Václav Červený and Petr Rychlovský

Charles University, Faculty of Science, Hlavova 8, 128 40 Prague 2, Czech Republic; e-mail: hranicek.jakub@email.cz

Abstract

The construction and optimization of new types of miniaturized flow-through electrolytic cells for electrochemical hydride generation in atomic absorption spectrometry (HG-AAS) were studied in this work. The aim of this work was to achieve comparable or higher generation efficiency while inner volume suppression. This is important for minimization of zone dispersion by connection of electrochemical hydride generation with chromatographic techniques (HPLC) in speciation analysis. The contribution of the miniaturized electrolytic cells to the signal dispersion should by minimal.

Five different types of miniaturized flow-through electrolytic cells with lead cathode and platinum anode were constructed in this work. In these cells the ion-exchange membrane was not used and therefore there was only one carrying electrolyte used for both of electrode chambers. For two of these cells higher sensitivity and better limit of detection for selenium determination with HG-AAS technique and electrochemical generation of selenium hydride were obtained then for classical thin-layer flow-through cell.

Keywords

Atomic absorption spectrometry; electrochemical generation; volatile hydride; efficiency; miniaturization; electrochemical cell; atomization

1. Introduction

Electrochemical generation (EcHG) is an alternative method of generation of volatile compound[1]. This method eliminates many complications coupled with classical method of chemical generation (CHG). For example, for analyte reduction electric current with electrolyte which consists of high pure mineral acids is used instead of alkaline solution of $NaBH_4$ needed in chemical generation.

The electrochemical generation of volatile compound technique is used as a derivatization technique in connection of separation techniques (HPLC) with detection by element selective spectroscopic method. This experimental formation is often applied in the speciation analysis to determine each form of an element[2]. The important requirement for this formation is minimal inner volume, especially for electrolytic cell. On the other hand, the efficiency should not be declined with decreasing inner volume of electrolytic cell. However, both of these requirements, high efficiency and minimal inner volume, are contradictory and it is necessary to find compromise.

Nowadays the thin-layer models of electrolytic cell[3,4], usually designed from plexiglass, teflon or polypropylene, are often used and therefore they are sufficiently examined and exist in various modifications[5,6]. There are ion-exchange Nafion membranes used for separation cathode and anode chambers and electrolytes. In the separated compartments there are electrodes of different types, shapes and materials (lead, carbon or platinum).

The aim of this work was construction and optimization of new types of flow-through electrolytic cells for electrochemical hydride generation with minimal inner

volume and high efficiency, which are operated in the mode of continual-flow analysis and flow-injection analysis.

2. Experimental
2.1 Construction types of the cells

Five types of miniaturized flow-through electrolytic cells were constructed in this work (see Fig.1). All of these new types of cells consist only of one piece of plexiglass with appropriate electrode chambers inside. Since no Nafion membrane is incorporated, there is only one carrying electrolyte which is common to both electrode chambers.
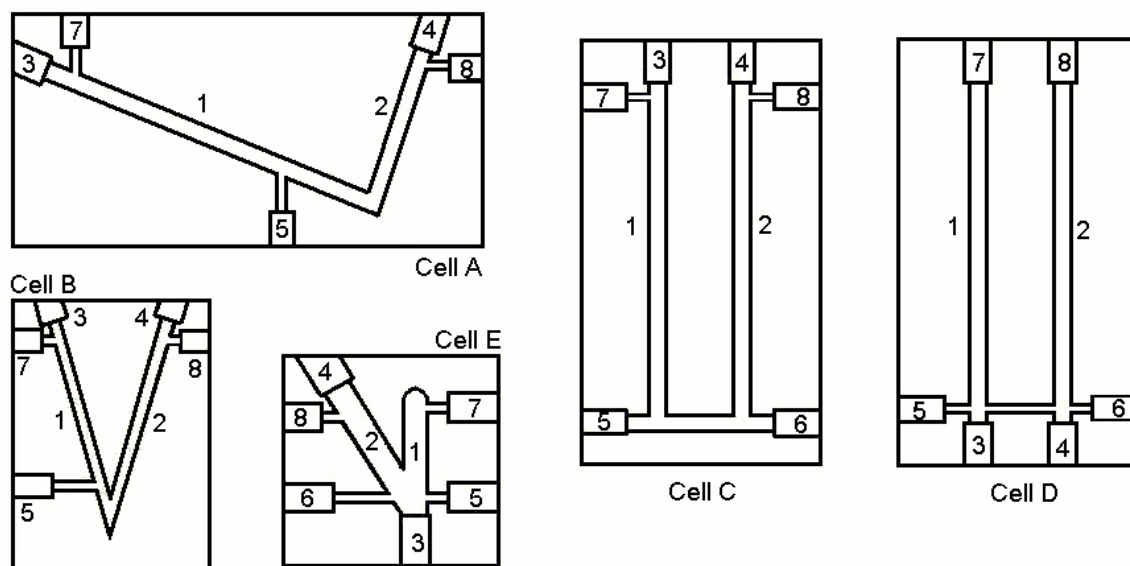
Fig.1 New flow-through electrolytic cells.
1 – cathode chamber, 2 – anode chamber, 3 – cathode holder, 4 – anode holder, 5,6 – electrolyte inlet (pure or containing analyte), 7 – outlet to gas-liquid separator, 8 – waste outlet

At first cells A and B were constructed. The electrolytic chambers are V-shaped. In the cathode chamber there is a lead-wire cathode and in the anode chamber there is a platinum-wire anode. There is only one electrolyte inlet coming to the cathode chamber, through witch the electrolyte flows into the cell. At first pure electrolyte flows through this inlet into the cell and is distributed into each electrolytic chambers. Afterwards electrolyte containing analyte flows into the cell. The products of reaction on the platinum anode are transported out of the cell into waste. Flow volume in anodic chamber is controlled by peristaltic pump so that anode is submerged and electrolyte mainly flows through the cathode chamber. The gaseous and liquid products from the cathode are transported by carrying gas (Ar) to the hydrostatic gas-liquid separator, where volatile compound of analyte (hydride in this case) is separated from liquid matrix and then transported into the externally heated quartz atomizer placed directly in spectral axis of the atomic absorption spectrometer (see Fig.2).
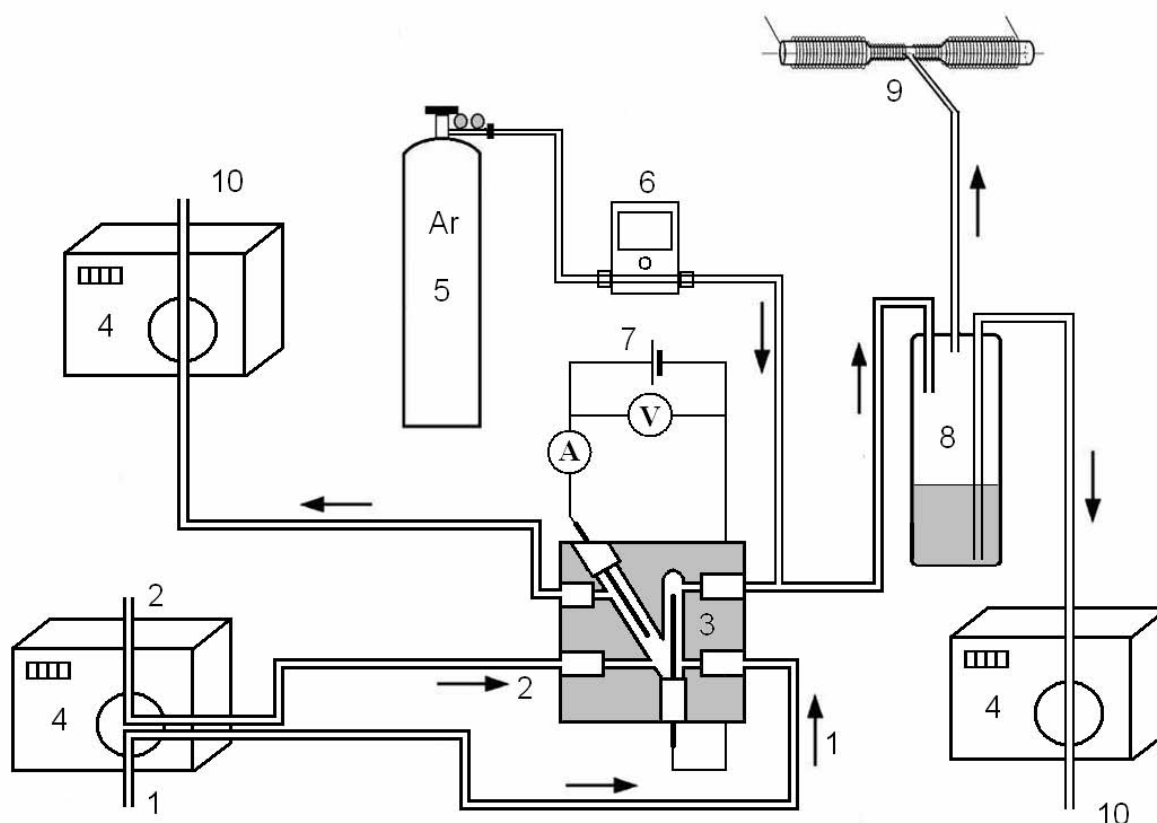
Fig.2 Instrumental setup for EcHG-AAS with cell E.
1 – catholyte, 2 – anolyte, 3 – flow-through electrolyte cell (type E), 4 – peristaltic pump, 5 – carrier gas, 6 – flow meter, 7 – electric current supply, 8 – gas-liquid separator, 9 – quartz tube atomizer, 10 - waste

In the following phase cells C and D were constructed. The electrode chambers are situated in parallel in these cells, they are connected by horizontal tube and there are two electrolyte inlets – one to transport pure electrolyte into the anode chamber and the other transport pure electrolyte/electrolyte with analyte into the cathode chamber. As in the previous cells (A, B), there is peristaltic pump to control anode flow volume.

Finally cell E was constructed. This cell is a combination of both previous groups of cells. Cell E is very small with miniature electrode chambers which are V-shaped and there are two electrolyte inlets.

To confront inner volume of newly constructed cells with comparative classic thin-layer cell (TL) see Table 1.

2.2 Instrumentation

For working parameters optimization and determination of basic characteristics spectrometer Pye Unicam 939 AA with Sb hollow cathode lamp (8 mA, 196.0 nm, spectral interval 1.0 nm) was used. For electrolyte transport peristaltic pump MasterFlex® L/S was used.

2.3 Reagents

All working selenium solutions of required concentration were prepared from analytical grade purity chemicals and standards (1.000 ± 0.002 g.dm^{-3} Se). For all dilution deionized distilled water purified with a Milli-QPLUS system was used. All electrolytes (H_2SO_4, HCl and H_3PO_4) were of high analytical purity. Ar of the 99.998% purity was used as the carrier gas.

3. Results and discussion

Selenium was used as the model element to optimize and prove new type of flow-through electrolytic cells. Optimized working parameters and basic characteristics for each cell were confronted with reference thin-layer flow-through cell.

Working parameters optimizations

For each newly constructed cell was necessary to optimize working parameters including shape and material of electrode, type and concentration of electrolyte, electrolyte flow rate, carrier gas flow rate, maximum generation current, anodic flow rate etc. In all of these cases the received signal corresponding with 60 μg.dm^{-3} Se solution was studied.

At first flow rate in anodic chamber was optimized. It was necessary to establish hydrostatic balance between influent and effluent electrolyte and gaseous products formed by electrode reactions using peristaltic pump to control anode flow rate. If anode flow rate was slow, the electrolyte was thrust from the anode chamber by gaseous products and after the electrolyte level fell under the end of electrode the electrolysis stopped. On the other hand, if the anode flow rate was fast, the same situation was observed in the cathode chamber. To ensure continual electrolysis in the electrolytic cells it was necessary to find optimized anode flow rate different for each cell.

When HCl (typical electrolyte used in classical thin-layer cells) was used as the electrolyte, there was no signal observed. The reason why no signal was observed is probably gaseous chlorine generated on the anode and consequently infiltrating into the cathode chamber and interfering with generated selenium hydride. Then H_3PO_4 was tested, but also without signal. Finally H_2SO_4 was used and the signal was observed. Therefore H_2SO_4 of concentration 1.0 mol.dm^{-3} was used for further experiments.

In these cells it was impossible to integrate carrier gas (Ar) before inlet into the cell, because small bubble of flowing carrier gas interrupted electrolyze. Due to this, it was necessary to integrate the carrier gas between cell output and gas-liquid separator to speed up transport of selenium hydride into the quartz atomizer. Typical optimal gas flow rate was approximately 10.0 ml.min^{-1}.

The dependence of the absorption signal on the electrolyte flow rate is not so significant. This flow rate value has only lower limit when electrolyze is interrupted.

The dependence curve of the absorption signal on the generation current has characteristic shape for each electrolytic cell. For low current values low absorption signals were obtained. From 0.15 to 0.35 A (for cell D) the signal rocketed and after 0.35 A the signal increased gradually and further on decreased slowly. For continual hydride generation it is better to use lower current than maximum value because the electrolyte does not get so warm and the lifetime of the generation cells is prolonged.

Finally the concentration of electrolyte (acid) was optimized. The dependence curve of absorption signal on the electrolyte concentration is downward sloping. As a consequence of this it would seem better to use very low electrolyte concentration to obtain the high signal. But in low concentration electrolyte, there is low concentration of particles able to conduct electric current and it is necessary to use high electric voltage and thus the electrolyte gets very warm. The optimal working parameters and inner volume of all cells are given in Table 1 and are compared with thin-layer electrolytic cell (TL).

Table 1 Optimal working parameters and inner volume.

Electrolytic cells	**E**	**D**	**TL**	**C**	**B**
Maximal generation current (A)	0.50	0.70	1.20	0.25	0.40
Carrier gas flow rate (ml·min^{-1})	10.0	20.0	20.0	10.0	10.0
Electrolyte flow rate (ml·min^{-1})	2.5	2.5	2.0	2.0	2.5
Electrolyte concentration (mol·dm^{-3})	1	1	1	1	1
Anode flow rate (ml·min^{-1})	5.3	7.0	---	3.5	1.6
Inner volume (mm^3)	214	353	999	339	318

Finding basic characteristics of selenium determination by EcHG-AAS using new types of electrolytic cells

Using optimal working parameters, the calibration values for selenium determination by EcHG-AAS for low (0 - 20 $\mu g.dm^{-3}$) and high (0 - 250 $\mu g.dm^{-3}$) concentrations were measured for cells B, C, D, E and thin-layer cell. Basic characteristic of selenium determination, including limit of detection, limit of determination, sensitivity, repeatability, correlation coefficient, linear dynamic range and other parameters were obtained by processing these calibrations. For summary of these characteristics see Table 2.

Table 2 Basic characteristics.

Electrolyte cells	**D**	**E**	**TL**	**C**	**B**
Limit of detection ($\mu g \cdot dm^{-3}$)	0.32	0.52	0.60	1.50	2.23
Limit of determination ($\mu g \cdot dm^{-3}$)	1.06	1.73	2.01	5.20	7.44
Sensitivity $\cdot\ 10^3$ ($dm^3 \cdot \mu g^{-1}$)	7.32	4.14	4.86	2.76	1.53
Repeatability (%)	0.56	0.53	0.62	1.78	1.40
Correlation coefficient	0.9988	0.9992	0.9995	0.9985	0.9982
Linear dynamic range ($\mu g \cdot dm^{-3}$)	1.06-100	1.73-100	2.01-100	5.20-100	7.44-100

4. Conclusion

New designs of flow through electrochemical cells were constructed and tested. These electrochemical cells enable to obtain sensitivity which is comparable (or higher) to original thin-layer cell at markedly lower generation electric current value. Thanks to their low inner volume (and minimal signal zone dispersion) compared to classical thin-layer flow-through cell it is possible to use these miniaturized cells as derivatization units after HPLC separation in speciation analysis of As or Se.

Acknowledgment

References

[1] Dědina J.; Tsalev D.: *Hydride Generation Atomic Absorption Spectrometry. John Wiley and Sons, Chichester, 1995.*

[2] Červený V.; Válková Z.; Rychlovský P.: „The application of electrochemical hydride generation as a derivatization step for HPLC-QFAAS determination of selected arsenic species" in *Book of Abstracts of Colloquium Spectroscopicum Internationale XXXIV, University of Antwerp, 200, p. 232.*

[3] Lin Y.H.; Wang X.R.; Yuan D.X.; Yang P.Y.; Huang B.L.; Zhuang Z.X.: *J. Anal. Atom. Spectrom. **7** (1992), 287.*

[4] Brockmann L.; Nonn C.; Golloch A.: *J. Anal. Atom. Spectrom. **8** (1993), 397.*

[5] Hueber D. M.; Winefordner J. D.: *Anal. Chim. Acta **316** (1995), 129.*

[6] Šíma J.; Rychlovský P.: *Chem. Listy **92** (1998), 676.*

THIOGLYCOLIC ACID AS ON-LINE PRE-REDUCTANT FOR SPECIATION ANALYSIS OF ARSENIC BY SELECTIVE HYDRIDE GENERATION-CRYOTRAPPING-AAS

Stanislav Musil[a,b], Tomáš Matoušek[a] and Petr Rychlovský[b]

[a] *Institute of Analytical Chemistry of the ASCR v.v.i., Víděňská 1083, 14220 Prague, Czech Republic; e-mail: stanomusil@biomed.cas.cz*
[b] *Charles University in Prague, Faculty of Science, Department of Analytical Chemistry, Albertov 6, 12843 Prague, Czech Republic*

Abstract

This work represents an improvement of current method of speciation analysis for determination of tri- and pentavalent inorganic, mono-, di- and trimethylated arsenicals using atomic absorption spectrometry (AAS) as a detector. The selective hydride generation based on pre-reduction is applied for differentiation of tri- and pentavalent arsenicals whereas the separation and preconcentration of arsine, methylarsine, dimethylarsine and trimethylarsine is carried out by means of cryotrapping. Presented study shows that 2% (m/v) L-cysteine currently used for pre-reduction of pentavalent arsenicals can be substituted by 1% (m/v) thioglycolic acid suitable for an on-line pre-reduction. Much faster reduction of pentavalent arsenicals (1-2 min) at 25°C with equal sensitivities as in the case of L-cysteine is achieved. The on-line pre-reduction is accomplished in a reaction coil where sample zone merges with thioglycolic acid. The suppression of axial dispersion and better mixing are achieved by means of air segments added to the sample and carrier flows. The standard calibrations measured with or without on-line pre-reduction indicate uniform and equal sensitivities. The possibility of standardization by water standards of single species (e.g. iAs^{III}) for quantification of all other As forms in urine is demonstrated in the recovery study. The limits of detection for all methylated arsenicals range between 30 and 50 pg·ml^{-1} and for iAs^{III} and iAs^{V} were between 100 and 140 pg·ml^{-1}.

Keywords

HG-AAS; arsenic; on-line pre-reduction; speciation; thioglycolic acid

1. Introduction

Tri- and pentavalent inorganic, mono-, di- and trimethylated arsenicals are required to be determined at ultra trace levels due to their high toxicity and mutagenic, teratogenic and carcinogenic effects[1-3]. The human metabolism of inorganic As (iAs) consists of the reduction of pentavalent arsenicals and the oxidative methylation of trivalent species that yields methylated arsenicals[4]. The conversion of species such as arsenite (iAs^{III}), arsenate (iAs^{V}), methylarsonite (MAs^{III}), methylarsonate (MAs^{V}), dimethylarsinite ($DMAs^{III}$), dimethylarsinate ($DMAs^{V}$) and trimethylarsine oxide ($TMAs^{V}O$) to their corresponding arsines by means of sodium tetrahydroborate ($NaBH_4$) is an underlying technique of the hydride generation (HG). The association of the HG with cryotrapping and gas chromatography (HG-CT) using atomic absorption spectrometry (AAS) for sensitive detection allows to separate arsines generated from iAs, MAs, DMAs and $TMAs^{V}O$ according to their boiling points and chromatographic properties of the trap. The distinguishing between tri- and pentavalent arsenicals is provided by the selective HG which can be based on the presence or absence of pre-reductant with –SH group, namely L-cysteine (L-cys) is commonly used[5-10]. Hydrides of trivalent arsenicals and $TMAs^{V}O$ are

selectively generated from Tris·HCl buffer (pH 6), whereas arsines of both tri- and pentavalent arsenicals are generated after pre-reduction from the same medium[9].

Nowadays an automatization of the analytical methods and a minimum sample pre-treatment are required. Therefore, replacement of the time-consuming off-line pre-reduction by the method with integrated pre-reduction step (on-line pre-reduction) is desirable. No loss of sensitivities, low consumption of all reagents and simplicity are the main requirements. The general limiting factor is the reaction rate of a pre-reduction agent with As species.

L-cys is not suitable for on-line pre-reduction because it needs about 1 hour to complete the reaction with iAs^V, MAs^V and $DMAs^V$ at room temperature[9,11]. The application of thioglycolic acid (TGA) for on-line pre-reduction was sugested in Ref.[11] for its short reaction time with inorganic and methylated pentavalent As species, but its application has not been reported yet.

The general aims of this study were to confirm the performance of TGA for the off-line pre-reduction of As species in comparison to commonly used L-cys and to develop a setup for the on-line pre-reduction integrated with the HG-CT system. Flow injection (FI) arrangement with batch separation and the multiatomizer[12] for atomization of arsines were chosen. The validation of the method is presented for As speciation in human urine samples.

2. Experimental
2.1 Instrumentation

The detection was performed by an atomic absorption spectrometer Perkin-Elmer 503 without background correction with arsenic EDL lamp System I (Perkin-Elmer) operated at 8 W. A multiple microflame quartz tube atomizer[12] heated eletrically to 900 °C with 40 ml·min^{-1} of air as outer gas was employed for atomization.

2.2 Standards and reagents

Deionized water (Ultrapur, USA) was used for preparation of all solutions. Working standards were prepared for individual species by serial dilution of stock solutions. Human urine diluted with deionized water (1:1) spiked with As species was employed for recovery study.

A reducing solution containing 1% (m/v) $NaBH_4$ (FLUKA, Germany) in 0.1% (m/v) KOH (Lach-Ner, s.r.o., Czech Republic) was prepared fresh daily. For analysis of urine samples 0.2 ml of 1% (m/v) solution of Antifoam B emulsion (Sigma, USA) per 100 ml of the reducing solution was added to prevent foaming. A 0.75 M TRIS·HCl buffer was prepared from a reagent grade Trizma®hydrochloride (Tris(hydroxymethyl)amino-methane hydrochloride, Sigma, Germany). L-cysteine hydrochloride monohydrate (L-cys·HCl·H_2O) (Merck, Germany) for off-line pre-reduction and thioglycolic acid (Fluka, Germany) for both off-line and on-line pre-reduction were used as pre-reduction agents.

2.3. Systems for HG
2.3.1 FI mode with off-line pre-reduction

A scheme of the system is shown in Fig.1a. All reagents were pumped by means of peristaltic pump (PP1) at the rates 1 ml·min^{-1}. The manifold was built from PTFE T-junctions and PTFE tubing. A sample was injected into flow of deionized water by a six-port injection valve with 597 µl sample loop volume. A plastic GLS with forced outlet capable to handle overpressure caused by resistance of a U-tube was employed. The cryogennic trap device consisted of the 305 mm long glass U-tube with 2.5 mm i.d. wrapped with a wire Ni80-Cr20 (0.6 mm o.d.; 5.275 Ω·m^{-1}; 15 Ω total resistance; Omega engineering, inc., USA) for gradual heating and filled with 0.92 g Chromosorb WAW-

DMCS 45/60, 15 % OV-3 (Supelco, USA). About ¾ of the U-tube was immersed into the 1.5 l Dewar flask with a liquid nitrogen during trapping of hydrides, while in the release phase the U-tube was heated by means of current of 2 A (30 V). The flow rates of carrier He (75 ml·min^{-1}) and H$_2$ (20 ml·min^{-1}) were employed in the whole course of analysis.
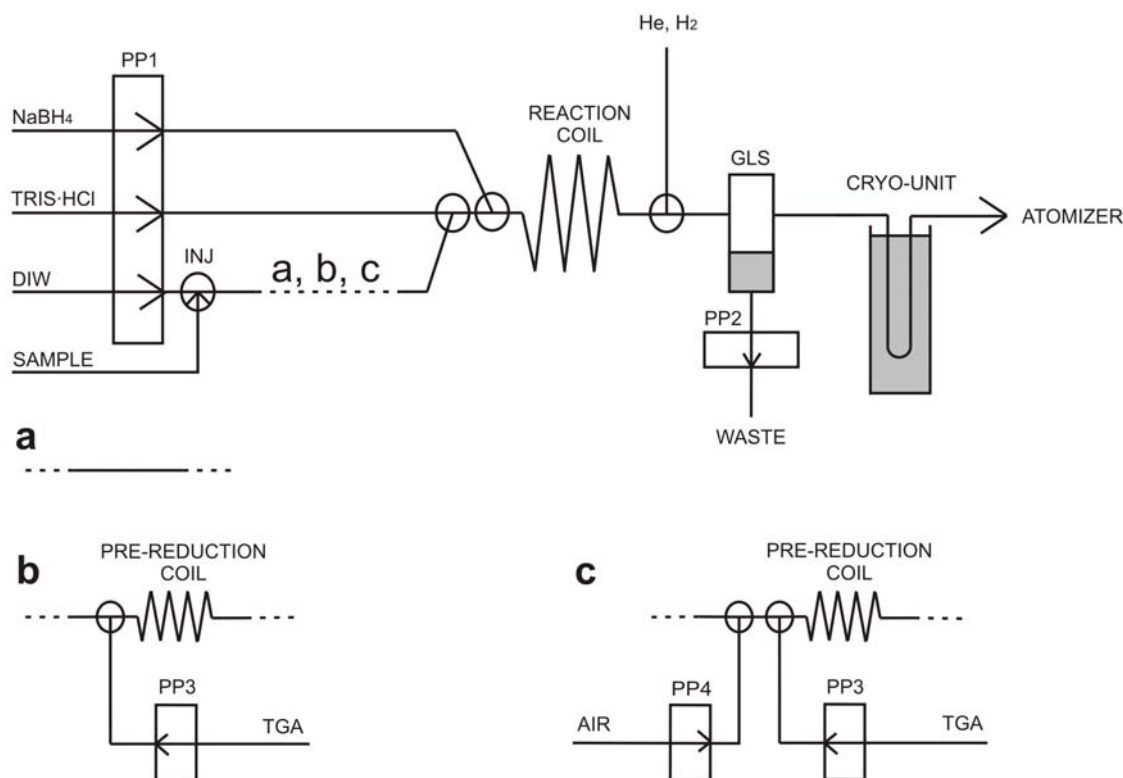
Fig.1 Experimental setups of HG-CT-AAS with off-line pre-reduction (a) and with on-line pre-reduction (b,c) *INJ – injection valve (0.6ml sample loop); GLS – gas-liquid separator; PP1-4 – peristaltic pumps.*

2.3.2 FI mode with on-line pre-reduction

The experiments with on-line pre-reduction of pentavalent arsenicals were carried out using the system displayed in Fig.1b. A peristaltic pump (PP3) was added to pump 5% (m/v) TGA at the rate 0.25 ml·min^{-1} (1% in each liquid segment after mixing, see Sec. 3.1). To form segmented flow of liquid (SFA), another peristaltic pump (PP4) was added to pump air into the manifold at the rate 0.15 ml·min^{-1} (Fig.1c). Both additional channels were built from PTFE T-junctions and PTFE tubing. Various pre-reduction coils were made from 1/16˝ o.d. PTFE tubing: 0.75 mm i.d. for 0.06 to 2.4ml coils and 1 mm i.d. for 2.9 and 3.5ml coils.

2.4 Procedure

Off-line pre-reduction: Pre-reducing agent was added to the standards/samples at least 1 hour prior to analysis. U-tube was imersed into liquid N$_2$ before the beginning of the cycle. It was started off by switching on the PP1 and after 3 s sample was manually injected by means of injection valve into a carrier flow (deionized water). The PP1 was switched off after 90 s; another 90 s was allowed to complete the reaction and transport arsines from the GLS to the U-tube. Then, the Dewar flask with liquid nitrogen was manually removed and volatilization stage could begin. Simultaneously, the heating of resistance wire was switched on and recording of signal (60s read window) started after 10s delay. At the end of the measurement, the PP2 was switched on and the waste liquid was removed from the GLS; the heating was left on for 30 s to dry the moisture from the U-tube. Total time of the procedure was 343 s.

On-line pre-reduction: The HG setup of Fig.1b,c was used. The whole procedure was similar to the procedure with off-line prereduction. The PP3 pumping TGA solution was running for 60 s only to cover the sample plug only, while the PP4 had been running 3 s before and in the course of the whole HG step when SFA was performed (Fig. 1c). The duration of the HG step depends on the pre-reduction coil volume: the time was 230 and 330 s for 2.4 and 3.5ml pre-reduction coils, respectively, when on-line pre-reduction without SFA was employed, and 90; 90; 120; 150; 160; 190; 210; 240 and 270 s for 0; 0.06; 0.5; 1; 1.4; 1.9; 2.4; 2.9 and 3.5ml pre-reduction coils, respectively, for measurements with SFA. The rest of the cycle was identical to the off-line pre-reduction.

3. Results and discussion
3.1 Off-line pre-reduction - comparison of L-cys and TGA

The performance of commonly used L-cys and proposed TGA as prereductants/ reaction modifiers in TRIS·HCl buffer reaction media for HG of sum of both tri- and pentavalent arsenicals in terms of sensitivity and repeatability was compared. It was found that L-cys can be used for off-line pre-reduction in a concentration range between 1 % and 3 % (m/v) of L-cys·HCl·H$_2$O added to a sample which provides the complete pre-reduction of iAs^V, MAs^V and DMAs^V. 2 % (m/v) of L-cys·HCl·H$_2$O was used for further experiments.

In the case of TGA, it was found that 0.5 % (m/v) is sufficient for complete pre-reduction. 1% (m/v) TGA in a sample solution was found optimal and used in experiments with on-line pre-reduction.
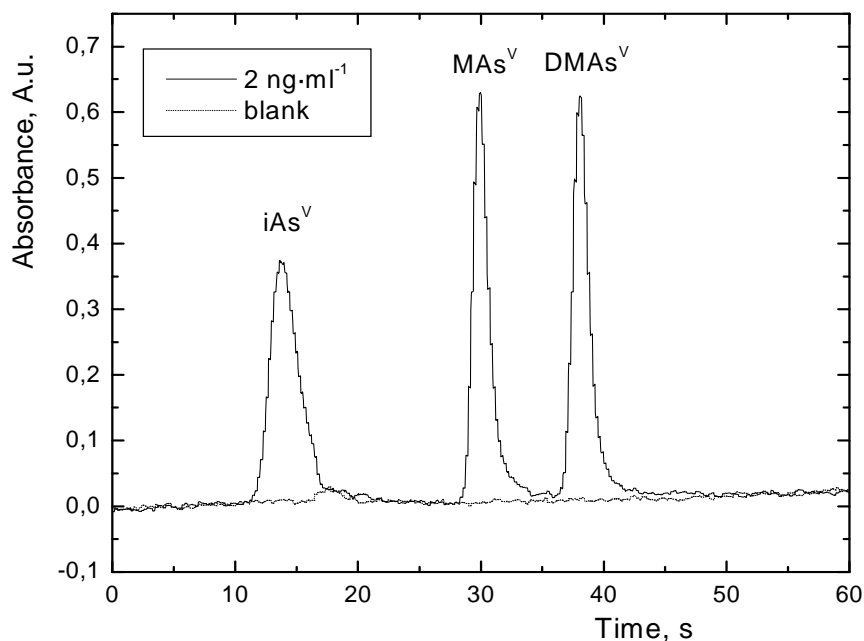
Fig.2 The typical chromatogram of arsenic species with 2% (m/v) L-cys·HCl·H$_2$O treatment; *2 ng·ml^{-1} As for each species*

The typical chromatogram of a mixed standard of pentavalent species obtained by means of off-line L-cys pre-reduction is ilustrated in Fig.2. No change in sensitivities or repeatabilities (RSD) using TGA instead of commonly used L-cys was found: The peak area responses of arsenicals treated with TGA with respect to signals measured with L-cys pre-reduction were 98.9 ± 3.0 % for iAs^V; 100.2 ± 3.1 % for MAs^V; 101.0 ± 2.3 % for DMAs^V.

3.2. On-line pre-reduction
3.2.1 Preliminary investigation

To achieve the optimum concentration of 1 % (m/v) of TGA in the sample/standard solution (see Section 3.1), the concentration of TGA 5 % (m/v) at the flow rate of 0.25 ml·min^{-1} in the separate channell was used. The on-line pre-reduction was tested with 2.4 and 3.5ml pre-reduction coils (Fig.1.b), but the efficiencies didn´t reach 100 % for all pentavalent arsenicals. The disadvantages were incomplete pre-reduction of MAs^V even in the larger coil, long time of pre-reduction, and increased content of total iAs in the blanks.

In the case when TGA is pumped only to the zone of the sample, the axial dispersion can cause that the whole zone may not contain optimum concentration of prereductant, as well as prolong the time necessary for purging a sample from the pre-reduction coil. The suppression of an axial dispersion and a better mixing can be achieved using SFA by means of air segments added to a sample and carrier flow (Fig.1.c). Air segmentation allowed to add TGA solely to the sample zone. The efficiencies of pre-reduction by SFA with 3.5ml pre-reduction coil as compared with off-line pre-reduction results for iAs^V, MAs^V and DMAs^V were 97.4 $\pm$ 2.6 %; 100.1 $\pm$ 2.0 % and 99.4 $\pm$ 2.5 %. Therefore the setup with SFA was applied for futher investigation.

3.2.2 Pre-reduction coil volume

The optimal pre-reduction coil volume (and corresponding reaction times of iAs^V, MAs^V and DMAs^V with TGA) were studied. Fig.3 shows that iAs^V is fully reduced in about 45 s, while complete pre-reduction of MAs^V and DMAs^V requires 115 s. Therefore the 2.4ml coil was found sufficient for complete pre-reduction with SFA.
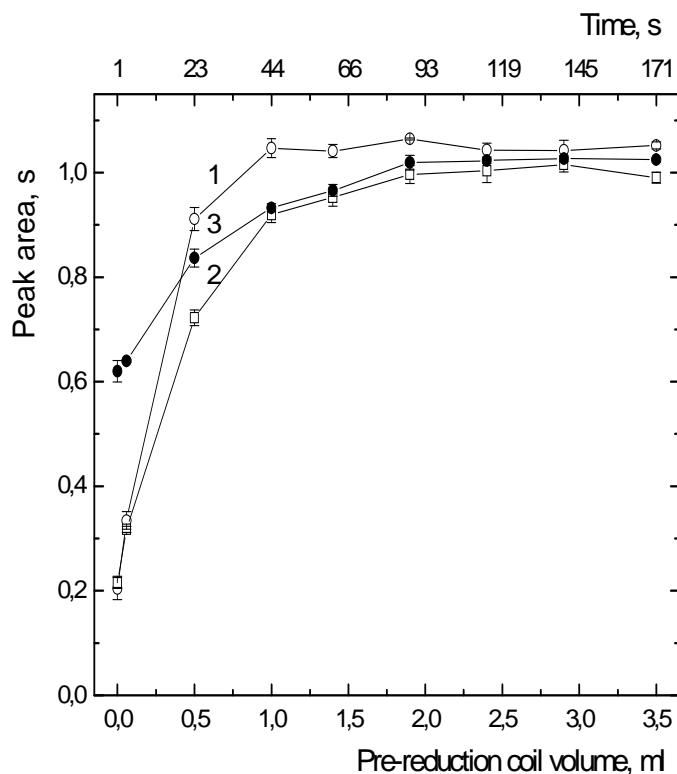
Fig.4 The dependence of the signal on the pre-reduction coil volume; *1 – iAs^V, 2 – MAs^V, 3 – DMAs^V (2 ng·ml^{-1} As each)*

3.2.3 Calibrations and LODs

Calibration graphs were tested for all forms. The comparison of slopes of calibrations shows good uniformity of sensitivities for iAs^{III} with and without pre-reduction, and iAs^V, MAs^V, DMAs^V after pre-reduction (Table 1). These results enable the

use of single species standardi-zation for quantification of all As forms[9] using on-line setup. Lower sensitivity of $TMAs^VO$ with the pre-reduction is probably caused by production of trimethylarsine at earlier stage. An unsufficient separation from liquid phase in the GLS and also transport losses of volatile compound before the GLS can play a role.

The limits of detection for iAs^{III} and iAs^V (Table 1) were caused by non-specific absorption and iAs^{III} content in the blanks. The relative LODs could be futher improved using greater sample loop volume, and in the case of iAs^{III} and iAs^V also by use of background correction.

Table 1 Slopes of calibrations, relative sensitivities (related to iAs^{III} sensitivity measured with on-line pre-reduction) and LODs (3σ, 597 µl sample); *concentration 0.25; 0.5; 1; 2 ng·ml^{-1} As each.*

As species	Slope, ml·s·ng^{-1}	Relative sensitivity, %	*LOD, pg·ml^{-1}*	*LOD, pg*
$iAs^{III\ (a)}$	0.420	92.1 ± 0.8	107	64
$iAs^{III\ (b)}$	0.456	100.0 ± 0.8	131	78
$iAs^{V\ (b)}$	0.450	98.7 ± 0.9	133	79
$MAs^{V\ (b)}$	0.447	98.0 ± 1.1	44	26
$DMAs^{V\ (b)}$	0.465	102.0 ± 1.1	48	29
$TMAs^VO^{\ (a)}$	0.432	94.7 ± 1.0	30	18
$TMAs^VO^{\ (b)}$	0.395	86.6 ± 1.5	45	27

[a] *Without pre-reduction (DIW instead of TGA was pumped to assure identical reaction time)*
[b] *On-line pre-reduction*

3.2.4 Recoveries of As species in urine matrix

A validation of the HG-CT method with on-line pre-reduction by TGA was carried out in human urine samples (diluted 1:1 by deionized water) spiked with inividual As forms. The recoveries of arsenic species (Table 2) verify the possibility using water standards of single specie for quantification of all As forms even in this matrices.

Table 2 Recoveries study – relative sensitivities (%) of As species in real biological matrix (urine and deionized water, 1:1) compared to water standards; *standard addition concentration 0; 1; 2 ng·ml^{-1} As each form.*

	iAs^{III}	iAs^V	MAs^V	$DMAs^V$	$TMAs^VO$
Without pre-reduction	99.0 ± 2.5	0	0	0	93.5 ± 1.6
On-line pre-reduction	102.6 ± 2.9	103.0 ± 1.0	100.1 ± 2.0	97.3 ± 3.3	n.d.

4. Conclusion

The selective HG procedure based on off-line pre-reduction by TGA acid is capable of resolution and quantification of inorganic and methylated arsenicals. TGA provides much faster reaction with all pentavalent arsenicals (1-2 min) compared to commonly used L-cys (30-60 min) which makes it suitable for on-line pre-reduction at room temperature. The standard calibrations measured with or without on-line pre-reduction indicated the uniform and equal sensitivities. The possibility of standardization by water standards of single species (e.g. iAs^{III}) for quantification of all other As forms in urine was demonstrated in the recovery study. Despite the analysis being prolonged by 2 mins as compared with off-line procedure, on-line pre-reduction simplifies sample pretreatment and increases sample throughput. This setup of pre-reduction should be also applicable for an automated system for the oxidation state specific speciation of inorganic and methylated arsenicals by selective hydride generation-cryotrapping-AAS.

Acknowledgement

References

[1] Hughes M.F.: *Environ. Health Persp.* **114** *(2006), 1790-1796.*

[2] Tsalev D.L.; Zaprianov Z.K.: *Atomic Absorption Spectrometry in Occupational and Environmental Health Practice, CRC Press, Boca Raton, Florida, (1983).*

[3] Valenzuela O.L.; Borja-Aburto V.H.; Garcia-Vargas G.G.; Cruz-Gonzales M.B.; Garcia-Montalvo E.A.; Calderon-Aranda E.S.; Razo L.M.: *Environ. Health Persp.* **113** *(2005), 250-254.*

[4] Cullen W.R.; McBride B.C.; Reglinski J.: *J. Inorg. Biochem.* **21** *(1984), 179-194.*

[5] J.Frank, M.Krachler, W.Shotyk: *Anal. Chim. Acta* **530** *(2005), 307-316.*

[6] Bortoleto G.G.; Cadore S.: *Talanta* **67** *(2005), 169-174.*

[7] Chen H.; Brindle I.D.; Le X.C.: *Anal. Chem.* **64** *(1992), 667-672.*

[8] Cordos E.A.; Frentiu T.; Ponta M.; Abraham B.; Marginean J.: *Chem. Spec. Bioavailab.* **18** *(2006), 1-9.*

[9] Matoušek T.; Hernández-Zavala A.; Svoboda M.; Langerová L.; Adair B.M.; Drobná Z.; Thomas D.J.; Stýblo M.; Dědina J.: *Spectrochim. Acta B (2007) accepted.*

[10] Welz B.; Šucmanová M.: *Analyst* **118** *(1993), 1417-1423.*

[11] Howard A.G.; Salou C.: *J. Anal. Atom. Spectrom.* **13** *(1998), 683-686.*

[12] Matousek T.; Dedina J.; Selecka A.: *Spectrochim. Acta B* **57** *(2002), 451-462.*

BILIRUBIN AND BILIVERDIN: STRUCTURAL STUDIES BY ELECTRONIC AND VIBRATIONAL CIRCULAR DICHROISM

Iryna Goncharova[a] and Marie Urbanová[b]

[a] *Institute of Chemical Technology, Prague, Technická 5, Department of Analytical Chemistry, 166 28 Prague 6, Czech Republic; e-mail:* gonchari@vscht.cz
[b] *Institute of Chemical Technology, Prague, Technická 5, Department of Physics and Measurements, 166 28 Prague 6, Czech Republic*

Abstract

Chiral recognition of bilirubin and biliverdin by poly(L-lysine), poly(D-lysine), and poly(L-arginine) and its micelles with dodecanoate ions at different pH was studied using a combination of vibrational and electronic circular dichroism. These systems were studied as the physiologically important model of the binding sites of the pigments and serum albumin. It was shown that biliverdin is more sensitive than bilirubin to pH in the complexes with polypeptides. Its conformation becomes more "closed" at acidic pH in the complexes with micellar systems with polylysine. Partial flattening and chiral self-association of bilirubin molecules takes place at higher pigment concentration in pigment-polypeptide systems. The inversions of ECD signals for the both pigments were observed in the systems with PLA at pH 8.5.

Keywords

Bilirubin; Biliverdin; Circular dichroism; Polypeptide; Chiral recognition

1. Introduction

Bilirubin (BR) and biliverdin (BV), toxic metabolites of heme in mammals are transported to the liver by serum albumin (SA) for further metabolism. In their most stable conformations, BR adopts folded ridge-tile molecular geometry whereas BV has a helical, lock-washer shape (Fig.1). In isotropic solvents the both pigments exist as racemic mixtures of isoenergetic M- and P- helical conformers[1].

Interest in the bilirubin-SA interaction arose when it became clear that high blood concentration of bilirubin is toxic to all tissues and causes irreversible brain damage[2]. These findings provided the motivation of study on the BR-SA binding mechanism for many years, making it one of the most studied of the SA-ligand interactions. The complex BV-SA is less studied but may be useful for understanding of the binding mechanism. One of the moot points are the lysine or arginine residues in SA binding sites involved in the complexation with the COO^- groups of the pigments.

Both the pigments exhibit optical activity in the presence of SA and it makes possible to use the circular dichroism techniques for their investigation.

In current study, we have employed the electronic circular dichroism (ECD) and for the first time vibrational circular dichroism (VCD) approaches in order to characterize the interaction of BR and BV with poly(L-lysine) (PLL), poly(D-lysine) (PDL), and poly(L-arginine) (PLA), which were chosen as simplified models of SA binding sites[3]. The goal of these experiments was to monitor how pH influences the pigments conformations in the complexes with the lysine and arginine residues.

Bilirubin
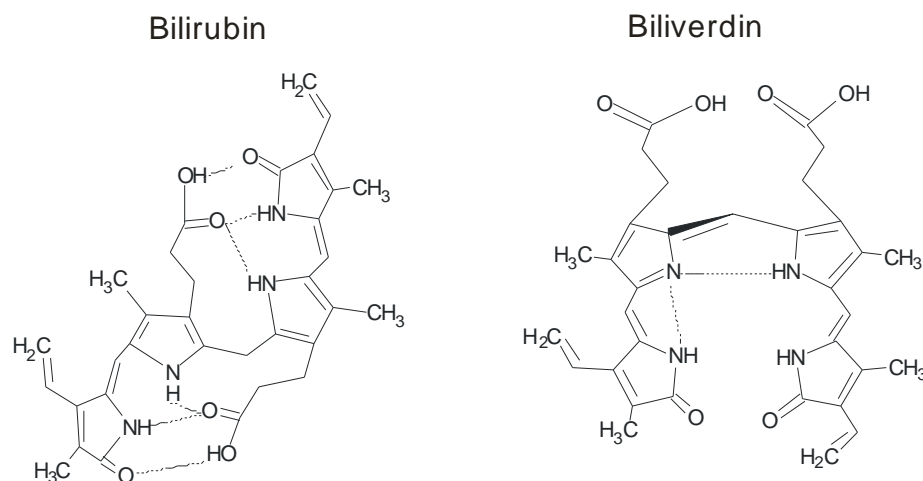
Biliverdin

Fig.1 Bilirubin-IX α ridge tile and biliverdin-IX α helical conformations showing intramolecular hydrogen bonds.

2. Experimental

2.1 Reagents

Poly(L-arginine) hydrochloride (M_w=35000 g mol^{-1}), poly(L-lysine) hydrobromide (M_w=44000g/mol), poly(D-lysine) hydrobromide (M_w=48000g/mol), dodecanoic acid (>98.0%), sodium hydroxide, hydrochloric acid, and D_2O (99.9% D) were supplied by Sigma/Aldrich and used as received.

Bilirubin-IXa and biliverdin-IXa hydrochloride (both Frontier Scientific) were used as salts.

2.2 Measurements by electronic circular dichroism

Double distilled water was used as a solvent for ECD measurements. Salts of BR or BV were added to the polypeptide solutions at pH = 10.8, concentration of the pigments was $1.5 \cdot 10^{-5}$ and $6 \cdot 10^{-5}$ mol L^{-1}. Nanoparticles were prepared according to the method described in Ref 4. Concentration of the poly(amino acid)s in solution were $3 \cdot 10^{-4}$ mol L^{-1}. All measurements were performed at room temperature and under nitrogen atmosphere. The ECD spectra were recorded on the Jasco J-810 spectropolarimeter using a quartz cell with a path length of 0.01 – 1 cm; the samples were flushed with dry ultrapurified nitrogen before and during the experiments. A slit program that afforded wavelength accuracy better than 0.5 nm and integration time of 2 s for each spectral point was used. The results are presented as mean molecular ECD intensities with respect to total pigment concentration.

2.3 Measurements by vibrational circular dichroism

Solutions in D_2O were used through all the VCD experiments. For VCD measurement, the pigments solution was added to the solution of peptide to achieve desired values of amount ratios. The concentration of peptides was kept at 0.24 mol L^{-1}. Complexes were prepared at temperature less then 10° C and the pH of the solutions was adjusted to 10.8 using NaOD. The final concentrations of the pigments were kept at 0.024, 0.034, and 0.048 mol L^{-1} for BR and at 0.034 mol L^{-1} for BV. For the micelle systems, polypeptides were mixed with sodium dodecanoate (C_{12}) at the room temperature and intensively shaken at pH=10.5. Concentration of the C_{12} ions was $5 \cdot 10^{-4}$ mol L^{-1}.

All samples were allowed to equilibrate for 30 minutes before the measurements and the stability of the samples was proved by comparison of the infrared absorption spectra recorded before and after each VCD measurement. VCD spectra were recorded in

the 1800–1350 cm^{-1} region at room temperature with a resolution of 8 cm^{-1} using a Fourier transform infrared spectrometer IFS-66/S (Bruker, Germany) equipped with a VCD/IRRAS module PMA 37 (Bruker) by a procedure that has been described in ref 5. A demountable cell with the CaF$_2$ windows and Teflon spacer of a 50 μm pathlength was used.

3. Result and discussion

The measurements for poly-lysine matrices were made at pH >10 to achieve the transition from the random coil to helical conformation. Taking into account that pigments form stereoselective complexes only with polypeptide in the helical conformation[1,3], recognition of BV and BR by PLA was not studied before, since the polypeptide PLA does not adopt helical conformational in aqueous soulution. Ref. 4 reports on nanoparticles of polypeptides with salt of dodecanoic acid (C$_{12}$) adopting their chains into predominantly α-helix conformation. In present study we use such systems where the uncomplexed parts of polypeptides provided potential binding sites for the bile pigments.

Biliverdin

Fig.2 shows ECD spectra of the BV complexes. Panel A shows complexes with neat PLL and PDL. BV interacting with PDL exhibits two broad ECD patterns with opposite signs typical to the P-helicity[1]. The BV spectrum induced by PLL is opposite.
Panel B shows ECD spectra of BV complexes with the PLL-C$_{12}$ nanoparticles at pH 5-10. ECD spectra of the BV complexes on the micelles differ form the BV complexes which were formed on pure PLL (c.f. panels A and B). The observed difference, the bisignate CD signals in the both UV and VIS regions, originates from conformational changes of the pigment accompanied by stabilizing a flatter or steeper helix type of chromophore. This fact can be interpreted as indication of a reduction of the torsion angle in the chromophore double bonds when the PLL-C$_{12}$ is used. BV adopts more "closed" conformation in this case than in complexes with pure PLL. In neutral and alkaline medium, the conformation of the pigment become more "opened" but it is still less opened than in its usual conformation. As for PDL-C$_{12}$ system, the spectra show the analogous behavior (spectra not shown); the only difference is the opposite sign of all patterns. This fact confirms that the observed ECD of the BV complexes is induced by the chirality of polylysine matrix.

Nanoparticles formed by PLA-C$_{12}$ produce stereoselective complexes with BV in the pH 5 – 11 and their spectra are shown in panel C. At pH 6.1 and 7.4, ECD spectra are very similar to the spectrum of the BV complexes with neat PLL (cf. panels A and C), chromophore has adopted a left-handed M-helicity. At pH > 9, the entire ECD spectrum inversed the signs. Right-handed P-helicity is preferable in the complexes at these conditions.

Fig.3 shows VCD of BV and its complexes. BV alone and BV-C$_{12}$ do not provide VCD spectra. High concentrations required for VCD enable to use only polylysine with the chain not longer than ~ 25 amino acid residues (MW 4000) for the experiments without nanoparticles (panel A, full line). In this case, the matrix was in random coil conformation mainly. The negative VCD signal at 1570 cm^{-1} is assigned to asymmetric COO$^-$ stretching vibrations of BV. This signal has been observed by us in VCD spectra of the complex formed by M-helical conformer of BV[6]. Similarly as in the ECD study, C$_{12}$ was used to stabilize the helical conformation of PLL, PDL and PLA. VCD spectra of BV-PLL-C$_{12}$ and BV-PDL-C$_{12}$ are shown in panel B. The signal at ~ 1570 cm^{-1} assigned to the COO$^-$ stretching vibration is used as a marker for the helicity sense of the pigment.
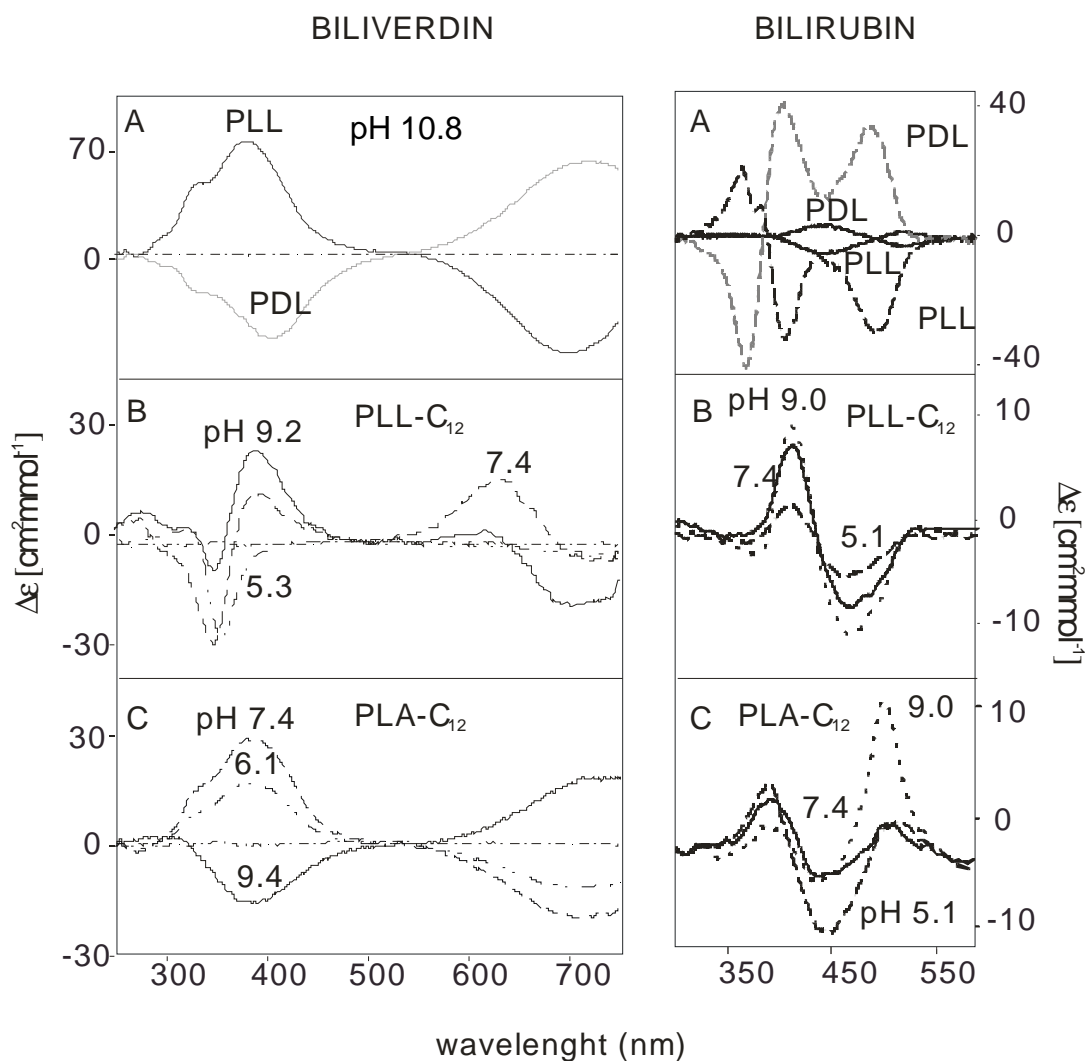
Fig.2 ECD spectra of the biliverdin and bilirubin and their complexes with (A) poly(L-lysine) (PLL) and poly(D-lysine) (PDL), BR/Lys = 1/20 (full lines) and BR/Lys = 1/5 (broken lines), (B) nanoparticles composed of dodecanoate ions (C_{12}) and poly(L-lysine), (C) nanoparticles composed of dodecanoate ions (C_{12}) and poly(L-arginine). *The numbers indicate pH of the systems.*

According these data, PLL forms a complex with M-helical conformer of BV which is in the agreement with the interpretation of ECD data. As for complexes with PLL-C_{12} and PDL-C_{12} particles, we can say that most probably BV adopts P-helical conformation with PLL-C_{12} and M-helices with PDL-C_{12}.

Panel C shows VCD spectra of PLA-BV-C_{12} complex at pH = 9.8. VCD spectrum induced by non-covalent interaction of PLA-C_{12} with BV shows and it is in agreement with ECD study a preference for the P-helicity.

Bilirubin

ECD spectra of pure BR and BR in complex with PLL and PDL are presented in Fig.2. High intensity of ECD spectra for BR/Lys = 5/1 suggest that the chiral self-association of BR molecules takes place. We interpret the observed enhanced of BR internal optical activity and the change of spectral pattern at higher concentration as a consequence of a partial flattening of BR in co-operative interactions between the pigment ligands fixed on the matrix in close vicinity to each other (oligomeric effect).

The ECD signal of BR with PLL-C_{12} (panel B) has a form of negative couplet, i.e. opposite to the situation for PLL. It means that BR adopts M-helicies in the system with

PLL-C$_{12}$ in whole range of studied pH. BR-PLA-C$_{12}$ possesses the ECD patterns of the same sign as in the case of BR-PLL-C$_{12}$ (panel C), therefore M-helical conformation is preferable in the pH range 5-8. When pH > 8.5, the ECD spectra inverts their signs and P-helical conformation is stable.
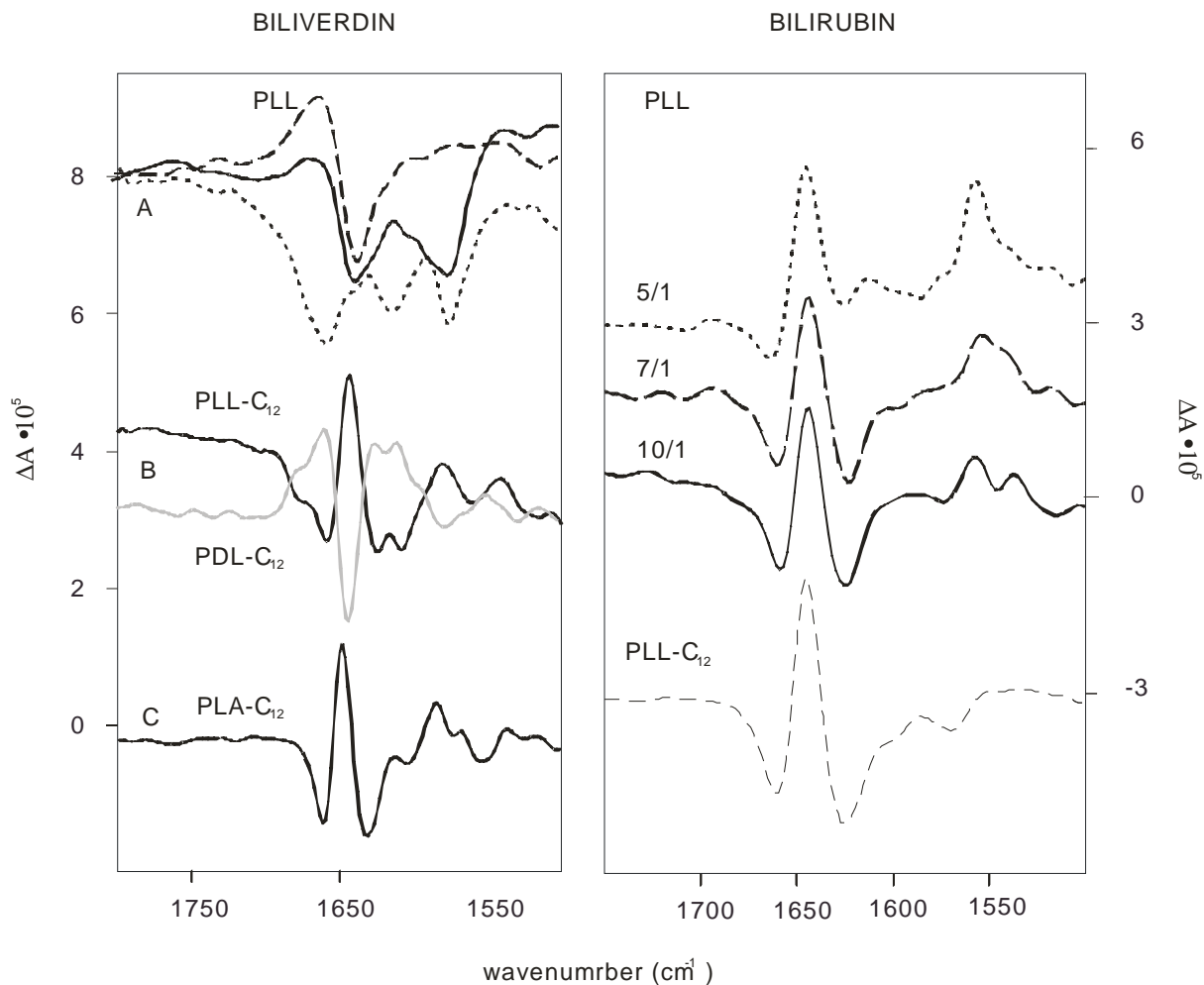
Fig.3 *(left)* VCD spectra of the biliverdin and bilirubin complexes.(A) complex of BV with poly(L-lysine) at pH = 9.6 (full line), pure poly(L-lysine) (broken line), complex of BV with β-cyclodextrin (dotted line), (B) complex of BV-PLL-C$_{12}$ and BV-PDL-C$_{12}$ (gray line) at pH = 10.5, (C) complex BV-PLA-C$_{12}$ at pH = 9.8; *(right)* complexes of BR with poly(L-lysine) at BR/Lys ratios 1/10,1/7,1/5 (pH =10.8), and complex of BR with PLL-C$_{12}$ at pH =10.5 (broken line).

VCD spectra of complexes with BR at molar ratios 10/1, 7/1, and 5/1 are shown in Fig.3. The VCD band at 1560 cm^{-1} is assigned to asymmetric COO$^-$ stretching vibrations for the BR-cyclodextrin complexes[6]. The corresponding VCD signal for BR-polylysine was observed at the 1565 cm^{-1}. The assignment of this band to the BR vibration is proved by the increase of its intensity in with the growth of BR concentration. The opposite VCD spectra were obtained when PDL was used as a matrix (spectrum is not shown). Compared to the complex BR-PLL, in the complex with C$_{12}$ the asymmetric COO$^-$ stretching vibration was inverted. These observations are in the agreement with ECD data: the M-helical conformer is more preferable in this case.

PLA forms complexes with P-helicies, stereoselective recognition is weaker in this system and only small changes were observed at VCD spectrum (spectrum not shown).

134

4. Conclusion

Both studied pigments stereoselectively bind to positively charged lysine and arginine residues. Moreover, self-association process was observed in the case of BR. Dianions of BR associated along the polypeptide chains probably and the angle between two chromophores decreased according to analysis of ECD data. The complexation is a function of pH and concentration. Addition of dodecanoate ions to the systems provides opposite complexation in the case of PLL and PLA for BV. The inversions of ECD signals for the both pigments were observed in the systems with PLA at pH 8.5.

Acknowledgment

References

[1] Boiadjiev S.E.; Lightner D.A.: *Tetrahedron-Asymmetr.* **10** *(1999), 607-655.*
[2] Petersen C.E.; Ha C.E.; Harohalli K.; Feix J.B.; Bhagavan N.V.: *J. Biol. Chem.* **275** *(2000), 20985-20995.*
[3] Dalagni M.; Darchivio A.A.; Giglio E.: *Biopolymers* **33** *(1993), 1553-1565.*
[4] General S.; Thunemann A.F.: *Int. J. Pharm.* **230** *(2001), 11-24.*
[5] Urbanova M.; Setnicka V.; Kral V.; Volka K.: *Biopolymers* **60** *(2001), 307-316.*
[6] Goncharova I.; Urbanova M.: *Tetrahedron-Asymmetr.* **18** *(2007), 2061-2068.*

COMPLEXES OF QUININE DERIVATIVES: VIBRATIONAL AND ELECTRONIC CIRCULAR DICHROISM STUDY

Ondřej Julínek[a] and Marie Urbanová[b]

[a] *Institute of Chemical Technology, Prague, Department of Analytical Chemistry, Technická 5, 166 28, Prague, Czech Republic, e-mail: ondrej.julinek@vscht.cz*
[b] *Institute of Chemical Technology, Prague, Department of Physics and Measurements, Technická 5, 166 28, Prague, Czech Republic*

Abstract

Chiral noncovalent complexes composed of *terc*-butyl-carbamoil-quinine or *terc*-butyl-carbamoil-quinidine and two enantiomers of 3,5-dinitrobenzoyl-leucine were studied via vibrational and electronic circular dichroism spectroscopy. VCD and IR absorption spectra of pure selectands and selectors were measured and their absorption bands were assigned. The formation of the favorable or unfavorable selectand-selector pairs leads to distinctly different ECD and VCD spectra. Some bands in VCD spectrum can be considered as the interaction markers typical of favorable pairs. These markers relate to the geometry changes of corresponding functional groups that intermediate the binding of selectand and selector. VCD spectroscopy can provide highly detailed structural information about the selectand-selector complex while ECD spectroscopy is feasible for rapid preliminary scans.

Keywords

VCD; ECD; Chiral complex; Chiral recognition; Diastereomeric complex; Quinine, Quinidine

1. Introduction

The development of novel stationary phases for chiral HPLC is very interesting field as the determination of enantiomeric purity is crucial for pharmacology and many sectors of modern chemistry. Cinchona alkaloids quinine and quinidine are chiral natural substances easily available. The possibility of their derivatization and relative low price makes them suitable selectors applicable in enantioseparation methods like enantioselective liquid-liquid extraction[1], chiral HPLC[2-7], chiral electrophoresis[8-10] or chiral electrochromato-graphy[11,12].
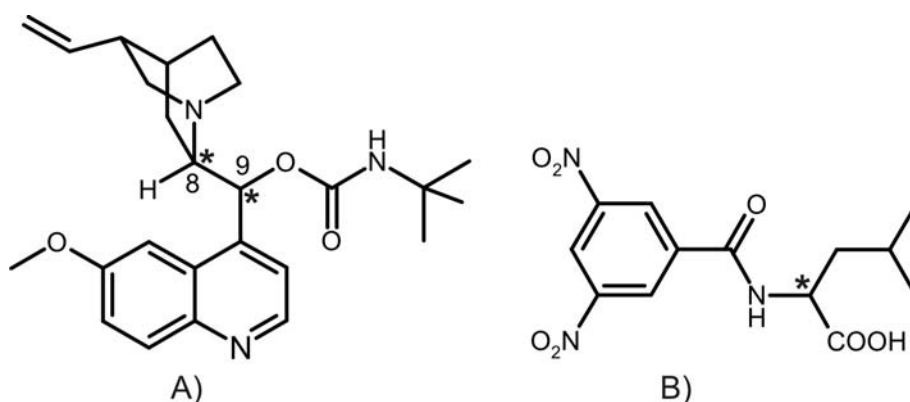
Fig.1 Structure of A) QN (8S, 9R) and QD (8R, 9S) selectors and B) DNB-L-Leu and DNB-D-Leu selectands.

Terc-butyl-carbamoil-quinine (QN) and *terc*-butyl-carbamoil-quinidine (QD) (Fig.1A) are the most employed cinchona alkaloid derivatives. They exhibit high affinity to 2,4-dinitrobenzoyl (DNB) amino acids, especially DNB-Leu (Fig.1B). QN and QD selectors are diastereoisomers with opposite configuration of binding center and therefore opposite configurational selectivity for chiral analytes. Due to the geometry of selectand and selector, QN interacts strongly with DNB-L-Leu and creates „favorable" complex while the interaction of QN and DNB-D-Leu is weaker and leads to formation of „unfavorable" complex. The opposite selector QD interacts strongly with DNB-D-Leu and its interaction with DNB-L-Leu is weak. High stability of the favorable complex is caused by the following types of weak interaction: hydrogen bond between amidic group of selectand and carbamate group of selector, ion pairing between carboxyl group of selectand and quinuclidine group of selector and π–π interaction between aromatic groups of selectand and selector (Fig.2).

The interaction of selectand and selector can be studied via common methods like HPLC[13,14], infrared absorption spectroscopy[15,16] and NMR[17] but more specialized techniques directly sensitive to the chirality can be also employed. Electronic and vibrational circular dichroism spectroscopy utilizes the phenomenon of different absorption coefficient of chiral molecules for left and right circularly polarized light. Circular dichroism (CD) spectrum of a molecule is difference of absorbance of left and right circularly polarized light depending on wavelenght of incident light. Two enantiomers have identical IR absorption spectra but different CD spectra; their spectra are symmetrical along the zero line. Achiral molecules exhibit zero CD signal. The differences between electronic circular dichroism (ECD) and vibrational circular dichroism (VCD) spectroscopy are the same as for their parent techniques – UV-VIS and IR absorption spectroscopy. Broad and low resolved peaks are typical of ECD spectroscopy, it measures electronic transitions of molecular orbitals and relates to the geometry of whole molecule. On the contrary VCD spectroscopy takes advantage of high resolved peaks that can be assigned to specific function groups in molecule. The fact that the sign and intensity of VCD band depends strongly on the geometry of corresponding group makes this technique very sensitive to small geometry changes in the molecule. This ability makes VCD method suitable to study interactions of chiral selectand-selector systems.
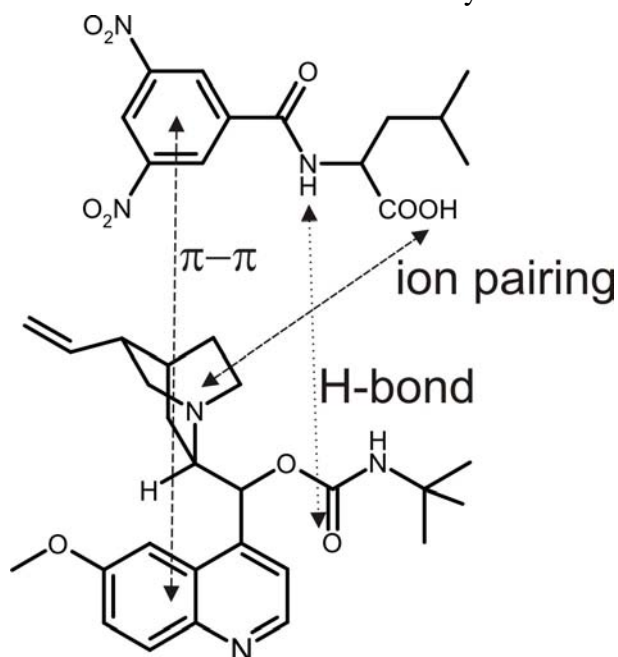

Fig.2 Weak interactions between the selectand and selector in the favorable complex.

2. Experimental
2.1 Reagents

The *terc*-butyl-carbamoil-quinine (QN), *terc*-butyl-carbamoil-quinidine (QD), 2,4-dinitrobenzoyl-L-leucine (DNB-L-Leu) and 2,4-dinitrobenzoyl-D-leucine (DNB-D-Leu) were synthetized[14,18] by prof. Lindner's group (Vienna, Austria). For ECD measurements, methanol of analytical reagent grade (Penta) was used as solvent. For VCD measurements, deutered methanol (MeOH-d4, 99,8 atom.% D, ISOSAR) was used.

2.2 ECD measurements

All ECD measurements were carried out on a Jasco J-810 spectropolarimeter using quartz cuvette with 0,1 mm optical pathlength. Parameters of the measurement: scanning speed 100 nm/min, band width 1 nm, standard sensitivity, 10 accumulations, room temperature.

2.3 VCD measurements

VCD and IR absorption spectra were recorded using a Fourier transform infrared spectrometer IFS-66/S equipped with a VCD/IRRAS module PMA 37 (Bruker, Germany) by a procedure described elsewhere[19]. VCD spectra were obtained as an average of 21 blocks, each block consisting of 2260 scans measured with spectral resolution of 4 cm^{-1} and a zero filling factor of 4. For all measurements a demountable cuvette A145 with CaF_2 windows and 50 µm optical patlength was used. The band assignment was done using charts with infrared characteristic group frequencies[20].

3. Results and discussion
Spectra of pure components

Fig.3A shows VCD and IR absorption spectra of DNB-D-Leu and DNB-L-Leu. These substances are enantiomers and therefore have identical IR absorption spectra. The most intensive absorption bands at 1549 cm^{-1} and 1348 cm^{-1} were assigned to asymmetric and symmetric vibration of nitro group, respectively. VCD spectrum in the region of vibration of asymmetric nitro group could not be measured due to high noise level. Two types of carbonyl group are presented in DNB-Leu: carboxyl group and amide group. The vibration band at 1655 cm^{-1} is assigned to the amide group, the band at 1720 cm^{-1} is assigned to vibration of non-dissociated carboxyl group and bands at 1592 cm^{-1} and 1388 cm^{-1} are assigned to asymmetric and symmetric vibration of dissociated carboxyl group, respectively. Intensity of concerned bands shows most carboxyl groups are presented in non-dissociated form. The bands of CH_3 asymmetric vibration at 1476 cm^{-1} and CH_2 scissors vibration at 1432 cm^{-1} are overlapped by amide II' vibration (in-plane N-D deformation vibration mixed with stretching C-N vibration).
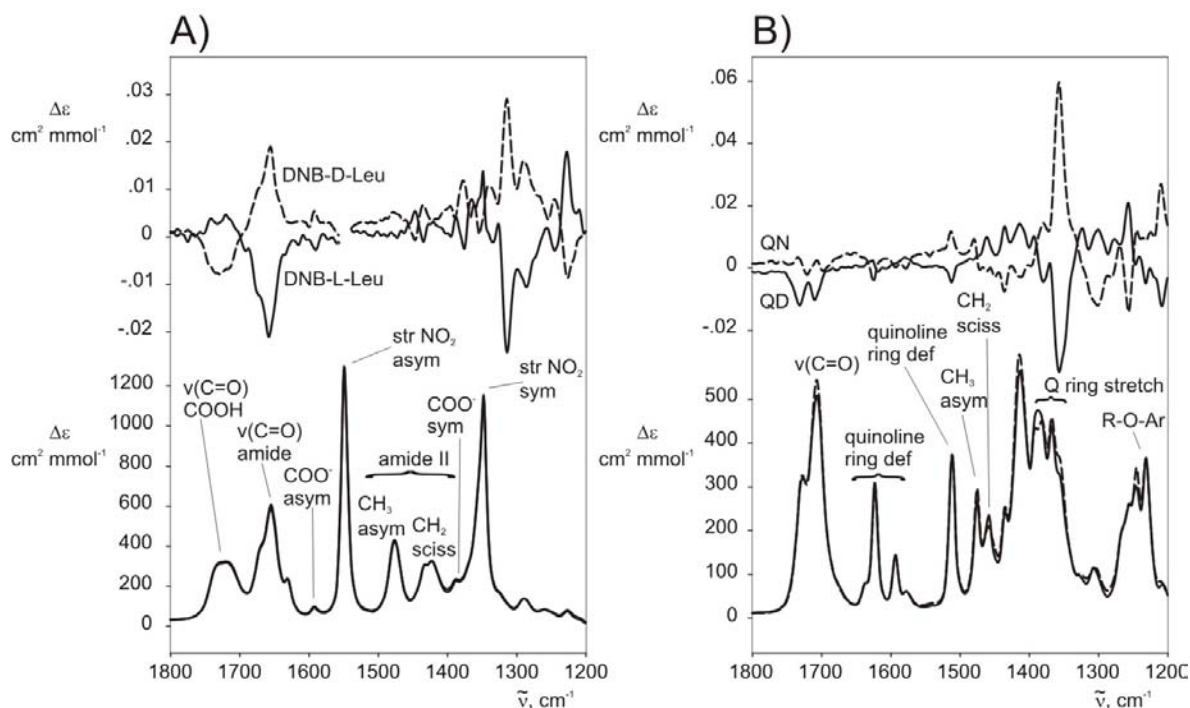
Fig.3 VCD and IR absorption spectra of both selectands and selectors in MeOH-d4.

Fig.3B shows VCD and IR absorption spectra of QN and QD selectors. QN and QD are diastereoisomers, so small difference between their IR absorption spectra can be observed. The band at 1707 cm^{-1} is assigned to the carbonyl group vibration. A group of bands at about 1600 cm^{-1} and the band at 1512 cm^{-1} belongs to various modes of quinoline ring deformation vibration. The bands at 1475 cm^{-1} and 1459 cm^{-1} are assigned to the CH$_3$ asymmetric vibration and the CH$_2$ scissors vibration, respectively. The stretching modes of quinoline group are manifested by several bands at about 1370 cm^{-1}. The vibration band at 1245 cm^{-1} is assigned to the ether connected to the aromatic group.

Spectra of complexes

Fig.4A shows VCD spectra of both favorable and unfavorable complexes in comparison with the pure components. Unfavorable pairs composed of selectand DNB-D-Leu and selector QN or selectand DNB-L-Leu and selector QD have noisy VCD spectra with bands of low intensity. On the other hand VCD spectra of favorable complexes composed of DNB-L-Leu selectand and QN selector or DNB-D-Leu selectand and QD selector exhibit VCD spectra with strong VCD bands. This difference corresponds with the character of favorable and unfavorable complex; the geometry of favorable complex is fixed by three interactions holding selectand-selector system in rigid chiral formation generating strong VCD signal with low level of noise, on the contrary in unfavorable complex, all these interactions are not available due to steric reasons, the selectand-selector system is more flexible and generates noisy VCD spectrum of low intensity.

Some VCD bands in the spectrum of favorable complex can be considered as interaction markers, these bands of high intensity are present in the spectra of favorable pairs only. The first interaction marker at 1621 cm^{-1} is assigned to deformation vibration of quinoline ring and is therefore the marker of π–π interaction of selectand and selector. The second interaction marker at 1581 cm^{-1} is assigned to asymmetric vibration of dissociated carboxyl group interacting with protonated quinuclidine group and is the marker of ion-pairing interaction. The last interaction marker at about 1410 cm^{-1} is unassigned so far.

Final assignment could be possible using ab-initio calculation of vibrational modes or using homologic series of selectands and selectors and their influence on the spectrum.

Fig.4B shows ECD spectra of pure selectands and selectors in comparison with favorable and unfavorable complexes. Again, ECD spectra of unfavorable complexes have the bands of low intensity, in fact the spectrum of unfavorable pair can be considered as the superposition of the corresponding selectand and selector spectrum. Spectra of favorable complexes have intensive ECD bands typical of organized chiral structure.
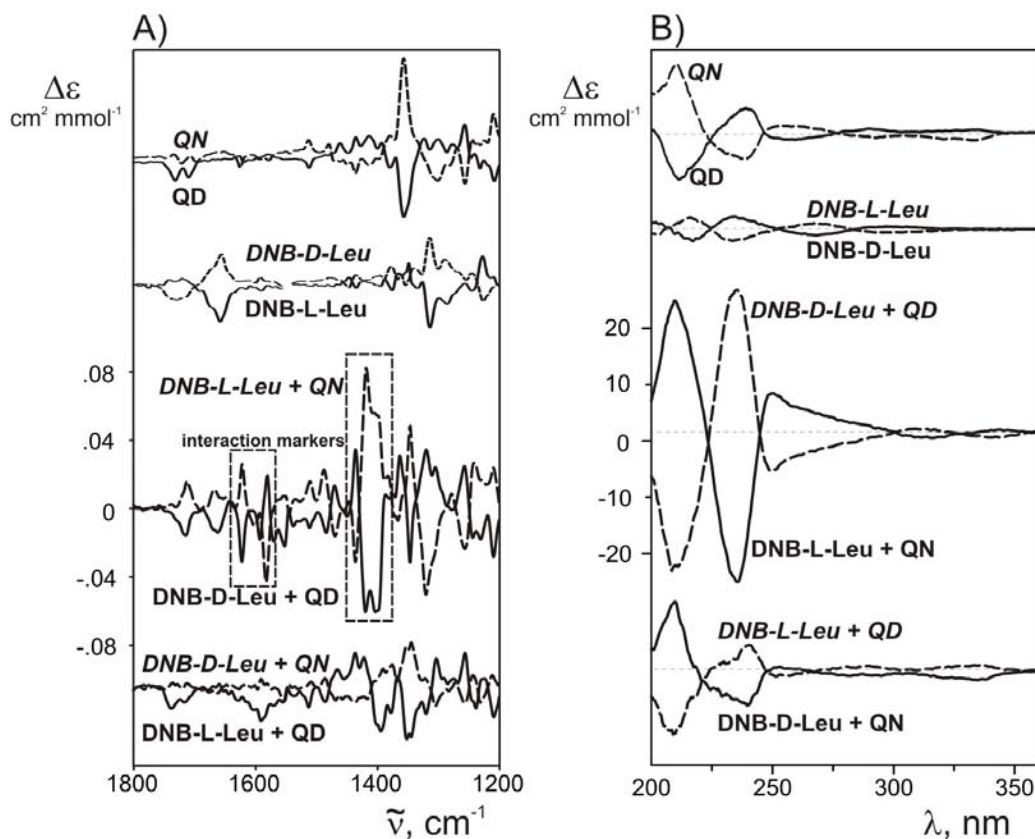
Fig.4 A) VCD and IR absorption and B) ECD and UV-VIS absorption spectra of favorable and unfavorable selectand-selector complexes in comparison with spectra of pure components.

4. Conclusion

VCD and ECD techniques were proved to be feasible tools to study cinchona derivative – DNB-Leu selectand-selector system. The complex chiroptical study combines advantages of rapid measurement and low sample consumption typical of ECD with high spectral resolution and conformational sensitivity of VCD. Favorable complex exhibit intensive CD bands in ECD spectrum allowing to use this spectroscopic method for rapid preliminary test of complex formation. VCD turns out to be a powerful method capable of detecting selectand-selector interaction and locating functional groups involved in the interaction.

Acknowledgement

References

[1] Kellner K. H.; Blasch A.; Chmiel H.; Lammerhofer M.; Lindner W.: *Chirality 9 (1997), 268-273.*

[2] Czerwenka C.; Lammerhofer M.; Maier N. M.; Rissanen K.; Lindner W.: *Anal. Chem. 74 (2002), 5658-5666.*

[3] Czerwenka C.; Lammerhofer M.; Lindner W.: *J. Pharmaceut. Biomed. 30 (2003), 1789-1800.*

[4] Czerwenka C.; Lammerhofer M.; Lindner W.: *J. Sep. Sci. 26 (2003), 1499-1508.*

[5] Gyimesi-Forras K.; Kokosi J.; Szasz G.; Gergely A.; Lindner W.: *J. Chromatogr. A 1047 (2004), 59-67.*

[6] Gyimesi-Forras K.; Leitner A.; Akasaka K.; Lindner W.: *J. Chromatogr. A 1083 (2005), 80-88.*

[7] Kacprzak K. M.; Maier N. M.; Lindner W.: *Tetrahedron Letters 47 (2006), 8721-8726.*

[8] Piette V.; Lammerhofer M.; Lindner W.; Crommen J.: *Chirality 11 (1999), 622-630.*

[9] Piette V.; Fillet M.; Lindner W.; Crommen J.: *J. Chromatogr. A 875 (2000), 353-360.*

[10] Piette V.; Lammerhofer M.; Lindner W.; Crommen J.: *J. Chromatogr. A 987 (2003), 421-427.*

[11] Lammerhofer M.; Lindner W.: *J. Chromatogr. A 829 (1998), 115-125.*

[12] Lammerhofer M.; Lindner W.: *J. Chromatogr. A 839 (1999), 167-182.*

[13] Lammerhofer M.; Maier N. M.; Lindner W.: *Am. Lab. 30 (1998), 71-75.*

[14] Lammerhofer M.; Franco P.; Lindner W.: *J. Sep. Sci. 29 (2006), 1486-1496.*

[15] Lesnik J.; Lammerhofer M.; Lindner W.: *Anal. Chim. Acta 401 (1999), 3-10.*

[16] Wirz R.; Burgi T.; Lindner W.; Baiker A.: *Anal. Chem. 76 (2004), 5319-5330.*

[17] Maier N. M.; Schefzick S.; Lombardo G. M.; Feliz M.; Rissanen K.; Lindner W.; Lipkowitz K. B.: *J. Am. Chem. Soc. 124 (2002), 8611-8629.*

[18] Mandl A.; Nicoletti L.; Lammerhofer M.; Lindner W.: *J. Chromatogr. A 858 (1999), 1-11.*

[19] Urbanova M.; Setnicka V.; Volka K.: *Chirality 12 (2000), 199-203.*

[20] Socrates G.: *Infrared and Raman Characteristic Group Frequencies: Tables and Charts*; *Chichester, 2001.*

141

PREPARATION AND CHARACTERIZATION OF NANOPARTICLES

Pavel Řezanka, Kamil Záruba and Vladimír Král

Institute of Chemical Technology Prague, Dept. of Analytical Chemistry, Technická 5, Prague 6, 166 28, Czech Republic; e-mail: pavel.rezanka@vscht.cz

Abstract

Several methods of size-controlled gold nanoparticles preparation are presented. Using different amount of reducing agent the particle size can be controlled in the range between 6 and 80 nm. Prepared nanoparticles were modified by three different ways and characterized by various techniques.

Keywords

Gold nanoparticles; preparation; modification; characterization; porphyrin

1. Introduction

Metal nanoparticles play important roles in different branches of science, such as nanoelectoronics, nonlinear optics, biological labeling, oxidation catalyst, etc[1]. Nanoparticles themselves also provide a pragmatic approach to multiscale engineering, functioning as 'building blocks' of regular shape and size for the fabrication of lager structures. Combination of synthetic design with directed assembly of nanoparticles into organized ensembles provides the direct control of physicochemical properties from the molecular to the macroscopic level. In this regard, functionalization of metal nanoparticles is a prerequisite to fabrication 2- and 3-dimensional structures.

Gold nanoparticles (GNP) are in the field of interest due to their unique properties, namely plasmon resonance and surface-enhanced Raman scattering (SERS) effect[1]. The plasmon resonance is the result of collective oscillations of GNP surface electrons upon interaction with visible light of a suitable wavelength. The extinction coefficients of GNPs are nominally in the range of 10^8-10^{10} dm^3 mol^{-1} cm^{-1} (ref. *2*), so it becomes an increasingly important colorimetric reporter to signify the events associated with interacting modified GNPs with analytes[3]. SERS effect is caused by enhancement (10^4-10^6) of the Raman signal and enables to study compounds that are immobilized on the surface of metal nanoparticles in low concentration[4].

The goal of this work is to develop methods of preparation of functional gold nanoparticles with different diameter, their modification and characterization.

2. Experimental
2.1 Reagents

All reagents were of analytical reagent grade or higher purity. Water used in all experiments was obtained from Merck (HPLC Lichrosolv®, R = 1 MΩ).

2.2 UV-Vis Spectroscopy

UV-Vis spectra were recorded on Varian Cary 400 SCAN UV-Vis spectrophotometer (USA). Solvents spectra were subtracted from all spectra. Data were collected from 200 nm to 900 nm with 1 nm resolution.

2.3 Transmission Electron Microscopy

TEM measurements were performed on a JEOL JEM-3010 microscope (Japan) operated at 300 kV. Samples were prepared by depositing 5 μL of the solution of the nanoparticles onto a carbon-coated copper grid and then allowed to air-dry before analysis.

2.4 Raman Spectroscopy

Raman spectra were collected using a Fourier transform near-infrared (FT-NIR) spectrometer Equinox 55/S (Bruker, Germany) equipped with a FT Raman module FRA 106/S (Bruker). A focused laser beam (100 mW) of a Nd:YAG laser (1064 nm, Coherent) was used to excite the Raman effect. Samples were made up in glass vials and placed on a motorized *X-Y-Z* sample stage. The scattered light was collected using a backscattering geometry. Interferograms were obtained using a quartz beam splitter and a Ge detector (liquid N_2 cooled). Typically, 1024 separate interferograms were accumulated and then processed by Fourier transformation using Blackman-Harris 4-term apodization and a zerofilling factor of 8 in order to obtain individual FT Raman spectrum.

2.5 Procedures

Preparation of Gold Nanoparticles

Used method is based on the reduction of Au^{3+} with citrate according to Turkevich *et. al.*[5]

Method A: 1 mL of 1% aqueous solution of the potassium tetrachloroaurate(III) and 2.5 mL of 1% aqueous solution of the trisodium citrate dihydrate were added to 100 mL of the boiling water (under reflux). Heating was continued for 10 minutes during which time the solution had changed color from pale yellow to gray-blue, to purple, and then to wine-red. After that, the reaction vessel was allowed to cool to room temperature.

Method B: 50 µL of 1% aqueous solution of the trisodium citrate dihydrate and 20 µL of 1% aqueous solution of the potassium tetrachloroaurate(III) were added to 2 mL of the boiling water in a closed vial. Heating was continued for 10 minutes during which time the solution had changed color from pale yellow to gray-blue, to purple, then to brightly red. After that, reaction vessel was allowed to cool to room temperature.

Method C: 20 µL of 1% aqueous solution of the potassium tetrachloroaurate(III) and 8.4 µL of 1% aqueous solution of the trisodium citrate dihydrate were added to 2 mL of the boiling water in a closed vial. Heating was continued for 10 minutes during which time the solution had changed color from pale yellow to gray-blue, to purple, and then to dark red. After that, the reaction vessel was allowed to cool to room temperature.

Method D: 20 µL of 1% aqueous solution of the potassium tetrachloroaurate(III) and 4 µL of 1% aqueous solution of the trisodium citrate dihydrate were added to 2 mL of the boiling water in a closed vial. Heating was continued for 10 minutes during which time the solution had changed color from pale yellow to gray-blue, to purple, and then to dark red. After that, the reaction vessel was allowed to cool to room temperature.

Method E: 300 µL of 1% aqueous solution of the potassium tetrachloroaurate(III) and 110 µL of 1% aqueous solution of the trisodium citrate dihydrate were added to 30 mL of the boiling water (under reflux),. Heating was continued for 30 minutes during which time the solution had changed color from pale yellow to gray-blue and then to brown. After that, the reaction vessel was allowed to cool to room temperature.

Modification of Gold Nanoparticles

Thiol derivatization: The solution of 3-mercaptopropanoic acid (MPA, 6.3 µL) in H_2O (1 mL) was added to the 100 mL of gold nanoparticle solution. The flask was capped and left to stand for 3 days in the dark.

One-step porphyrin derivatization: The solution of porphyrin-brucine conjugate[6] (Por-Bru, 10 mg, Fig.1) in MeOH (2 ml) was added to the 100 mL of gold nanoparticle solution. The flask was capped and left to stand for 3 days in the dark.
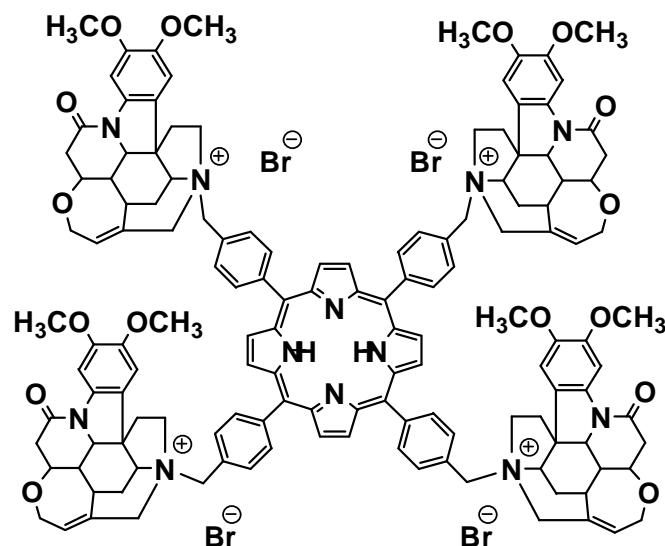
Fig.1 Structure of porphyrin-brucine conjugate.

Two-step porphyrin derivatization: The solution of 3-mercaptopropanoic acid (6.3 μL) in H_2O (1 mL) was added to the 100 mL of gold nanoparticle solution. The flask was capped and left to stand for 3 days in the dark. Then, the solution of porphyrin-brucine conjugate (10 mg, Fig.1) in MeOH (2 ml) was added. The flask was capped and left to stand for 3 days in the dark.

Cleaning of Gold Nanoparticles

Unbound species and reaction byproducts were removed in the supernatant after centrifugation. The nanoparticles were repeatedly redispersed in water or methanol.

Characterization of Gold Nanoparticles

Modified nanoparticles were characterized by UV-Vis spectro-scopy, TEM and Raman spectroscopy.

3. Results and discussion

Gold nanoparticles were prepared by modified procedures originally published by Turkevich[5] and characterized by various techniques, namely TEM and UV-Vis. A monodisperse colloid solution of circle shaped GNP was prepared by method A. Their average diameter was 14.7 nm (Fig.2) with the maximum of absorbance at 518 nm, which corresponds with TEM[7].
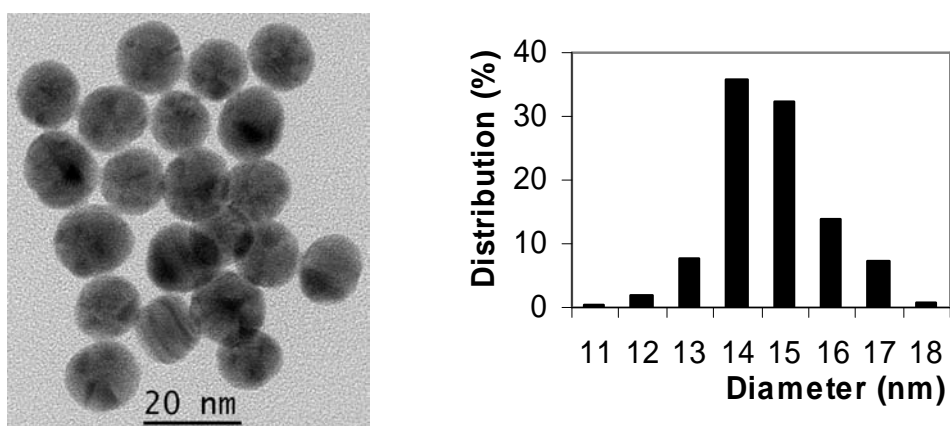
Fig.2 TEM image and size distribution of gold nanoparticles prepared by method A. *Size distribution was obtained by measuring of 500 nanoparticles in an arbitrarily chosen area of a TEM image.*

Comparing diameters obtained from TEM for nanoparticles prepared by methods B, C, D and E with wavelengths of the maximum absorbance (Fig.3), it is possible to determine approximately the diameter of new prepared nanoparticles only by measuring UV-Vis spectra. Experimental results are in the agreement with the previously published data[7-9].
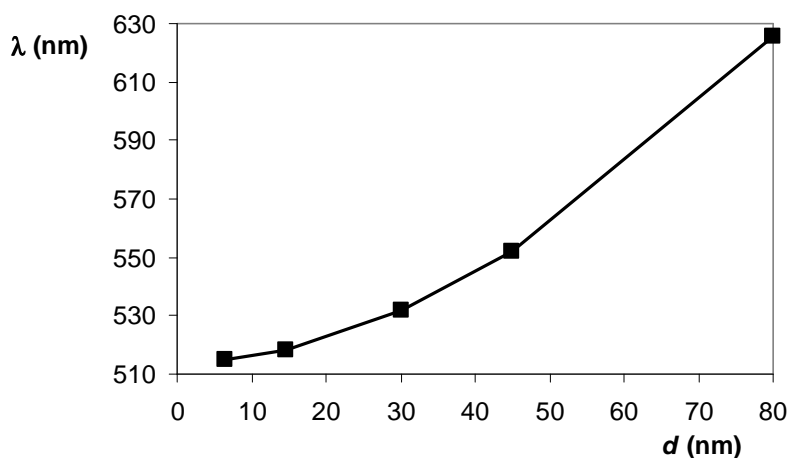
Fig.3 Dependence of wavelength of the maximum absorbance on the diameter of gold nanoparticles.

Immobilization of porphyrin derivative (Fig.1) was carried out by addition of porphyrin derivative solution in methanol to GNP (one-step method) or to GNP premodified with 3-mercaptopropionic acid (MPA) (two-step method). Successful modification was confirmed by UV-Vis spectroscopy. Spectra of modified GNP showed the red shift of the maximum absorbance (λ_{max}) of 2-40 nm (ref. *10*).
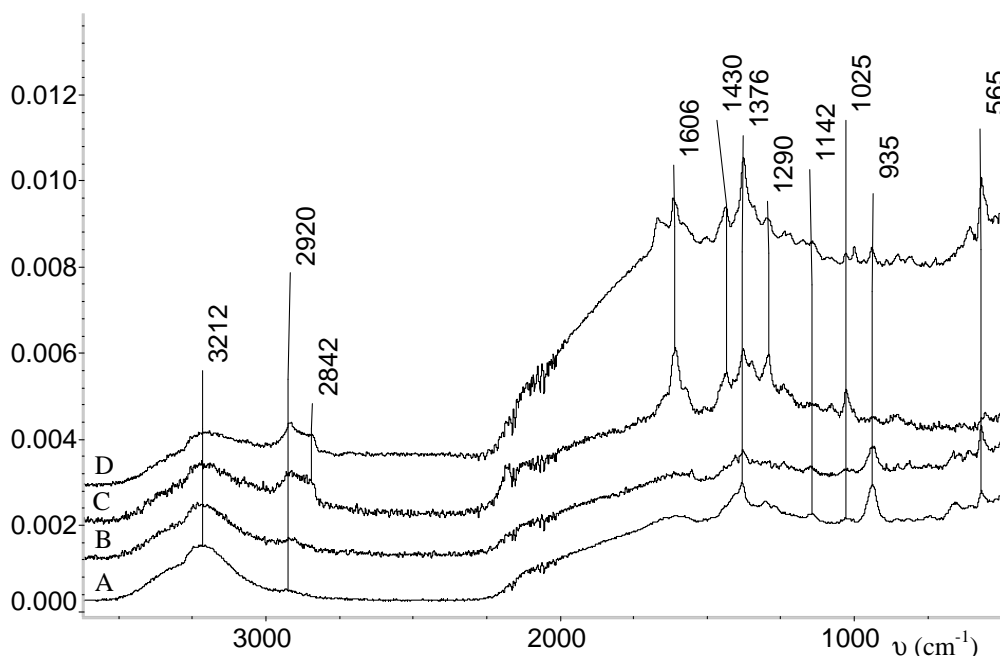
Fig.4 Raman spectra of gold nanoparticles modified with MPA (A), MPA and porphyrin derivative (B), citrate (C, freshly prepared GNP) and porphyrin derivative (D).

Analysis of the Raman spectra (Fig.4) confirmed immobilization added compounds on the surface of gold nanoparticles. After addition of MPA or porphyrin derivative to the prepared GNP (spectrum C) and centrifugation, spectra significantly changed (spectra A and D). After addition porphyrin derivative to the GNP modified with MPA (spectrum A) and centrifugation, the spectrum didn't changed significantly (spectrum B) but UV-Vis spectra confirmed immobi-lization of the porphyrin derivative.

4. Conclusions

In the present work the preparation of gold nanoparticles with various diameter has been presented. Prepared nanoparticles were modified with porphyrin derivative by one- and two-step methods and modified nanoperticle were characterized by UV-Vis spectroscopy, SERS spectroscopy and TEM.

For the future development of sensor application of nanoparticles, the possibility of using SERS to determination of immobilized compounds concentration on the surface of gold nanoparticles will be studied.

Acknowledgment

References

[1] Daniel M.C.; Astruc D.: *Chem. Rev. 104 (2004), 293-346.*
[2] Link S.; El-Sayed M.A.: *J. Phys. Chem. B 103 (1999), 8410-8426.*
[3] Drechsler U.; Erdogan B.; Rotello V.M.: *Chem. Eur. J. 10 (2004), 5570-5579.*
[4] Kneipp K.; Kneipp H.; Itzkan I.; Dasari R.R.; Feld M.S.: *Chem. Rev. 99 (1999), 2957-2975.*
[5] Turkevitch J.; Stevenson P.C.; Hillier J.: *Discuss. Faraday Soc. 11 (1951), 55-57.*
[6] Král V.; Pataridis S.; Setnička V.; Záruba K.; Urbanová M.; Volka K.; *Tetrahedron 61 (2005), 5499-5506.*
[7] Gittins D.I.; Caruso F.: *J. Phys. Chem. B 105 (2001), 6846-6852.*
[8] Link S.; El-Sayed M.A.: *J. Phys. Chem. B 103 (1999), 4212-4217.*
[9] Turkevich J.; Garton G.; Stevenson P.C.: *J. Colloid Sci. Suppl. 1 (1954), 26-35.*
[10] Templeton A.C.; Pietron J.J.; Murray R.W.; Mulvaney P.: *J. Phys. Chem. B 104 (2000), 564-570.*

VOLTAMMETRIC DETERMINATION OF 2-NITROPHENOL AT BORON-DOPED DIAMOND FILM ELECTRODE

Jana Musilová[a], Jiří Barek[a], Pavel Drašar[b] and Karolina Pecková[a]

[a] *Charles University in Prague, Faculty of Science, Department of Analytical Chemistry, UNESCO Laboratory of Environmental Electrochemistry, Hlavova 2030, 12843 Prague 2, Czech Republic; e-mail: Jana.Musilova@seznam.cz*
[b] *Institute of Chemical Technology, Faculty of Food and Biochemical Technology, Technická 5, 16628 Prague 6, Czech Republic*

Abstract

The voltammetric behavior of 2-nitrophenol (2-NP) was investigated by differential pulse voltammetry at boron-doped diamond film electrode (BDDFE). The electrochemical reduction and oxidation has been studied in Britton-Robinson buffer over a pH range of about 2 – 12. Optimum conditions have been found at pH 4 for reduction and pH 11 for oxidation. Limits of detection were 6.10^{-6} mol.L^{-1} for electrochemical oxidation of 2-NP and 4.10^{-7} mol.L^{-1} for electrochemical reduction.

Keywords

Boron-doped diamond film electrode, Differential pulse voltammetry, 2-Nitrophenol

1. Introduction

Boron doped diamond is a novel and versatile electrode material, which have gained popularity in a variety of electrochemical applications.[1-3] The use of conductive diamond films as an electrode material in electrochemistry has been reviewed by Fujishima et al.[4] Nowadays, there are several commercial suppliers of BDDFE, including Element Six (UK), Windsor Scientific (UK), Adamant Technologies (Swiss), Condias (Germany), Sumitomo (Japan) and sp3 Diamond Technologies (USA).[5]

Nitrophenols are nitroaromatic derivatives present in some industrial wastewaters as they are widely used as intermediates in industries such as pesticides, herbicides, dyes and manufacturing solvents. They are considered to be potentially carcinogenic and mutagenic.[6] Pesticides based on simple nitrophenols are generally not allowed today but some of than are still used as growth stimulators in agriculture.[7] US EPA has restricted the concentration of 2-nitrophenol, 4-nitrophenol and 2,4-dinitrophenol in natural water to be less than 10 μg/L.[6] Moreover, this substance is a suitable model of nitrated explosives.[8]

2. Experimental

Voltammetric measurements were carried out using Eco-Tribo Polarograph with software PolarPro version 5.1 (Polaro-Sensors, Prague, Czech Republic) in a three-electrode system – platinum wire electrode (Monokrystaly, Turnov, Czech Republic) as auxiliary electrode, Ag/AgCl reference electrode RAE 113 (1 mol.L^{-1} KCl, Monokrystaly, Turnov, Czech Republic) and boron-doped diamond electrode (3 mm diameter, Windsor Scientific, UK) as working electrode.

The polarization rate 20 mV.s^{-1}, the pulse ±50 mV and the modulation amplitude 80 ms were used in differential pulse voltammetry (DPV).

The stock solution of 2-NP 1.10^{-3} mol.L^{-1} (Sigma-Aldrich, Prague, Czech Republic) was prepared by dissolving an accurately weighed amount of the pure substance in 100 ml of redestilled water.

The required amount of the stock solution was placed in 10 mL volumetric flask and was diluted to the mark with a Britton-Robinson (BR) buffer of appropriate pH.

Oxygen was removed from the measured solutions by bubbling with nitrogen for five minutes.

Prior use in electrochemical measurement and also for renewing electrode's surface BDDFE was activated by cycling the potential in virgorously stirred aqueous 1M HNO$_3$ between -2.5 and +2.5 V vs. SCE until a stable signal was detected (5-10 cycles with 0.1 V.s^{-1} scan rate).

3. Results and discussion
3.1 Electrochemical reduction

First, the influence of pH on DPV curves of 1.10^{-4} mol.L^{-1} 2-NP at BDDFE was investigated in BR buffer of appropriate pH (Fig.1 and 2). All curves were measured 5 times. First measurement always gave higher peaks and thus was not evaluated. The best developed and highest peak was obtained in BR buffer pH 4 (Fig.1). The calibration measurements were carried out for concentrations from 2.10^{-7} to 1.10^{-4} mol.L^{-1} 2-NP. The calibration dependence in $(2-10).10^{-6}$ mol.L^{-1} range is depicted in Fig.3. The concentrations lower than 2.10^{-7} were not detectable. The parameters of calibrations curves are sumarized in Table 1.
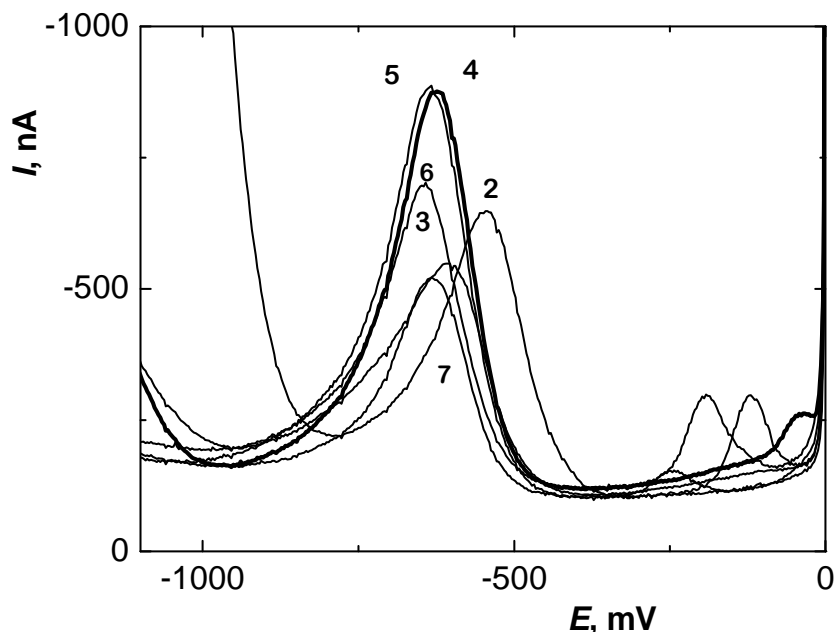
Fig.1 Selected DP voltammograms of 2-NP (c = 1.10^{-4} mol.L^{-1}) using electrochemical reduction at BDDFE in BR buffer, pH 2-7. *The values of pH are at each curve.*
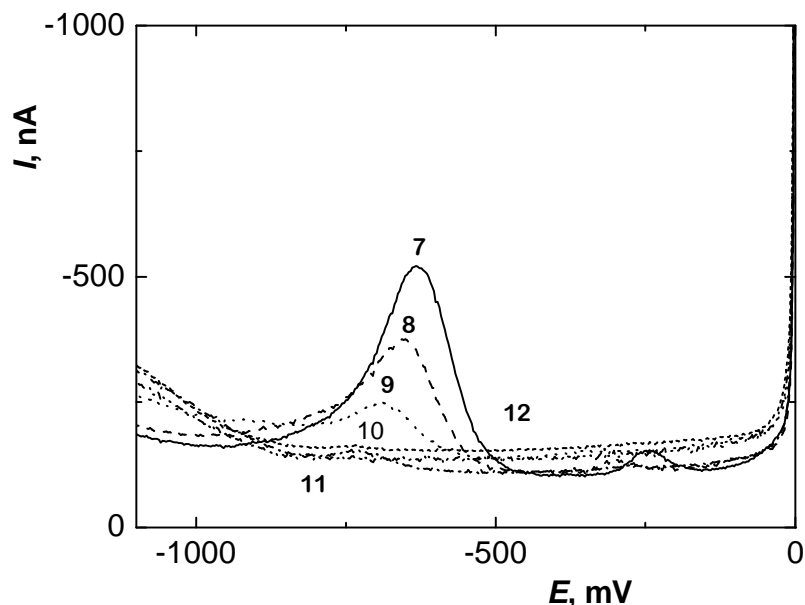
Fig.2 Selected DP voltammograms of 2-NP (c = 1.10^{-4} mol.L^{-1}) using electrochemical reduction at BDDFE in BR buffer, pH 7-12. *The values of pH are at each curve.*
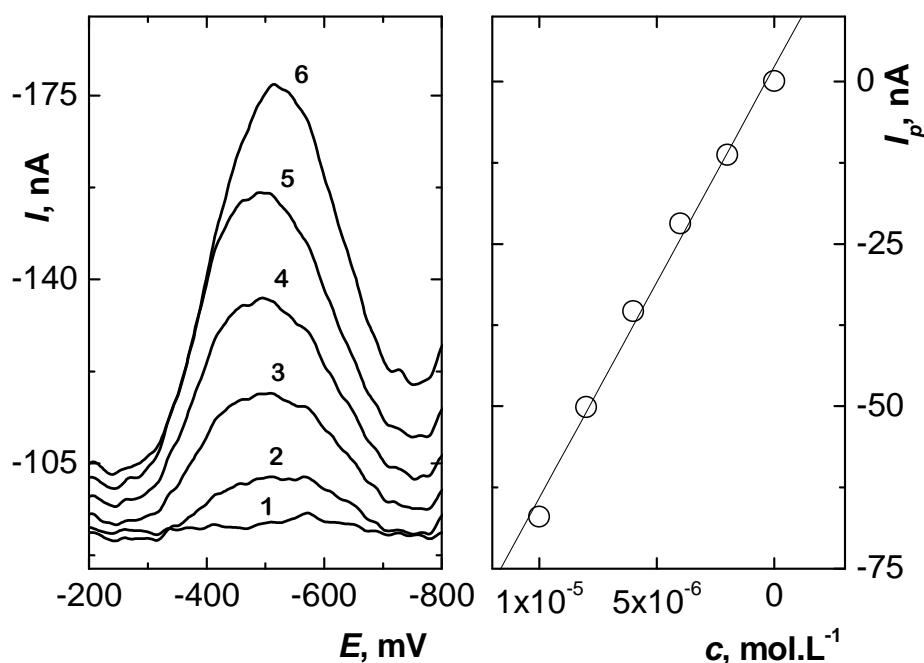
Fig.3 DP voltammograms and calibration dependence for 2-NP using electrochemical reduction at BDDFE in BR buffer pH 4, *c(2-NP): 0 (1), 2.10^{-6} (2), 4.10^{-6} (3), 6.10^{-6} (4), 8.10^{-6} (5), 10.10^{-6} (6) mol.L^{-1}.*

3.2 Electrochemical oxidation

First, the influence of pH on DPV curves of 1.10^{-4} mol.L^{-1} 2-NP at BDDFE was investigated in BR buffer with corresponding pH (Fig.4 and 5). All curves were measured 5 times. During electrochemical oxidation became evident passivation of electrode's surface and thus the peak was decreasing with increasing number of measurements. For evaluation of pH dependence the second measurements after activation were used. The best developed and highest peak for electrochemical oxidation was obtained in BR buffer pH 11 (Fig.5). The calibration measurements were carried out for concentration ranges (2-

149

10).10^{-6} (Fig.6) and (2-10).10^{-5} mol.L^{-1}. However, the calibration dependence in (2-10).10^{-5} mol.L^{-1} range was not linear due to passivation of electrode's surface. The concentrations lower than 2.10^{-6} were not detectable. The parameters of calibrations curves are sumarized in Table 1.
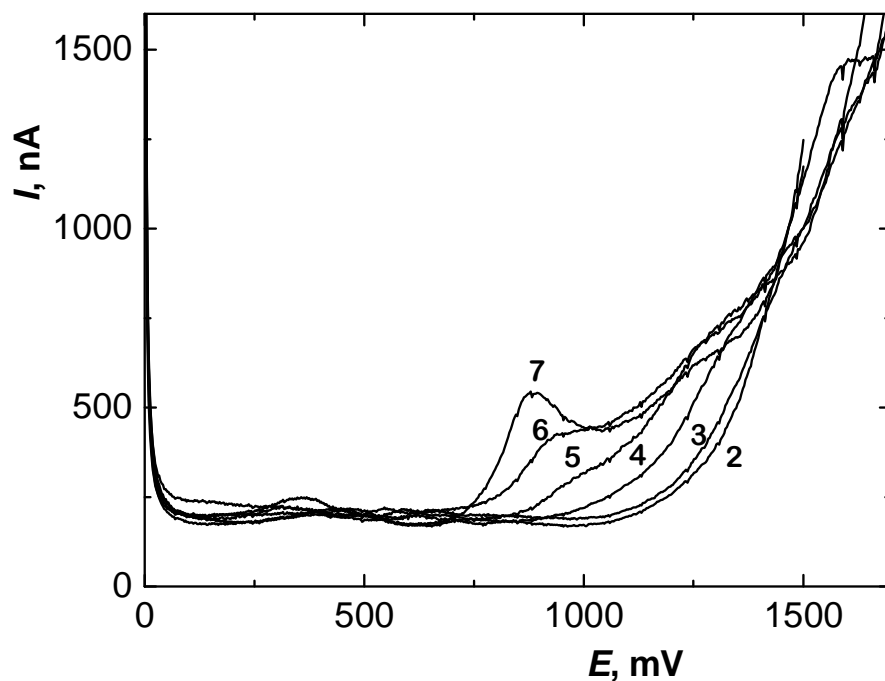

Fig.4 Selected DP voltammograms of 2-NP (c = 1.10^{-4} mol.L^{-1}) using electrochemical oxidation at BDDFE in BR buffer, pH 2-7. *The values of pH are at each curve.*
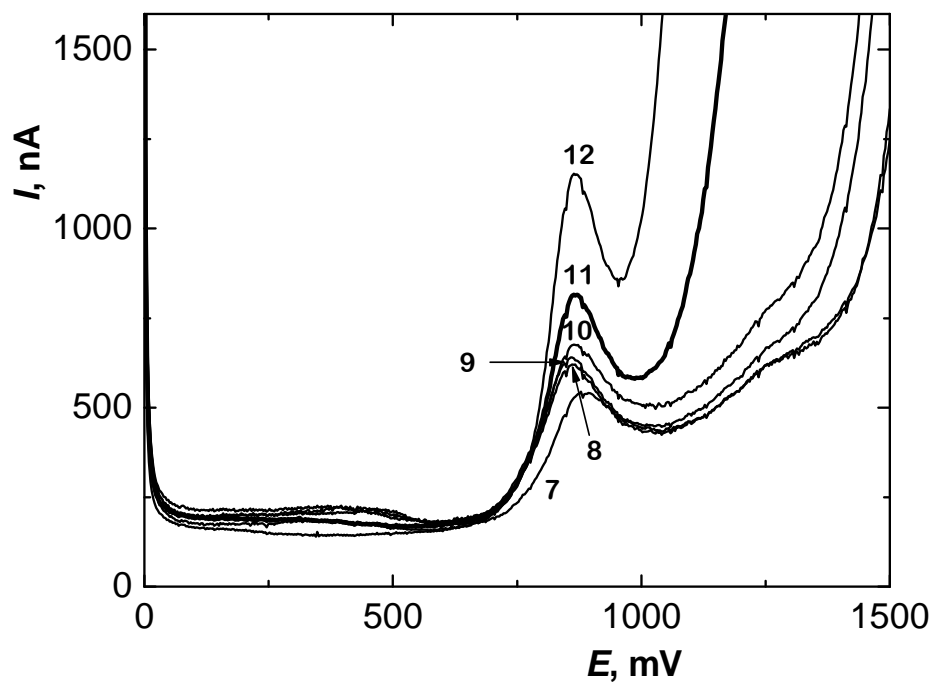
Fig.5 Selected DP voltammograms of 2-NP (c = 1.10^{-4} mol.L^{-1}) using electrochemical oxidation at BDDFE in BR buffer, pH 7-12. *The values of pH are at each curve.*
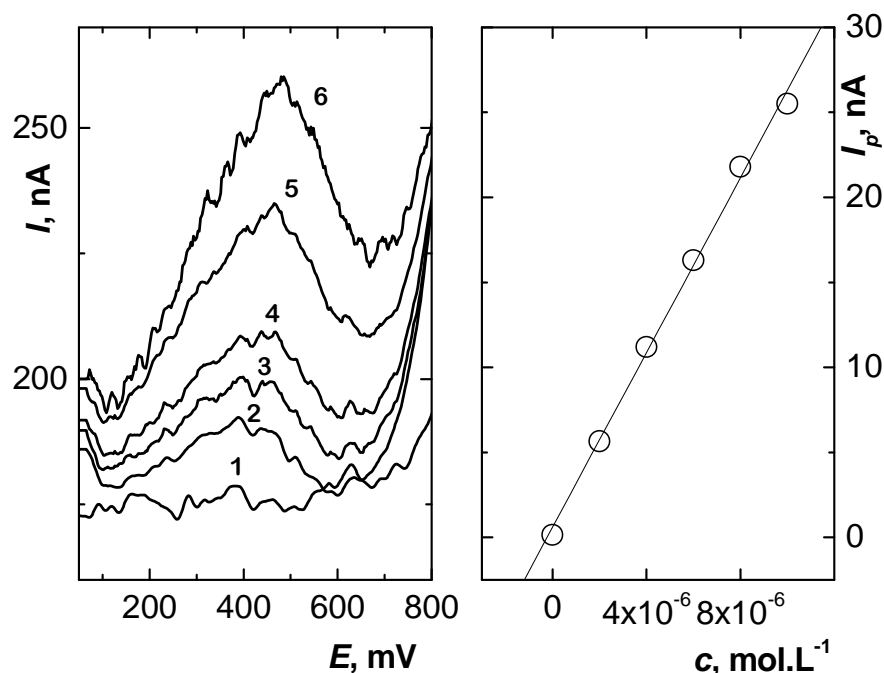
Fig.6 DP voltammograms and calibration dependence for 2-NP using electrochemical oxidation at BDDFE in BR buffer pH 11, *c(2-NP): 0 (1), 2.10^{-6} (2), 4.10^{-6} (3), 6.10^{-6} (4), 8.10^{-6} (5), 10.10^{-6} (6) mol.L^{-1}.*

Table 1 Parameters of the calibration straight lines for the determination of 2-NP by DPV at BDDFE in B-R buffer pH 4 (reduction) and pH 11 (oxidation).

Concentration [mol.L^{-1}]	Slope [nA.mol^{-1}.L]	Intercept [nA]	Correlation coefficient	L_Q [mol.L^{-1}]
$(2 - 10).10^{-6}$ (ox)	$2.6.10^6$	0.6	0.9985	6.10^{-6}
$(2 - 10).10^{-5}$ (red)	$-4.9.10^6$	6.4	0.9981	-
$(2 - 10).10^{-6}$ (red)	$-6.6.10^6$	2.3	0.9961	-
$(2 - 10).10^{-7}$ (red)	$-1.9.10^7$	-0.2	0.9962	4.10^{-7}

4. Conclusion

It can be concluded that BDDFE can be used to determine a wide variety of inorganic and organic compounds using electrochemical reduction and oxidation. Limits of detection were 6.10^{-6} mol.L^{-1} for electrochemical oxidation of 2-NP and 4.10^{-7} mol.L^{-1} for electrochemical reduction. It can be expected that this aproach can be used for the detection of trace amounts of nitrated explosives as well.

Acknowledgement

References

[1] Chailapakul O.; Siangproh W.; Tryk D.A.: *Sensor Letters **4**, (2006), 99*.
[2] Pleskov Y.V.: *Russ. J. Electrochem. **38**, (2002), 1275*.
[3] Compton R.G.; Foord J.S.; Marken F.: *Electroanalysis **15**, (2003), 1349*.

[4] Fujishima A.; Einaga Y.; Rao T.N.; Tryk D.A.: *Diamond electrochemistry. Elsevier, Amsterdam*, 2005.

[5] Barek J.; Fischer J.; Navratil T.; Peckova K.; Yosypchuk B.; Zima J.: *Electroanalysis* **19**, *(2007), 2003*.

[6] Jinadasa K.; Mun C.H.; Aziz M.A.; Ng W.J.: *Water Science and Technology* **50**, *(2004), 119*.

[7] Kolektiv autorů SRS: *List of the Registered Plant Protection Products. The state phytosanitary administration, Brno*, 2006.

[8] Zaleska A.; Hupka J.: *Waste Management & Research* **17**, *(1999), 220*.

VOLTAMMETRIC DETERMINATION OF 6-AMINOQUINOLINE AT A CARBON FILM ELECTRODE

Ivan Jiránek and Jiří Barek

Charles University in Prague, Faculty of Science, Department of Analytical Chemistry, UNESCO Laboratory of Environmental Electrochemistry, Hlavova 2030, 128 43 Prague 2, Czech Republic; email: jiranek@natur.cuni.cz

Abstract

Determination of 6-aminoquinoline (6-AQ) by differential pulse voltammetry (DPV) and direct current voltammetry (DCV) at carbon film electrode (CFE) was developed.

Keywords

Differential Pulse Voltammetry, Direct Current Voltammetry, Carbon Film Electrode, 6-Aminoquinoline

1. Introduction

Development of methods for monitoring of various detrimental biological active substances in environment is one of the most important tasks of modern analytical chemistry. Electrochemical methods are especially suitable for this purpose and represent very effective tool for analysis of electrochemically active substances. These methods are very sensitive, inexpensive and represent an independent alternative to prevalent spectrometric and separative methods. Modern electrochemical methods are well described in monographs[1,2].

The studied substance, 6-aminoquinoline (6-AQ) has genotoxic effects and belongs to dangerous pollutants of environment[3,4]. On the other hand, derivatives of aminoquinolines including 6-AQ are connected with antimalarial and potential anticancer agents[5-7]. Thanks to presence of amino group, 6-AQ is easily determinable on the basis of anodic oxidation.

The aim of this study was to find out optimal conditions for determination of 6-AQ using modern voltammetric methods, namely differential pulse voltammetry (DPV) and direct current voltammentry (DCV) at a carbon film electrode (CFE) and to set the limit of quantification.

In present we are testing a newly developed type of CFE[8]. The idea of this concept consists in covering of any solid electrode's surface by a film that is composed of conductive microparticles and nonconductive polymer. Such electrode has properties similar to material that microparticles are made from, so it is an elegant way how to reversibly change the potential window of original electrode. Conductive microparticles provide the electric contact between analyzed solution and conductive part of electrode. Carbon, resp. graphite is material with wide potential window which is suitable for anodic oxidations. Problem with passivation of the film's surface can be solved very simply by wiping the old film off with a filter paper and immersing the electrode's surface into conductive ink solution to form a new film. However, when a suitable electrochemical pretreatment of the film electrode is applied, the same film can be used for reproducible measurements for several days.

We use for measuring silver solid amalgam electrode (AgSAE) covered by a carbon film (CF-AgSAE). We have chosen this combination because AgSAE's properties are very similar to mercury electrodes and we assume that a film electrode will be used only for anodic oxidations whereas AgSAE would rather be used for cathodic reductions.

So when it is necessary to carry out measurement on the basis of cathodic reduction it suffices to wipe the film off and original AgSAE can be used.

2. Experimental Part
2.1 Reagents

The stock solution of 6-aminoquinoline (98%, Aldrich Chem. Co.) in deionized water ($c = 1 \cdot 10^{-3}$ mol·L^{-1}) was prepared by dissolving 0.01442 g of the substance in 100 ml of deionized water. More diluted solutions were prepared by exact dilution of the stock solution with deionized water. All solutions were kept in dark at laboratory temperature and in glass vessels. Other chemicals (boric acid, glacial acetic acid, phosphoric acid, sodium hydroxide, potassium chloride, all p.a. purity) were supplied by Lachema Brno, Czech republic. Deionized water from Millipore, USA, was used. The conductive carbon ink solution was prepared by mixing 0.01 g of polystyrene, 0.09 g of carbon powder (crystalline graphite 2 μm, CR 2 Maziva Týn, Czech Republic). The mixture was thoroughly homogenized by intensive agitation and sonication for 3 minutes.

2.2 Apparatus

Voltammetric measurements were carried out using Eco-Tribo Polarograph driven by software PolarPro version 5.1 (Polaro-Sensors, Prague). The software worked under the operational system Microsoft Windows XP (Microsoft Corp.).

All measurements were carried out in a three-electrode system. Platinum wire as an auxiliary electrode, silver/silver chloride reference electrode RAE 113 (1 mol·L^{-1} KCl, Monokrystaly Turnov, Czech republic) and CFE (AgSAE, disk diameter 0.55 mm, covered by carbon ink film) as a working electrode were used.

The scan rate 20 mV·s^{-1}, the pulse amplitude 50 mV and pulse width 80 ms were used unless stated otherwise.

Better reproducibility of determinations at CFE was assured by a suitable electrochemical regeneration of CFE. Optimal results were obtained by the application of 50 potential jumps between -200 mV and +600 mV for 0.3 s.

2.3 Procedures

Appropriate amount of 6-AQ stock solution or more diluted solution (0.02 – 1 mL) was measured out into a voltammetric vessel and filled up to 10 mL with Britton-Robinson (BR) buffer of appropriate pH. All curves were measured 3 times. The parameters of calibration curves (e.g. slope, intercept, limit of determination) were calculated using statistic software Adstat. This software uses confidence bands ($\alpha = 0.05$) for calculation of the limit of determination (L_Q). It corresponds to the lowest signal for which relative standard deviation is equal to 0.1 (Ref. *9*).

3. Results and Discussion
3.1 Differential Pulse Voltammetry at a Carbon Film Electrode

The dependence of height of peaks on pH was investigated. From DP voltammograms follows that 6-AQ gives one well developed anodic peak in the whole investigated pH region (Fig.1). Other strongly irreversible and badly developed peak was observed at less positive potential and is not analytically useful. The best developed peak was obtained in BR buffer pH 5 medium, which was further used for measuring calibration curves. Parameters of calibration curve are summarized in Table 1. DP voltammograms and calibration plot corresponding to the lowest attained concentration range are for the sake of illustration depicted in Fig.2. Because of the problems with electrode passivation in higher concentration range the calibration curve was not linear and the points were more scattered. Therefore, those results are not given in Table 1.
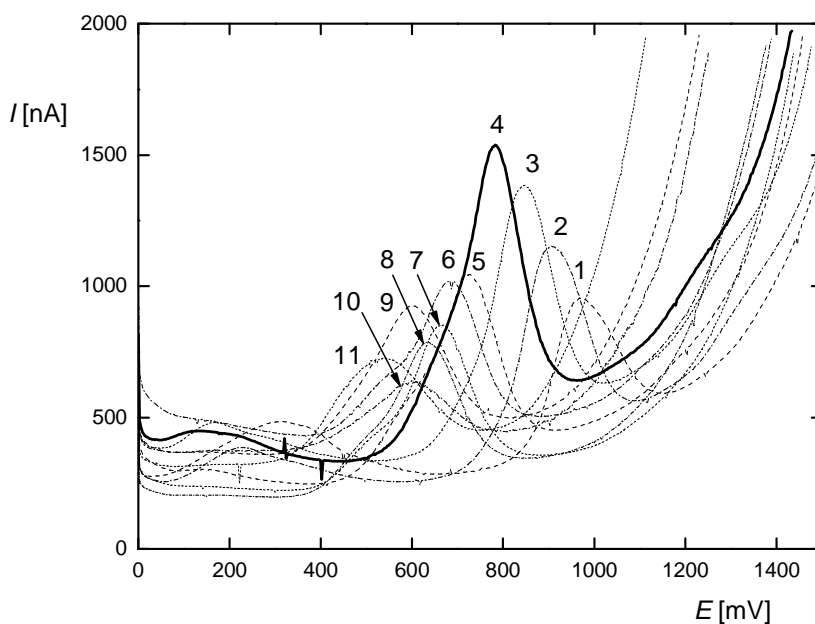
Fig.1 Differential pulse voltammograms of 6-AQ (c = $1 \cdot 10^{-4}$ mol·L^{-1}) at CFE *in BR buffer, pH 2.0 (1), 3.0 (2), 4.0 (3), 5.0 (4), 6.0 (5), 7.0 (6), 8.0 (7), 9.0 (8), 10.0 (9), 11.0 (10) and 12.0 (11).*
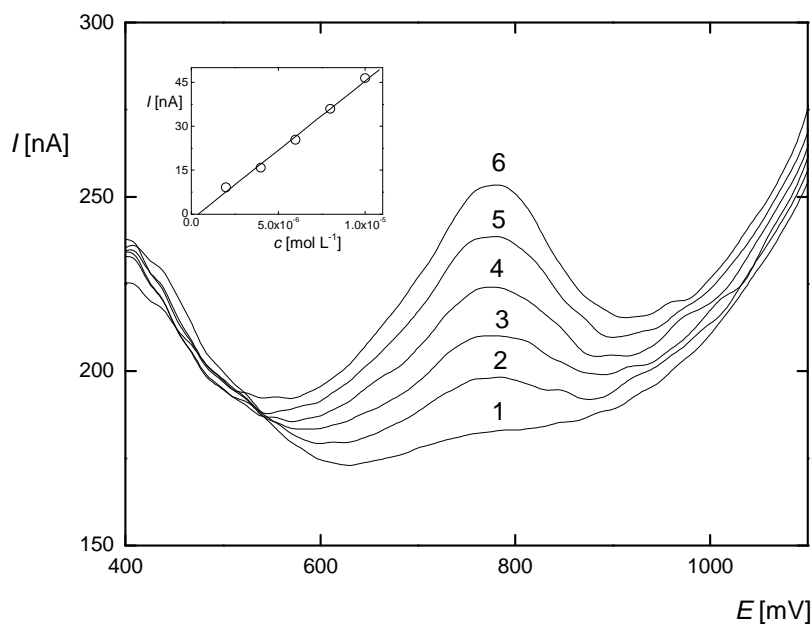
**Fig.2** DP voltammograms and calibration plot of 6-AQ at CFE *in BR buffer pH 5 medium at the lowest* attained concentrations. *c(6-AQ) = 0 (1), $2 \cdot 10^{-6}$ (2), $4 \cdot 10^{-6}$ (3), $6 \cdot 10^{-6}$ (4), $8 \cdot 10^{-6}$ (5), and $1 \cdot 10^{-5}$ (6) mol·L^{-1}.*

Table 1 Parameters of calibration straight line for DPV determination of 6-AQ at CFE *in BR buffer pH5 medium.*

Concentration mol·L^{-1}	Slope μA·mol^{-1}·L	Intercept μA	Correlation coefficient	L_Q mol·L^{-1}
$(2-10) \cdot 10^{-6}$	$4.73 \cdot 10^{6}$	-1.8	0.9978	$3 \cdot 10^{-6}$

155

3.2 Direct Current Voltammetry at a Carbon Film Electrode

6-AQ gives one anodic wave in the whole investigated pH region (see Fig.3). The best developed wave was obtained in BR buffer pH 5 medium. This medium was further used for measuring of calibration curves. Parameters of calibration dependence is summarized in Table 2 and voltammograms connected with the lowest attained concentration range is shown in Figure 4 for illustration.
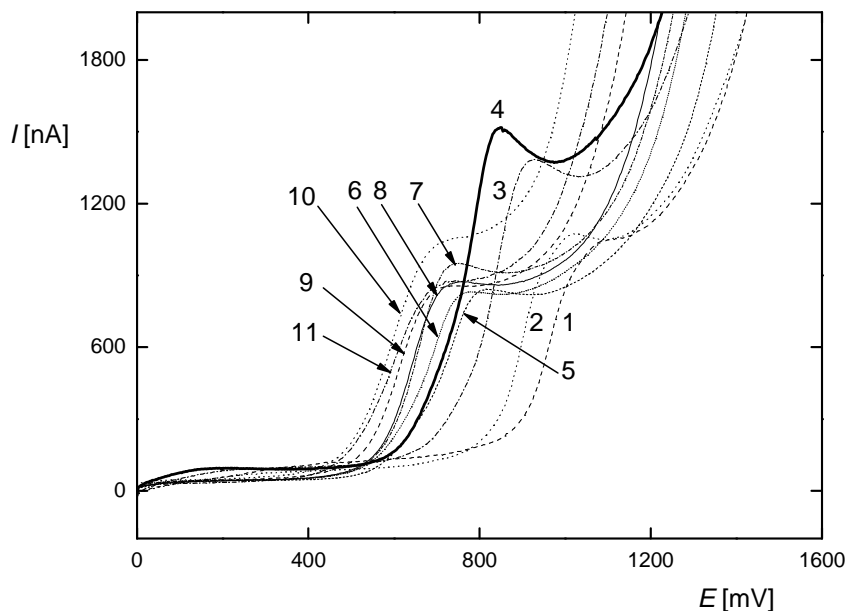

Fig.3 Differential pulse voltammograms of 6-AQ (c = $1 \cdot 10^{-4}$ mol·L^{-1}) at CFE *in BR buffer, pH 2.0 (1), 3.0 (2), 4.0 (3), 5.0 (4), 6.0 (5), 7.0 (6), 8.0 (7), 9.0 (8), 10.0 (9), 11.0 (10) and 12.0 (11).*
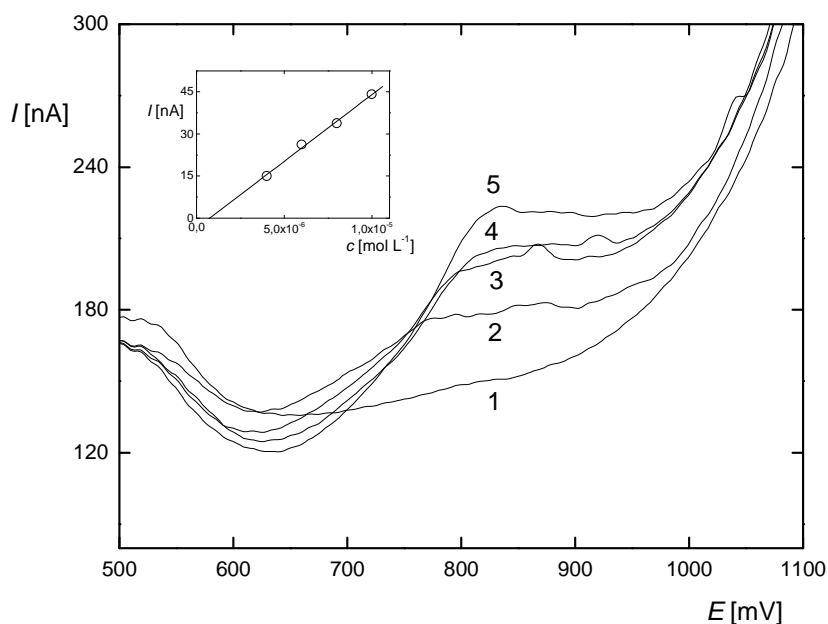

Fig.4 DP voltammograms and calibration plot of 6-AQ at CFE *in BR buffer pH 5 medium at the lowest attained concentrations. c(6-AQ) = 0 (1), $4 \cdot 10^{-6}$ (2), $6 \cdot 10^{-6}$ (3), $8 \cdot 10^{-6}$ (4) and $10 \cdot 10^{-6}$ (5) mol·L^{-1}.*

Table 2 Parameters of calibration straight line for DCV determination of 6-AQ at CFE *in BR buffer pH 5 medium.*

Concentration mol·L^{-1}	Slope µA·mol^{-1}·L	Intercept µA	Correlation coefficient	L_Q mol·L^{-1}
$(4 - 10) \cdot 10^{-6}$	$4.74 \cdot 10^{6}$	-3.4	0.9991	$4 \cdot 10^{-6}$

4 Conclusion

By DP Voltammetry at CFE, the limit of quantification of 6-AQ equal to $3 \cdot 10^{-6}$ mol·L^{-1} was reached. By DC Voltammetry at CFE, the limit of quantification of 6-AQ equal to $4 \cdot 10^{-6}$ mol·L^{-1} was reached. It is obvious that DPV is the method of choice because the peaks are better developed and more easily evaluable.

Acknowledgements

References

[1] Wang J.: *Analytical Electrochemistry, 2nd edition. VCH, Weinheim 2000.*

[2] Bard A.J.; Faulkner L.R.: *Electrochemical Methods: Fundamentals and Applications, 2nd edition. John Wiley, New York 2001.*

[3] Zima J.; Stoica A.I.; Zítová A.; Barek J.: *Electroanalysis 18 (2006), 158-162.*

[4] http://monographs.iarc.fr/monoeval/crthgr02a.html, *accessed March, 10, 2005.*

[5] Green N.; Hu Y.H.; Janz K.; Li H.Q.; Kaila N.; Guler S.; Thomason J.; Joseph-McCarthy D.; Tam S.Y.; Hotchandani R.; Wu J.J.; Huang A.R.; Wang Q.; Leung L.; Pelker J.; Marusic S.; Hsu S.; Telliez J.B.; Hall J.P.; Cuozzo J.W.; Lin L.L.: *J. Med. Chem. 50 (2007), 4728-4745.*

[6] Aragon P.J.; Yapi A.D.; Pinguet F.; Chezal J.M.; Teulade J.C.; Chapat J.P.; Blafne Y: *Chem. Pharm. Bull. 52 (2004), 659-663.*

[7] Vlahov R.; Parushev, Vlahov J.: *Pure Appl. Chem. 62 (1990), 1303-1306.*

[8] Yosypchuk B.; Barek J.; Fojta M.: *Electroanalysis 18 (2006), 1126-1130.*

[9] Meloun M.; Militký J.: *Statistické zpracování experimentálních dat na osobním počítači. Finish, Pardubice 1992.*

PREPARATION OF SERS-ACTIVE SUBSTRATES WITH LARGE SURFACE AREA FOR RAMAN SPECTRAL MAPPING AND TESTING OF THEIR SURFACE NANOSTRUCTURE

Vadym Prokopec[a], Jitka Čejková[b], Pavel Matějka[a] and Pavel Hasal[b]

[a] *Department of Analytical chemistry, Institute of Chemical Technology Prague, Technická 5,166 28 Prague 6, Czech Republic; e- mail: Vadym.Prokopec@vscht.cz*
[b] *Department of Chemical Engineering, Institute of Chemical Technology Prague, Technická 5,166 28 Prague 6, Czech Republic*

Abstract

Surface enhanced Raman scattering (SERS) is a powerful technique of signal detection at a low concentration. One of the main requirements for the substrate to be SERS-active is the proper roughness of its surface. Different SERS-active Au and Ag substrates suitable for spectral mapping were prepared using procedures consisted of electrochemical deposition of metal layer and roughening with oxidation-reduction cycles (ORC). The nanostructures of the surfaces were tested using Atomic Force Microscopy (AFM). Monolayers formed both by covalent and non-covalent linkages to the metal surface were detected and Raman spectral maps were measured. The relations among the nanostructures, optimal roughening, type of linkage of the analyte to the surface and the Raman signal enhancement were studied.

Keywords

SERS-active substrate, AFM, nanostructure, spectral map

1. Introduction

SERS is one of the methods which can give molecularly specific information about adsorbate-surface interactions. It demonstrates increased sensitivity over its non-enhanced counterpart and it has been used for the detection of molecules[1]. SERS-active metals enhance the intensity of the signal and allow the analysis of very thin (even submono-molecular) layers. Commercially fabricated surfaces are based on vacuum thermal evaporation[2] or sputtering coating[3] of gold particles onto proper material, plasmon treatment[4], laser deposition[5] but all these procedures require expensive instruments. In this work SERS-active substrates are fabricated on the surface of massive platinum targets using different electrochemical procedures.

The essential factor which influences the enhancement is the proper morphology (roughness) of the SERS-active surface on the nanostructure level[6]. One of the techniques used for the monitoring of the nanostructures is Atomic Force Microscopy, which is ideal for quantitative measurements of nanometer scale surface roughness[7]. The other important parameter of signal enhancement is an analyte adsorption to the surface. Depending on chemical structure of the species several mechanisms could be responsible for the interaction of an analyte with the surface: direct chemical bonding with covalent interactions (self-assembled monolayers (SAM) could be formed), physical sorption or non-covalent interactions[8]. SAMs can be used for (bio-) chemical sensors[9,10] or in molecular recognition[11].

This study was aimed at testing of different ways of preparation of SERS-active gold and silver substrates with large surface area with monolayers of the analyte on their surface, monitoring of surface nanostructure by AFM technique and Raman spectral mapping of prepared surfaces in scale up to several millimeters. The main goal is the achievement of optimal enhancement of the signal and its relation with the morphology of

the surface in nanoscale. All substrate preparation procedures were adjusted to formation of uniform surface in "macroscopic" (comparable with the size of the target) scale.

2. Experimental
2.1 SERS-active surfaces fabrication

All experiments were performed on massive platinum targets (diameter 10 mm, thickness 2 mm), which were then coated by gold or silver layer. Platinum targets were firstly polished with metallographic paper, alumina and calcium carbonate consecutively to obtain clean surface. Polished targets were immersed into the "piranha solution" for 30 minutes and finally washed with redistilled water. After the pretreatment the electrochemical procedure of gold or silver deposition followed. Both procedures were performed in the electrochemical cell, where flat gold or silver electrode was used as anode and platinum target was a cathode. The solution of $K[Au(CN)_2]$ mentioned in [11] was used for gilding procedure. Silver coating was performed from prepared bath which contained $[Ag(NH_3)_2]^+$ prepared from Ag_2O by dissolution in 30% ammonia.

2.2 ORC treatment

For some substrates oxidation-reduction cycles (ORC) treatment on both gold and silver surfaces was performed in a three-compartment cell. This was made using EG&G Princeton potentiostat/galvanostat. Gold or silver coated target, a thin platinum wire and silver/silver chloride (Ag/AgCl) were employed as working, counter and reference electrodes, respectively. Typically, gold coated target was cycled in a deoxygenated aqueous solution of 0.1M KCl from -0.28 to +1.22 V versus Ag/AgCl at 50 mV s^{-1} for 50 scans without any duration at the cathodic and anodic vertex. Silver coated target was typically cycled in a deoxygenated aqueous solution of 0.1M KCl from -0.3 to +0.3 V versus Ag/AgCl at 5 mV s^{-1} for 5 scans also without any duration at the cathodic and anodic vertex. Table 1 shows details of the deposition procedures.

2.3 Deposition of organic substances

Compounds A, B and C (Fig.1), which could serve as spacers for the selective receptors, were deposited. Deposition processes were performed from solutions of A, B and C in the volatile alcohols (either methanol or ethanol). Concentration range from 10^{-3} to 10^{-5} mol.L^{-1} was tested. Fabricated SERS-active substrate was immersed into the sample solution, usually for 24 hours. After that the target was took out of the solution and thoroughly rinsed with solvent and redistilled water repeatedly.

2.4 FT-Raman spectroscopy

FT-Raman spectra of samples were collected on a FT-Raman spectrometer (Bruker Optics). A 4-cm^{-1} spectral resolution was used for data accumulation. FT-Raman spectrometer was equipped with a TLC mapping stage (Bruker Optics).
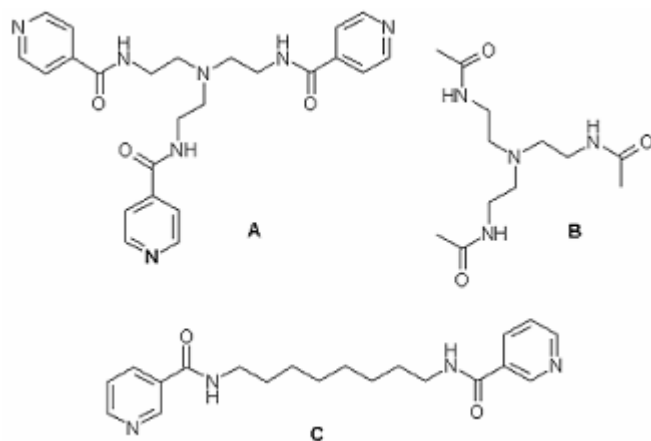
Fig.1 Compounds used in the study.

2.5 Spectral mapping

Spectral mapping was performed on above described spectrometer. The mapping area on the surface was selected from 10 x 10 (100 acquisition points) up 27 x 27 (729 acquisition points). The distance between points was set at 500 μm. Each single spectrum from the map was measured with 128 scans. During the processing of spectral mapping results different procedures were used to obtain several types of maps. The first type, so called „chemical" mapping, where the map was constructed on the base of intensity of one or several bands in the spectra, was performed in Opus (Bruker Optics) software. Maps of the second type were based on correlation coefficient of individual spectra and selected template (usually the mean spectrum) and on Principal Component Analysis (PCA) and were made in Matlab 6.5 software (The MathWorks Inc., USA).

2.6 Atomic force microscopy

The samples were imaged by atomic force microscope Ntegra (NT-MDT, Russia) in the tapping mode. Silicon tips NSG10 (NT-MDT, Russia) with typical resonant frequency of 255 kHz, force constant of 11.5 N/m and curvature radius of 10 nm were used. Scanning by sample configuration was selected. For scanning of larger areas the scanner with maximal range 100 x 100 μm and for scanning of smaller areas the scanner with maximal range 5 x 5 μm were used. The roughness was evaluated using Nova software.

3. Results and discussion
3.1 Gold SERS - active substrates preparation

Due to the fact that all imperfections of the surface should be flattened by covering with metal layer and because of big size of the targets the metal coating process lasted for at least 20 minutes. The duration of the first (lower current) and second (higher current) step of coating was optimized from the point of view of nanostructure of the substrate surface and the enhancement of the compound signal. It was found that gold SERS-active substrate prepared according to procedure G1 {Table 1A} was not suitable for the detection of the analytes and spectral mapping, because the signal of compound was very weak (Fig.2a) and there was low S/N ratio level in all spectra. On the contrary, when the procedure G2 was used, the signal of compounds was much higher and spectra showed high S/N ratio level (Fig.2b). AFM images of substrates showed that gold layer on the surface consisted of small gold nanoparticles (Fig.3A), which are responsible for the surface enhancement of Raman bands observed. Different size of gold nanoparticles causes the differences in morphological properties of substrate in nanoscale range. Gold nanoparticles prepared according to G1 were more rounded (diameter 200 – 300 nm),

while on the substrate G2 they had oval shape (500 – 700 nm in length). The average roughness of the surface was 47 ± 3 nm for G1 and 71 ± 2 nm for G2. The current density applied during the gold coating process and the duration of particular step affects the size of individual gold nanoparticles and the nanomorphology of the surface. With higher current and longer time the size of gold particles increases.
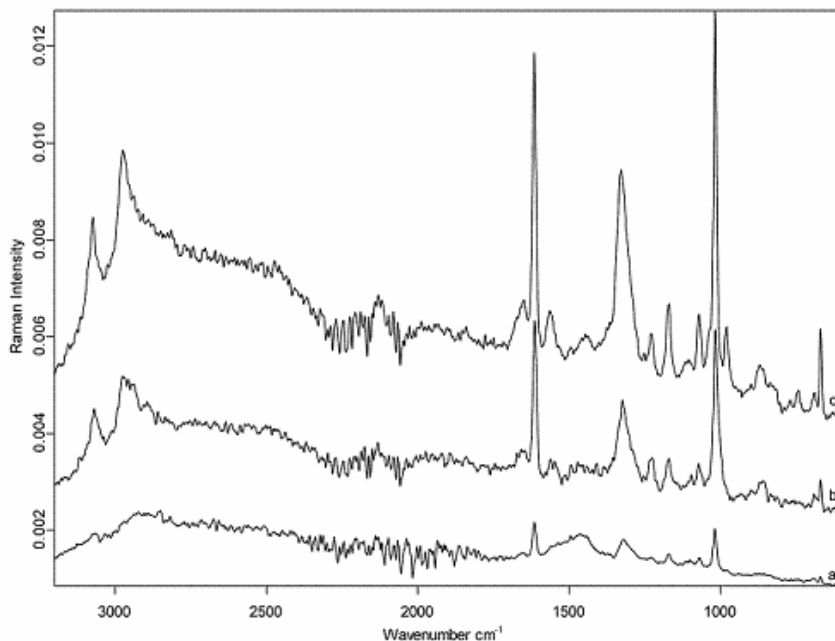

Fig.2 Details of FT-Raman spectra of compound C (10^{-3} mol·L^{-1}) measured on the surface of gold SERS-active substrates. *Spectra were measured on Au substrate prepared according to procedure G1 (a), G2 (b) and G3 (c)*
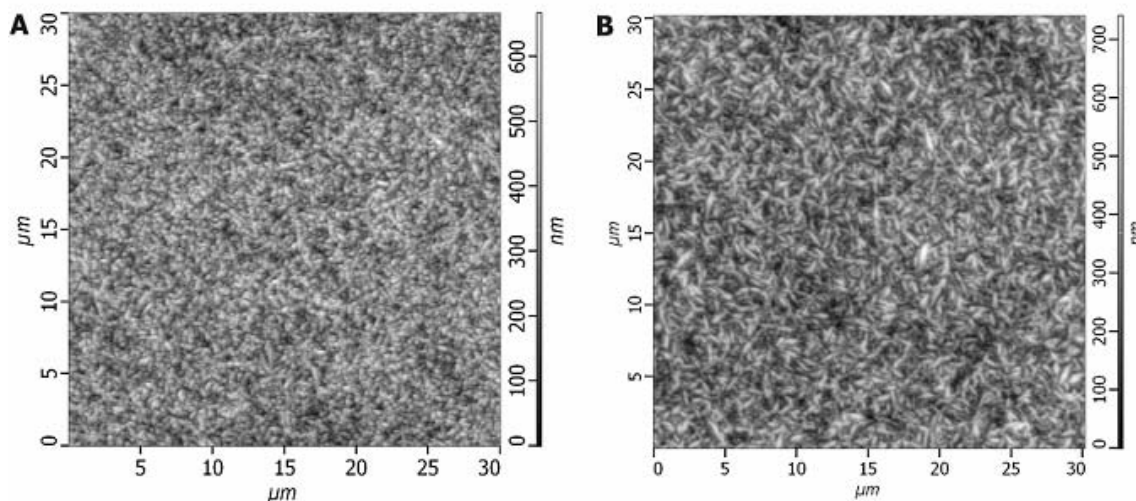

Fig.3 AFM images of gold SERS-active substrates prepared according to the procedure (A) G2 and (B) G3. *Images were scanned over the area 30x30 μm.*

161
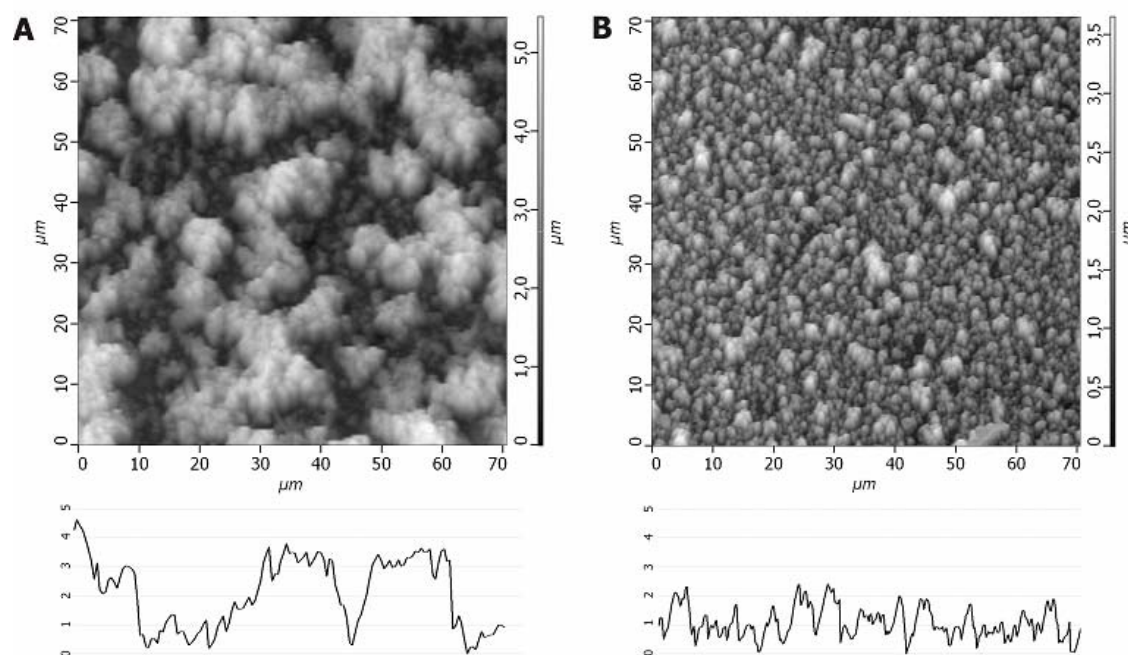
Fig.4 AFM images of silver SERS-active substrates prepared according to the procedure (A) S2 and (B) S4. *Images were scanned over the area 70x70 μm.*

Gold substrate prepared according to G2 was suitable for the detection of the analyte and spectral mapping but when concentration of organic solution lower than 10^{-3} mol·L^{-1} was applied there was only weak signal of the deposited compound with very low level of S/N ratio in measured spectra, which was not acceptable for spectral mapping. After gold coating procedure G3, which included ORC treatment, had been applied, it was found that substrate was suitable not only for the detection of deposited analyte at concentration 10^{-3} mol·L^{-1} (Fig.2c) but also up to 10^{-4} mol·L^{-1} and spectra from collected maps showed high intensity of all Raman bands and proper S/N ratio. AFM images of these substrates showed that the size of gold nanoparticles was bigger (700 – 900 nm in length) than in case of G2 and their shape changed (Fig.3B). After ORC treatment the particles became like long rollers. Average roughness (76 ± 1 nm) was also higher.

3.2 Silver SERS - active substrates preparation

Silver substrates compared to the gold ones had better enhancement of the signal. This can be caused by completely different morphological properties of the surface. From AFM imaging it was found that individual silver particles are of ca. 10 times bigger in surface roughness dimension than in case of gold substrates, i.e. ca. 500 - 800 nm for silver and ca. 45-90 nm for gold. The procedure S1 was less suitable for the detection and spectral mapping than the S2, which is analogical to G2 in gold coating. Average roughness of S1 and S2 substrates was 454 ± 28 nm and 548 ± 42 nm, respectively. Procedure S3 was also tested, where only constant current was applied during the whole process. AFM image showed that in this case silver particles were even bigger than in S2 (up to 5 μm) {Fig.4A} and average roughness was 902 ± 28 nm. But the surface was uniform neither in nanoscopic nor in macroscopic scale, so this procedure was further rejected. When silver substrate prepared according S2 was further treated with ORC (procedure S4 in Table 1B), its surface became more uniform: silver particles had comparable size and there were no visible differences in surface morphology (Fig.4B). Average roughness was 479 ± 17 nm. Section profiles for surface morphologies of samples are shown in Figure 4 as well. When layer was prepared by S2, particles clustered and formed non-uniform domains, whereas in case of S4, layer was less rugged and particles

162

were distributed uniformly. The detection of analyte deposited from the solution with concentration 10^{-5} mol·L^{-1} was made on this substrate. The quality of spectra allows evaluation of spectral maps.

3.3 Spectral mapping

Spectral maps were measured on the substrates, where the spectrum of the analyte showed adequate S/N ratio. The S/N ratio is critical factor for spectral mapping, because an increase of the individual spectrum accumulation time caused dramatic extension of the whole map collection time. As long as there were no detectable interferences in the spectra of surface of substrate prior the deposition of compounds, all Raman bands detected on the surface after deposition were caused by the layers. The integration method for chemical mapping was selected depending on the compound deposited. Strong bands typical for the individual functional groups were chosen for this purpose in order to compare spectral information in different points of the substrate surface. Fig. 5 shows spectral maps measured on silver SERS-active substrate prepared according to S4 (Table 1) with compound A on its surface deposited from the solution with concentration 10^{-4} mol·L^{-1}. Mapping area was 10x10 points. First two maps (Fig.5A, 5B) are constructed with the use of integration method based on the comparison of intensity of two bands of pyridine: in-plane deformation vibrations of pyridine ring and C=C and C=N ring stretching vibrations. The integration of the spectra from the third map (Fig.5C) was made in terms of the bands of C-N stretching vibrations of secondary amides. In the fourth map (Fig.5D) bands of CH_2 group stretching vibrations were compared. As it can be seen from Fig.5, all these maps show the same features of spectral homogeneity in wide area of examined substrate surface. There are some differences in map on Fig.5D comparing to three previous maps, which can be caused by changes in orientation of long aliphatic chains of the molecule in different points of the surface. The band selection can help to compare the information in terms of different functional groups but the enhancement factor for the whole molecule is affected only by nanostructure of the substrate. Different approaches were used to prepare maps 5E and 5F. Map 5E is based on correlation of individual spectra with a central spectrum of the whole area. Some differences are visible but the similarity of most points of the map is apparent. In the case of PCA map (5F) based on the value of a selected principal component more differences among individual points can be seen, because complete spectral information is used and the first few principal components describe a majority of variance.

163
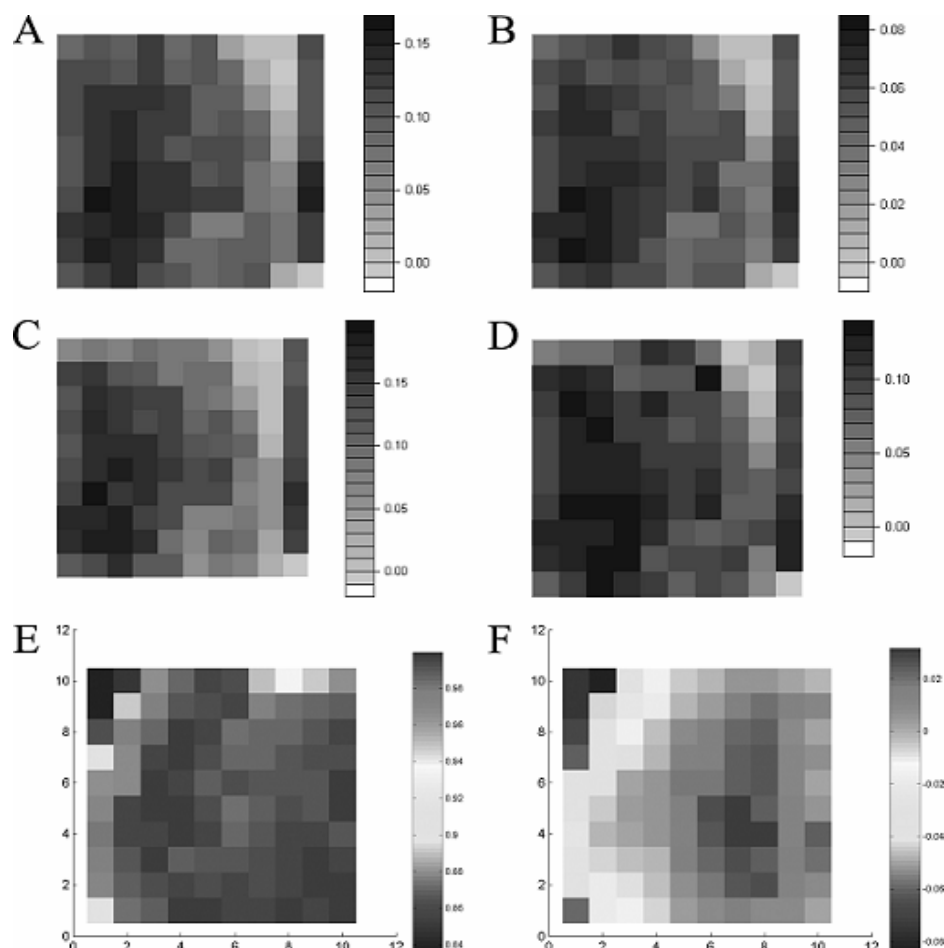
Fig.5 Comparison of various Raman spectral maps of silver SERS-active substrate with deposited compound A on the surface. Maps of intensity of characteristic Raman bands (A-D) {See Results and discussion}, correlation map based on the correlation with the mean spectrum (E) and PCA map based on the intensity of second principal component (F) are showed.

Table 1 Conditions of SERS-active surfaces preparation
ORC treatment was always performed as the third step, conditions for both gold and silver substrates were defined in Experimental

A) Gold substrates

Procedure	Step No.	Used current (mA)	Time (min)	ORC treatment
G1	1	7	25	no
	2	15	5	
G2	1	7	10	no
	2	15	20	
G3	1	7	10	yes
	2	15	20	

B) Silver substrates

Procedure	Step No.	Used current (mA)	Time (min)	ORC treatment
S1	1	5	10	no
	2	15	5	
S2	1	5	5	no
	2	15	10	
S3	1	15	15	no
S4	1	5	5	yes
	2	15	10	

4. Conclusions

Methods of preparation of gold and silver SERS-active substrates with large surface area were optimized for deposition of compounds on the surface and "macroscopic" Raman mapping. The substrates match all requirements of proper morphology of the surface in nanoscale and its uniformity in macroscale. Combination of Raman spectroscopy with AFM could be used for this purpose.

Different methods of spectral maps generation based on comparison of intensity of several Raman bands of the deposited compound were applied. The comparison of "chemical" maps and correlation or PCA maps for the monitoring of homogeneity of compound layer on the surface and the dissimilarities in interaction of the compound with the surface in different points was showed.

Acknowledgements

References

[1] Smith E.; Dent G.: In *Modern Raman Spectroscopy, A practical approach*, *John Willey and Sons (ed.), Ltd., 2005*, *113-133.*

[2] Yan W.; Bao L.; Mahurin S.M.; Dai S.: *Appl. Spectroscopy.* **58** *(2004), 18.*

[3] Pan Z.; Zavalin A.; Ueda A.; Guo M.; Groza M.; Burger A.; Mu R.; Morgan S.H.: *Appl. Spectroscopy* **59** *(2005), 782.*

[4] Rosenberg M.; Sheehan D.P.; Petrie J.R.: *J. Phys. Chem. A.* **108** *(2004), 5573.*

[5] Geddes C.D.; Parfenov A.; Roll D.; Fang J.; Lakowicz J.R.: *Langmuir.* **19** *(2003), 6236.*

[6] Liu Y.C.; Hwang B.J.; Jian W.J.: *Materials Chemistry and Physics.* **73** *(2002), 129.*

[7] Chen H.; Wang Y.; Dong S.; Wang E.: *Spectrochimica Acta Part A.* **64** *(2006), 343.*

[8] Ulman A.: In *An Introduction to Ultrathin Organic Films: From Langmuir-Blodgett to Self-Assembly. Academic Press, Boston, 1991***.**

[9] Subramanian A.; Irudayaraj J.; Ryan T.: *Sensors and Actuators B* **114** *(2006), 192.*

[10] Choi S.H.; Lee J.W.; Sim S.J.: *Biosensors and Bioelectronics* **21** *(2005), 378.*

[11] Zaruba K.; Matejka P.; Volf R.; Volka K.; Kral V.; Sessler J.L.: *Langmuir*, **18** *(2002), 6896.*

HPLC METHOD TO DETERMINE THE RESIDUAL CONCENTRATION OF ESTRONE DURING MOUSE SPERM CAPACITATION *IN VITRO*

<u>Marie Vadinská</u>[a], Zuzana Bosáková[a], Eva Tesařová[b], Jitka Vašinová[c], Michaela Jursová[c] and Kateřina Dvořáková-Hortová[c]

[a] *Department of Analytical Chemistry, Faculty of Science, Charles University in Prague, Albertov 2030, 128 40 Prague 2, Czech Republic*
[b] *Department of Physical and Macromolecular Chemistry, Faculty of Science, Charles University in Prague, Albertov 2030, 128 40 Prague 2, Czech Republic*
[c] *Department of Developmental Biology, Faculty of Science, Charles University in Prague, Viničná 7, 128 44 Prague 2, Czech Republic*

Abstract

   This work presents a high performance liquid chromatography HPLC method with UV detection to determine the status of estrone during mouse sperm capacitation *in vitro*. The proposed method enables to ascertain a free estrone, and the estrone bound to the bovine serum albumin in capacitation medium. A reversed-phase separation mode using a Symmetry C18 column with a mobile phase composed of acetonitrile, methanol and water at the ratio 23/34/53 (v/v/v) was applied.

Keywords

   HPLC; endocrine disruptors, estrone; sperm; capacitation

1. Introduction

   Endocrine-disrupting chemicals (EDCs) are known as industrial and environmental contaminants, and can be found in the water of many rivers, lakes, seas, etc. EDCs interfere with the function of the endocrine system of both wildlife and humans[1]. It was reported that these compounds affect ecosystems, e.g. feminization of wild fish living downstream from wastewater effluent[2]. EDCs detected in environmental waters derive from factory effluent, from wastewater of plant treatment, and from residential wastewater. Some environmental estrogens have a natural origin. 17β-Estradiol (E2) and its main metabolites - estriol (E3) and estrone (E1) - along with their conjugates are naturally present at higher levels in females than in males[3]. Metabolism of estrone and progesterone mainly takes place in the liver. The lipophilic steroid hormones are conjugated with glucuronic acid or sulfate, which increases their water solubility. They are excreted as glucuronide and sulphate into the urine. Therefore, urinary estrogens may be a good marker to estimate the exposure level to these environmental estrogens[4].

   Environmental estrogens can also simulate the behavior of natural hormones due to binding to their receptors[5]. Estrogens can block the bond of hormones to receptors or simply block synthesis of certain hormones. They can also prevent the transport of hormones in the blood stream or alter their excretion from the body. Among others, environmental hormones are known to be responsible for decreasing the number of sperm in men. Pesticides are one source of these emissions, which stay in the food chain for decades. Hence, estrogenous compounds, present in food, plastic wrapping and water bottles represent potentially harmful substances to the health of man.

   A recent study[6] *in vivo* reported an important genetic difference in sensitivity to estrones between various kinds of mice. Environmental estrogens bind to estrogen receptors and mimic the actions of estrone, including inhibition hypothalamic gonadotropin-releasing hormone secretion, which decreases follicle-stimulating hormone (FSH) and luteinizing hormone (LH) secretion, thereby leading to a lower testicular

function. Estradiol and several estrogenic xenobiotics also act towards an increase of germ cell apoptosis and a sperm count decrease. Capacitation is the key event in the study of sperm behavior prior to fertilization. Only capacitated sperm are sufficiently active and are able to fertilize. *In vivo* location of capacitation occurs in the uterus and oviducts and it is facilitated by substances of the female genital tract. For obvious reasons it is difficult to study these events *in vivo*. Therefore *in vitro* experiments precisely simulating an *in vivo* environment are crucial for closer understanding of the process, when sperm gain the ability to fertilize an ovum. However, in order to study the effects of hormones such as estrone on sperm during *in vitro* capacitation, it is crucial to find out how much of the free estrone is available for cells in the sample. Therefore, how much of estrone is bound to bovine serum albumin (BSA) present in M2 capacitation medium due to a strong binding of estrone to BSA[7].

Specific alternative methods using antibodies such as enzyme-linked immunosorbent assay (ELISA) with a simple solid-phase extraction (SPE) were developed for the analysis of estrone in an aquatic environment[8,9]. The limits of detection dropped down to a tenth, and in some cases, to a thousandth of a microgram per liter. Among the analytical techniques, gas chromatography-mass spectrometry[10-12] and high-performance liquid chromatography-mass spectrometry[13-15] were commonly used for determining estrones in wastewater and soil. High-performance liquid chromatography (HPLC) with ultraviolet (UV) or fluorescence detection were also developed for determining estrones in real water samples (limit of detection ~ $\mu g \cdot L^{-1}$)[16].

The aim of this work is to develop the HPLC method with UV detection for determining free estrone available to cells (see Fig.1) in a specific biological sample, in our case sperm. The freshly collected mouse spermatozoa were capacitated *in vitro* within the presence of estrone. The residual concentration of estrone during and after capacitation was monitored on an experimental time scale.
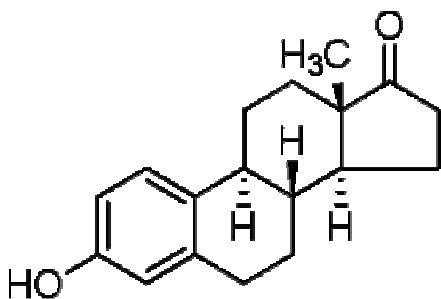

Fig.1 The structure of estrone (E1)

2. Experimental
2.1 Instrumentation

The HPLC equipment (Pye Unicam, Cambridge, UK) comprised of a PU 4015 pump, a PU 4020 UV detector and a Rheodyne injection valve Model 7725i (Cotati, CA, USA) with a 20 μl sample loop. The samples were injected with a Hamilton syringe (Reno, Nevada, USA). Signal was processed and data were handled with the CSW 32 PC software (DataApex, Prague, Czech Republic). A commercially available steel column Symmetry C_{18} (150 x 4.6 mm I.D., octadecyl bonded to silica gel, particle size 5 μm) was purchased from Waters (Milford, Massachusetts, USA).

The concentration of spermatozoa in 1 ml was assessed in a haemocytometer chamber according to a standard protocol under a 100x magnification. The motility of spermatozoa was checked under a light microscope (Zeiss, Czech Republic), and viability was evaluated under a fluorescence microscope (Olympus, Czech Republic).

2.2 Reagents and Experimental Conditions

Methanol (MeOH) and acetonitrile (ACN), both of them a HPLC grade purity, were purchased from Sigma-Aldrich (Chromasolv, Stienheim, Germany). Ethanol and paraffin oil were obtained from P-LAB (Czech Republic), M2 laboratory mouse *in vitro* fertilizing medium was delivered by Sigma-Aldrich (Stienheim, Germany). Deionized water (Milli-Q water purification system Millipore, Milford, MA, USA) was used in all experiments. For viability a check-up, sperm were dyed using a life-dead sperm staining kit (Molecular Probes, Invitrogen, Czech Republic).

The stock solution of estrone ($10g.mL^{-1}$), (Sigma Aldrich, Czech Republic) was prepared by the dilution of an appropriate amount of standard E1 in ethanol and was stored at 5 °C. The individual concentrations of estrone for calibration measurements were obtained by the adding of an appropriate amount of stock solution into the M2 medium.

The experiments were carried out at laboratory temperature (22 ± 2 ºC). The UV detection was performed at the wavelength of 200 nm. The mobile phase consisted of methanol, acetonitrile, and water was sonicated for 20 min prior to use. The mobile phase flow rate was $1mL·min^{-1}$.

2.3 Sperm Capacitation *in vitro*

Laboratory BALB/c mice, purchased from Velaz (Prague, Czech Republic), were maintained and housed at the animal facilities of the Faculty of Science, Charles University, Prague. All animal procedures were carried out in strict accordance with the Animal Scientific Procedure, Art 1991, and subjected to review by the local ethics committee.

Mouse spermatozoa were recovered from the *cauda epididymidis* by placing its very distal region into a M2 *in vitro* fertilizing medium containing 0.4% bovine serum albumin for 10 minutes at 37 °C in 5% CO_2 in air. Sperm stock was diluted for the required concentration (5×10^6 sperm $.mL^{-1}$) into the 100 µL drop of M2 medium under paraffin oil in 35 mm Petri dishes[17]. Each drop contained estron of the concentration 200 $µg.L^{-1}$. The motility of the sperm population was checked throughout the whole experiment by a light inverted microscope with a thermostatically controlled stage at 37 °C. Spermatozoa were capacitated for up to 90 minutes. At time 0 and then after 30, 60 and 90 min of incubation a drop with spermatozoa was collected, and centrifuged for 5 min at 10 000 rpm. Individual supernatants were further investigated for the remaining amounts of free estrone. Parallel controls without presence of estrone were run throughout the whole experiment to check whether sperm viability and motility was not altered by an addition of estrone.

3. Results and Discussion
3.1 Optimization of separation conditions

Based on the results reported for the separation of estrone and estradiol (contained in drug preparations) in the literature[18], the separation system consisted of a C_{18} stationary phase and methanol, acetonitrile and water as mobile phase constituents were selected for determining estrone in a specific biological sample – M2 medium supernatant after centrifugation of capacitated sperm. The M2 medium is a complex mixture, containing inorganic and organic components, which especially BSA (4%) can cause difficulties during the separation process. To attain the sufficient resolution between estrone and the other constituents of M2 media, various volume ratios of MeOH, ACN and water were tested as mobile phase compositions. As the compromise among analysis time, resolution and peak symmetry, the mobile phase composed of MeOH/ACN/water 34/23/53 (*v/v/v*) was selected for the determining and subsequent quantification of estrone in the M2

medium. The chromatograms of the M2 medium itself and the M2 medium spiked with estrone are shown in Figs.2 and 3, respectively.
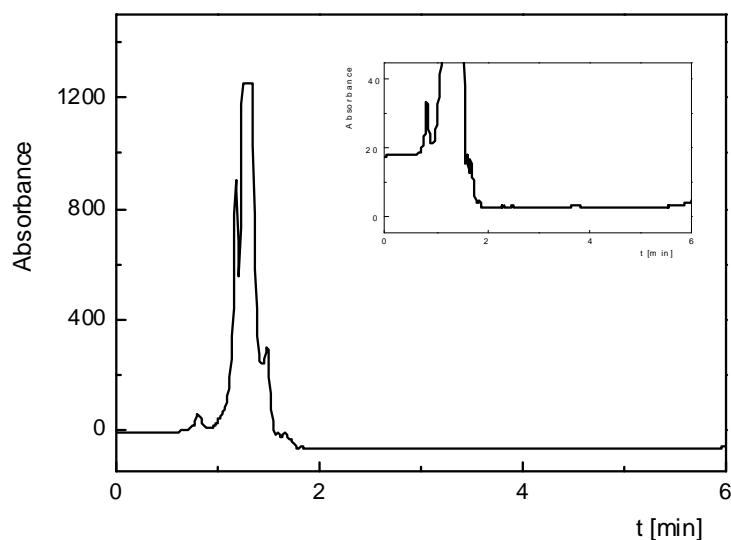

Fig.2 Chromatogram of M2 medium (Insert: enlarged section of chromatogram); E*xperimental conditions: Symmetry C$_{18}$ column, mobile phase composition - 34/23/53 (v/v/v) MeOH/ACN /water; flow rate 1 mL·min^{-1}, λ = 200 nm.*
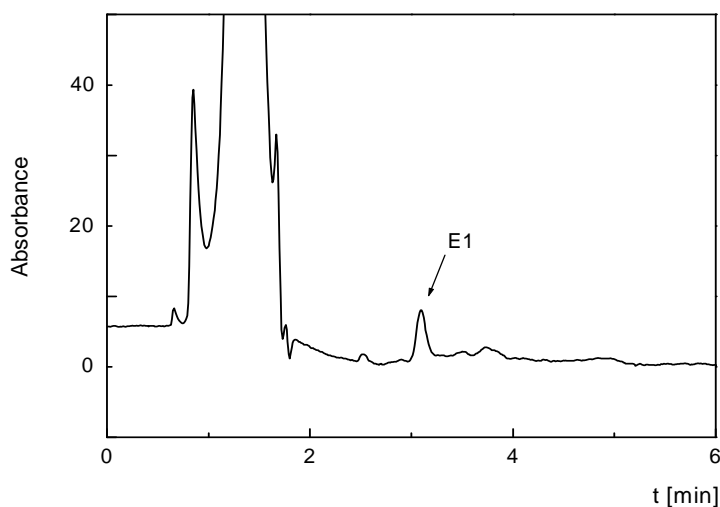

Fig.3 Chromatogram of separation of 200 μg L^{-1} estrone in M2 medium; E*xperimental conditions: Symmetry C$_{18}$ column, mobile phase composition - 34/23/53 (v/v/v) MeOH/ACN /water; flow rate 1 mL ·min^{-1}, λ = 200 nm.*

3.2 Calibration of estrone

At optimized separation conditions (described above), the calibration of estrone in M2 medium was carried out. With respect to the biological purpose (see section 2.3), the highest measured concentration of estrone in M2 medium was 200 μg·L^{-1}. The calibration curve was measured over a concentration range from 50 to 200 μg·L^{-1}. Measurements at all concentration levels were repeated four times and the mean values of the peak areas were subjected to linear regression (see Fig.4). A satisfactory fit between the experimental points and linear calibration curve was observed.
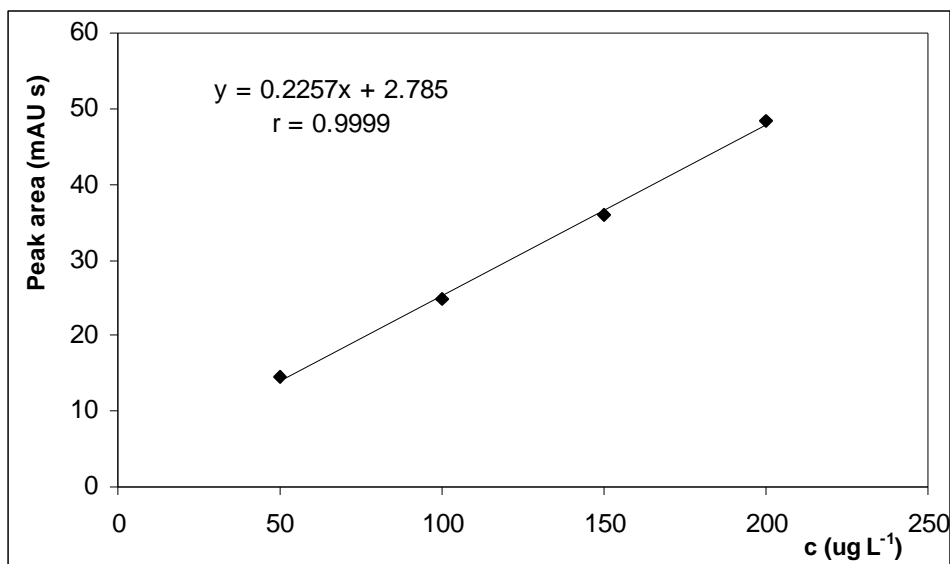
Fig.4 Calibration curve of estrone; E*xperimental conditions: Symmetry C_{18} column, mobile phase composition - 34/23/53 (v/v/v) MeOH/ACN /water; flow rate 1 mL ·min^{-1}, λ = 200 nm.*

3.3 Determining of the residual concentration of estrone in M2 medium after sperm capacitation *in vitro*

Supernatants collected (see para. 2.3) at time 0, 30, 60 and 90 min of sperm capacitation *in vitro* were investigated for the residual concentration of E1. Under optimized separation conditions, the residual estrone concentrations were monitored at each experimental time. In order to eliminate inaccuracies caused by manipulation with samples, appropriate controls (E1 + M2) without sperm were prepared in parallel. Fig.5 shows the separation of supernatant collected at time 0 min of sperm capacitation *in vitro*.

It is obvious by comparing Fig.4 and 5 that both chromatograms are almost the same.
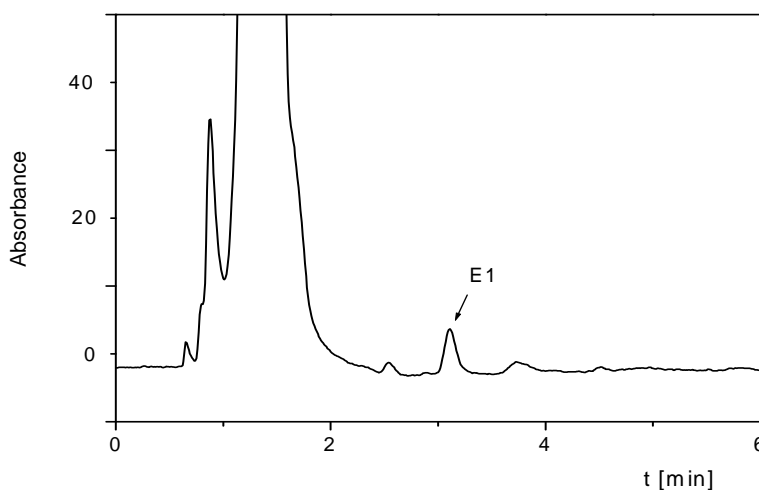
Fig.5 Chromatogram of supernatant (200 μg·L^{-1} E1 + M2 + sperm) at time 0 min; E*xperimental conditions: Symmetry C_{18} column, mobile phase composition - 34/23/53 (v/v/v) MeOH/ACN /water; flow rate 1 mL·min^{-1}, λ = 200 nm.*

The analysis of estrone in the samples (supernatants) was performed in triplicates. The mean peak areas (A) of estrone in experimental and parallel control samples are listed in Table 1.

Table 1 Average values of the peak area (*A*) of estrone in supernatants
Experimental conditions: Symmetry C₁₈ column, mobile phase composition - 34/23/53 (v/v/v) MeOH/ACN/water; flow rate 1 mL ·min⁻¹, λ = 200 nm.

Time of capacitation [min]	A [mAU s]	
	Experimental sample	Control sample
0	49.25	48.60
30	48.64	48.66
60	47.28	48.70
90	43.91	48.68

Experimental sample – supernatant 200 μg·L⁻¹ of E1 + M2 + sperm
Control sample – supernatant 200 μg·L⁻¹ of E1 + M2 without sperm added

Mean peak areas of the experimental samples were implemented into a calibration equation (see Fig.5) for the calculation of residual concentrations of estrone after the time-dependent capacitation of sperm *in vitro*. Dependency of the residual concentration of E1 on the time elapsed from capacitation of sperm is depicted in Fig.6. The attained results clearly demonstrate the almost parabolic decrease of E1 concentration in experimental samples within this time.
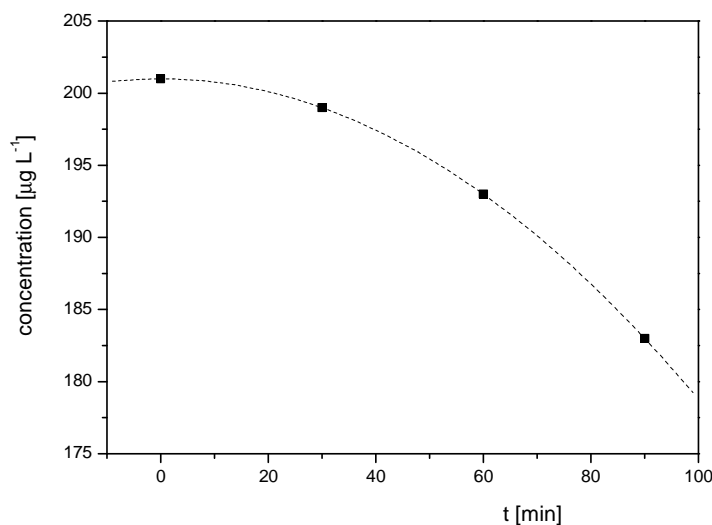

Fig.6 Dependency of a residual concentration of estrone on the time of sperm capacitation *in vitro*.

4. Conclusion

The proposed analytical method proved to be suitable for the detection and quantification of the residual concentration of estrone in sperm capacitation medium containing BSA. Our results show that the level of free estrone available for cells in the medium can be determined throughout the ongoing capacitation of mouse spermatozoa *in vitro*. Comparing experimental samples with controls, a quantity of the E1 bound to the BSA can also be ascertained. Therefore, in conclusion, HPLC method with UV detection represents an important tool to determine the amount of environmental estrogens, in our case estrone, bound to sperm cells at a specific time of capacitation *in vitro*.

Acknowledgement

References

[1] Colborn T.; vom Saal F.S.; Soto A.M.: *Environ. Health Perspect. **101** (1993), 378.*

[2] Sumpter J. P.: *Toxicol. Lett. **737** (1995), 82.*

[3] Mitani K.; Fujioka M.; Kataoka H.: *J. Chromatogr. A **1081** (2005), 218.*

[4] Mao L.; Sun C.; Zhang H.; Li Y.; Wu D.: *Anal. Chim. Acta **522** (2004), 241.*

[5] Reiner J.; Vriese E.; Blaty H.; Vermeulen N. P. E.: *Anal. Biochem. **357** (2006), 85.*

[6] Spearow J. L.; Doemeny P.; Sera R.; Leffler R.; Barkley M.: *Science **285** (1999), 1259.*

[7] Tan E.; Lu T.; Pang K. S.: *J. Pharmacol. Exp. Ther. **297** (2001), 423.*

[8] Huang C. H.; Sedlak D. L.: *Environ. Toxicol. Chem. **20** (2001), 133.*

[9] Li Y.; Wang S.; Lee N. A.; Allan R. D.; Kennedy I. R.: *Anal. Chim. Acta **503** (2004), 171.*

[10] Nakamura S.; Sian T. H.; Daishima S.: *J. Chromatogr. A **919** (2001), 275.*

[11] Liu R.; Zhou J. L.; Wilding A.: *J. Chromatogr. A **1022** (2004), 179.*

[12] Kawaguchi M.; Ishii Y.; Sakui N.; Okanouchi N.; Ito R.; Inoue K.; Saito K.; Nakazawa H.: *J. Chromatogr. A **1049** (2004), 1.*

[13] Fawel J. K.; Sheahan D.; James H. A.; Hurst M.; Scott S.: *Water Res. **35** (2001),1240.*

[14] Lopez de Alda M. J.; Barcelo D.: *J. Chromatogr. A **892** (2000), 391.*

[15] Rodriguez- Mozaz S.; Lopez de Alda M. J.; Barcelo D.: *Anal. Chem. **76** (2004), 6998.*

[16] Penalver A.; Pocurull E.; Borrull F.; Marce R. M.: *J. Chromatogr. A **964** (2002), 153.*

[17] Bavister B.D.: *Gamete Res. **23** (1989), 139.*

[18] Nováková L.; Solich P.; Matysová L.; Šícha J.: *Anal. Bioanal. Chem. **379** (2004), 781.*

VOLTAMMETRIC DETERMINATION OF EPINEPHRINE AT A MODIFIED MINIATURIZED CARBON PASTE ELECTRODE

Zuzana Jemelková, Jiří Zima and Jiří Barek

Charles University in Prague, Faculty of Science, Department of Analytical Chemistry, Albertov 6, 128 43 Prague 2, Czech Republic; e-mail: Zuzana.Jemelkova@seznam.cz

Abstract

Nowadays, the application of electrochemical methods has been evolving in pharmaceuticals determination area and the need for high sensitivity and selectivity for the biomolecules has been increasing. In this article, a modified miniaturized carbon paste electrode (miniCPE) is proposed for the voltammetric determination of epinephrine. The solution of epinephrine was measured in the concentration range $1 \cdot 10^{-6}$ - $1 \cdot 10^{-5}$ mol·dm^{-3} and the limit of detection of epinephrine at a bare miniCPE was $5 \cdot 10^{-7}$ mol·dm^{-3}. For the decrease of limits of detection a poly (eriochrome black T) chemically modified carbon paste electrode was tested. The solution of epinephrine was measured in the concentration range $8 \cdot 10^{-7}$ - $1 \cdot 10^{-5}$ mol·dm^{-3}. Using differential pulse voltammetry the anodic peak of epinephrine obtained with modified miniCPE was approximately 3 times higher than peak of epinephrine obtained with bare carbon paste electrode and the limit of detection decreased to $2 \cdot 10^{-7}$ mol·dm^{-3}.

Keywords

Epinephrine; voltammetry; modified carbon paste electrode

1. Introduction

In the end of 1950's the team of Professor Adams evolved carbon paste electrode (CPE) as a new electrode material[1]. In following years the modifications of carbon paste were performed. An effort to extend the usage of CPE leads to preparation of new carbon paste, which contained not only carbon powder and paste liquid but also chemical or biological modificator. Nowadays, the scientists endeavour to do miniaturization of known electrodes. The miniaturized carbon paste electrode (miniCPE) is suitable for the determination of low amounts of solutions.

Epinephrine is an adrenal medulla hormone. It occurs also in sympathetic postganglionic terminal and in some parts of central nervous system. It is sympathicus activator and humoral transmitter of sympathetic excitement to target tissue[2]. Epinephrine falls into the catecholamines group. The principal catecholamines are norepinephrine, epinephrine and dopamine. Catecholamines include compounds with a dihydroxyphenyl group and an amino group. By electrochemical oxidation, catecholamines are easily converted into quinone species[3]. There are a number of disorders involving catecholamines, including neuroblastoma, pheochromocytoma, chemodectina, familial paraganglioma syndrome, dopamine-ß-hydroxalase deficiency, and tetrahydrobiopterin deficiency. So the efficient methods are necessary for the determination of catecholamines.

Methods for epinephrine assay and study are HPLC[4-6], capillary electrophoresis[7,8] and flow injection analysis[9-11]. Very often used detection methods are fluorescence, chemiluminescence and mass spectrometry.

2. Experimental
2.1 Reagents

All reagents were of analytical-reagent grade and all solutions were prepared with water obtained from a Millipore Q-plus System (Millipore, Bedford, MA, USA). Epinephrine was purchased from Zentiva (Prague, Czech Republic) as a solution containing epinephrini hydrochloridum 1.2 mg (epinephrinum 1 mg) in 1 cm^3 of injection solution. Carbon paste was prepared by mixing 250 mg of carbon powder "CR2" (crystal graphite 2µm, Maziva Týn s.r.o., Týn nad Vltavou) and 0.1 cm^3 of mineral oil Nujol (Fluka, Buchs). All experiments were carried out in Britton-Robinson (B-R) buffer solution prepared by mixing 0.2 $mol·dm^{-3}$ sodium hydroxide with acidic solution (0.4 $mol·dm^{-3}$ each of boric acid, phosphoric acid and acetic acid – all p.a., Sigma Aldrich, USA). Eriochrome black T for modification of CPE was obtained from Lachema Brno, Czech Republic.

2.2 Apparatus

A 4330 Conductivity & pH Meter (Jenway Ltd., Essex, UK) fitted with the combined glass electrode was employed to measure the pH of the solutions. Differential pulse voltammograms were obtained with PalmSens (Palm Instruments BV) controled by PalmSensPC software (Ivium Technologies, Netherland). Appropriate measurements were carried out in the three-electrode system consisting of working carbon paste electrode and miniaturized carbon paste electrode, respectively (both Vývojové dílny, Univerzita Pardubice, Czech Republic), silver/silver chloride, 3 $mol·dm^{-3}$ KCl reference electrode RE-5B (BASi, USA) and a platinum wire as the auxiliary electrode (Monokrystaly, Turnov, Czech Republic). Instrumental parameters were: applied potential range 0 to +1000 mV; scan rate 20 $mV·s^{-1}$; pulse amplitude +50 mV, pulse time 0.070 s.

2.3 Procedures

Techniques used for voltammetric determination of epinphrine were differential pulse voltammetry (DPV) and adsorptive stripping voltammetry (AdS DPV). DPV measurements were performed in an unstirred and not de-aerated B-R buffer at a laboratory temperature. Accumulations were performed in the stirred, not de-aerated B-R buffer solution. $1·10^{-4}$ $mol·dm^{-3}$ stock solution was prepared diluting 0.183 cm^3 of epinephrini hydrochloridum in B-R buffer of appropriate pH. The prepared stock solution was kept in cold and dark. The detection limits were calculated as the concentration of an analyte which gave a signal three times the background noise (*S/N* = 3).

The miniaturization of CPE led to decrease of consumption of analyte and other chemicals. In case of classical CPE, the volume of measured solution is 10 cm^3. 1 cm^3 of solution is enough for determination with miniCPE.

For the decrease of limits of detection it is appropriate to use the accumulation of analyte on the surface or to the bulk of carbon paste and to modify the carbon paste. The eriochrome black T was used to modify the miniCPE.

3. Results and Discussion
3.1 Bare carbon paste

The influence of pH on voltammetric behaviour of epinephrine in Britton-Robinson (B-R) buffer pH 2 – 12 was studied (Fig.1). Concentration of measured epinephrine solution was $1·10^{-5}$ $mol·dm^{-3}$. DPV at CPE was used as a measuring technique. In B-R buffer media pH 2 - 7 was obtained one peak of epinephrine, that broadened in more alkaline media. In B-R buffer pH 11 and 12, no peak of epinephrine was recorded and the potential window narrowed down. For the following calibration measurements, B-R buffer pH 6 was chosen based on the peak shape and peak height.
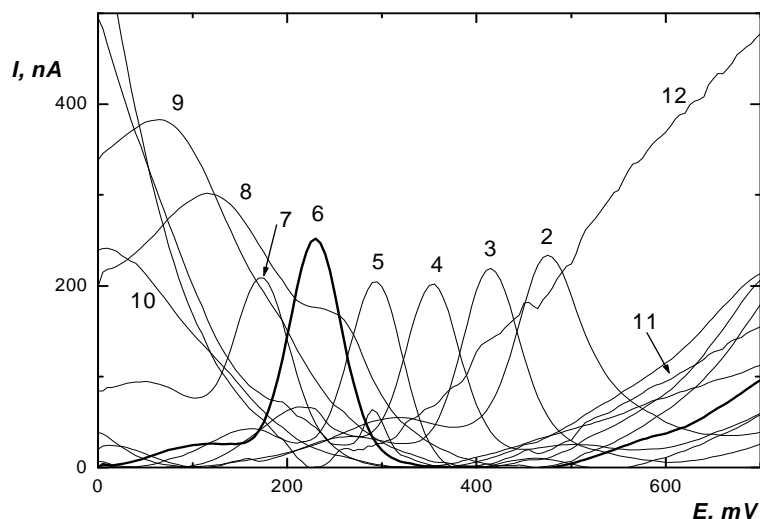
Fig.1 The pH dependency of epinephrine; voltammograms of $1 \cdot 10^{-5}$ mol·dm^{-3} epinephrine; *measured by DPV at CPE in B-R buffer media pH 2 – 12. The numbers indicate pH of base electrolyte.*

The curves of epinephrine were measured in the range of concentration $8 \cdot 10^{-7}$ - $1 \cdot 10^{-5}$ mol·dm^{-3}. In lower concentration it was impossible to evaluate the peak of epinephrine. Curve parameters and correlation coefficient for dependency of epinephrine peak height on epinephrine concentration obtained using linear regression method are shown in Table 1.

Table 1 The dependency of peak height of epinephrine on the eliminating step of modification of miniCPE.

	range (mol·dm^{-3})	slope ($\mu A \cdot \mu mol^{-1} \cdot dm^{3}$)	intercept (μA)	correlation coeficient
CPE	$8 \cdot 10^{-7}$ - $1 \cdot 10^{-5}$	0.0195	+ 0.0018	0.997
miniCPE	$1 \cdot 10^{-6}$ - $1 \cdot 10^{-5}$	0.0179	+ 0.0087	0.998
modified miniCPE	$8 \cdot 10^{-7}$ - $1 \cdot 10^{-5}$	0.0164	+ 0.0155	0.996

One of the advantages of voltammetric methods is the possibility to accumulate the compound on the electrode surface or in the bulk of the electrode. This results in significantly lower limits of detection for the compound. An AdS DPV at CPE was used as a measuring technique for the determination of epinephrine. Fig.2 shows the dependency of peak heights and areas on accumulation potential E_a with the time of accumulation 60 s. It is evident, that epinephrine did not accumulate on the carbon paste, because different accumulation potentials gave very similar values of peak heights. The influence of accumulation time on peak heights and areas using accumulation potential 350 mV was negligible too so that epinephrine does not accumulate on the surface of the carbon paste and AdS DPV can not be used for lowering the epinephrine limit of detection.

175
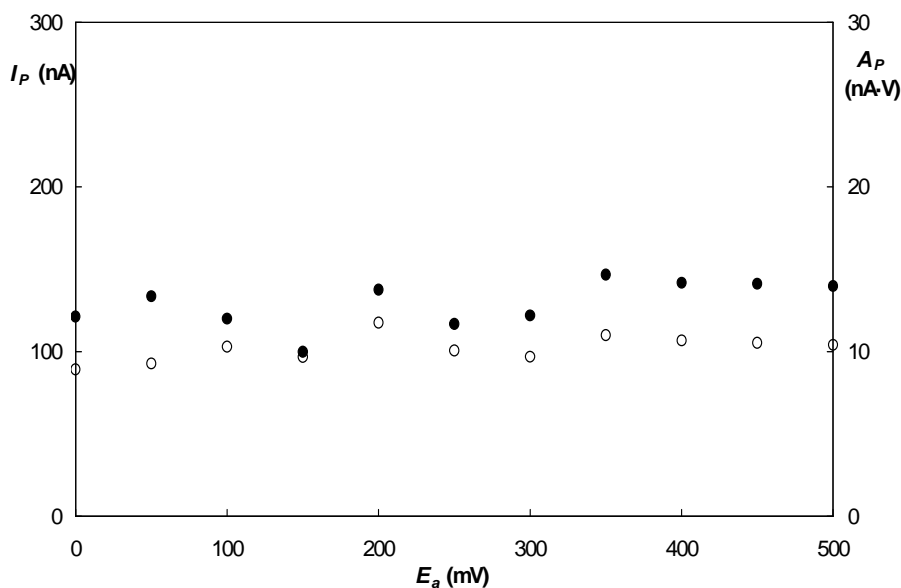
Fig.2 Dependency of peak heights I_P (nA ●) and areas A_P (nA·V ○) on accumulation potential E_a (mV); *B-R buffer pH 6; time of accumulation 60 s, c (epnephrinei) = $1·10^{-6}$ mol·dm^{-3}.*

The same procedure was used in measurements employing miniCPE. The influence of pH on voltammetric behaviour of epinephrine was studied in Britton-Robinson (B-R) buffer pH 2 – 12 (Fig.3). Concentration of measured epinephrine solution was $1·10^{-5}$ mol·dm^{-3}. DPV at CPE was used as a measuring technique. B-R buffer pH 6 was chosen for the following calibration measurements.
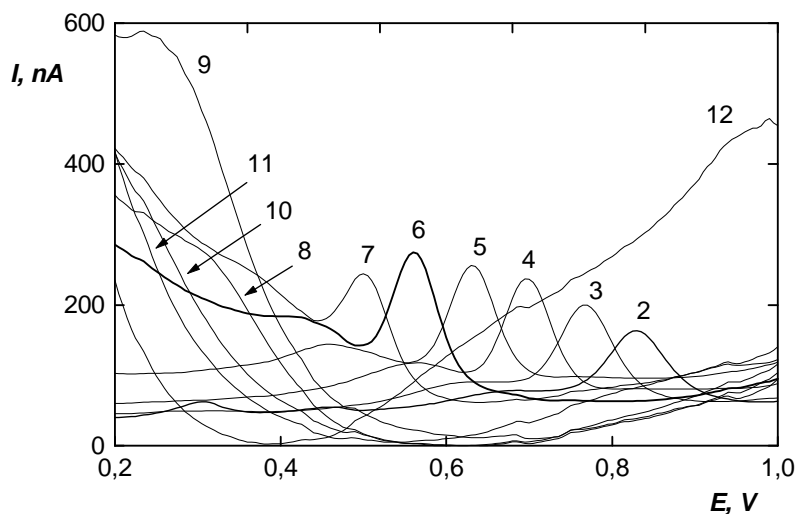

Fig.3 The pH dependency of epinephrine; voltammograms of $1·10^{-5}$ mol·dm^{-3} epinephrine; *measured by DPV at miniCPE in B-R buffer media pH 2 – 12. The numbers indicate pH of base electrolyte.*

The curves of epinephrine were measured in the range of concentration $1·10^{-6}$ - $1·10^{-5}$ mol·dm^{-3}. Curve parameters and correlation coefficient for dependency of epinephrine peak height on epinephrine concentration obtained using linear regression method are shown in Table 1. An AdS DPV at miniCPE was used as a measuring technique for the accumulation of epinephrine. The results obtained using miniCPE are compared with those obtained with classical CPE (Fig.4).
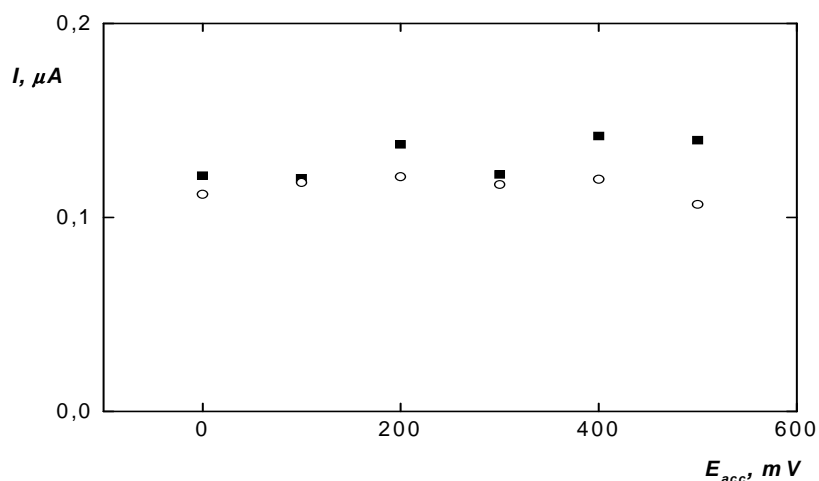
Fig.4 Dependency of peak heights I_P (nA) of epinephrine on accumulation potential E_a (mV); *B-R buffer pH 6; time of accumulation 60 s, c (epnephrinei) = 1·10⁻⁶ mol·dm⁻³, working electrode CPE (■), miniCPE (○);*

3.2 Modified carbon paste

For the decrease of limits of detection the modification of carbon paste was tested. A poly (eriochrome black T) chemically modified carbon paste electrode was prepared by cycling the potential between -0.4 and +1.5 V in the presence of 0.01M NaOH containing 0.5mM eriochrome black T. Than the film was washed with deionised water. To eliminate untreated eriochrome black T the cycling of potential between -0.2 and +0.8 V in the presence of Britton-Robinson buffer was used.

The DP voltammograms of epinephrine in the media of Britton-Robinson buffer, pH 2 – 12, were measured (Fig.5). In acidic media, there was another peak, which belongs obviously to EBT. This peak was decreasing towards the neutral media. But in basic media, pH > 8, also the peak of epinephrine was not able to evaluate. The solution of epinephrine was measured in the Britton-Robinson buffer, pH 7 in the concentration range $8·10^{-7}$ - $1·10^{-5}$ mol·dm⁻³. Curve parameters and correlation coefficient for dependency of epinephrine peak height on epinephrine concentration obtained using linear regression method are shown in Table 1. The accumulation of epinephrine to the bulk of electrode was tested, but either employing the modificator did not lead to better results (Fig.6). When the accumulation time higher than 60 s was used, the peak was divided in two. Then it was unable to evaluate separate peaks because of their covering.
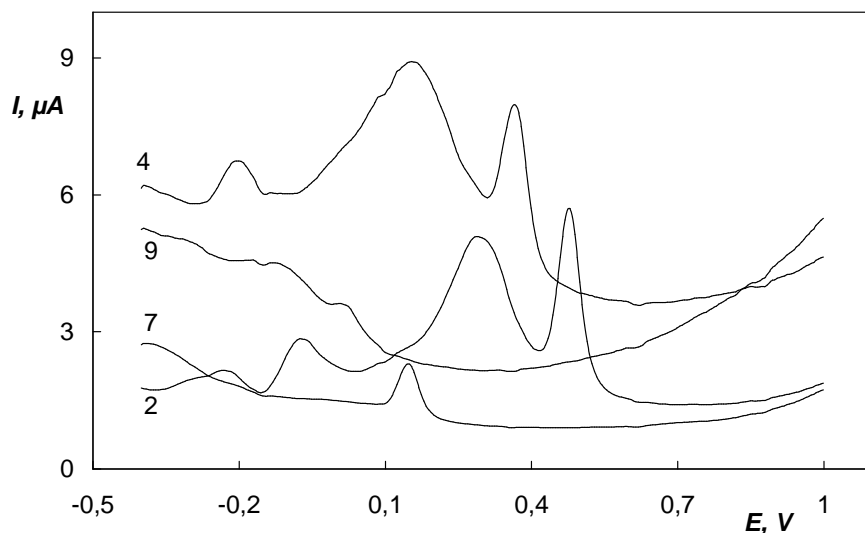
Fig.5 The pH dependency of epinephrine; v*oltammograms of $1 \cdot 10^{-4}$ mol·dm^{-3} epinephrine; measured by DPV at miniCPE in B-R buffer media pH 2 – 12. The numbers indicate pH of base electrolyte.*
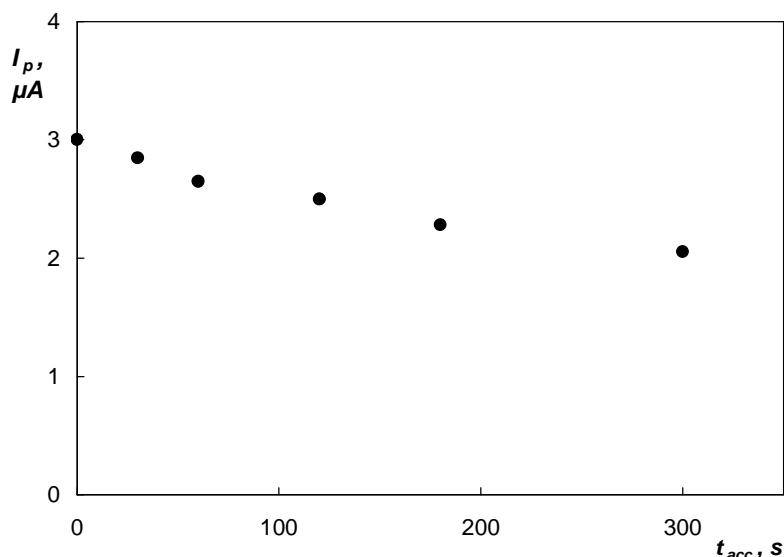

Fig.6 Dependency of peak heights I_P (nA) of epinephrine on accumulation time t_{acc} (s); *B-R buffer pH 6; potential of accumulation -0,1 V, c (epnephrinei) = $1 \cdot 10^{-5}$ mol·dm^{-3}.*

4. Conclusion

The miniaturized CPE was made to allow the measurements in lower amount of solution and to decrease the consumption of all chemicals. At a bare miniCPE the $5 \cdot 10^{-7}$ mol·dm^{-3} limit of detection was achieved and the epinephrine did not accumulate neither on the surface nor in the bulk of the carbon paste. The EBT was tested as a suitable modificator of carbon paste for determination of epinephrine. Using differential pulse voltammetry the anodic peak of epinephrine obtained with modified miniCPE was approximately 3 times higher than peak of epinephrine obtained with bare miniCPE and the limit of detection decreased to $2 \cdot 10^{-7}$ mol·dm^{-3}. Using of AdS DPV method did not lead to lower limits of detection, because epinephrine did not accumulate either in the modified carbon paste.

Acknowledgment

References

[1] Adams R.N.: *Anal. Chem. 30 (1958), 1576.*

[2] Wenke M.: *Farmakologie*, Avicenum, Praha *(1984)*

[3] Koštíř J.: *Biochemie*, Avicenum, Praha *(1974)*

[4] Sanchez A.; Toledo-Pinto E.A.; Menezes M.L.: *Pharm. Research 50 (5), (2004,) 481.*

[5] Carrera V.; Sabater E.; Vilanova E.; Sogorb M.A.: *J. Chrom. B 847 (2007), 88-94.*

[6] Pyo W.Y.; Jo C.H.; Myung S.W.: *Chromatographia 64 (2006), 731-737.*

[7] Sabbioni C.; Saracino M.A.; Mandrioli R.; Pinzauti S.; Furlanetto S.; Gerra G.; Raggi M.A.: *J. Chromatogr. A 1032 (2004), 65-71.*

[8] Kumarathasan P.; Vincent R.: *J. Chromatogr. A 987 (2003), 349-358.*

[9] Sanger-van de Griend C.E.; Ek A.G.; Widahl-Nasman M.E.: *J. Pharm. Biomed. Anal. 41 (2006), 77-83.*

[10] Wei S.L.; Song G.Q.; Lin J.M.: *J. Chromatogr. A 1098 (2005), 166-171.*

[11] Zhao C.; Shao C.; Li M.; Jiao K.: *Talanta 71 (2007), 1769-1773.*

VOLTAMMETRIC DETERMINATION OF 4-NITROPHENOL USING SILVER AMALGAM PASTE ELECTRODE

Abdul Niaz[a], Jan Fischer[b], Jiří Barek[b], Bogdan Yosypchuk[c], Sirajuddin[a] and Muhammad Iqbal Bhanger[a]

[a] *National Centre of Excellence, in Analytical Chemistry, University of Sindh, Jamshoro 76080, Pakistan*
[b] *Charles University in Prague, Faculty of Science, Department of Analytical Chemistry, UNESCO Laboratory of Environmental Electrochemistry, Hlavova 2030, 12843 Prague 2, Czech Republic, e-mail: barek@natur.cuni.cz*
[c] *J. Heyrovsky Institute of Physical Chemistry of ASCR, v. v. i., Dolejšova 3, 182 23 Praha 8, Czech Republic.*

Abstract

A differential pulse voltammetric (DPV) method was developed for the determination of 4-nitrophenol (4-NP) at a silver amalgam paste electrode (AgA-PE) in Britton-Robinson buffer pH 3.0. The experimental parameters, such as pH of Britton-Robinson buffer and activation and regeneration potential of electrode surface were optimized. The reduction peak currents were linear with the concentration of 4-NP from 2×10^{-7} to 1×10^{4} mol.l^{-1} with the correlation coefficient of R= 0.9997. The method showed reproducible results with R.S.D (n= 45) 1.7%. The limit of quantification (LOQ) was 3.2×10^{-7} mol L^{-1}. The method was successfully applied for the direct determination of 4-NP in drinking water.

Keywords

Voltammetry; 4-Nitrophenol; Silver amalgam paste electrode; Drinking water

1. Introduction

Phenol and substituted phenols are known to be widespread as components in natural and industrial waste mostly from petroleum, gas, wood, textile, pharmaceutical, papermaking, insecticide, and dyestuff industries. The toxicity of these compounds have been well understood to humans, animals and plants, they give an undesirable taste and odor to drinking water, even in very low concentration. For these reasons, many of the phenols have been included in the environmental legislation. In particular 4-NP is one of the nitrophenols in the U.S. Environmental Protection Agency List of Priority Pollutants[1,2]. 4-NP is a hazardous substance which can cause a high environmental impact due to its toxicity and persistence. The origin of contamination comes from manufacturing, chemical industry and agricultural practices[3]. Moreover, organophosphorus pesticides yield nitrophenols as major degradation products[4]. Consequently, monitoring of nitrophenols is a matter of concern for environmental control. Similarly, there is an ever increasing demand for electrochemical determination of trace amounts of nitrated explosives for which new types of electrodes are actively sought.

The determination of nitrophenols is usually accomplished by means of chromatographic separation with spectrometric detection. Due to easy instrumentation and low eqiupments costs, however, voltammetric thechniques are particularly usefull for the analysis of a wide variety of organic compounds[5]. Various electroanalytical techniques have been proposed for the determination of nitrophenols, mainly polarography, cyclic voltammetry (CV), differential pulse voltammetry (DPV) and adsorptive stripping voltammetry (AdSV) at different type of electrodes[6-16].

Non toxic solid amalgam electrodes were found to be suitable sensors for the determination of nitrophenols in water[15]. Recently, a silver amalgam paste electrode (AgA-PE) as an active electrode material for the reduction processes has been developed by

research group of Prague[17]. Due to easily renewable surface, good mechanical stability, high rate of electrode processes, simple handling with regeneration of the surface by an electrochemical pretreatment in the same solution of analyte, the AgA-PE is the most suitable material for the electrochemical measurements. Therefore, the present study aimed to investigate a differential pulse voltammetric (DPV) method for the determination of trace amounts of toxic 4-NP in drinking water using a non-toxic silver amalgam paste electrode and to compare the results at this electrode to those at mercury meniscus modified silver solid amalgam electrode (m-AgSAE) and classical hanging mercury drop electrode (HMDE).

2. Experimental
2.1 Reagents and solution

All reagents were of analytical grade. A stock solutions of 1.10^{-3} mol.l^{-1} 4-NP was prepared by dissolving 0.0139 g of the substance (C. A. S. Registry Number: [100-02-7]; 98%, Sigma-Aldrich, Germany) in 100 mL deionized water. Britton–Robinson buffer was used as a supporting electrolyte. De-ionized water was produced by a Milli-Q plus system. Other chemicals were obtained from Lachema Brno (Czech Republic) in p.a. purity. All the chemicals were used without any further purification.

2.2 Apparatus

DPV experiments were performed using computer controlled Eco-Tribo Polarograph with Polar Pro software, version 5.1 for Windows XP (both Polaro-Sensors, Prague, Czech Republic) in combination with a typical three electrode system: a platinum foil as an auxiliary electrode and silver/silver chloride (1M-KCl) RAE 113 (Monokrystaly, Turnov, Czech Republic) as a reference electrode. The working electrode was silver amalgam paste electrode (AgA-PE) with 10% silver.

The way of preparation of AgA-PE was described in previous papers[17]. A mixture of mercury and 10 % of fine silver powder (particle size 2 – 3.5 μm, Aldrich) was vigorously mixed for 60 s in dental amalgams preparation unit Dentomat compact (Degussa, Brazil). A small amount of the amalgam paste was put inside the pipette tip and an electrical connection with the steel wire was made and then the surface was smoothed on glass surface.

2.3 Procedure

Before starting the experiment, as well as after electrode passivation or every pause longer than one hour, the electrochemical activation of AgA-PE was carried out in 0.2 M KCl at -2200 mV under stirring of the solution for 300 seconds followed by rinsing with distilled water. Where not stated otherwise, work with AgA-PE was carried out at a scan rate of 20 mVs^{-1}, pulse amplitude of -50 mV, pulse duration of 100 ms, sampling time of 20 ms beginning 80 ms after the onset of the pulse and interval between pulses of 100 ms. A short electrochemical regeneration of AgA-PE lasting about 30s preceded each measurement. For regeneration study the appropriate values of the potential and the time of regeneration were inserted in the program of the used computer-controlled instrument so that the regeneration of AgA-PE was always carried out automatically. The voltammetric measurements were carried out by taking appropriate amount (1-1000 µL) 4-NP from the stock solution (c = 0.1 mmol.l^{-1}) and added into a10-mL volumetric flask, which was filled up to the mark with corresponding Britton-Robinson buffer in deionized water and then transferred into an electrochemical cell. Oxygen was removed from measured solutions by purging with nitrogen for 5 minutes under stirring. The calibration curves were measured in triplicate and evaluated by the least squares linear regression method. The limits of determination were calculated as the tenfold standard deviation from 12 analyte

determinations at the concentration corresponding to the lowest point on the appropriate calibration straight line[18]. All the measurements were performed at laboratory temperature. Determination of 4-NP in drinking water was carried out by calibration plot method.

3. Results and discussion
3.1 Activation and regeneration of AgA-PE

Voltammetric measurements were performed at 11 different new surfaces of AgA-PE for each 5 repeated measurements without activation and regeneration procedure in Britton-Robinson buffer pH 6.0 were carried out, in order to observe the reproducibility of current signal after renovation of electrode. The statistical results are shown in the Table 1. It can be seen from the table that the current values are practically the same and the reproducibility is better than 10% for all different combinations, which means that each new AgA-PE showed reproducible results.

Table 1 Voltammetric measurements of 4-NP at different surfaces of AgA-PE without activation and regeneration *in Britton-Robinson buffer pH 6.0, C(4-NP) = 4.10^{-5} mol.l^{-1}, given values are peak currents in nA.*

No.of electrode used	1	2	3	4	5	6	7
Measur: 1	-35.39	-37.18	-30.62	-26.71	-24.07	-28.70	-40.33
= 2	-34.26	-39.73	-31.15	-33.70	-30.62	-29.30	-38.35
= 3	-30.96	-39.22	-30.70	-35.63	-32.34	-29.66	-41.24
= 4	-28.34	-39.10	-30.84	-35.53	-33.80	-30.83	-42.69
= 5	-27.48	-39.72	-30.21	-35.75	-33.66	-29.84	-43.24
Averg	*-31.29*	*-38.99*	*-30.70*	*-33.46*	*-30.89*	*-29.67*	*-41.17*
St.dev	3.13	0.94	0.31	3.46	3.60	0.70	1.75

No.of electrode used	8	9	10	11	Averg	St. dev
Measur: 1	-29.37	-45.50	-44.05	-30.58	*-33.86*	*7.14*
= 2	-31.87	-38.76	-43.48	-29.17	*-34.58*	*4.80*
= 3	-32.17	-35.91	-43.30	-28.06	*-34.47*	*5.00*
= 4	-33.07	-33.43	-42.71	-28.37	*-34.43*	*5.13*
= 5	-33.43	-32.71	-41.60	-28.71	*-34.21*	*5.32*
Averg	*-31.98*	*-37.26*	*-43.03*	*-28.98*	*-34.31*	*4.93*
St.dev	1.42	4.63	0.83	0.88	-	-

After the reproducibility of each new surface of electrode has been confirmed, the electrochemical activation study was performed at the same surface of AgA-PE in 0.2 M KCl at -2200 mV under stirring of the solution for 300 seconds followed by rinsing with distilled water. The statistical results obtained for 12 activation cycles of each 7 repeated measurements are shown in the Table 2. These reveal that activation improved the current signal up to 2 activation cycles and then the signal became stable after employing further activation cycle with a relative standard deviation equal to 7%. Thus before starting the experiment or after passivation, activation is necessary for each new surface of AgA-PE to get optimum results.

Table 2 Activation of AgA-PE using the same surface *in 0.2 M KCl, C(4-NP) =4.10⁻⁵mol.l⁻¹, activation potential = -2200 mV and activation time = 300s. given values are peak currents in nA.*

No. Of activation	without actv.	Actv-1	2	3	4	5	6	7
Meas: 1	-17.41	-66.43	-97.06	-102.20	-95.01	-94.22	-93.60	-94.53
= 2	-31.10	-72.58	-95.04	-98.95	-93.91	-92.68	-90.52	-92.48
= 3	-43.58	-68.62	-90.68	-94.76	-91.12	-90.34	-88.25	-89.57
= 4	-43.34	-67.87	-87.24	-92.99	-88.73	-88.93	-86.96	-89.24
= 5	-42.49	-66.50	-88.21	-92.19	-87.32	-90.13	-86.07	-88.37
= 6	-42.08	-66.49	-84.20	-91.46	-87.53	-88.77	-85.50	-87.79
= 7	-41.78	-65.81	-82.92	-91.26	-87.50	-87.71	-84.47	-87.40
Averg	*-37.39*	*-67.75*	*-89.34*	*-94.83*	*-90.16*	*-90.39*	*-87.91*	*-89.91*
St.dev(%)	26%	3%	6%	4%	4%	3%	4%	3%

No. Of activation	8	9	10	11	12	Aveg	St .dev
Meas: 1	-88.59	-89.98	-108.2	-107.70	-103.2	*-97.66*	7%
= 2	-87.62	-90.44	-108	-107.00	-97.91	*-95.87*	7%
= 3	-83.71	-90.60	-104.7	-104.40	-95.83	*-93.09*	7%
= 4	-82.60	-85.57	-102.7	-101.20	-94.22	*-90.95*	7%
= 5	-85.95	-85.97	-101.9	-99.88	-93.83	*-90.89*	6%
= 6	-84.44	-85.45	-101.4	-99.75	-91.70	*-89.81*	7%
= 7	-81.91	-84.64	-101.1	-98.39	-92.08	*-89.03*	7%
Averg	*-84.97*	*-87.52*	*-104*	*-102.66*	*-95.54*	*-92.47*	7%
St.dev(%)	3%	3%	3%	4%	4%	-	-

3.2 The influence of pH on voltammetric behavior of 4-NP

The influence of pH on the differential pulse voltammograms of tested 4-NP is represented by Fig.1. It can be seen from the figure that at pH 3 the highest, well developed and therefore most easily evaluated peak was obtained.

Repeated measurements revealed quite pronounced passivation of the electrode, probably by products of the electrode reaction, resulting in decreasing peaks moving toward more negative potentials. Effect of passivation of the electrode surface was reduced by the above described electrochemical activation but settings of regeneration potentials have strong impact on signal stability and, therefore, optimal regeneration potentials had to be found for 4-NP. The best results were obtained at (E_{reg1}) = -1050 mV and (E_{reg2}) = 200 mV with R.S.D of about 1.7 % after 45 repetitive measurements, see Table 3.

Using optimum experimental conditions linear calibration curves were obtained in high and low concentration ranges (depicted in Fig. 2, 3 and 4) in Britton-Robinson buffer pH 3.0 with pulse amplitude and scan rate -50mV and 20mVs⁻¹ , respectively and (E_{reg1}) = -1050 mV and (E_{reg2}) = 200 mV. The parameters of thus obtained calibration curves are summarized in Table 4.
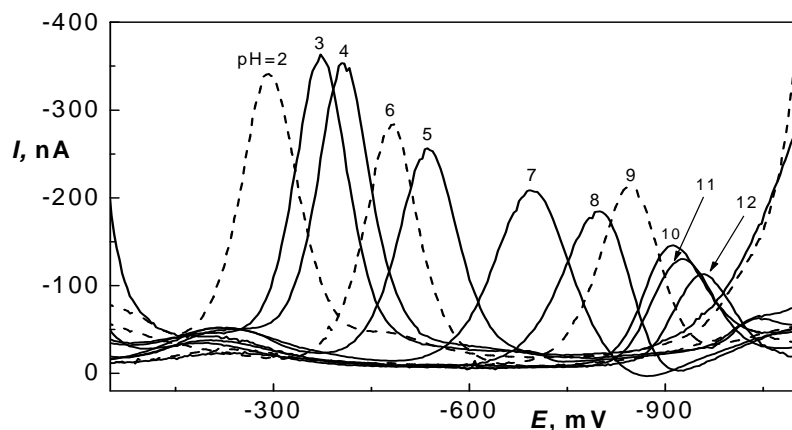
Fig.1 Differential pulse voltammograms of 4-NP at AgA-PE *in Britton-Robinson buffer pH 2 to 12 (numbers above curves correspond to given pH), c(4-NP) = 1.10^{-4} mol.L^{-1}.*

Table 3 Experimentally found optimal values of regeneration potentials of AgA-PE for 4-NP *in Britton-Robinson buffer pH 3.0. Concentration of 4-NP is 1.10^{-4} mol.l^{-1}and scan rate is 20mVs^{-1}.*

| No. of electrode	Serial No. of measurement	$E_{reg\,1}$ [mV]	$E_{reg\,2}$ [mV]	I_{p1meas} [nA]	I_{p2meas} [nA]	$I_{p45meas}$ [nA]	$I_{p\,Min}$ [nA]	$I_{p\,Max}$ [nA]	Rel. st. dev.	Avegrage [nA]
1	1	-1000	200	-119.6	-117.6	-105.00	-101.3	-119.6	3.5%	-108.01
1	1	-1000	100	-144.9	-161.3	-140.50	-140.5	-161.8	4.4%	-151.08
1	2	-1000	100	-52.64	-51.32	-50.25	-41.44	-52.64	5.4%	-47.31
1	1	-1050	100	-69.39	-70.02	-77.47	-69.39	-77.47	2.5%	-73.56
1	2	-1050	100	-85.89	-86.79	-80.85	-69.87	-87.68	5.1%	-81.44
1	3	-1050	100	-75.40	-76.44	-80.40	-74.50	-80.40	1.6%	-78.32
1	1	-1050	0	-104.9	-104.4	-97.04	-94.74	-104.9	2.4%	-98.73
1	1	-1050	200	-98.39	-98.71	-93.31	-90.29	-99.50	1.9%	-95.83
2	2	-1050	200	-155.7	-156.3	-151.80	-150.8	-156.7	1.1%	-153.53
3	3	- 1050	200	-149.4	-150.2	-142.20	-135.5	-150.2	2.1%	-142.28
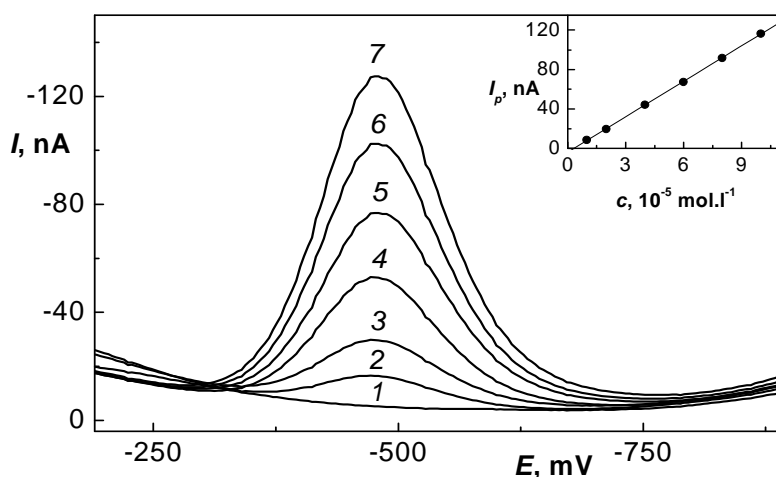
Fig.2 Differential pulse voltammograms of 4-NP at AgA-PE *in Britton-Robinson buffer pH 3.0 in the concentrations of (1) 0.10^{-5}, (2) 1.10^{-5} (3) 2.10^{-5}, (4) 4.10^{-5}, (5) 6.10^{-5}, (6) 8.10^{-5}, (7) 1.10^{-4} mol.l^{-1}.The pulse amplitude and scan rate are 50mV and 20mVs^{-1} , respectively. Regeneration potential (E_{reg1}) is -1050 and (E_{reg2}) is 200mV,*

184
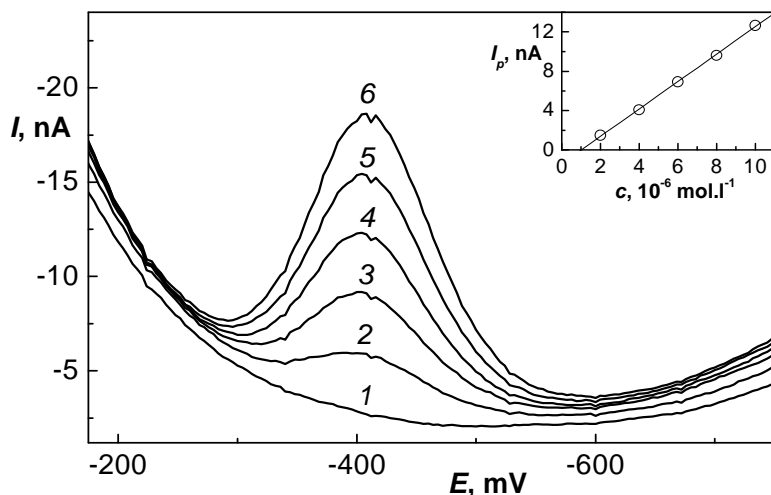
Fig.3 Differential pulse voltammograms of 4-NP at AgA-PE *in Britton-Robinson buffer pH 3.0 in the concentrations of (1) 0.10^{-6}, (2) 2.10^{-6} (3) 4.10^{-6}, (4) 6.10^{-6}, (5) 8.10^{-6}, (6) 1.10^{-5} mol.l^{-1}. The pulse amplitude and scan rate are 50 mV and 20 mV.s^{-1}, respectively. Regeneration potential (E$_{reg1}$) is -1050 and (E$_{reg2}$) is 200 mV.*
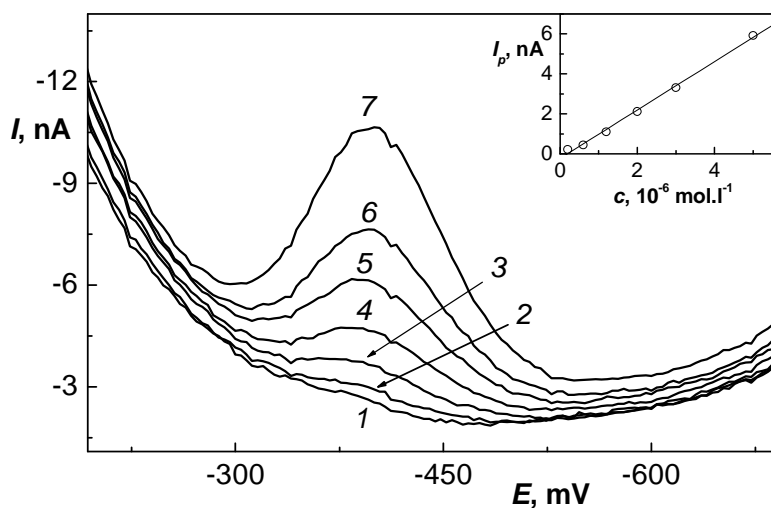

Fig.4 Differential pulse voltammograms of 4-NF at AgA-PE *in Britton-Robinson buffer pH 3.0 in the concentrations of (1) 0.10^{-7}, (2) 2.10^{-7} (3) 6.10^{-7}, (4) 1.10^{-6}, (5) 2.10^{-6}, (6) 3.10^{-6}, (7) 5.10^{-6} mol.l^{-1}. The pulse amplitude and scan rate are 50 mV and 20 mV.s^{-1}, respectively. Regeneration potential (E$_{reg1}$) is -1050 and (E$_{reg2}$) is 200 mV.*

185
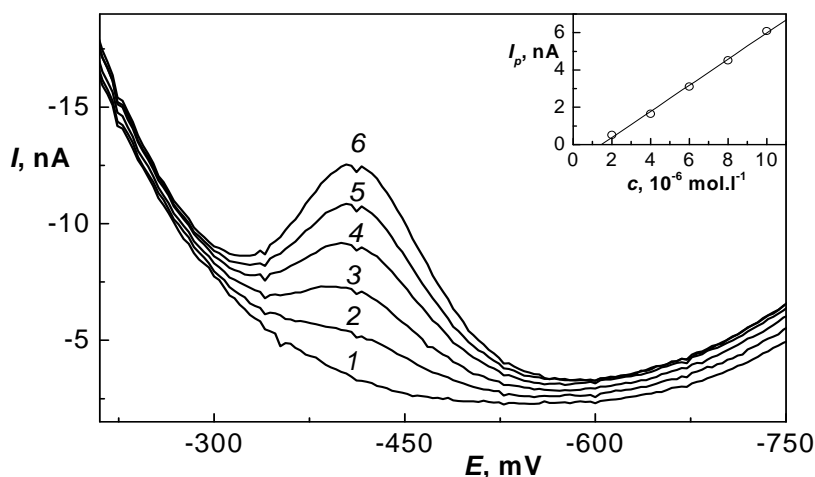
Fig.5 Differential pulse voltammograms of 4-NF in tape water (5ml) at AgA-PE i*n Britton-Robinson buffer (5 ml) pH 3.0. Concentrations of 4-NP in 5 ml drinking water are (1) 0, (2) 2.10^{-6} (3) 4.10^{-6}, (4) 6.10^{-6}, (5) 8.10^{-6}, (6) 1.10^{-5} mol.l^{-1}. The pulse amplitude and scan rate are 50 mV and 20 mV.s^{-1}, respectively. Regeneration potential (E_{reg1}) is -1050 and (E_{reg2}) is 200 mV.*

In order to check the application of the proposed method, the determination of 4-NP was carried out in drinking water. For this purpose a calibration curve was measured (shown in Fig.5) using 5 ml of drinking water containing 20 – 100 µL (2.10^{-6} – 1.10^{-5} mol.l^{-1}) of 1.10^{-3} mol.l^{-1} 4-NP and 5 ml Britton-Robinson buffer pH 3.0 which makes together a final volume of 10 ml. The parameters of thus obtained calibration curves are summarized in Table 4.

These results confirmed the possible application of the proposed method in drinking water. All the results obtained at HMDE, m-AgSAE, AgA-PE are summarized in the Table 4. These results indicate that better sensitivity can be obtained at AgA-PE in comparison to m-AgSAE, although HMDE is still the best electrode. However, for some electrochemical application AgA-PE can by useful and applicable alternative to HMDE.

Table 4 Parameters of the calibration straight lines for the determination of tested 4-NP *in the concentration range of 0.2-100 µmol.L^{-1} using DPV at HMDE, m-AgSAE and AgA-PE in a Britton-Robinson buffer.*

Electrode	pH	E_{reg1} [mV]	E_{reg2} [mV]	Concentration range [mol.L^{-1}]	Slope [nA.mol^{-1}L]	Intercept [nA]	R	LOQ [mol.L^{-1}]
HMDE	6.0	-	-	$(2-10)\cdot10^{-6}$	$-7.5.10^{6}$	-0.70	0.9998	-
				$(2-10)\cdot10^{-7}$	$-7.4.10^{6}$	-0.17	0.9992	$1.3.10^{-7}$
m-AgSAE	6.0	-1200	0	$(2-10)\cdot10^{-5}$	$-1.3.10^{6}$	7.07	0.9994	-
				$(2-10)\cdot10^{-6}$	$-1.4.10^{6}$	0.41	0.9995	$4.2.10^{-7}$
AgA-PE	3.0	-1050	200	$(1-10)\cdot10^{-5}$	$-1.2.10^{6}$	3.9	0.9999	-
				$(2-10)\cdot10^{-6}$	$-1.4.10^{6}$	1.4	0.9997	-
				$(0.2-3)\cdot10^{-6}$	$-1.2.10^{6}$	0.23	0.9980	$3.2.10^{-7}$

4. Conclusion

It is concluded from all these results that AgA-PE is a suitable sensor for the determination of micromolar and submicromolar concentrations of 4-NP. The limit of determination of 4-NP using DPV at AgA-PE is lower than for m-AgSAE. Due to efficient electrochemical regeneration, the AgA-PE gives better reproducibility with excellent signal stability given by lower pasivation of electrode surface. Furthermore, fairly good reproducibility (RSD lower than 10%) of surface renovation has been observed. The easy renovation of electrode surface makes the method easier than the use of other solid electrodes and thus it represents an effective and simpler alternative to the HMDE. It can be expected that AgA-PE will be useful for determination of trace amounts of nitrated explosives.

References

[1] US Environmental Protection Agency, *Fed. Regist.,* **44** *(1979), 233.*
[2] US Environmental Protection Agency, *Fed. Regist.,* **52** *(1989), 131.*
[3] Christophersen M.J.; Cardwell T.J.: *Anal. Chim. Acta* **323** *(1996),39.*
[4] Castillo M.; Domingues R.; Alpendurada M.F.; Barcelo D.: *Anal. Chim. Acta* **353** (1997), *133.*
[5] Barek J.; Cvacka J.; Muck A.; Quaiserova V.; Zima J.: *Fresenius J. Anal. Chem.* **369** *(2001), 556.*
[6] Zietek M.: *Mikrochim. Acta* **2** (1975), *463.*
[7] Barek J.; Ebertová H.; Mejstrík V.; Zima J.: *Collect. Czech. Chem. Commun.* **59** *(1994), 1761.*
[8] Hernandez L.; Hernandez P.; Vicente J.: *Fresenius J. Anal. Chem.* **345** *(1993), 712.*
[9] Rodriguez I.N.; Leyva J.A.N.; de Cisneros J.L.H.H.: *Anal. Chim. Acta* **344** *(1997), 167.*
[10] Rodríguez I.N.; Leyva J.A.N.; de Cisneros J.L.H.H.: *Analyst* **122** *(1997), 601.*
[11] Rodriguez I.N.; Zamora M.B; Salvador J.M.B.; Leyva J.A.M; Hernandez-Artiga M.P; de Cisneros J.L.H.H.: *Mikrochim. Acta* **126** *(1997), 87.*
[12] Cuiling S.; Gaiping Xu.; Wang and Cui D.: *Talanta* **54** *(2001), 115.*
[13] Pedrosa V.D.; Codognoto L.; Avaca L.A.: *J. Braz. Chem. Soc.* **14** *(2003), 530.*
[14] Huang W.; Yang C.; Zhang S.: *Anal-bio. Anal. Chem.* **372** *(2003), 703.*
[15] Fischer J.; Vanourkova L.; Danhel A.; Vyskocil V.; Cizek K.; Barek J.; Peckova K.; Yosypchuk B.; Navratil T.: *Int. J. Electrochem. Sci.,* **2** *(2007), 226.*
[16] Ni Y.; Wang, L.; Kobot S.: *Anal. Chim. Acta* **431***(2001), 101.*
[17] Yosypchuk B.; Sestakova I.: `Electroanalysis `**`20`**` (2008), accepted.`
[18] Christian G.D.: *Analytical Chemistry, 6th ed., John Willey & Sons: Inc., New York, 2004, p. 113.*